INFORMATION TO USERS

This manuscript has been reproduced from the microfilm master. UMI films the text directly from the original or copy submitted. Thus, some thesis and dissertation copies are in typewriter face, while others may be from any type of computer printer.

The quality of this reproduction is dependent upon the quality of the copy submitted. Broken or indistinct print, colored or poor quality illustrations and photographs, print bleedthrough, substandard margins, and improper alignment can adversely affect reproduction.

In the unlikely event that the author did not send UMI a complete manuscript and there are missing pages, these will be noted. Also, if unauthorized copyright material had to be removed, a note will indicate the deletion.

Oversize materials (e.g., maps, drawings, charts) are reproduced by sectioning the original, beginning at the upper left-hand corner and continuing from left to right in equal sections with small overlaps.

ProQuest Information and Learning
300 North Zeeb Road, Ann Arbor, MI 48106-1346 USA
800-521-0600

To my Mother and Father

CONDUCTIVITY AND ION-PAIR FORMATION IN ACETONE SOLUTION AS A FUNCTION OF PRESSURE AND TEMPERATURE

by

W. A. Adams

A thesis submitted in partial fulfillment of the requirements for the degree of Doctor of Philosophy

Department of Chemistry
University of Ottawa
Ottawa, Canada

August, 1967

K. J. Laidler
Professor of Chemistry
Research supervisor

W. A. Adams
Ph.D. Candidate

PREFACE

The mechanism of ionic motion in non-aqueous electrolyte solutions is a problem which has not yet been satisfactorily solved. Temperature and pressure coefficients of the limiting equivalent conductivity permit calculation of activation parameters which help to characterize the mechanism of the conductance process. The purpose of the present work is to obtain, over a wide range of temperature and pressure, new experimental results to add to the small body of reliable data now available.

The thermodynamics of the solvation of ions in non-aqueous media has not been widely studied. Ion-pair dissociation constants, which can be obtained from electrical conductivity measurements of electrolyte solutions, permit thermodynamic parameters of dissociation to be calculated. These quantities offer a new insight into both the nature of the ion pairs formed in non-aqueous solution and the variations in ionic solvation brought about by changes in temperature and pressure.

In connection with these studies in acetone, the work described in Appendix I has been published in the following paper: The effects of pressure and temperature on the structure of liquid acetone, W. A. Adams and K. J. Laidler. Can. J. Chem. 45, 123 (1967).

ACKNOWLEDGEMENTS

The author is grateful to Professor K. J. Laidler for the encouragement he provided throughout the course of these investigations. Professor Laidler's versatility has contributed to an appreciation of many different aspects of the work. Discussions with Professor B. E. Conway have been of great assistance. Thanks are also due to R. Martin for advice concerning the apparatus and for many discussions of high-pressure chemistry. Technical help was received from the University of Ottawa Computing Center staff, the workshop staff of the Chemistry Department, and three summer students who all gave generously of their time.

A National Research Council Scholarship and a Government of Ontario Graduate Fellowship are acknowledged with gratitude.

TABLE OF CONTENTS

LIST OF FIGURES

LIST OF TABLES

ABSTRACT

The equivalent conductivities of tetramethylammonium iodide, tetraethylammonium iodide, and tetra-n-propylammonium iodide in acetone solution were determined at temperatures of 25° to 55°C, and at pressures from atmospheric to 1.1 kbar. The results have been analysed by the Shedlovsky method. The limiting equivalent conductivities have been interpreted in terms of activated complex theory; the energies of activation for conductivity at constant pressure and at constant volume, and the volumes of activation for conductivity, were calculated. The hole free-volume theory of liquids has been discussed for different solvent systems and found to give a satisfactory explanation for the observed pressure and temperature coefficients of conductivity, viscosity, and self-diffusion in several solvents. The magnitude of the limiting ionic equivalent conductivity has been shown to depend in a critical way on the ionic radius and on the relative strengths of the ion-solvent and the solvent-solvent interactions.

The ion-pair dissociation constants determined from the Shedlovsky analysis were used to calculate the enthalpy, the internal energy at constant volume, the entropy, the volume, and the Gibbs free energy of dissociation. The sign and magnitude of these parameters over the range of conditions of temperature and pressure investigated indicated that the free ions in acetone solution are extensively solvated and that, depending on the conditions, solvent-shared or solvent-separated ion pairs are formed.

The compressibility of acetone has been redetermined at temperatures of 25° to 55°C, and at pressures from atmospheric to 1.1 kbar. The results have been fitted to the Tait equation, and values

of $(\partial P/\partial T)_V$ and of the internal pressure have been calculated. The heat capacity at constant volume has also been deduced as a function of pressure and temperature. The variation of these and other derived quantities has been shown to lead to conclusions about structural changes in the liquid.

CHAPTER 1

INTRODUCTION

1. General Introduction

Experimental and theoretical research on the thermodynamics of electrolyte solutions has been devoted mainly to the problems of aqueous solutions. However, water has many special properties which divert attention from those properties of electrolyte solutions which are common to many solvent systems, but which are not obvious in aqueous systems because of the unique hydrogen-bonded structure. Furthermore, even in aqueous systems few studies of electrolyte solutions have been carried over a sufficient range of temperature, volume, and pressure to indicate the complexity of the parameters which are usually measured only at 25°C and atmospheric pressure. Acetone, an organic solvent capable of dissolving many organic and inorganic salts to a concentration which permits the measurement of the electrical conductivity to a reasonable precision, was the solvent used in the present studies. Acetone is readily available in a form containing only water as an impurity. The large compressibility makes a wide range of volumes accessible for study without the need of maintaining very high pressures. At room temperature and atmospheric pressure acetone is close to its boiling point (56.2°C) and would be expected to show fewer features of the short range ordering characteristic of different solvent-solvent interactions specific to a given solvent than if the liquid studied were close to its freezing point. It is thought that the conductivity behaviour of salts in acetone solutions in the range of temperature from 25°C to 55°C and of pressure from 1 to 1100 bar, should reflect a pattern which is common to many solvent systems.

Blokker (1) studied the conductivities of LiCl, LiBr, LiI, NaI, KI, CaI_2, and i-Am_4NI in acetone solution from 25°C to 218°C (the critical constants of acetone are T_c = 235°C, P_c = 47 atmospheres, and ρ_c = 0.268 g ml^{-1} (2)) in a closed vessel at several concentrations. The equivalent conductivities were tabulated for these conditions. The density of the solvent in equilibrium with the vapour was determined at six temperatures between 25° and 218°C in order to obtain the equivalent conductivities. The conductance of i-Am_4NI was found to decrease with time. This observation was also made in the present work for n-Bu_4NI and it is thought to be the result of a reverse Menschutkin reaction in which trialkylamine and alkyl iodide are non-ionic products of the decomposition of tetraalkylammonium iodide. Other difficulties experienced by Blokker were the crystallization of the more concentrated solutions of LiCl, NaI, KI, and CaI_2 salts at higher temperatures. Blokker did not calculate the limiting equivalent conductivities or ion-pair dissociation constants from the concentration dependence of the observed equivalent conductivities. However, a decrease in the equivalent conductivity with temperature was ascribed to ion-pair or triple-ion formation. Some results calculated from these data are shown in Table 1.1.

A study of several salts in acetonitrile (ϵ = 36.8 at 25°C) between 15° and 30° by Minc and Werblan (3) has resulted in an analysis of the mechanism of ion-pair formation and conductivity, and is similar to that undertaken for acetone solutions in the present work. Minc and Werblan did not, however, measure the conductivity as a function of pressure. The salts studied were $LiClO_4$, $NaClO_4$, $KClO_4$, $RbClO_4$, $CsClO_4$, and Et_4NClO_4.

Table 1.1 (a)

Enthalpy of Ion-Pair Dissociation of Some Salts in Acetone Solution Calculated from the Data of Blokker (1)

(kcal mole^{-1})

	Temperature (°C)						
Salt	30	60	90	120	150	180	210
LiCl	-9.9	-10.5	-13.2	-19.6			
LiBr	-2.6	-2.0	-1.9	0.3	1.0	4.6	9.2
LiI	-1.8	-0.5	-1.7	-1.1	-2.2	1.9	0.1
NaI	-1.9	-2.0	-3.2	-3.7	-5.5	-7.4	-11.1
KI	-2.2	-2.6	-3.5	-4.7			
i-Am_4NI	-0.8	-0.8	-1.2	-1.5			
CaI_2	-1.1	-0.7	-0.8	-1.6	-4.7	-5.7	-4.3

Table 1.1 (b)

Energy of Activation for Conductivity at Constant Pressure for Some Salts in Acetone Solution Calculated from the Data of Blokker (1)

(kcal mole^{-1})

	Temperature (°C)						
Salt	30	60	90	120	150	180	210
LiCl	1.4	0.3	-0.8	-1.9			
LiBr	0.9	0.5	0.0	-1.7	-3.0	-5.6	-8.9
LiI	1.6	0.8	0.9	0.0	-0.6	-4.2	-5.4
NaI	1.2	0.8	0.4	-0.4	-0.8	-1.5	-2.4
KI	1.3	1.2	1.0	0.2			
i-Am_4NI	1.6	1.3	1.0	0.8			
CaI_2	1.3	0.9	0.2	-0.8	-1.6	-2.9	-4.4

Notes on Table 1.1

1. The energy of activation for conductivity at constant pressure, E_p, was obtained by plotting $\ln \Lambda$ against the temperature for the results given by Blokker at several concentrations. E_p at infinite dilution was estimated by plotting the slopes from these graphs against concentration for each temperature and extrapolating to zero concentration.

2. The enthalpy of ion-pair dissociation was estimated from E_p and $\Delta H_d + 2E_p$ obtained in the following way. The temperature dependence of $\ln(K_d \Lambda_o^2)$, which is the slope of the Ostwald dilution law plot of $c\Lambda$ against Λ^{-1}, allows the calculation of $\Delta H_d + 2E_p$. This procedure is discussed in Chapter 3.

3. The enthalpy of dissociation is negative, the process is exothermic, except for LiBr and LiI at higher temperatures where the E_p obtained by extrapolation is almost certainly in error because there were insufficient points to extrapolate to a concentration region of negligible ion-pair formation.

All of the salts, with the exception of Et_4NClO_4, were found to be associated to ion pairs in acetonitrile. The free-energy of dissociation was found to be positive, increasing with increases in the ion size. The dissociation is exothermic for $LiClO_4$ (-0.3 kcal $mole^{-1}$) and $NaClO_4$ (-1.57 kcal $mole^{-1}$) and endothermic for $KClO_4$ (0.41 kcal $mole^{-1}$), $RbClO_4$ (1.60 kcal $mole^{-1}$), and $CsClO_4$ (3.25 kcal $mole^{-1}$). The entropies of dissociation are negative for the salts of the small cations (about -10 e.u. for $LiClO_4$ and $NaClO_4$) and increase to a small positive value for $CsClO_4$ (2.8 e.u.). These results were taken to indicate the removal of solvent from the solvation layer of the alkali ions by the perchlorate ions in the ion-pair formation process. The cation-anion interaction increases with the decreasing size of the cation, the smaller cations releasing more solvent on association. Consequently ion-pair dissociation produces a greater negative entropy change for smaller cations. The heat of dissociation becomes more endothermic with increasing cation size, reflecting the weaker cation-anion interaction in the ion pairs formed with larger cations. It is concluded by Minc and Jerblan that contact ion pairs are formed in acetonitrile. This view is not thought to be correct, since the entropy changes of dissociation measured were not sufficiently negative, about -20 e.u. would have been more reasonable, to correspond to the production of two singly charged ions from the neutral state of the contact ion pair. The results obtained would appear to be more consistent with either a solvent-separated or a solvent-shared model of the ion pair. Considerations of the applicability of different models of the ion pairs formed in solution will be discussed more fully in Chapter 4.

The limiting equivalent conductivities were analyzed by Minc and Werblan using the Eyring theory of absolute reaction rates (4) and the individual ionic activation parameters were estimated. It is suggested, on the basis of differences observed in these activation parameters, that the larger ClO_4^-, Et_4N^+, and Cs^+ ions undergo translation in solution without the primary solvation layer, the smaller cations Li^+ and Na^+ with their primary solvation solvent molecules. In the latter case, the mechanism of the movement of the ions is determined by the solvent molecules in the second solvation layer. K^+ and Rb^+ ions have a mechanism of ionic migration intermediate between these two extremes.

There is a fundamental difficulty which has not yet been satisfactorily resolved in connection with the activation theory of ionic mobility. This has to do with division of the activation parameters into the ionic contributions. This problem has been discussed by Hills (5) and can be illustrated by the following analysis which is carried out for temperature changes, but could equally well have been done for pressure changes. The energies of activation for conductivity at constant volume, E_V, and at constant pressure, E_p, are defined by the equation

$$E_V / RT^2 = \left(\frac{\partial \ln \Lambda_o}{\partial T}\right)_V = \frac{1}{\Lambda_o}\left(\frac{\partial \Lambda_o}{\partial T}\right)_V$$

$$= \frac{1}{\Lambda_o}\left(\frac{\partial}{\partial T}(\lambda_+^\circ + \lambda_-^\circ)\right)_V \qquad (1.1)$$

where R is the gas constant

T is the temperature in $^\circ K$

Λ_o is the limiting equivalent conductivity

λ_+° and λ_-° are the limiting ionic equivalent conductivities

The limiting transport number is given by $\lambda^{\circ}_{\pm}/\Lambda_{o}$, equation (1.1) can be written as

$$E_V / RT^2 = \left[t^{\circ}_{+}\left[\frac{\partial}{\partial T} \ln \lambda^{\circ}_{+}\right]_{V} + t^{\circ}_{-}\left[\frac{\partial}{\partial T} \ln \lambda^{\circ}_{-}\right]_{V} \right]_{P}$$

$$= t^{\circ}_{+} E^{+}_{V} + t^{\circ}_{-} E^{-}_{V} \qquad (1.2)$$

where t°_{+} and t°_{-} are the limiting transport numbers for the cations and anions respectively

The ionic parameters can be seen to be additive only if t°_{+}, $t^{\circ}_{-} \neq f(T,P)$, in which case E_V and E_P are simple sums of the ionic contributions. Until measurements of the transport numbers as a function of temperature and pressure are available this point can not be settled. However, by studying a series of salts which contain a common ion, the effect of the variation in the anion or cation can be estimated.

The compressibility of liquid acetone was measured in the present work for the conditions 25° to 55°C and 1 to 1100 bar pressure and several thermodynamic properties of the system were evaluated. This work is reported in Appendix I. The values of these parameters enabled various mechanisms of ionic mobility and ion-pair formation to be investigated.

The conductivities of the iodide salts of tetramethylammonium ion (Me_4N^+), tetraethylammonium ion (Et_4N^+), and tetra-n-propylammonium ion ($n\text{-}Pr_4N^+$) were investigated over the above-mentioned range of temperature and pressure. From measurements of the concentration dependence of the equivalent conductivity, the ion-pair dissociation

constants and the limiting equivalent conductivities were obtained as functions of the temperature and pressure of the system. The detailed interpretation of these results emphasizes the importance of molecular properties of the solvent. The structural properties of liquids are of special relevance. The part played by solvent structure in ionic solvation and the energetics of solvation in non-aqueous media are two aspects of prime importance to the problem of the mechanism of ionic mobility and ion-pair formation in acetone solution. For this reason the next two sections of this chapter deal with liquids and solvation, both from a somewhat general point of view. Unfortunately, there are still far too few experimental thermochemical measurements on non-aqueous electrolyte solvent systems for it to be possible to make very many generalizations on their behaviour. It is just this uncertainty as to what features are to be expected and are general for all solvents, and what features are particular to a given solvent, which makes the interpretation of measurements of this kind such an interesting if sometimes frustrating task.

2. Liquids

A General Introduction

The liquid state possesses characteristics of both the gaseous and solid states of matter. Unlike a crystalline solid which is defined primarily in terms of the orderly spacial arrangement of molecules or ions extending over a macroscopic region, the liquid displays a regularity of arrangement of its molecules over only a few molecular diameters. This short-range order is not present to the same extent in gases. Another criterion which can be used to distinguish between the gaseous and liquid states is the molecular free path. When the molecules separate beyond a certain distance,

the intermolecular forces are negligible and a molecule travels from one interaction to the next without being influenced by neighbouring molecules. When the density of a fluid, even above the critical point, is such that molecules can not translate without being in the range of interaction of a neighbouring molecule, it is more convenient to treat the fluid on the basis of theories of the liquid state (6).

A rather special class of liquids are the glasses. A glass when cooled does not undergo the discontinuous change in properties that most liquids experience when they freeze. According to Angell (7), the high viscosity of liquids as they approach the glass transition is due to configurational restrictions to relaxation at high density. On the basis of experimental work with ionic melts at low temperatures, the liquid state is viewed by Angell as being continuous through the crystallization temperature and terminating in a glass transition. A glass, therefore, can be thought of as a liquid which, for the time scale of the experiment of interest, has a negligible configurational entropy.

The liquid state is intermediate between that of the crystalline solid and the dilute gas. Models which attempt to idealize certain features of the liquid state to enable the experimental properties to be theoretically estimated therefore extend from the extremes of the lattice model to the kinetic model. There are two other main features to be considered in proposing a model for a liquid: first, whether the intermolecular forces are spherically symmetric, permitting a simple central force law to be used between molecules, and secondly, the problems raised by mixed solvents or ionic melts which contain several species interacting amongst themselves to varying degrees.

A theory which is based on a model making use of a central force law acting between hard-sphere molecules may be able to predict the experimental properties of a condensed noble gas such as liquid neon or liquid krypton, but it will not be adequate to represent a liquid of polyatomic molecules which are not spherical and have localized centers of attraction for neighbouring molecules. The choice of a model to represent a liquid, therefore, depends on the nature of the molecules constituting the liquid of interest and on the range of temperature and pressure which are to be studied. These considerations define the extent to which the intermolecular forces determine the properties of the system.

3 Structure in Electrolyte Solutions

Recently much emphasis has been placed on the important role which the properties of the solvent play in determining the thermodynamic behaviour of electrolyte solutions, transport properties, and reaction kinetics in solution. Water and aqueous solutions have naturally attracted the greatest attention because of their biological importance. Satisfactory explanations of ionic hydration (8), viscosity of aqueous electrolytes (9,10,11), mobility of ions in aqueous solution (12), and effects of the variation of the temperature and pressure on viscosity and electrical conductivity in aqueous solutions (13,14,15) have emphasized the importance of the short-range forces of the ions which perturb the bulk solvent structure in the immediate environment of the ion. The key to this approach to electrolyte solutions lies in an understanding of the structural properties of the solvent. Theories of the structure of liquid water are of such current interest that many excellent recently published reviews are available. Some of these are referred to

by Conway (16) in an extensive critical review of solvation and structural aspects of electrolyte solutions.

In this review attention is directed to some work concerned with liquid-water structure by Falk and Ford (17). The infrared spectrum of HDO at low concentrations in H_2O and D_2O was studied over a 130° range of temperature in order to avoid complications which occur in the spectrum of pure H_2O or D_2O. These difficulties make a simple interpretation of the spectrum of H_2O or D_2O in terms of either a mixture model or a continuum model extremely difficult. No absorption which could be attributed to non-hydrogen-bonded OH or OD groups was observed at even the highest temperature of 130°C. Since the vibrational spectrum detects species having a life-time as short as 10^{-13} seconds, the existence of free unbonded monomer water in the liquid, even at high temperatures, is in doubt. There is thought to exist a broad distribution of bond strengths extending from ice-like hydrogen bonds to the weak interactions between molecules in the vapour. The distribution shifts in the direction of lower bond strengths as the temperature is raised. Of great interest would be a similar study of the pressure dependence of the infrared absorption of HDO in solutions of H_2O and D_2O. The effect of pressure on the distribution of bond strengths could then be compared with the effect of temperature. The evidence reviewed by Conway (16) supports the view of Lennard-Jones and Pople (18) who considered that hydrogen bonds could exist even if they were 40° to 50° non-linear. Any model which postulates species to exist in liquid water on the basis of some proportion of hydrogen bonds being either completely broken or fully formed is, on the evidence above, bound to be rather arbitrary. The wide range of hydrogen

bonded to non-hydrogen bonded ratios estimated by various workers in different attempts to produce a structural model of liquid water, and collected by Falk and Ford (17), indicate the weakness of the mixture approach to this problem. Water can be represented by a model in which the strong four-fold chemical interaction of the water molecules produces a net-like structure extending throughout the whole volume of the liquid. However, the thermal energy of the molecules distorts the special regularity of the lattice to such an extent that regions of lower density and regions of higher density can have a fluctuating existence throughout the liquid. Variations in the external conditions of pressure and temperature and variations in the internal pressure by the addition of solute, will bring about a stabilization or a disruption of such a lattice. This close analogy between the model used to describe water and the model of ice I is not a common observation for liquids in general. X-ray and neutron diffraction studies (6,19) indicate that there is some degree of short-range order in liquids. However, it is the absence of the long-range order found in crystalline solids that is most characteristic of the liquid state. Evidence thought to indicate the non-existence of flickering clusters of ice-like water, which are discussed by Frank and Wen (20), has been found in the measurements of the light scattering of liquid water by Mysels (21). The turbidity is thought to be entirely a result of pressure fluctuations. A good example of the difference in the degree of order between liquids and solids has been discussed by Hildebrand (22). This is shown by the striking differences between the X-ray scattering due to the liquid and powdered forms of gallium under nearly identical conditions. For this reason the structural model of non-aqueous polar liquids should not be expected to resemble the

crystalline solid as much as the structural model of liquid water resembles ice.

The considerations above for water are not presented as an attempt to sum up the most acceptable and recent views as to the nature of the structure of liquid water. The extensive review of Kavanau (23) has indicated the complexity of this problem and the large number of conflicting interpretations to be found in the literature based on the same body of experimental evidence. The object of this short discussion of water structure has been rather to suggest the need for great caution when phenomena occurring in aqueous and non-aqueous solvents are to be compared. There is little justification for generalizing conclusions based on the results of experiments in aqueous media to non-aqueous media, because of the great structural differences between these two classes of solutions.

There is ample evidence that where strongly directional intermolecular forces are absent, and the molecules are compact and symmetrical, the liquid phase will have a structure of maximum randomness in terms of the radial distribution function (24). As stated by Hildebrand and Scott (24), for such liquids, "There is no quasi-crystalline or lattice structure; there are no 'holes' of definite size or shape, no discrete molecular frequencies or velocities, and no distinguishable 'gas-like' or 'solid-like' molecules". The characteristics of a polar liquid will result from a superposition on the behaviour observed for normal liquids, such as CCl_4, where the intermolecular forces are only London forces (dispersion forces), of the special behaviour due to the polar interactions. Liquid acetone is discussed in Appendix I for the conditions of temperature and pressure which were used in the experiments. Some aspects of acetone not discussed there will be developed below.

C Some Properties of Acetone

Electron diffraction studies by Allen, Bowen, Sutton, and Bastiansen (25) have indicated the following bond lengths in acetone: C=O, 1.22± 0.03 Å; C-C, 1.55±0.02 Å; and C....O, 2.40± 0.02 Å. From these bond lengths a C-C-O angle of 119.6± 3 °, that angle expected for sp^2 bonding, is calculated. Electrostatic interactions between the oxygen and the methyl groups must be compensated by a steric interaction between the methyl groups which leads to a nearly perfect trigonal plane structure for the molecule. These dimensions and the C-C-O angle are, within the tolerances listed, the same as those given by Zeidler (26). The molecular radius is given by Zeidler as 2.8 Å. This radius corresponds to that determined by Allen, Bowen, Sutton, and Bastiansen (25) for acetone in the gas phase.

An estimate of the shape of the acetone molecule has been made by Wilson (27) based on the bond lengths and the van der Waals radii given by Pauling (28). A sketch of this model is given in Figure 1.1 showing two views: (a) a direction perpendicular to the plane of the molecule, and (b) a direction lying in the plane of the molecule. The dipole moment which is shown in this sketch is seen to be buried in the center of the molecule. The shape is roughly spherical, but not so spherical that preferential orientation would be of no importance when the molecules were close-packed.

D X-ray Diffraction

There is in the literature only one X-ray diffraction study of liquid acetone. This work was published in 1949 and was done by Danilov, Zubko, and Danilova (29). The data from this X-ray experiment were presented in terms of the intensity of X-rays as a function of the

Figure 1.1. Sketch of the acetone molecule based on the van der Waals radii (a) perpendicular to the plane of the molecule
(b) in the plane of the molecule

(a)

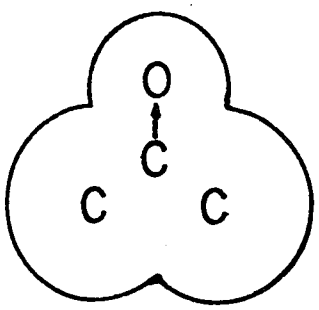

(b)

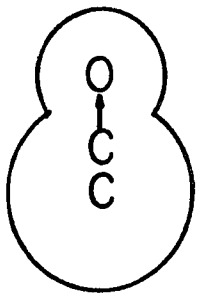

sine of half of the angle between the X-ray beam and the observed scattering in the Debye-Scherrer camera divided by the wave length of the X-rays, $\frac{\sin\theta/2}{\lambda}$. Scattering intensity as a function of $\frac{\sin\theta/2}{\lambda}$ was obtained for water and pure acetone as well as a mixture of 1 mole of acetone to 2.5 moles of water at $18.5 \pm 1.5^{\circ}C$. Although great care was taken to eliminate background scattering from both the sample container and air in the camera, and patterns were obtained using two different sources of monochromated X-rays, it is not possible to estimate the scattering intensity corresponding to a given value of $\frac{\sin\theta/2}{\lambda}$ to better than ± 5 % from the graphs given in the paper. To obtain structural information from such intensity curves it is highly desirable to convert them into the form of molecular distribution functions (19). Early studies of liquid paraffins, alcohols, and acids, however, were interpreted by Stewart (30) and many others by the use of Bragg's law and such a method, according to Kruh (19), does give a crude estimate of distances at which density maxima occur. The conversion of the intensity data to a radial distribution function was attempted, but the results indicated that the uncertainty in the primary intensity data would make a calculation of the number of nearest neighbours by integrating the distribution function over the peak corresponding to the average separation of first neighbours quite ambiguous. This result is perhaps to be expected in view of the conclusion of Kruh (19) that diffraction experiments can account well for intramolecular structure of molecules, but that the interpretation of intermolecular ordering in terms of unique structures from diffraction experiments is a form of "wishful analyzing". Recently, however, Harris and Clayton (31) have successfully analyzed the X-ray diffraction patterns of liquid CF_4 and obtained molecular distribution

functions at three temperatures. Making use of scattering data gathered over a wide range of $\frac{\sin\theta/2}{\lambda}$, and paying careful attention to possible errors in the treatment of the data, intermolecular interaction distances and the number of molecules associated with each distance were calculated at three temperatures. Tests were made to find the effect that taking different ranges of $\frac{\sin\theta/2}{\lambda}$ would have on the molecular distribution function. The shape of the molecular distribution function in the region of intermolecular distances was found to be largely a result of peaks in the intensity at small values of $\frac{\sin\theta/2}{\lambda}$. The acetone intensity function in Figure 1.2 taken from Danilov, Zubko, and Danilova (29), shows one main peak at $\frac{\sin\theta/2}{\lambda} = 0.13 \pm 0.01$ which is analogous to the peak at $\frac{\sin\theta/2}{\lambda} = 0.12 \pm 0.01$ found by Harvey (32) for liquid ethyl alcohol at -75°C and the peaks at $\frac{\sin\theta/2}{\lambda} = 0.13 \pm 0.01$ for liquid methyl alcohol at 25°C and -75°C found by Harvey (33). Radial distribution functions constructed by Harvey for methyl and ethyl alcohol give almost no structural information about the number of neighbouring molecules. The existence of peaks was established at a distance at which hydrogen bonding between neighbouring molecules is probable. The acetone intensity curve resembles the 25°C methanol intensity curve since it shows no indication of a peak between the main peak at $\frac{\sin\theta/2}{\lambda} = 0.115$ and 0.37. Liquid acetone and methanol at 25°C are both far removed from their freezing points (-98°C for methanol and -95.4°C for acetone). Both liquids would, therefore, be expected to show only a small degree of order relative to the order found in water at room temperature.

Figure 1.2. Experimental curve for liquid acetone at $18.5 \pm 1.5^{\circ}C$ X-ray scattering intensity against $\sin(\theta/2)/\lambda$ measured by Danilov, Zubko, and Danilova (29)

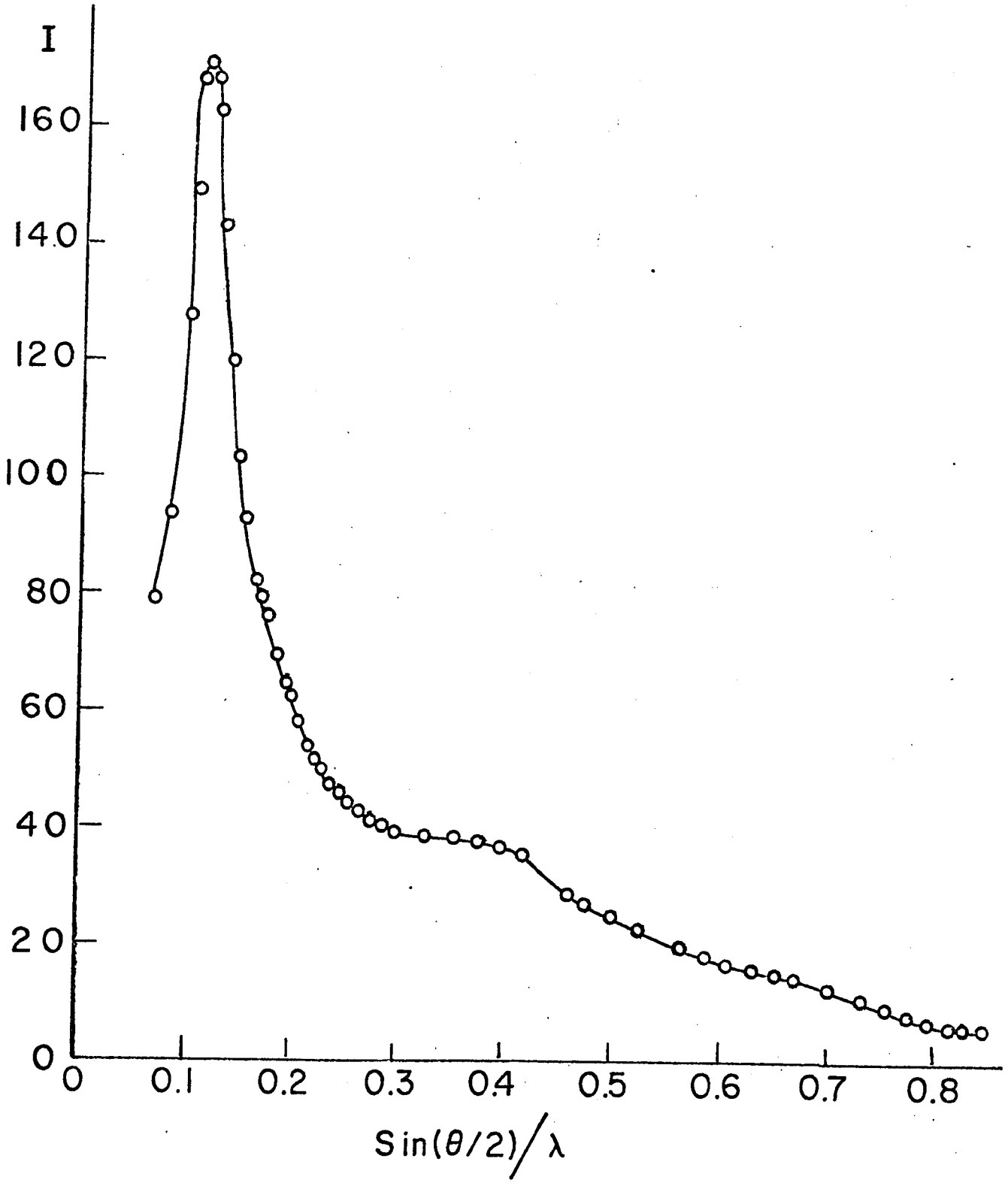
I
160
140
120
100
80
60
40
20
0
0
0.1
0.2
0.3
0.4
0.5
0.6
0.7
0.8
Sin(θ/2)/λ

E Effect of Pressure on Liquids

The sign and magnitude of the freezing temperature-pressure coefficient are strongly influenced by the degree of structure present in the liquid; the coefficients for several liquids are: water, -9.0 deg $kbar^{-1}$, ethyl alcohol, +9.8 deg $kbar^{-1}$, and carbon tetrachloride, +35.0 deg $kbar^{-1}$ (34). At atmospheric pressure, the freezing point of acetone is about -95°C. Pressure raises the freezing point of acetone by approximately 13.5 deg $kbar^{-1}$. Bridgman (35) found that acetone, unlike eleven other polar organic liquids studied, which were liquid between 20° and 80°C up to 12,000 kg cm^{-2}, froze at 20°C for a pressure of 8,000 kg cm^{-2}. Although the freezing curve was not studied carefully over a wide temperature range, at 40°C the freezing pressure was found to be about 10,000 kg cm^{-2}. Bridgman's results indicate that the compression of acetone produces an effect of about the same magnitude on its freezing point as that produced by the compression of liquids known to have a high degree of short-range order such as the alcohols. Detailed studies of the phase changes of water illustrate the complexity of behaviour found when there are strongly directional intermolecular forces present. There is little reason to believe that a theory of the thermodynamic behaviour of a dipolar aprotic solvent should be easier to develop than a theory which satisfactorily accounted for the complex behaviour of water. Variation of the isothermal compressibility, the isobaric expansivity, the internal energy, the heat capacities at constant pressure and volume, and other properties of dipolar aprotic solvents, show the most complex and irregular behaviour when measured as a function of density and temperature (35, 36).

3. Solvation

A General Introduction

The presence of an ion in a liquid brings about local changes in the medium by means of the electrostatic interaction of the ionic field with the solvent molecules, and by the disruption that the volume of the ion causes in the packing of the solvent molecules. The ionic mobility in solution at infinite dilution is intimately related to the extent of the interactions between the solvent and the ions. The degree of association of an electrolyte into ion pairs is determined to a large extent by the ion-solvent interactions, since the force acting between cations and anions is through the solvent close to the ions. At the surface of very large ions, the field is weak enough for the surrounding solvent to be satisfactorily considered to have the same properties as the bulk solvent, to a first approximation. Small singly-charged ions or multiply-charged ions interact strongly with the solvent to bind the nearest neighbouring solvent molecules into a spherical shell called by Bockris (37) the primary solvation shell. The solvent molecules not immediately next to the ion, but having their solvent properties somewhat modified by the presence of the electrostatic field of the ion, are considered to make up the secondary solvation shell.

The number of degrees of freedom of the molecules in the primary solvation shell which are restricted is not a constant for different ions (38, 39). Solvent molecules may be able to translate in two dimensions on the surface of some ions as well as exchanging with solvent molecules in the secondary solvation shell. In general, the nature of the interaction between cations and anions to the solvent molecules, even when the cation and the anion have the same radius,

differs because of the asymmetry of the solvent molecules.

The interaction energy between an ion and the different solvent molecules surrounding it varies considerably. The designation of the number of solvent molecules involved in total solvation or specifically in either primary or secondary solvation is, therefore, entirely dependent on the nature of the experiment used to measure the solvation number. The arbitrary nature of solvation numbers has been pointed out by Verrall (40), Nightingale (41), Samoilov (42), and others. To illustrate the ambiguous meaning of the quantitative estimates that have been made of hydration numbers, Verrall and Samoilov gathered together sets of ionic hydration numbers from different sources. These estimates varied widely. The effective assignment of a specific number of solvent molecules to an ion, such that the combined ion-solvent entity has a permanent existence in the solution, is considered by Samoilov (42) to represent a poor approximation to the real mechanism of ionic solvation. Solvation can be analyzed in terms of the effect the ion has on the free-energy barrier which solvent molecules must overcome to undergo motion between equilibrium positions in the liquid. In such an analysis, the molecules in the primary solvation shell are those molecules with the greatest perturbation of the free-energy barrier to motion, but no great distinction between solvent molecules next to the ion and those in the secondary solvation region is made. Solvent molecules with sufficient energy exchange with the neighbouring solvent molecules at a rate determined by the free-energy barrier. Samoilov (42) has introduced the concept of positive and negative solvation which involves the idea of solvent exchange. Positive solvation occurs when the solvent molecules exchange less rapidly in the neighbourhood of the ion than they do in the bulk solvent. Negative solvation results from an

enhanced rate of exchange of solvent molecules near the ion relative to the exchange rate in the bulk solvent.

Frank (43) has discussed the problem of selecting a model which corresponds sufficiently well to the "reality" of the physical system of ions in solution and yet is still amenable to mathematical treatment. The Born (44) equation utilizes only the size of the ion and the macroscopic dielectric constant of the medium to calculate the ionic free energy of solvation, ΔG_{si}.

$$\Delta G_{si} = \frac{-N (z_i e)^2}{2r_i} (1 - 1/\epsilon) \qquad (1.3)$$

where N is Avogadro's number

z_i is the number of charges on the ion

e is the electronic charge

r_i is the ionic radius in solution

ϵ is the dielectric constant of the solvent

This equation predicts the correct order of magnitude of the solvation free energy. It also emphasizes the electrostatic origin of the solvation free energy. The Born equation has been modified by Laidler and Pegis (45) to obtain better agreement with experiment by taking into account the fact that the dielectric constant is a function of the electrical field of the ion. The use of the Born equation or the modified Born equation to calculate thermodynamic properties of ionic solutions requires an integration from the surface of the ion to infinity. Desnoyers, Verrall, and Conway (46) have commented that the difficulty with this type of treatment is that the correct radius to be used in the integration is uncertain because the solvent is considered to be a continuum near the ion where the molecular nature of the solvent is of primary importance. The crystal ionic radius

is thought to lie closer than the gas-phase ionic radius to the ionic radius in solution (46). This conclusion is based on the view that ions in solution and in crystals are subject to about the same electrostatic pressure. Hamann (34) and Whalley (47) have considered variations of the ionic radius in solution brought about by the external pressure and the internal electrostatic pressure. For large compressible ions such as the tetraalkylammonium ions, the variation in the ionic radius, or in the size of the cavity containing the ion in the solution, is probably quite large when such ions are transfered from the gas phase to solution or when they are placed in an environment with a different internal pressure. These considerations indicate the difficulties experienced in choosing the most appropriate ionic radius in a treatment of ionic solvation by the continuum model.

The approach taken by Desnoyers, Verrall, and Conway (46) is to consider only the effect produced by the field of the ion on the solvent surrounding the ion. This treatment combines a continuous medium model, by which is calculated the effective compression of the solvent produced by different electric field strengths, with a molecular model of the solvent near the ion. The problems associated with estimating solvation numbers of ions have been alluded to, and these probably limit somewhat the usefulness of this type of calculation, for example in estimating the electrostriction volume.

Thermodynamic properties of infinitely dilute electrolytic solutions have also been calculated by means of statistical mechanics using molecular models by Bernal and Fowler (48) and others. These calculations have been reviewed by Conway and Bockris (49) and by Golden and Gutbezahn (50). In general they give results in good agreement with experiment. However, the experimental heats and entropies of solution obtained must be converted to an individual ionic basis before

comparison with theory. This uncertainty tends to obscure the significance found in the good agreement between these theories and experiment.

B Individual Ionic Solvation

The Born model, for ions of a given size, predicts no variation in the calculated thermodynamic properties of solvation with the sign of the charge on the ion. Conway, Verrall, and Desnoyers (39) have discussed the work of Verwey (51) and the more recent work of Vaslow (52) in which a non-radial distribution of solvent dipoles at cations and anions is postulated. There is expected to be a significant difference between the thermodynamic parameters of solvation of cations and anions. In hydrogen-bonding solvents anions are solvated by ion-dipole interactions upon which is superimposed a strong hydrogen-bonding which is strongest for small anions. However, in dipolar aprotic solvents, such as dimethylsulphoxide, N,N-dimethylformamide (D.M.F.), and acetone, anions are solvated by ion-dipole interactions upon which is superimposed only an interaction due to the mutual polarizability of the anion and the solvent molecules which is greatest for the large anions. The solubility of KCl is greater in methanol than in D.M.F. even though they have about the same dielectric constant, while KI with a larger more polarizable anion, is more soluble in D.M.F. than in methanol (53). Parker (54) has illustrated how the differences in these two classes of anionic solvation can be used to explain the effects of solvent on rates of reaction, on conductance, on spectra of anions, and other phenomena involving anions. Cation solvation is extensive in those solvents having a negative charge localized on a bare oxygen atom, for example in acetone or dimethyl sulphoxide. Parker (54) reports that lithium salts form solvates with acetone and dimethyl sulphoxide and that the solutions formed are very viscous. The

solvation of cations is presumed to occur in dipolar aprotic solvents by electron-donor interactions of the solvent with the cation. The lack of anion solvation in these solvents is indicated by the limiting equivalent conductivity data gathered by Parker; these show that anions of the same crystallographic size as cations are much more conducting in acetone or D.M.F. than these same anions are, relative to cations having the same crystallographic radius, in methanol or water. The change of solvent from water to acetone has been found by Winstein, Savedoff, Smith, Stevens, and Gall (55) to cause a reversal in the degree of nucleophilicity of the halides from $I^- > Br^- > Cl^-$ to $Cl^- > Br^- > I^-$ in the SN2 reactions of lithium halides with alkyl halides. This observation was made on the basis of rate constants corrected for the extent of ion-pair formation in the lithium halide.

C Ionic Solvation in Acetone

As was mentioned above, the boiling point and freezing point of acetone at atmospheric pressure are 56.2° and -95.4°C respectively. The temperature for acetone which corresponds to 25°C, or room temperature, for water is about -53°C. The effect of ions in causing a disruption of the structure in acetone at 25°C will be a minimum since little structure is present at this temperature because of the thermal motion of the molecules. However, the ability of external pressure to bring about a change in volume of the solvent is at a maximum under these circumstances since the solvent is most compressible near its boiling point. Therefore, although ions have a net structure-making effect in acetone at atmospheric pressure, for the reason outlined above, at high pressures the ions must compete with enhanced dipole-dipole interactions between the solvent molecules, and the structure-making ability of the ions is reduced.

The thermodynamics of solutions of $NaClO_4$ in acetone have been compared with the analogous aqueous solutions by Mishchenko and Sokolov (56). The integral heat of solution of $NaClO_4$ in acetone, ΔH_m, as well as the pressure of the saturated acetone vapour above the solutions, were measured at 25°C. From these data, the relative partial molal enthalpy of the solvent, $\bar{L}_1$, and the non-ideal portion of the relative partial molal entropy, $(\bar{S}_1 - \bar{S}_1^\circ)_{ni}$, were calculated using the equations (57,58,59)

$$\bar{L}_1 = \frac{m^{3/2}}{2 \times 17.22} \left(\frac{d(\Delta H_m^\circ)}{d m^2}\right) \qquad (1.4)$$

and $$(\bar{S}_1 - \bar{S}_1^\circ)_{ni} = (\bar{L}_1 - RT \ln(a_1/N_1))/T \qquad (1.5)$$

where m is the molality of the solution

ΔH_m° is the standard integral heat of dissolution

R is the gas constant

T is the temperature in °K

a_1 is the activity of acetone refered to pure acetone as the standard state

N_1 is the mole fraction of solvent in the solution

It is shown that $\bar{L}_1$ is negative in these solutions; that is, the processes of solution are exothermic. In aqueous solutions, the values of $\bar{L}_1$ are smaller and positive, that is, solution is an endothermic process. Further, in the concentration range of 0 to about 4.5 molal, $d\bar{L}_1/dm = -370$ cal mole^{-2} in acetone, while in water $d\bar{L}_1/dm = +11$ cal mole^{-2}. The absolute value of the derivative is some thirty times greater in acetone than in water. The function $(\bar{S}_1 - \bar{S}_1^\circ)_{ni}$ is a measure of the change in the regularity of the solvent on the addition of one mole of the solvent to an infinitely large quantity of solution of a given concentration. In the same concentration range

the addition of $NaClO_4$ to water results in a calculated value of $(\bar{S}_1-\bar{S}_1^o)_{mi}$ which becomes increasingly positive with concentration, while in acetone the function $(\bar{S}_1-\bar{S}_1^o)_{mi}$ becomes increasingly negative with concentration, having values an order of magnitude greater than the corresponding aqueous values ($(\bar{S}_1-\bar{S}_1^o)_{mi}$ = -3.0 e.u. at m = 4 molal). The added $NaClO_4$ results in a marked increase in the ordering of the solvent molecules in the acetone solutions and a slight net disordering in the aqueous solutions. This is the expected result since in acetone at 25°C the solvent is highly disordered compared to water at this temperature.

The results discussed above are compared with new data, including the temperature dependence of the heat of dissolution of NaI and $NaClO_4$ in acetone and NaI in methanol, by Mishchenko and Sokolov (60). It was found that the exothermicity of the integral heat of solution decreases in the order $Mg(ClO_4)_2$>NaI>$NaClO_4$>NaCNS>KCNS>NH_4CNS, suggesting that the heat of solvation is primarily a property of the cations. This agrees with the postulated low interaction between anions and dipolar aprotic solvents. The integral heat of solution becomes more negative with decreasing concentration for all of the salts investigated. This is ascribed to the solvation of ions released from the more neutral ion paired state. Mishchenko and Sokolov have calculated the degree of dissociation from ebullioscopic and conductimetric measurements for NaI in acetone. The concentration region 0.1 to 0.3 molal, where a very rapid decrease in ΔH_m occurs, was found to be the same concentration region where the degree of dissociation increases markedly with a further decrease in concentration. A rough calculation of the heat of dissociation of ion pairs in NaI acetone solution indicates that this

quantity is about -3.0 kcal mole^{-1}. In aqueous medium an increase in concentration causes the opposite behaviour in ΔH_m, i.e. the exothermicity increases. In acetone the desolvation of the ions caused by ion-pair formation as the concentration of salt is increased evidently predominates over the effect of closer approach. It was found that at 10°, 25°, and 40°C, the ΔH_m against molality curves were parallel. The temperature coefficient of ΔH_m was found to be about +45 cal deg^{-1}mole^{-1} in acetone (in methanol $(d\Delta H_m/dT)_P < 0$), whereas in this temperature region in water the same parameter is about -35 cal deg^{-1} mole^{-1}. The temperature coefficient of ΔH_m is given in terms of the molar heat capacities by the equation

$$\left(\frac{d\Delta H_m}{dT}\right)_P = C_P(\text{solution}) - (C_P(\text{salt}) + N_1 C_P(\text{solvent})) \qquad (1.5)$$

where C_P is the heat capacity as indicated for a 1 mole solution of salt

N_1 is the number of moles of solvent

Since the coefficient in equation (1.5) is positive in acetone, the heat capacity of the solution is greater than $C_P(\text{salt}) + N_1 C_P(\text{solvent})$ and the structure of the solution is, therefore, enhanced by the ions. In aqueous solutions the same coefficient is generally negative. This is understood to indicate the breakdown of solvent structure. The second derivative $(d^2\Delta H_m/dT^2)_P$ is positive in aqueous solutions, which also emphasizes the importance of the solvent structure in solvation. The thermal degradation of solvent structure is greatest at high temperatures, and this causes the increase with temperature in the exothermicity to become more positive. This result supports the view that the behavior of water toward ions near its boiling point is closer to the behaviour of acetone toward ions near room temperature, as expected from structural considerations.

There is strong evidence to support the view that Na^+ ions in acetone are solvated by four acetone molecules. Below 25.5-25.7°C, NaI is known to separate from the saturated solution as $NaI.3CH_3COCH_3$ (61). Nishchenko and Sokolov (60) have determined the heat of formation of this solvate from NaI and acetone at 10°C to be -15.67±0.01 kcal $mole^{-1}$. From steric considerations, the solvation number of Na^+ ion is four and of the ClO_4^- ion is eight. Nishchenko and Sokolov (56) have estimated that $NaClO_4$ solutions should undergo rapid change in the thermodynamic properties of solution, based on these solvation numbers, at a molality of about 1.44, for which complete solvation would be expected. The evidence for a break in the $\bar{L}_1$ and $(\bar{S}_1-\bar{S}_1^o)_{ni}$ functions near a concentration of 1.44 molal is not conclusive. The $\bar{L}_1$ function does become rapidly more negative between 1 and 2 molal for $NaClO_4$ solutions, but the $(\bar{S}_1-\bar{S}_1^o)_{ni}$ function decreases with concentration smoothly with no sign of a break at 1.44 molal.

From these solubility studies it can be concluded that anions are not greatly solvated in dipolar aprotic solvents such as acetone. Cations, on the other hand, interact quite strongly with such solvents. The evidence suggests that small cations such as Na^+ favour four coordination in acetone solution. The effect of ions on the solvent structure of acetone at atmospheric pressure between 10° and the boiling point is to increase the amount of order. This has been shown by the behaviour of the relative partial molal enthalpy of acetone and the relative partial molal entropy of acetone in the solutions of several salts. The importance of these conclusions in the interpretation of transport behaviour of ions and ion-pair formation in acetone will be discussed below in connection with the results of the present work.

CHAPTER 2

EXPERIMENTAL

1. Materials

A Acetone

The acetone was obtained commercially as either Fisher Electronic Grade or G.C. Spectrophotometric Quality 'Baker Analyzed' Reagent Grade. Fisher acetone was used for the work with Me_4NI and Et_4NI, while Baker acetone was used for the n-Pr_4NI work. As is discussed in Appendix I with respect to compressibility and specific volume, water is the most serious impurity found in acetone, and is most difficult to remove. Although both grades of acetone were claimed by the manufacturers to contain no significant impurities other than water, according to Thirion and Craven (62) a commonly found contaminant is isopropyl ether. Using a cloud-point method suggested in this paper, the isopropyl ether content of the Fisher acetone was estimated to be less than 0.005% by weight. The Baker acetone was not tested, but the accompanying certificate of analysis indicated that the only significant impurity was water, present at 0.02% by weight. Removal of the small traces of water was accomplished by batch drying in stoppered flasks with Linde 4 Å Molecular Sieves, in the form of 1/16 inch pellets, as described by Meeker, Critchfield, and Bishop (63). These workers showed that treated by this method, acetone initially containing 0.45% by weight water, in 2.5 hours contained 0.007% water, and after 21 hours, 0.001% water. After using this procedure, which was carried out in a dry nitrogen atmosphere inside a polyethylene glove bag available

commercially from the I&R Company, Cheltenham, Pa., U.S.A. the acetone was distilled slowly through a packed column and the middle fraction collected and stored under dry nitrogen. The acetone was treated in a dry nitrogen-filled glove bag as were all the operations carried out in the preparation of solutions and the filling of conductivity cells.

The removal of trace quantities of water was verified by two independent methods. Immediately prior to making up the solutions, the purified acetone was combined into one lot and a sample tested for its specific conductance in a specially designed conductance cell with large platinum electrodes. The results indicated a significant reduction in the specific conductance after the treatment with molecular sieves. This observation confirmed that the water content was reduced, based on conductance studies of potassium iodide solutions using various grades of acetone which were done by Dippy and Hughes (64). The Fisher Electronic Grade acetone as purchased had a specific conductance of $5.9 \times 10^{-7} \Omega^{-1} cm^{-1}$; after treatment just before it was used the specific conductances were as follows: for the Me_4NI solutions, $2.08 \times 10^{-8} \Omega^{-1} cm^{-1}$, for the Et_4NI solutions, $2.85 \times 10^{-8} \Omega^{-1} cm^{-1}$. The Baker acetone, with an initial specific conductance of $8.00 \times 10^{-6} \Omega^{-1} cm^{-1}$, did not have as low an initial value as did the Fisher acetone. After purification, just before the $n\text{-}Pr_4NI$ solutions were prepared, the specific conductance was $9.64 \times 10^{-8} \Omega^{-1} cm^{-1}$.

The second check for trace water was a series of nuclear magnetic resonance (n.m.r.) spectra which were run on samples of the Fisher acetone taken at different stages in the purification process.

It has been reported by Muller (65) that in dilute solutions of water in acetone the chemical shift of water is -2.8 p.p.m. from T.M.S. A possible contamination of the sieve-dried acetone by diacetone alcohol was suggested by Muller to account for the appearance of a peak at 0.9 p.p.m. from acetone and a peak at about -0.5 p.p.m. from acetone. The positions of these peaks were verified by spectra, obtained on acetone doped with diacetone alcohol, in which it is proposed that the 0.9 p.p.m. peak is a methyl peak and the -0.5 p.p.m. peak a CH_2 peak. Muller also observed that the largest impurity peak height was less than 1/3 the peak height of the C^{13} satellites of acetone. The peak observed at -2.8 p.p.m. is therefore ascribed to water. This peak was reduced in height relative to the C^{13} satellite peak heights from 0.87, for the untreated acetone, to 0.23 for the treated. Since the naturally occuring abundance of C^{13} is 1.11% (66), this indicates approximately .06% water by weight in the treated acetone. This value agrees well with the 0.001% water by weight found in acetone sieve-dried for 21 hours by Meeker, Critchfield, and Bishop (63). The percentage water by weight in the acetone was estimated as follows:

$$\text{weight \% water in acetone} \leq 1.11/2 \times (0.23/2)/(1.00/3) \times 18/58$$

$$\leq .06$$

The bracketed numbers 2 and 3 take into account the number of protons in water and acetone respectively which contribute to the absorption; 18 and 58 are the molecular weights of water and acetone, 1.11 is divided by 2 because there are two C^{13} peaks, and the other numbers are explained above. Contamination from diacetone alcohol, as suggested by Muller, was

investigated by examining an n.m.r. spectrum taken on the undistilled sieve-dried acetone. The peak thought to be due to the methyl group, at 0.9 p.p.m. from acetone, was barely detectable from the background in the distilled sieve-dried acetone, but could be seen in the treated but undistilled acetone. The peak at -0.5 p.p.m. from acetone, thought to be due to CH_2, appeared close to the water peak and was slightly smaller than the water peak in both spectra. This trace amount of diacetone alcohol was not thought to be significant for this work.

Other physical properties of the acetone that were measured are reported in Appendix I.

B Water

The water used to prepare the potassium chloride solutions required for determining the cell constants of the conductivity cells, was the same as that used in the compressibility experiments described in Appendix I.

C Tetra-n-alkylammonium Iodides

The tetramethylammonium iodide (Me_4NI) and the tetra-n-propylammonium iodide ($n\text{-}Pr_4NI$) were Eastman Reagent Grado chemicals; the tetraethylammonium iodide (Et_4NI) was obtained from the Columbia Organic Chemicals Co., Inc. All the salts were dried for 24 hours or more *in vacuo* at 60 to 100°C just before the solutions were prepared. The salts were shielded from direct light as much as possible to prevent decomposition. As well as determining the melting points of these compounds, which are shown in Table 2.1 compared to literature values, it was thought advisable to determine the purity by another method.

Table 2.1 Melting Points of Tetra-n-alkylammonium Iodides

Salt	Melting Point (°C)	
	This work	Literature value Reference
Me_4NI	380±10	greater than 230 (67)
Et_4NI	303±1	decomposition 300 (68)
n-Pr_4NI	277±1	decomposition 280 (69)

Using the Volhard method for iodide according to Kolthoff and Sandell (70), the percentage iodide relative to the theoretical amount of iodide expected in the sample was found to be: for n-Pr_4NI, 99.6±0.4, 99.3±0.3, and 99.1±0.6; for Me_4NI, 99.9±0.2. The Et_4NI was not tested for percentage iodide. These results indicated that the salts were sufficiently pure and they were used without further treatment.

D Potassium Chloride

Reagent-grade potassium chloride was dried *in vacuo* at 110°C for 24 hours and then used to make up aqueous solutions for the determination of cell constants without further treatment.

2. Apparatus

A Conductivity Bridge

An RC-18 conductivity bridge manufactured by Industrial Instruments Inc., Cedar Grove, N.J., U.S.A. was used to measure the conductance of the solutions. The resistance in ohms or the electrolytic conductance in micromhos was read directly from six decade dials. The bridge was based on an A.C. Wheatstone-bridge measuring circuit with a Wagner ground balance connection and had a two-inch oscilloscope

which was used as a balance detector. Capacitive balance was achieved by means of built-in variable capacitors and for high conductance cell capacity, a capacity decade box was added externally across the cell. The limit of error for this instrument was stated by the manufacturer to be 0.1% of the decade resistance reading over the range 500-50,000 ohms. Two frequencies, nominally 1000 and 3000 c.p.s. were supplied by the generator in the bridge. Since the conductivity was found to be frequency dependent, it was necessary to check these frequencies against a reliable frequency meter. A Frequency Meter and Discriminator Type 1142-A, manufactured by the General Radio Co., indicated that the 1000 c.p.s. position gave 1046.5 c.p.s. and the 3000 c.p.s. position gave 2890.0 c.p.s.

B Conductivity Cells

High-Pressure Conductivity Cells

Ten cells were constructed according to a design of Hills (71), shown in Fig. 2.1. Pressure distortion of the cell and resultant changes in the cell constant are avoided by a ring and rod arrangement of the electrodes. This type of cell was tested by Ovenden (72) and found to have a cell constant independent of pressure over a range of 2000 atmospheres. Durable, metal-to-glass seals were produced by electrowelding tungsten leads to the platinum electrodes and sealing the joint in the glass. Advantage was thereby taken of the strong mechanical properties of the glass to tungsten joint while the solution was only in contact with platinum. Only one cell out of the ten, made in this fashion, developed a leak

Figure 2.1. High-pressure conductivity cell.

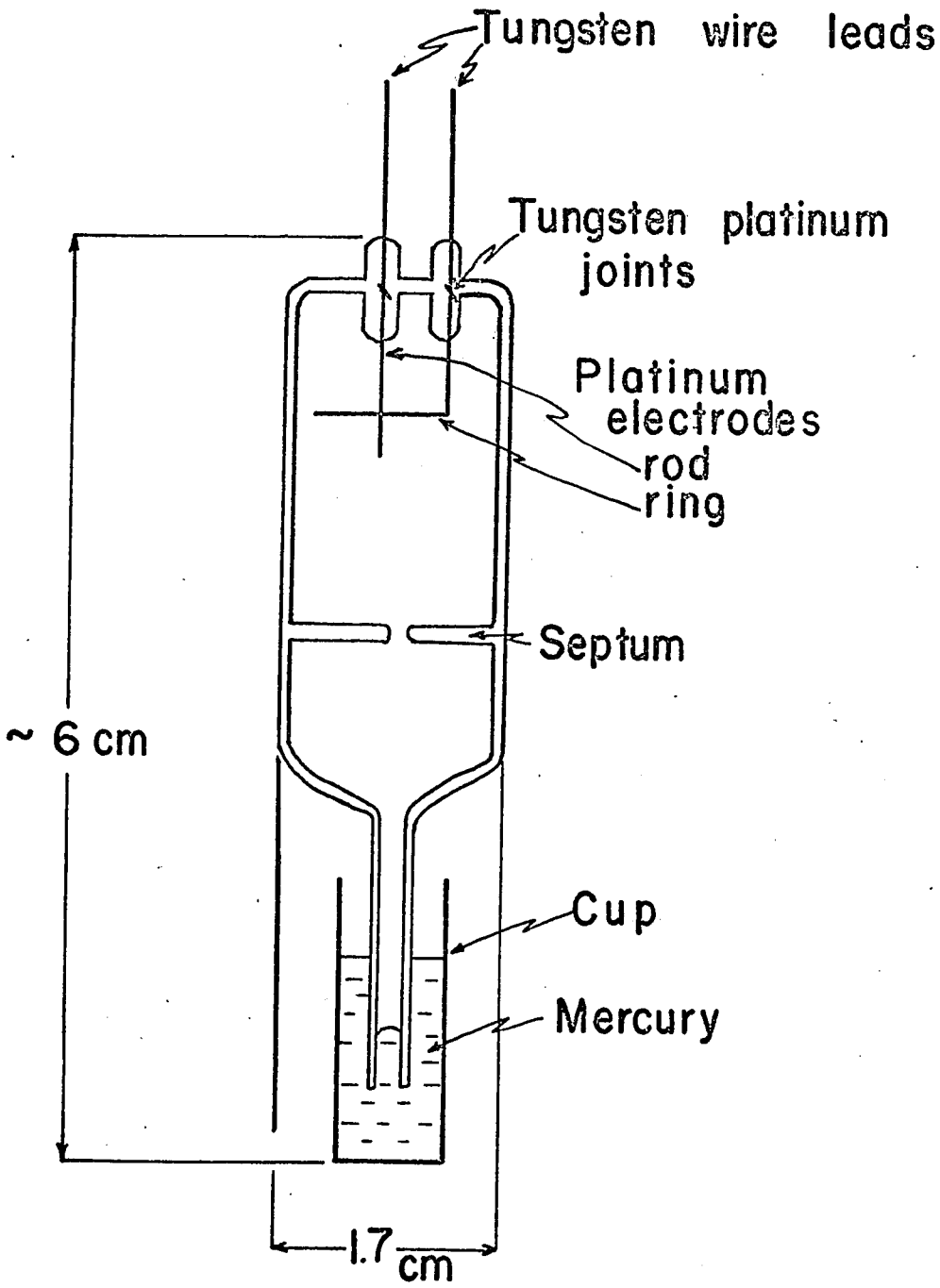
Tungsten wire leads
Tungsten platinum joints
Platinum electrodes
rod
ring
Septum
~ 6 cm
Cup
Mercury
1.7 cm

at this type of seal in over one year's use. A pierced glass septum was built into each cell as shown in Fig. 2.1, to isolate the portion of solution surrounding the electrodes from movement of the pressure-transmitting mercury piston. The cell constant was therefore independent of the position of the mercury piston in the cell stem.

Atmospheric-Pressure Conductivity Cells

Three Shedlovsky-type cells designed for dilute solutions were constructed as shown in Fig. 2.2 from 50 ml Erlenmeyer flasks. (73). The solution between the electrodes could be removed and replaced by tilting the cell back and forth. When this was done, no evidence for a "shaking effect", such as that found by Prue and Sherrington (74), was encountered. This was probably because the electrodes were not platinized and adsorption of ions on the electrodes was therefore minimized. A double seal was used to prevent loss of acetone from evaporation at high temperatures. The outer joint, shown in Fig. 2.2, was greased and the cap held in position by two springs. In this way, a pressure of dry nitrogen slightly greater than one atmosphere was kept over the inner ungreased stopper. The cells were filled almost completely with solution to avoid having to make a concentration correction for the acetone vapour in the dead space of the cell.

Solvent Conductivity Cell

This cell was constructed as shown in Fig. 2.3 from a one-liter flask and was fitted with a thermometer. Large electrodes were placed close together to obtain a small cell constant, so that an accurate solvent correction could be made. As in the two cells described above, the electrodes were not platinized. Photographs of the

Figure 2.2. Atmospheric-pressure conductivity cell.

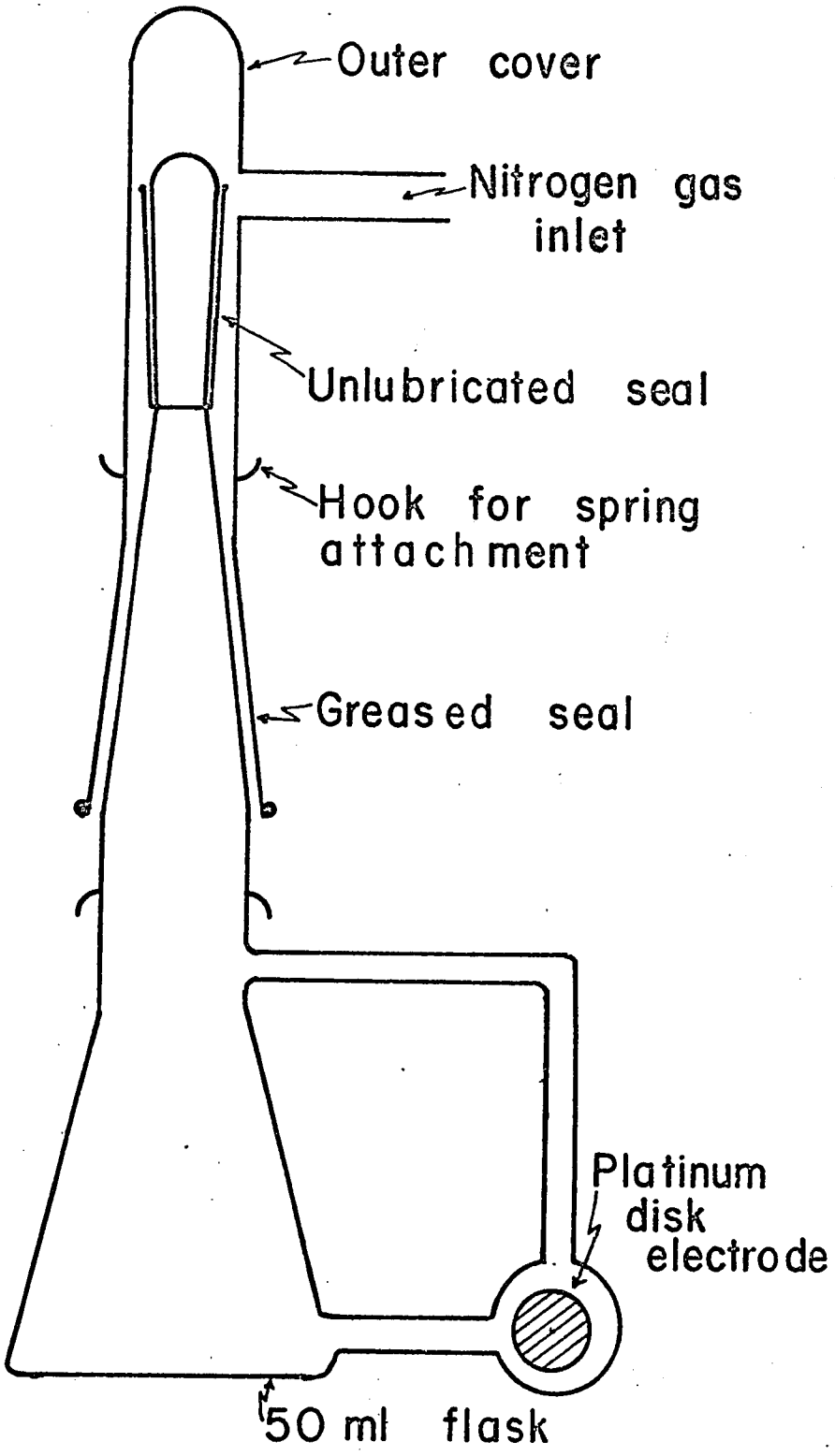
Outer cover
Nitrogen gas inlet
Unlubricated seal
Hook for spring attachment
Greased seal
Platinum disk electrode
50 ml flask

(Side view)

Figure 2.3. Solvent conductivity cell.

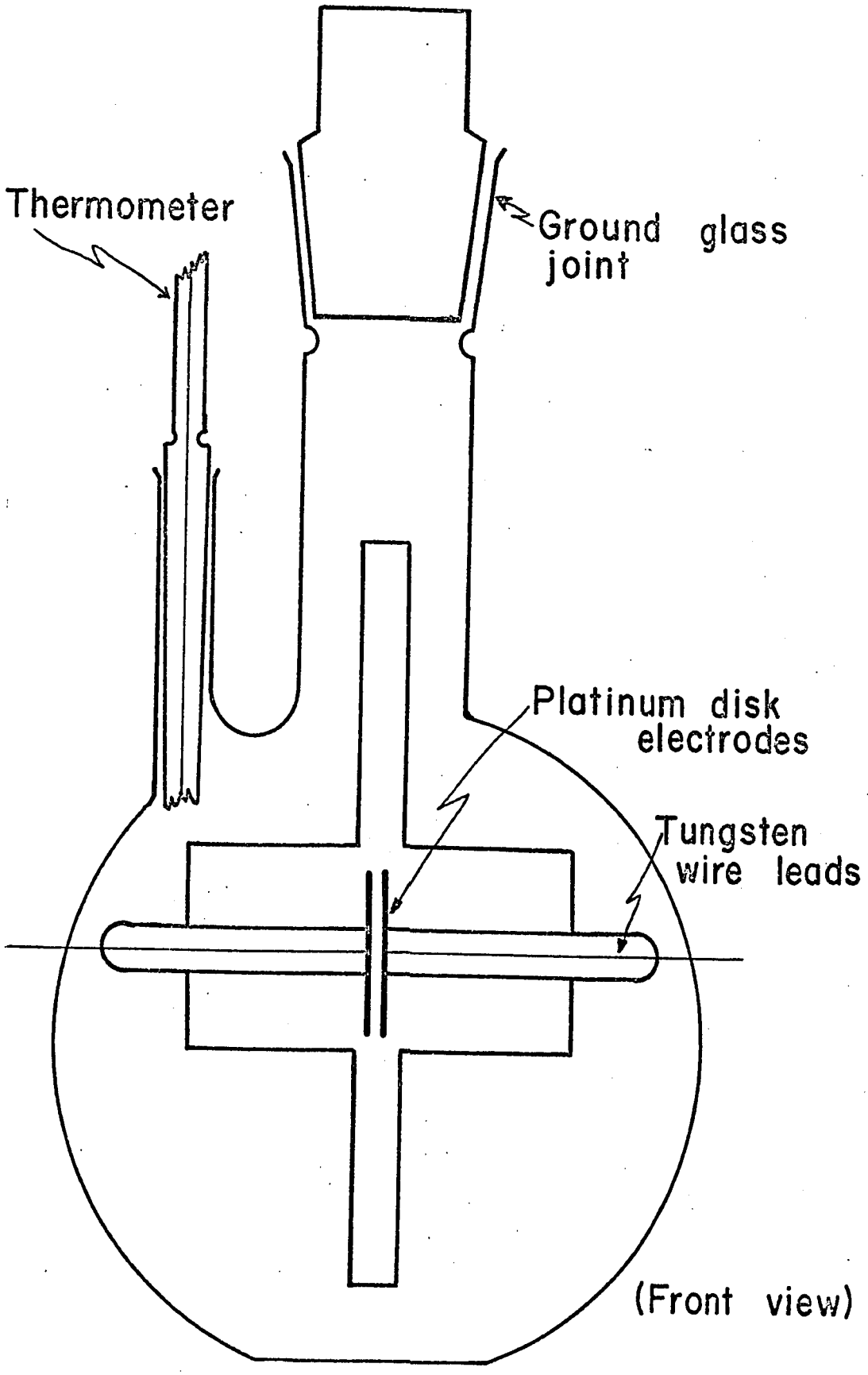
Thermometer
Ground glass joint
Platinum disk electrodes
Tungsten wire leads
(Front view)

conductivity cells are shown in Fig. 2.4.

C Thermostat

A 35-gallon container constructed from a 45 gallon drum was placed in a wooden box and insulated around the outside with vermiculite to reduce heat transfer. A light oil, DICL-N35, obtained from the Imperial Oil Company Ltd., was used to fill the container as a thermostatting fluid. The temperature was controlled by an intermittent heating coil turned off and on by a mercury micro-set thermoregulator, with a range of 50 to 220°F and a sensitivity of ± 0.01°C, combined with an electronic relay, both of which were manufactured by the Precision Scientific Co., Chicago, Ill., U.S.A. A second heating unit whose input could be adjusted by means of a variac, and a cooling coil of copper tubing through which cold tap water was circulated, were used to obtain the optimum heating cycle at each temperature. Two heavy duty induction motors were used to circulate the oil rapidly and smoothly by means of propellers. The top of the thermostat was covered by plexiglass to minimize heat losses at the surface of the oil.

The temperature of the thermostat was measured with two thermometers at each temperature. The four calibrated Beckmann thermometers are described in Appendix I. One of the two mercury-in-glass total immersion thermometers, manufactured by the Brooklyn Thermometer Co., Springfield Gardens, N.Y., U.S.A., was used with the appropriate Beckmann thermometer at each temperature. The calibration of these thermometers was carried out by the Division of Applied Physics,

Figure 2.4. Photographs of the conductivity cells:

(a) high-pressure conductivity cell,

(b) atmospheric conductivity cell, and

(c) solvent conductivity cell.

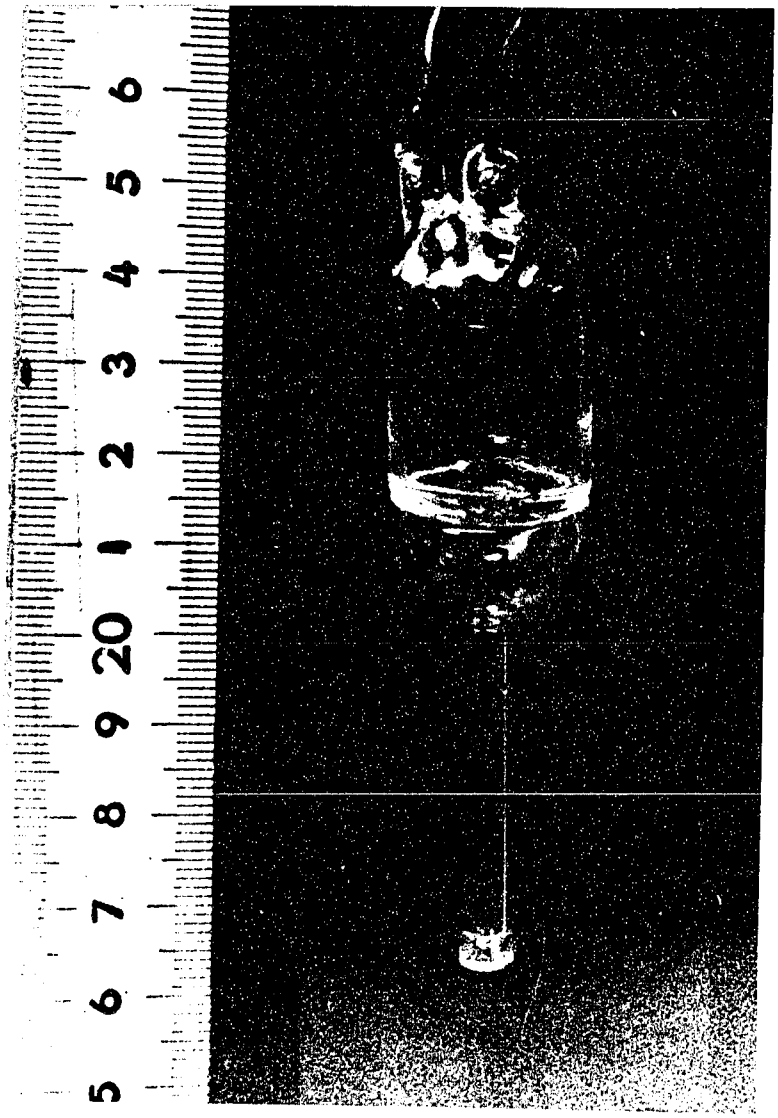

(a)

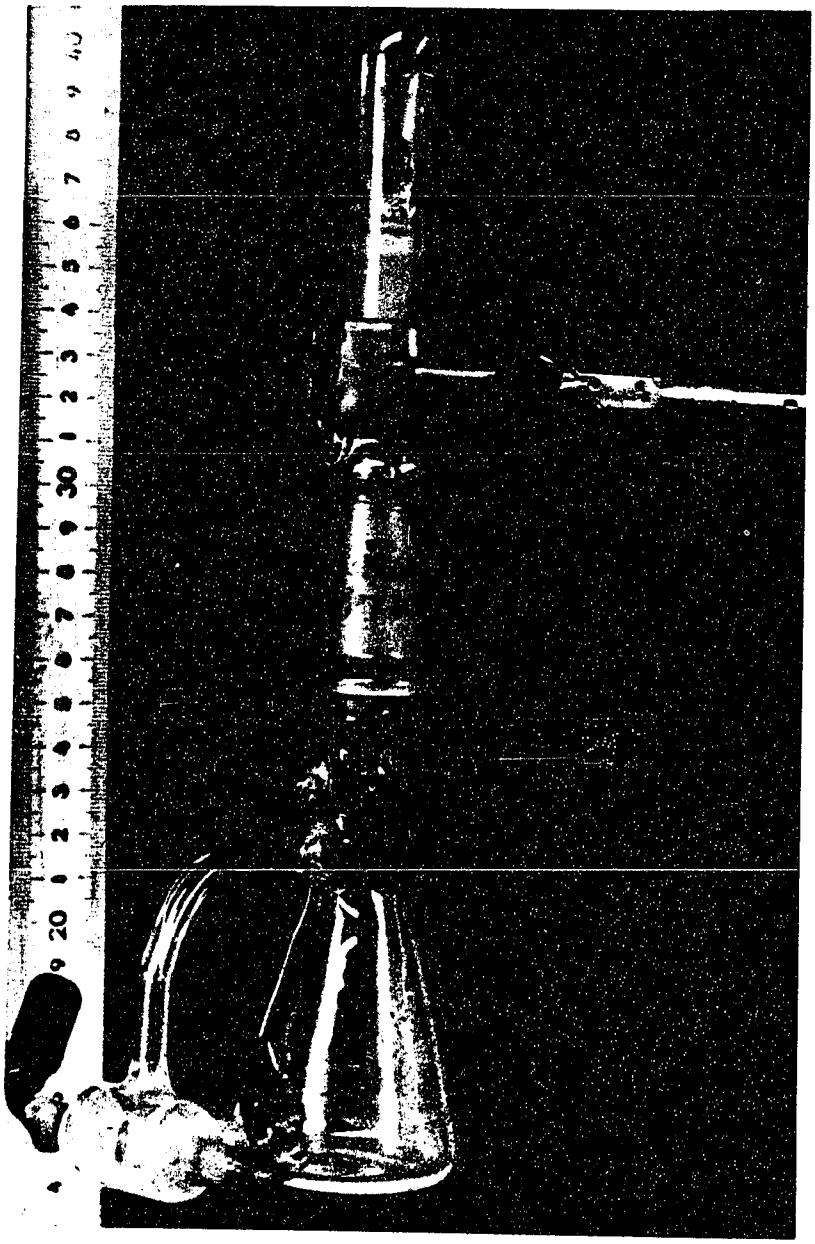

(b)

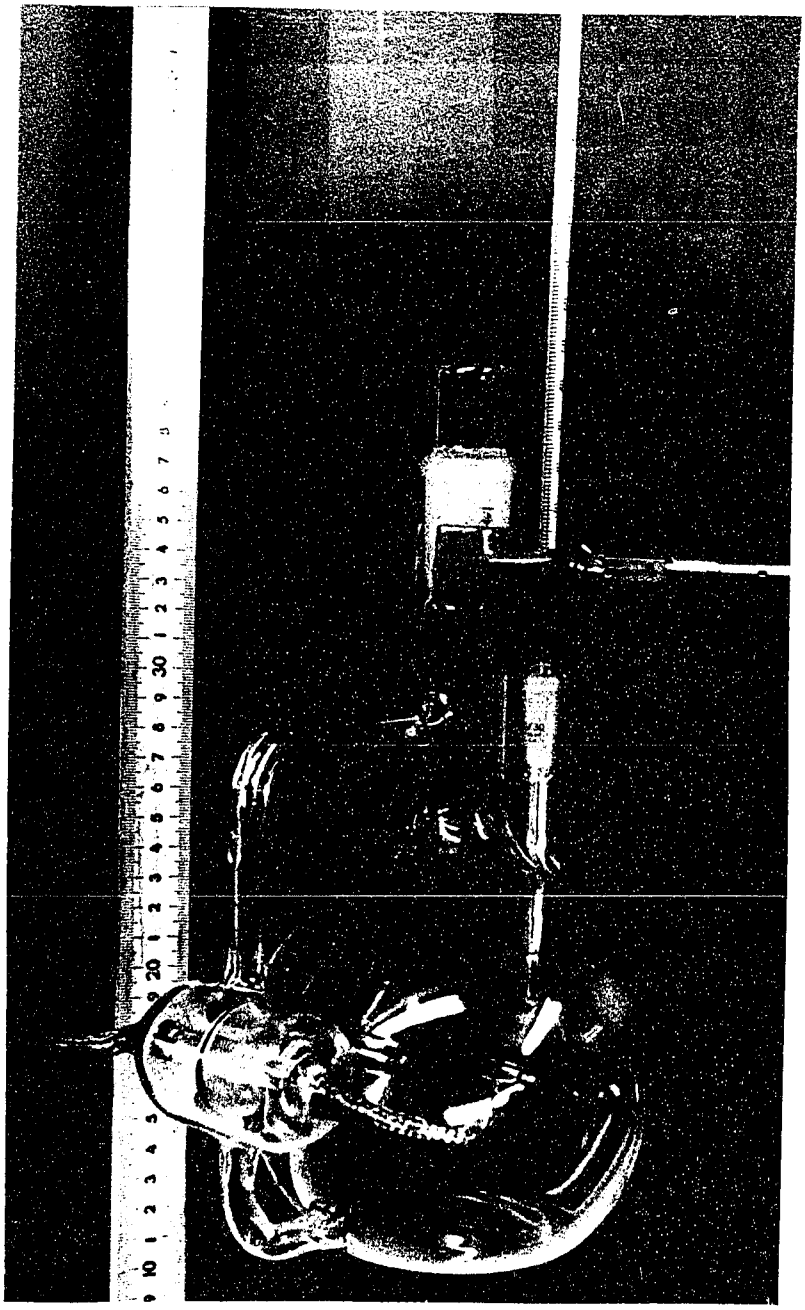

(c)

National Research Council, Ottawa, N.R.C. Report No. APH 1341 and 1341/1. These thermometers had an accuracy of ±0.005°C. One was calibrated at 25 and 35°C and the other at 45 and 55°C. The temperature in the thermostat was constant to ±0.01°C and variations throughout the thermostat were less than ±0.01°C.

A bead-type thermister of about 25,000 ohms resistance at room temperature was placed against the inside of the top of the high pressure vessel and cemented into position with epoxy resin glue. This thermister was used as a probe in situ to determine when the temperature had stabilized after compression or decompression of the system. The thermister was able to withstand the pressure, although it may have been protected somewhat by the coating of epoxy resin glue.

D High-Pressure System

A diagram of the high-pressure system is shown in Fig. 2.5. A photograph of the high-pressure equipment installed in the thermostat also showing the conductivity bridge appears in Fig. 2.6. The more important components are described below. The high-pressure valves, tubing, and other fittings were obtained from one or other of the two manufacturers of high-pressure equipment in Erie, Pennsylvania, listed below.

High-Pressure Vessel

A two-liter capacity vessel, number OM-2000, manufactured by Autoclave Engineers, Inc., Erie, Pa., U.S.A., was modified by this company to accept two electrical leads. The method by which the leads were introduced into the vessel was to seal, with a ceramic material,

Figure 2.5. Diagram of the high-pressure system.

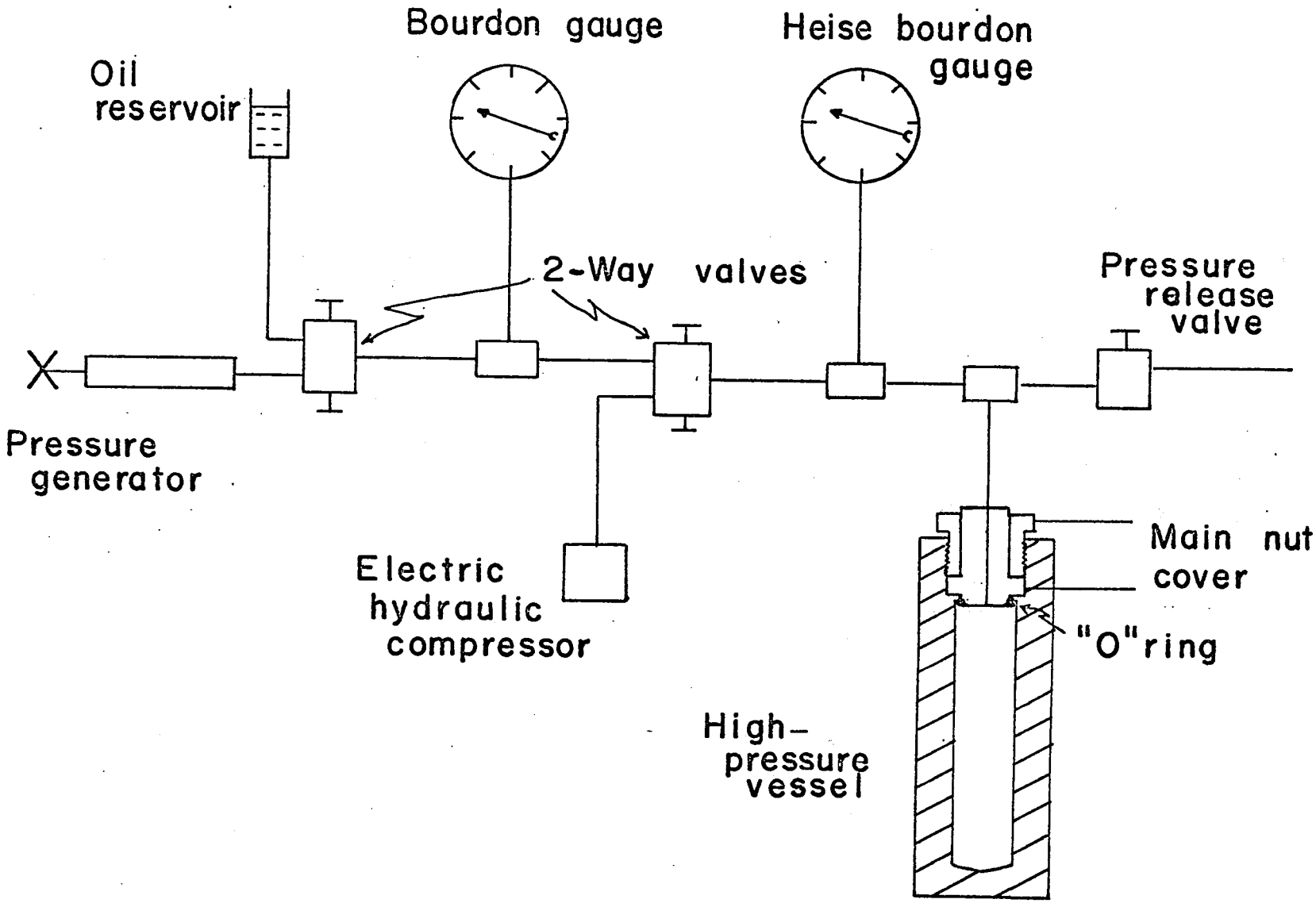
Bourdon gauge
Heise bourdon gauge
Oil reservoir
2-Way valves
Pressure release valve
Pressure generator
Electric hydraulic compressor
Main nut cover
"O" ring
High-pressure vessel

Figure 2.6. Photograph of the apparatus.

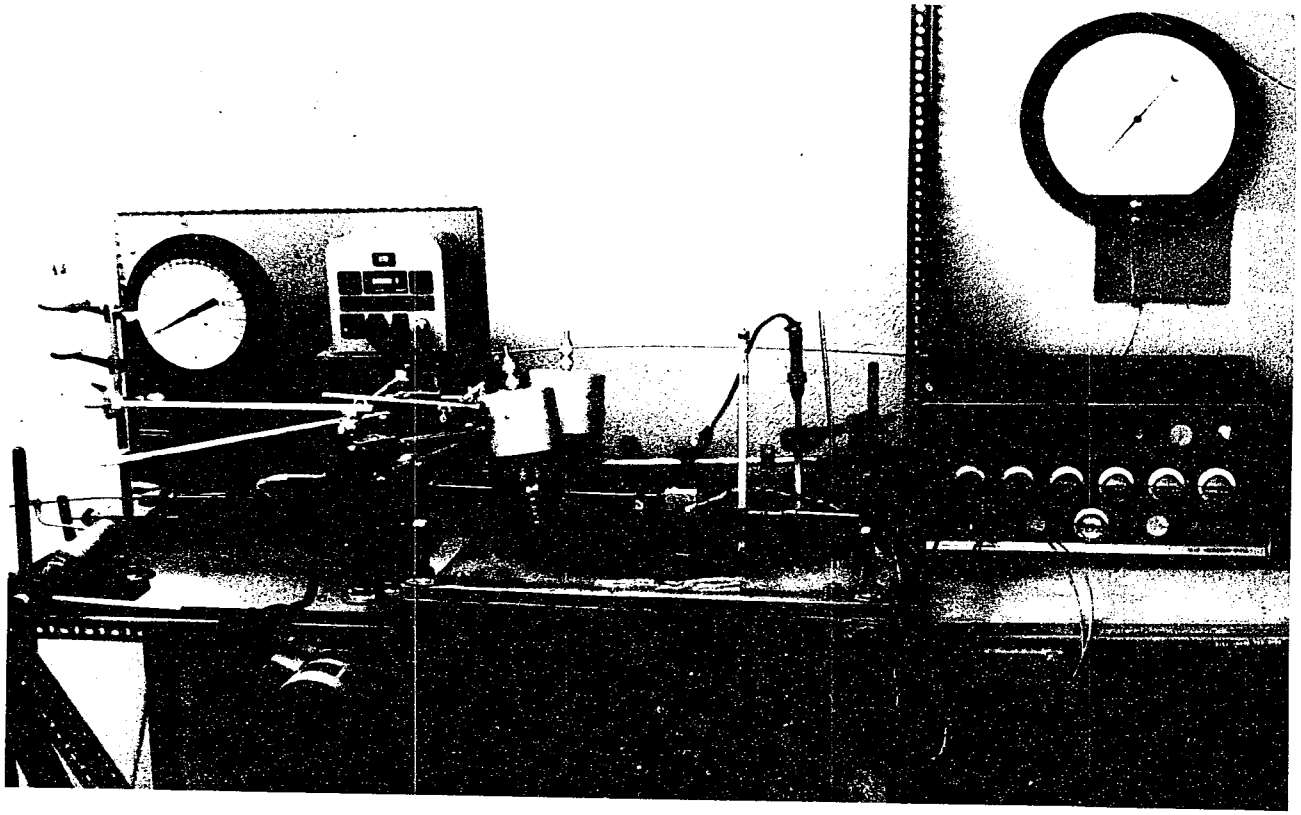

0.030-inch kovar wire into a thin conical nickel sleeve. This sleeve was then force-fitted into a 3/32-inch hole in the vessel top which had been coned to fit the nickel sleeve on the inside. The vessel was constructed from 410 stainless steel and was equipped with an "O" ring closure. The working pressure of the vessel was 30,000 p.s.i. at 250°F.

One of the electrical leads described above was removed and in its place a ten-wire lead was installed into the vessel. Varnished copper wire, of small enough diameter that ten wires could fit through the 3/32-inch hole, was worked carefully back and forth in the hole, while "Duro" epoxy resin glue, manufactured by the Woodhill Chemical Corporation, Cleveland, Ohio, U.S.A., was run into the hole and coated on the wires. When it was certain that no air pockets remained in the hole, plugs were placed at each end to prevent the glue from running out, and the leads were arranged so as not to be in contact with each other or the top of the vessel. When the glue had hardened the arrangement was tested successfully to 30,000 p.s.i. at room temperature with no leak and no change in the ten electrical connections into the vessel. The wires on the inside and outside of the top were connected to nine-pin octyl sockets. On the inside of the vessel, the socket was connected to a nine-pin base on the high pressure conductivity cell holder into which eight of the cells could be clipped and held in place by springs, as shown in Fig. 2.7. On the outside of the vessel, the socket was connected to a nine-pin base, which took the leads through a shielded cable to a PA 1001

Figure 2.7. High-pressure conductivity cell holder.

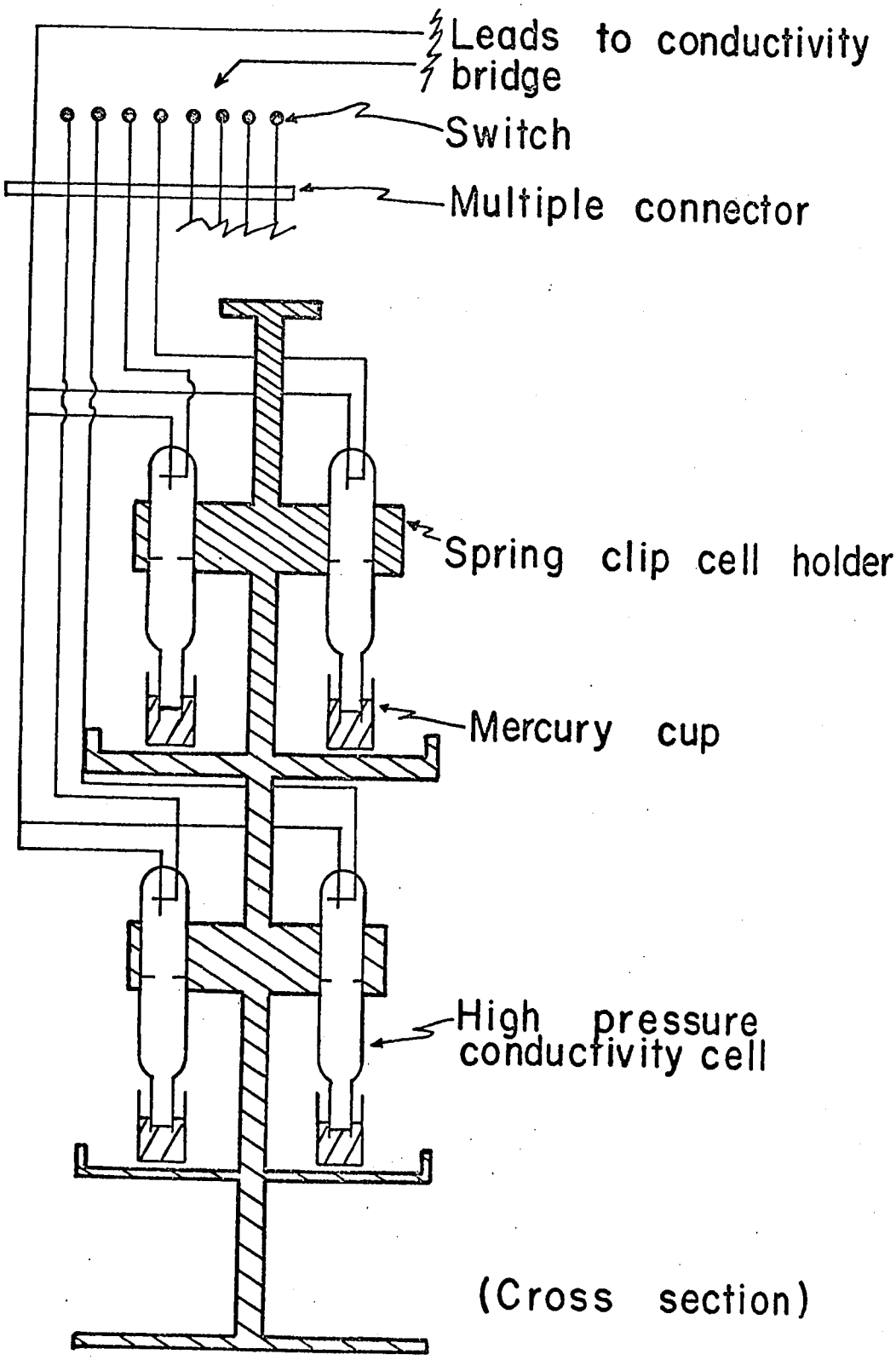
Leads to conductivity bridge
Switch
Multiple connector
Spring clip cell holder
Mercury cup
High pressure conductivity cell
(Cross section)

Centre Lab rotary switch. From this switch a coaxial cable led to the conductivity bridge. A common ground was used for all of the conductivity cell connections in the vessel, which itself was a ground for one of the leads going from the rotary switch to the conductivity bridge. The two extra leads into the vessel, to make up a total of eleven, were used to connect the thermister to the rotary switch and from there to the bridge.

High-Pressure Gauges

A twelve inch, 0-30,000 p.s.i. bourdon tube gauge was obtained from the Heise Bourdon Tube Co., Inc., Newton, Conn., U.S.A. The gauge was calibrated by the manufacturer and found to be accurate within 0.1% of the full scale reading. A second bourdon gauge was used to check the calibration of the above described gauge as outlined in Appendix I.

A smaller bourdon gauge, the Marsh Gauge No. 100, was obtained from the Steam and Industrial Equipment Ltd., Quebec, P.Q. This gauge was used as an indicator when reducing or augmenting the pressure with the hand pressure generator. In this way, a rapid change in pressure was avoided when the valve separating the pressure vessel, the hand pressure generator, and the oil reservoir was opened.

Compressors

The hand pressure generator was a $5\frac{1}{2}$ ml capacity unit obtained from the High Pressure Equipment Co., Erie, Pa., U.S.A. The design of this generator was the same as that described in Appendix I in connection with the compressibility measurements.

Pressure could be raised quickly by means of an electrically driven, hydraulic compressor, No. 46-2245, manufactured by the American Instrument Co., Silver Spring, Maryland, U.S.A.

The pressure transmitting medium was Duo Seal Pump Oil obtained from the Welch Scientific Co., Skokie, Ill., U.S.A.

3. Procedure

A Preparation of Solutions

Acetone Solutions

The dried salt was weighed on a balance enclosed in a dry-nitrogen-filled polyethylene glove bag and carefully placed in a preweighed 500 ml volumetric flask. Care was taken to carry out this operation in subdued light. Flasks of solution were kept covered with aluminum foil. These precautions were necessary to prevent decomposition of the salt which was detected by a slight yellowing if the salt or solutions of the salt were exposed to strong light. After eight portions of salt were weighed into the flasks, these were filled in another nitrogen-filled glove bag, with the dried acetone whose conductivity had just been measured in the solvent conductivity cell. The flasks were then stoppered and a polyethylene sheet wrapped around the top and held in place by an elastic band to preclude evaporation of acetone or contamination of the solution by atmospheric moisture. The flasks were then weighed to the nearest 0.1 g and the vacuum-corrected mass of the solutions calculated. The molar concentration of the solutions at different temperatures and pressures was calculated on the basis that the density of the solutions was the same as that of

pure acetone given in Table 2.2. The flasks in which the solutions were prepared contained teflon-coated magnetic stirring bars so that the salts, which were hard to dissolve, especially Me_4NI, could be stirred with magnetic stirrers. To ensure full solution of each salt, the eight prepared solutions were stored overnight, while being stirred, in a refrigerator at 10°C.

Potassium Chloride Solutions

These solutions were made up by weight and the molar concentrations calculated as for the acetone solutions.

B Cleaning the Conductivity Cells and Flasks

Flasks

Volumetric flasks were treated with warm cleaning solution, and then rinsed with tap water, distilled water, double distilled water, and finally spectrograde acetone. They were then dried with compressed dry nitrogen, stoppered, and stored in a glove bag until used.

Conductivity Cells

The cells were filled with nitric acid and placed in a beaker of boiling water. After this treatment they were rinsed with distilled water. Water was squirted into the narrow stems of the high-pressure cells from a polyethylene wash bottle. The polyethylene bottles used in the filling and rinsing of the high-pressure cells were seasoned by being stored several months while containing double-distilled water which was changed periodically. To ensure the complete rinsing of the high-pressure cells, a device was constructed in which distilled water

Table 2.2

Specific Volume of Acetone

($ml\ g^{-1}$)

Pressure (bar)	Temperature (°C) 26.61	35.00	45.01	54.83
1.0	1.2778	1.2938	1.3137	1.3341
137.9	1.2577	1.2726	1.2899	1.3078
275.8	1.2405	1.2546	1.2699	1.2861
413.7	1.2254	1.2389	1.2528	1.2677
551.6	1.2120	1.2250	1.2378	1.2516
689.5	1.2000	1.2125	1.2244	1.2375
827.4	1.1890	1.2018	1.2124	1.2248
965.3	1.1790	1.1910	1.2014	1.2133
1103.2	1.1698	1.1815	1.1914	1.2028

could be circulated continuously through the cells. The cells were rinsed overnight before being used for conductivity measurements. After this rinsing, the cells were subjected to the same procedure as was used to prepare the flasks.

C Filling Procedure

The clean high-pressure cells were placed in a glove bag. The eight solutions prepared the previous day were taken from the refrigerator and placed in the glove bag for transfer to the cells, one at a time. A small seasoned polyethylene bottle, one of eight, was then filled with solution and the appropriate cell was filled through the stem with that solution. The filled cell was then inverted stem down into a small cup of triple-distilled mercury, and the complete unit then carefully clipped into the cell holder. When all eight high pressure cells were filled and clipped into the holder, the cell holder containing the cells was placed into the high-pressure vessel, the electrical socket connections made through the top of the vessel, and the retaining ring screwed down.

Enough solution was prepared so that fresh solution could be used to fill the atmospheric cells at each of the four temperatures at which measurements were made. These cells were also filled in a dry-nitrogen atmosphere in a glove bag. Three solutions could be equilibrated at the same time in atmospheric pressure cells in the thermostat while being maintained under nitrogen pressure.

D Measurement Procedure

Frequency Dependence of Resistance

As suggested by Jones and Bollinger (75), where there is a danger that platinum-blacked electrodes might catalyze an undesirable reaction in the solution, or if dilute solutions are being studied, it is better to use untreated platinum electrodes for conductivity measurements. However, when smooth platinum electrodes are used to measure the A.C. resistance of solutions, it has been found by Jones and Christian (76), that the resistance decreases with increasing frequency due to the frequency dependence of electrode processes. The true ohmic resistance of electrolytes is independent of the frequency at audio frequencies, because the Debye-Falkenhagen effect (77), associated with ionic atmosphere relaxation, occurs to a significant extent only at radio frequencies (78). An extrapolation to infinite frequency of the measured resistance of the electrolyte-filled conductivity cell, against the appropriate function of frequency in the audio frequency range, should allow the extraction of the true electrolyte resistance, R_t. In acidic aqueous solutions, Jones and Christian (76) found that their results for bright platinum electrodes could be expressed by the equation

$$R_t = R_f + kf^{-\frac{1}{2}} \qquad (2.1)$$

where R_t is the true electrolyte resistance, independent of f

R_f is the resistance of the cell at frequency f

f is the frequency and k is a constant

In a study of the electrodeposition of copper at solid electrodes, Bockris and Conway (79) have found linear plots when the resistance

for the electrode reaction was taken to be an inverse-square-root function of the frequency. As suggested by Robinson and Stokes (78) however, such a frequency dependence as is given by equation (2.1) is not always found. For example, it has been shown by Nanney and Gilkerson (80), that the dispersion of conductivity of tetra-n-butyl-ammonium picrate solutions in benzene and substituted benzene mixtures of low dielectric constant, is not a simple function of frequency, but probably reflects ion-pair relaxation effects.

Experiments were undertaken using a wide-range oscillator which was calibrated with the frequency meter described earlier in connection with the conductivity bridge. A Wheatstone bridge, utilizing a General Radio frequency-discriminating null detector, was used to measure the resistance of the high-pressure and the atmospheric-pressure cells over a range of frequencies. Temperature was controlled at $25.0 \pm 0.1^{\circ}C$ by immersing the cells in an oil thermostat. For both type of cells, the most linear plots of measured resistance, R_f, as a function of frequency, over the range of 0.7 to 10 kilocycles per second, were obtained using the inverse-square-root function as in equation (2.1) above. When one of the high-pressure cells was lightly platinized, the frequency dependence of the measured resistance was greatly reduced. With aqueous potassium chloride solutions it was found that the extrapolated resistance, using equation (2.1) with results from the unplatinized cell, gave very close to the same conductance as that from the platinized cell. The frequency dependence of the

resistance of acetone solutions was of the same order as that of the aqueous potassium chloride solutions, approximately 1% of the measured resistances. A small frequency correction was therefore applied using equation (2.1) and the measured resistances at the two frequencies supplied by the conductivity bridge. The resistances listed in Appendix II are those measured for both frequencies at all the conditions of temperature and pressure studied for each set of concentrations for the different salts.

Cell Constants

The conductivity cells were calibrated according to a procedure suggested by Lind, Zwolenik, and Fuoss (81). These workers derived the conductivity equation which was thought to best represent the data for aqueous potassium chloride up to about 0.01 molar at 25°C. Each conductivity cell was cleaned, filled, and the cell resistance measured at 25.00°C. Using the specific conductance of the solution calculated from the equation in the above reference, and the measured cell resistance, the cell constant was obtained by multiplication. This procedure was repeated until the average deviation from the mean for three or more separate determinations was found to be less than 0.2-0.3%. The cell constants were assumed to be independent of pressure and temperature. The results of these measurements are shown in Table 2.3 along with the average deviation from the mean associated with each cell constant.

Table 2.3

Conductivity Cell Constants (cm^{-1})

Solvent Cell		0.01992(0.00003)
Atmospheric-Pressure Cells	1.	0.2935(0.0001)
	2.	0.2772(0.0004)
	3.	0.2267(0.0004)
High-Pressure Cells	1.	0.2998(0.0001)
	2.	0.2830(0.0003)
	3.	0.3165(0.0001)
	4.	0.3110(0.0009)
	5.	0.3170(0.0002)
	6.	0.3354(0.0002)
	7.	0.3018(0.0003)
	8.	0.3154(0.0003)

High-Pressure Conductivity Measurements

The cells were filled with solution, clipped into the cell holder, and this unit connected to the bridge after it had been fitted into the high-pressure vessel; resistance measurements of the set of cells and the thermister were then made until no variation with time was found. This condition indicated that the solutions were at the same temperature as the thermostat. After assembly and testing as described above, six cells were functioning correctly and continued to function throughout the four days required to complete a pressure study of conductivity at four temperatures for each experiment reported.

The measurements proceeded from the work at 25.61°C to the work at 54.83°C on the fourth day with nine pressures being studied at each temperature. It required approximately one hour to allow the temperature to return to a constant value after the solution was compressed by 2000 p.s.i. This rate of temperature change was noted by measuring the resistance of the solutions at both frequencies, in order of decreasing concentration, and repeating this set of measurements until satisfactory agreement was found between successive sets of measurements. The atmospheric-pressure resistances were redetermined at several temperatures after compression at a given temperature, to ensure that the resistances measured were reproducible and that it was safe to assume that no contamination of the solutions had occurred. The temperature was then raised for the next set of readings the following day. Some of these repeat determinations are shown in brackets in the

tables of Appendix II where all of the resistance measurements are given for the solutions studied.

Atmospheric-Pressure Conductivity Measurements

The atmospheric-pressure cells were filled and clamped in the thermostat beginning with the most concentrated solution and working through the three cells in rotation to the least concentrated solution. These cells were left in the thermostat for approximately one hour until they reached constant temperature, at which time the resistance at both frequencies was measured. When the resistance of a cell was recorded, another cell was put into the thermostat to equilibrate while the first cell was rinsed several times with electronic-grade acetone, dried with nitrogen and filled with the next solution.

CHAPTER 3

RESULTS AND CALCULATIONS

1. Equivalent Conductivity

A small frequency correction was applied to the resistance measured at each pressure and temperature, by assuming, as has been discussed above, that the resistance measured at two frequencies could be extrapolated according to equation (2.1). The specific conductance was then calculated by multiplying the inverse of the corrected resistance by the appropriate cell constant according to the equation

$$K_{sp} = R_t^{-1} \times \text{cell constant} \qquad (3.1)$$

A correction for solvent conductance was then applied by subtracting the specific conductance of the solvent from the values of K_{sp} obtained as described above. The concentrations of salt, in moles per liter, were then used with the corresponding $(K_{sp})_{corrected}$ to obtain the equivalent or molar conductivities according to the equation.

$$\Lambda = (K_{sp})_{corrected} \times 10^3 / (\text{concentration}) \qquad (3.2)$$

All of equivalent conductivities are not recorded explicitly, but can easily be calculated from the resistances given in Appendix II and the cell constants in Table 2.2. In Table 3.1 are shown the equivalent conductivities calculated for Et_4NI from the atmospheric cells and the high-pressure cells at 26.61°C, as well as the results at 965.3 bar pressure. To show the nature of the calculations in detail, the example above will be used throughout this chapter as an illustration. The solvent correction was small enough that it was not thought necessary to vary the correction term at different temperatures or pressures.

Table 3.1

Equivalent Conductivity of Et_4NI

Cells	Temperature (°C)	Pressure (bar)	Concentration (mole l^{-1})x10^4	Equivalent Conductivity ($cm^2\Omega^{-1}$ $mole^{-1}$)
atmospheric	26.61	1.0	11.25	166.5
			9.729	169.3
			8.770	171.2
			6.589	177.1
			5.746	178.7
			3.341	186.6
			3.292	186.1
			1.068	196.4
	45.01		10.94	190.8
			9.463	193.6
			8.531	195.8
			6.409	204.5
			5.589	205.4
			3.250	217.4
			3.202	215.2
			1.039	228.2
high pressure	26.61		11.25	163.4
			9.729	167.5
			8.770	167.8
			3.341	185.9
			3.292	185.5
			1.068	198.0

Table 3.1 (cont.)

Equivalent Conductivity of Et_4NI

Cells	Temperature (°C)	Pressure (bar)	Concentration (mole l^{-1})x10^4	Equivalent Conductivity ($cm^2\Omega^{-1}mole^{-1}$)
high pressure	45.01	1.0	10.94	188.5
			9.463	192.8
			8.531	193.6
			3.250	214.6
			3.202	218.0
			1.039	230.7
	26.61	965.3	12.19	112.7
			10.54	115.0
			9.505	114.8
			3.621	124.1
			3.567	123.9
			1.158	130.6
	45.01		11.97	130.8
			10.35	132.7
			9.328	133.3
			3.554	144.3
			3.501	144.4
			1.136	153.7

2. Dielectric Constant of Acetone

The dielectric constants for the four temperatures at atmospheric pressure were calculated from an equation given by Maryott and Smith (82):

$$\log_{10} \epsilon(T) = \log_{10} 20.70 - 0.205\ (T-25.00) \qquad (3.3)$$

This equation was satisfactory for the 26.61° and 35.00°C temperatures as given; however at 45.01° and 54.85°C the calculated dielectric constants were modified by a small negative correction term based on the experimental value measured by Grimm and Patrick (83), of 17.70 at 56.2°C, and that obtained from equation (3.3) of 17.87. This correction term is shown in the equation

$$\epsilon(T) = \epsilon(T)_{\text{equation (3.3)}} - 0.17\ (T-40.00)/16.2 \qquad (3.4)$$

The values of the dielectric constant (d.e.c.) estimated at atmospheric pressure are shown in Table 3.2.

There are two experimental investigations reported in the literature on the effect of pressure on the d.e.c. of liquid acetone. One of these investigators was Kyropoulos (84), whose measurements up to 3000 kg cm^{-2} at 500 kg cm^{-2} intervals at 20°C, were fitted by Owen and Brinkley (85) to an equation of the form of the Tait equation. The results fitted this equation quite well, the average deviation between the calculated and experimental d.e.c. being 0.08%, while the maximum deviation of the same was 0.19%. The temperature dependence of the d.e.c. as a function of pressure has recently been investigated by Hartmann, Neumann, and Rinck (86) who have reported new d.e.c. data at 20, 35, and 50°C at twelve pressures between atmospheric pressure

Table 3.2

Dielectric Constant of Acetone

Pressure (bar)	Temperature (°C) 26.61	35.00	45.01	54.83
1.0	20.54	19.75	18.78	17.82
137.9	20.96	20.17	19.26	18.33
275.8	21.33	20.54	19.65	18.72
413.7	21.65	20.87	20.00	19.08
551.6	21.94	21.17	20.30	19.39
689.5	22.21	21.44	20.58	19.66
827.4	22.47	21.70	20.84	19.92
965.3	22.70	21.93	21.09	20.16
1103.2	22.92	22.15	21.31	20.38

and 1800 atmospheres. It was thought that more consistent results would be obtained if the data of Kyropoulos were not used to obtain d.e.c. data at the conditions of interest. The approach taken is one of several which were reported on by Hartmann, Neumann, and Rinck in attempts to find a suitable empirical formula to represent the experimental d.e.c. data. The temperature-dependent constant B(T), from the Tait-equation fit of the compressibility data given in Appendix I, was used to fit experimental d.e.c. data over a range of pressure, to obtain a varying value of the other 'constant' A which appears in the equation

$$\frac{1}{\epsilon(P^0)} - \frac{1}{\epsilon(P)} = A \log_{10} \frac{B(T) + P}{B(T) + P^0} \qquad (3.5)$$

The A values were plotted first against pressure to obtain the values of A at the pressures of interest. These A were then plotted against temperature and a set of 36 values of A obtained, each number corresponding to a condition of interest. Combined with the d.e.c. data previously calculated for atmospheric pressure, the Tait constants B(T) from the compressibility data were used with the set of A values, to calculate the dielectric constants of acetone shown in Table 3.2 by means of equation (3.5). As a test of this empirical method, the d.e.c. was calculated from the direct fit of the experimental data to the Tait equation at 689.5 bar pressure and 35.0°C and compared with the d.e.c. calculated as outlined above. The results agreed to 0.05%.

3. Viscosity of Acetone

At one atmosphere pressure, the best viscosity data for acetone over the range of room temperature to the boiling point are those obtained by Howard and McAllister (87). The viscosities at the four temperatures and atmospheric pressure given in Table 3.3 were interpolated from a graphical treatment of these.

The only measurements reported on the effect of pressure on the viscosity of liquid acetone are those of Bridgman (88). These experiments were carried out at 30° and 75°C and Bridgman reports in the paper the ratio of the viscosity observed at pressures up to 12,000 atmospheres to the atmospheric-pressure viscosity at 30°C. Unfortunately in the pressure region of interest, values of the ratio are only given for 500, 1000, 2000, and 4000 atmospheres. As a consequence of this, it was necessary to find an equation which was known to reproduce accurately the pressure and temperature dependence of the viscosity of pure liquids. An equation which has often been applied to the viscosity of liquids and has been discussed in terms of the effect of pressure on the parameters involved by Kuss (89), is

$$\eta = C \exp (E_{act} / RT) \qquad (3.6)$$

where C is a constant, T is the temperature in degrees K, and R is the gas constant. If C is independent of temperature and pressure and E_{act} is independent of temperature, then the viscosity, $\eta(P)$, can be calculated from the equations

$$\eta(P) = \eta^{0} \exp (gP) \qquad (3.7)$$

Table 3.3

Viscosity of Acetone

($mg\ cm^{-1} sec^{-1}$)

Pressure (bar)	Temperature (°C) 26.61	35.00	45.01	54.83
1.0	2.968	2.756	2.530	2.325
137.9	3.272	3.030	2.773	2.541
275.8	3.590	3.316	3.028	2.768
413.7	3.894	3.594	3.277	2.993
551.6	4.191	3.866	3.525	3.218
689.5	4.459	4.116	3.755	3.430
827.4	4.727	4.368	3.990	3.648
965.3	4.976	4.602	4.208	3.851
1103.2	5.235	4.840	4.425	4.050

and

$$g = \frac{1}{RT} \left(\frac{\partial E_{act}}{\partial P}\right)_T \qquad (3.8)$$

However, when points were taken from the graphs given by Bridgman (88), it was found that the activation energy, E_{act}, was not a linear function of pressure, so that C had to be considered to be a function of pressure. For the purposes of the calculation, E_{act} was assumed to be independent of the temperature at all pressures. This was found to be the case for the viscosities reported by Howard and McAllister (87) at atmospheric pressure. The pressure dependence of E_{act} was calculated from the results of Bridgman using equation (3.6) at each pressure. With these results, pressure-dependent values of $\log_{10}C$ were calculated from the 30°C viscosity data. Graphical interpolation was then carried out to obtain a set of E_{act} and $\log_{10}C$ at the pressures of interest. From this information, equation (3.6) was used to calculate viscosities at all the temperatures and pressures of interest. These values were multiplied by the ratio of the atmospheric viscosity of Howard and McAllister to that of Bridgman at each of the four temperatures, to obtain the final set of viscosities which are shown in Table 3.3.

4. Concentration Dependence of the Equivalent Conductivity

A Kohlrausch Treatment

The Onsager equation, which is a theoretically derived expression first suggested by Kohlrausch (90) as an empirical relationship between Λ and concentration, is

$$\Lambda = \Lambda_o - S c^{\frac{1}{2}} \qquad (3.9)$$

where c is the molar concentration of salt. The intercept at zero concentration is called the limiting equivalent conductivity, Λ_o. For unassociated, symmetrical, 1-1 electrolytes, the limiting slope at zero concentration, S_{exp}, of the equivalent conductivity plotted as a function of the square root of the concentration, is closely approximated by the expression due to Onsager (91) given below:

$$S = 8204 \times 10^{2} \Lambda_o / (\epsilon T)^{1.5} + 82.5 / \eta (\epsilon T)^{0.5} \qquad (3.10)$$

where ϵ is the dielectric constant of the solvent

T is the temperature in degrees K

and η is the viscosity in g cm^{-1} sec^{-1}

If the experimentally measured Onsager slopes obtained from the fit of Λ to the square root of the concentration had been found to be close to those calculated from equation (3.10), then the conclusion would have been that the salts were unassociated. The experimental Onsager slopes of the three salts studied at atmospheric pressure, given in Table 3.4, were obtained by least-mean-square (l.m.s.) fitting of the equivalent conductivity data to equation (3.9) on an I.B.M. 360 computer. Table 3.4 also lists the limiting equivalent conductivities from these plots. The three sections of the table represent the data obtained from (a) the high-pressure conductivity cells, (b) the atmospheric-pressure conductivity cells, and (c) the combined data from both (a) and (b). This calculation was performed on the conductivity data obtained at high pressures as well, and the results are recorded in Tables 3.5, 3.6, and 3.7. The program for this calculation constitutes the first part of the Shedlovsky

Table 3.4

Experimental Onsager Slope, S_{exp}, and Limiting Equivalent Conductivity at Atmospheric Pressure, Λ_o

	Temperature (°C)							
	26.61		35.00		45.01		54.83	
(a)	S_{exp}	Λ_o	S_{exp}	Λ_o	S_{exp}	Λ_o	S_{exp}	Λ_o
Me_4NI	2166	222.5	2144	231.6	2446	253.2	2740	272.7
Et_4NI	1484	212.9	1562	226.1	1878	250.0	2081	267.3
n-Pr_4NI	1318	195.0	1487	210.2	1753	230.5	2108	251.8
(b)								
Me_4NI	1888	218.8	2137	236.0	2455	256.6	3065	276.8
Et_4NI	1299	209.9	1442	225.6	1684	246.0	1888	265.0
n-Pr_4NI	1188	193.3	1342	208.5	1570	227.7	1780	245.7
(c)								
Me_4NI	2007	220.3	2208	235.2	2502	256.0	2925	275.1
Et_4NI	1389	211.5	1499	226.0	1780	248.0	1981	266.2
n-Pr_4NI	1246	194.1	1406	209.3	1654	229.0	1934	248.7

Table 3.5

(a) Experimental Onsager Slope, S_{exp}, and Limiting Equivalent Conductivity, Λ_o.

units: S_{exp}, $((cm^2\Omega^{-1}mole^{-1})x(mole\ l^{-1})^{-\frac{1}{2}})$

Λ_o, $(cm^2\Omega^{-1}mole^{-1})$

Me_4NI Temperature (°C)

Pressure (bar)	26.61		35.00		45.01		54.83	
	S_{exp}	Λ_o	S_{exp}	Λ_o	S_{exp}	Λ_o	S_{exp}	Λ_o
1.0	2166	222.5	2144	231.6	2446	253.2	2740	272.7
137.9	1847	206.0	1819	215.5	2095	234.9	2319	252.3
275.8	1620	192.2	1588	201.5	1839	219.6	2014	235.8
413.7	1415	179.8	1366	188.7	1637	206.5	1782	221.5
551.6	1224	168.4	1285	179.0	1491	195.0	1678	210.8
689.5	1079	158.3	1166	169.3	1339	184.6	1550	200.3
827.4	964	149.5	1077	160.9	1237	175.6	959	178.1
965.3	884	142.1	991	153.0	1145	167.1	1314	181.2
1103.2	824	135.3	920	146.2	1071	159.6	874	164.1

(b) Theoretical Onsager Slope Calculated from the Terminal Shedlovsky

	Iteration			
1.0	716.5	769.0	854.0	945.2
137.9	644.4	693.5	767.1	846.6
275.8	584.7	630.1	696.4	768.4
413.7	535.4	577.1	638.2	703.6
551.6	493.6	534.4	589.3	651.1
689.5	458.8	497.7	548.4	606.1
827.4	428.5	465.6	512.6	549.6
965.3	403.3	437.8	481.6	531.4
1103.2	380.1	413.3	454.2	490.7

Table 3.6

(a) Experimental Onsager Slope, S_{exp}, and Limiting Equivalent Conductivity, Λ_o

units: S_{exp}, $((cm^2\Omega^{-1}mole^{-1})x(mole\ l^{-1})^{-\frac{1}{2}})$

Λ_o, $(cm^2\Omega^{-1}mole^{-1})$

Et_4NI

Pressure (bar)	Temperature (°C) 26.61		35.00		45.01		54.83	
	S_{exp}	Λ_o	S_{exp}	Λ_o	S_{exp}	Λ_o	S_{exp}	Λ_o
1.0	1484	212.9	1562	226.1	1878	250.0	2081	267.3
137.9	1307	198.4	1375	210.2	1636	231.0	1816	247.8
275.8	1170	185.1	1230	196.6	1454	215.6	1617	231.4
413.7	1045	173.3	1114	184.5	1290	201.5	1458	217.3
551.6	952	163.3	1036	174.6	1204	190.4	1330	204.9
689.5	863	153.8	955	165.4	1087	180.0	1192	193.2
827.4	791	145.5	885	157.3	1011	171.0	1115	183.3
965.3	734	138.1	826	149.5	945	162.8	1061	175.5
1103.2	683	131.4	772	142.4	888	155.4	995	167.7

(b) Theoretical Onsager Slope Calculated from the Terminal Shedlovsky

	Iteration			
1.0	706.4	764.8	853.4	941.0
137.9	636.8	688.7	764.8	843.0
275.8	577.3	625.3	693.2	764.1
413.7	528.5	572.9	633.3	699.2
551.6	488.1	530.0	584.3	644.5
689.5	454.0	493.7	543.4	598.1
827.4	424.2	462.0	507.5	557.4
965.3	398.7	434.2	476.7	524.6
1103.2	375.7	409.1	449.4	494.5

Table 3.7

(a) Experimental Onsager Slope, S_{exp}, and Limiting Equivalent Conductivity, Λ_o.

units: S_{exp}, $((cm^2\Omega^{-1}mole^{-1})x(mole\ l^{-1})^{-\frac{1}{2}})$

Λ_o, $(cm^2\Omega^{-1}mole^{-1})$

n-Pr_4NI

Pressure (bar)	Temperature (°C) 26.61		35.00		45.01		54.83	
	S_{exp}	Λ_o	S_{exp}	Λ_o	S_{exp}	Λ_o	S_{exp}	Λ_o
1.0	1318	195.0	1487	210.2	1753	230.5	2108	251.8
137.9	1156	181.2	1305	194.9	1534	213.8	1852	233.1
275.8	1039	169.3	1195	183.2	1424	200.3	1617	217.4
413.7	940	159.0	1078	172.1	1244	187.5	1468	204.1
551.6	862	149.8	988	162.3	1177	178.2	1348	192.6
689.5	797	141.6	912	153.7	1087	168.7	1268	182.7
827.4	738	134.5	847	146.1	1015	160.3	1163	173.4
965.3	688	127.9	794	138.9	951	152.9	1092	165.4
1103.2	645	121.8	747	132.4	898	146.0	1030	158.0

(b) Theoretical Onsager Slope Calculated from the Terminal Shedlovsky

	Iteration			
1.0	678.0	738.3	820.3	912.8
137.9	610.4	664.1	736.4	817.3
275.8	553.7	604.3	668.7	740.9
415.7	507.6	554.0	611.4	677.8
551.6	468.7	511.6	566.0	625.0
689.5	436.4	476.5	526.4	581.2
827.4	408.5	445.8	491.7	542.3
965.3	384.4	418.9	462.3	509.3
1103.2	362.2	394.9	435.9	480.2

treatment described in part C of this section and which is listed in Appendix III. A detailed example of this calculation is given for Et_4NI in part C of this section below. The theoretical limiting Onsager slopes calculated from equation (3.10) for the three compounds studied are also recorded in parts (b) of Tables 3.5, 3.6, and 3.7. These calculations indicated that the equivalent conductivity data were not a linear function of the square root of concentration according to the relationship suggested by equation (3.9). The observed slopes were more negative than those calculated from equation (3.10). This suggests that there is some ion association.

B Ostwald Dilution Formula

The fundamental hypothesis made by Arrhenius (92) was that the degree of dissociation, α_d, is given by the relation

$$\alpha_d = \Lambda/\Lambda_o \qquad (3.11)$$

For the dissociation of a weak 1-1 electrolyte, the Ostwald Dilution law (93) follows from this result:

$$K = \Lambda^2 c / \Lambda_o(\Lambda_o - \Lambda) \qquad (3.12)$$

The apparent dissociation constant, K, and the limiting equivalent conductivity, Λ_o, can be obtained simultaneously from a plot of Λ^{-1} against Λc, as can be seen from a rearrangement of equation (3.12).

$$\Lambda^{-1} = \Lambda_o^{-1} + K^{-1} (\Lambda_o)^{-2} \times c\Lambda \qquad (3.13)$$

This approach involves two serious approximations in which the effect of ionic interactions are neglected. The first is that equation (3.11) should not involve Λ_o, but the equivalent conductivity of a hypothet-

ically fully dissociated state for the salt in question, at the concentration of ions present which is responsible for Λ. The second has to do with activity coefficients, which are not considered in the Ostwald Dilution law formulation. The thermodynamic dissociation constant for the ionization of a weak 1-1 electrolyte is

$$K_d = \frac{y_\pm^2 \alpha_d^2 c}{y_u (1-\alpha_d)} \qquad (3.14)$$

where $y_\pm$ is the mean molar activity coefficient of electrolyte

y_u is the molar activity coefficient of undissociated solute

The ratio of the activity coefficients, $y_\pm^2 / y_u$, is assumed to be equal to one. According to Harned and Owen (94) at high dilutions of weak electrolytes in aqueous solution, or of strong electrolytes in solvents of low dielectric constant, these errors are small and almost compensating.

Some l.m.s. calculations were done on the computer, in order to obtain, with equation (3.13), rough estimates of the limiting equivalent conductivity and the dissociation constant. These results are not reported since the calculations described in part C do not involve the approximations mentioned above. However, the dissociation constants and equivalent conductivities obtained were very close to those calculated by the Shedlovsky treatment. The same trends for different salts and varying conditions of temperature and pressure were found in the more exact method of Shedlovsky. The comment of Harned and Owen (94) seems to be justified for these electrolytes in acetone, as was suggested above.

C Shedlovsky Extrapolation Method

The Shedlovsky extrapolation method (95, 96) is an iterative procedure by which successively better estimates of the limiting equivalent conductivity are used to estimate the ion-pair dissociation constant, K_d. It has been used by Sears, Wilhoit, and Dawson (97) to determine limiting equivalent conductivities and dissociation constants of potassium thiocyanate and tetra-n-butylammonium iodide ($n\text{-}Bu_4NI$) in acetone solution at several temperatures within the range 25 to -50°C. It was also used by Savedoff (98) on a number of lithium and tetra-n-butylammonium salts in acetone solution at 25°C.

The Shedlovsky extrapolation method is outlined below and the equations which appear in the computer program are discussed. The program, listed in Appendix III, was written in Fortran IV (E) language for use on the I.B.M. 360 computer at the Computing Center of the University of Ottawa. A subroutine program which made use of a method of weighted least squares to fit polynomials of up to degree fifteen to sets of paired data by a method outlined by Hildebrand (99), was obtained from the National Research Council Computation Centre. An empirical equation due to Shedlovsky (95), which is based on the Onsager equation (3.9), is used to represent the conductivity of a hypothetical electrolyte which is assumed to be completely dissociated:

$$\Lambda = \Lambda_o - (A/\Lambda_o)\, S\, c^{\frac{1}{2}} \qquad (3.15)$$

The observed conductivity divided by that calculated from equation (3.15) is then set equal to the degree of dissociation:

$$\alpha_d = (\Lambda/\Lambda_o) + (\Lambda/\Lambda_o^2)\ S\ (\alpha_d c)^{\frac{1}{2}} \tag{3.16}$$

A new variable, Z, is then defined by

$$Z = S\ (\Lambda c)^{\frac{1}{2}} \Lambda_o^{-1.5} \tag{3.17}$$

After a set of equivalent conductivities and concentrations, for a given condition of temperature and pressure, have been selected from the whole set of data for a given salt read into the computer, the calculation of a set of Z values is carried out by the program with a value of the Onsager slope calculated from equation (3.10). The limiting equivalent conductivity chosen for this first iteration, is that obtained from the Kohlrausch treatment outlined in part A. Equation (3.16) can be simplified by substituting the new variable Z, and the degree of dissociation is then given by

$$\alpha_d = (\Lambda/\Lambda_o)\left[\frac{Z}{2} + \left\{1 + \left(\frac{Z}{2}\right)^2\right\}^{\frac{1}{2}}\right]^2 \tag{3.18}$$

A second new variable is then defined in terms of Z:

$$S(Z) = \left[\frac{Z}{2} + \left\{1 + \left(\frac{Z}{2}\right)^2\right\}^{\frac{1}{2}}\right]^2 \tag{3.19}$$

The program uses the first set of calculated Z values to obtain a set of S(Z) from equation (3.19). Equations (3.18), (3.19), and (3.14) are now combined to obtain

$$\frac{1}{\Lambda^{S(Z)}} = \frac{1}{\Lambda_o} + \frac{c\Lambda y_\pm^2 S(Z)}{K_d (\Lambda_o)^2} \tag{3.20}$$

This is rearranged to facilitate calculations as follows:

$$\Lambda^{S(Z)} = \Lambda_o - \frac{c\Lambda^2 y_\pm^2 S^2(Z)}{K_d \Lambda_o} \tag{3.21}$$

Before the final calculation, which involves a curve fit of $\Lambda S(Z)$ as a function of $c\, y_{\pm}^2 \Lambda^2 S^2(Z)$ to obtain a new estimate of Λ_o and a value of K_d, it is necessary to evaluate the activity coefficients $y_{\pm}$. The Debye-Hückel formula for the activity coefficient in its limiting form, which follows as equation (3.22), given by Robinson and Stokes (100), was used to calculate the activity coefficients:

$$\log_{10} f_{\pm} = - A |z_1 z_2| \alpha_d^{\frac{1}{2}} I^{\frac{1}{2}} \qquad (3.22)$$

where z_1 and z_2 are the charges carried by cations and anions; for the salts studied $z_1 = z_2 = I$

I is the ionic strength defined as $\frac{1}{2} c (n_1 z_1^2 + n_2 z_2^2)$ where n_1 and n_2 are the number of cations and anions resulting from the dissociation of one 'molecule' of salt of concentration c, and therefore I= c in moles per liter for the salts studied.

α_d is the degree of dissociation

A is a constant for a given temperature and pressure as below

$$A = \frac{1.8246 \times 10^6}{(\epsilon T)^{1.5}} \quad \text{mole}^{-\frac{1}{2}}\, l^{\frac{1}{2}}\, (\text{deg K})^{1.5} \qquad (3.23)$$

The ion-size correction term which appears in the denominator of the Debye-Hückel formula was neglected because it is negligible in comparison to one, for the dilute solutions studied. The formula which appears in the computer program is given by the equation

$$y_{\pm}^2 = \left[\exp \left(\frac{1.5848 \times 10^6 (\alpha_d c)^{\frac{1}{2}}}{(\epsilon T)^{1.5}} \right) \right]^{-1} \qquad (3.24)$$

It should be noted that the molar activity coefficient is called for

in the equations derived in the Shedlovsky treatment, while equation (3.22) represents the mean rational activity coefficient, $f_{\pm}$. The two activity coefficients are related by the following equation given by Harned and Owen (101):

$$\log f_{\pm} = \log y_{\pm} + \log \left\{ \frac{d}{d_o} + \frac{c\,(n M_1 - M_2)}{1000\, d_o} \right\} \qquad (3.25)$$

where d and d_o are the densities of the solution and the solvent respectively

M_2 and M_1 are the molecular weights of solute and solvent

c is the concentration of solute

n is the number of moles of ions produced per mole of solute

For the solutions studied, d could be approximated by d_o and the second term in the brackets involving the concentration was negligible compared to one, so that the two activity coefficients were identical for the present treatment.

After the quantities S, Z, S(Z), and $y_{\pm}^2$ were evaluated, they were printed out by the computer. Then $\Lambda S(Z)$ was fitted as a linear function of $c\, y_{\pm}^2 \Lambda^2 S^2(Z)$ and the intercept recorded as the first estimate of Λ_o; K_d calculated from the slope $-(K_d \Lambda_o)^{-1}$ was also recorded as the first estimate of the dissociation constant. If this new Λ_o did not agree with the estimate of Λ_o used for that iteration to better than ±0.05%, the new Λ_o was used to recalculate S, Z, S(Z), and $y_{\pm}^2$ and the calculation of the Shedlovsky linear fit repeated. The

program was set to carry out this iteration seven times or until the specified agreement was reached. Three iterations were usually required.

Table 3.8 gives the Onsager slopes calculated from equation (3.10) using the limiting equivalent conductivity which was employed in the final Shedlovsky iteration. Parts (a), (b), and (c) represent, respectively, the results obtained at atmospheric pressure with the high-pressure cells, the results of the atmospheric cells, and the combined data from both sets of cells. Parts (b) of Tables 3.5, 3.6, and 3.7 as mentioned above report the Onsager slopes calculated from equation (3.10) using the Λ_o of the high-pressure results, again for the final Shedlovsky iteration.

Table 3.9 contains the limiting equivalent conductivities calculated by the Shedlovsky method at atmospheric pressure from (a) the high-pressure cells, (b) the atmospheric-pressure cells, and (c) the combined data from (a) and (b). The numbers in brackets in this and later tables represent estimates which are related to the errors in these quantities. The meaning of these error estimates will be discussed in section 7 of this chapter. Table 3.10 contains the limiting equivalent conductivities calculated by the Shedlovsky method at high pressures. Tables 3.11 and 3.12 are the analogous tables of the dissociation constants obtained from the Shedlovsky treatment.

In Table 3.13 are recorded values obtained for some of the quantities of the Shedlovsky treatment of the Et_4NI salt. From this

Table 3.8

Theoretical Onsager Slope Calculated from the Terminal Shedlovsky Iteration at Atmospheric Pressure ($(cm^2\Omega^{-1}mole^{-1})x(mole\ l^{-1})^{\frac{1}{2}}$)

	Temperature (°C)			
	26.61	35.00	45.01	54.83
(a)				
Me_4NI	716.5	769.0	854.0	945.2
Et_4NI	706.4	764.8	853.4	941.0
$n\text{-}Pr_4NI$	678.0	738.3	820.3	912.8
(b)				
Me_4NI	714.2	778.3	861.9	947.2
Et_4NI	703.3	765.2	848.3	939.0
$n\text{-}Pr_4NI$	676.7	737.3	817.4	905.2
(c)				
Me_4NI	715.1	774.7	859.0	946.0
Et_4NI	704.9	765.1	850.9	940.1
$n\text{-}Pr_4NI$	677.3	737.8	818.8	908.9

Table 3.9

Limiting Equivalent Conductivity at Atmospheric Pressure

($cm^2\Omega^{-1}mole^{-1}$)

	Temperature (°C)			
	26.61	35.00	45.01	54.83
(a)				
Me_4NI	213.3(3.9)	222.9(3.4)	243.5(3.7)	261.8(3.9)
Et_4NI	207.3(1.1)	220.4(1.2)	243.0(1.7)	259.5(1.7)
n-Pr_4NI	190.6(1.8)	205.1(1.6)	224.3(2.0)	244.4(2.1)
(b)				
Me_4NI	211.9(2.5)	228.2(2.6)	247.7(2.9)	262.9(9.4)
Et_4NI	205.5(0.4)	220.6(0.6)	240.1(1.1)	258.4(1.3)
n-Pr_4NI	189.9(0.5)	204.5(0.7)	222.8(1.0)	240.1(1.6)
(c)				
Me_4NI	212.5(2.1)	226.1(3.2)	246.2(2.8)	262.3(5.4)
Et_4NI	206.4(1.0)	220.6(1.2)	241.6(1.1)	259.0(1.5)
n-Pr_4NI	190.2(1.0)	204.7(1.0)	223.5(1.2)	242.1(1.6)

Table 3.10

Limiting Equivalent Conductivity

($cm^2 \Omega^{-1} mole^{-1}$)

Me_4NI	Temperature (°C)			
Pressure (bar)	26.61	35.00	45.01	54.83
1.0	213.3(3.9)	222.9(3.4)	243.3(3.7)	261.8(3.9)
137.9	198.0(3.5)	207.9(3.2)	226.2(3.4)	242.9(3.5)
275.8	185.1(3.3)	194.8(2.9)	211.9(3.1)	227.5(3.2)
413.7	173.6(3.0)	182.8(3.0)	199.5(2.9)	214.1(3.0)
551.6	163.1(2.8)	173.5(2.5)	188.6(2.7)	203.7(3.0)
689.5	153.7(2.5)	164.3(2.4)	178.9(2.6)	193.5(3.2)
827.4	145.4(2.3)	156.3(2.2)	170.2(2.4)	173.7(2.1)
965.3	138.4(2.1)	148.8(2.1)	162.2(2.3)	175.5(2.5)
1103.2	131.9(2.0)	142.3(2.2)	155.0(2.1)	160.9(2.3)
Et_4NI				
1.0	207.3(1.1)	220.4(1.2)	243.0(1.7)	259.5(1.7)
137.9	193.4(1.1)	205.1(1.2)	224.8(1.4)	240.9(1.7)
275.8	180.6(1.1)	191.9(1.1)	210.0(1.3)	225.0(1.8)
413.7	169.2(0.9)	180.2(1.0)	196.5(1.2)	211.5(1.7)
551.6	159.6(0.9)	170.7(0.9)	185.4(1.7)	199.5(1.7)
689.5	150.5(0.8)	161.8(0.9)	175.6(1.2)	188.5(1.4)
827.4	142.5(0.7)	153.9(0.8)	166.9(1.1)	178.6(2.2)
965.3	135.3(0.7)	146.3(0.8)	158.9(1.1)	171.1(1.7)
1103.2	128.8(0.7)	139.4(0.8)	151.7(1.1)	163.4(1.7)

Table 3.10 (cont.)

Limiting Equivalent Conductivity

($cm^2 \Omega^{-1} mole^{-1}$)

n-Pr_4NI

Pressure (bar)	Temperature (°C) 26.61	35.00	45.01	54.83
1.0	190.6(1.8)	205.1(1.6)	224.3(2.0)	244.4(2.1)
137.9	177.4(1.7)	190.4(1.5)	208.3(1.8)	226.3(2.5)
275.8	165.8(1.6)	179.0(1.9)	195.2(1.5)	211.4(2.0)
413.7	155.9(1.5)	168.4(1.8)	182.9(1.6)	198.6(1.9)
551.6	146.9(1.5)	158.8(1.7)	173.8(2.1)	187.5(1.8)
689.5	138.9(1.4)	150.5(1.7)	164.7(2.0)	177.8(1.8)
827.4	132.0(1.3)	143.1(1.6)	156.5(1.9)	168.9(1.7)
965.3	125.5(1.3)	136.0(1.6)	149.3(1.8)	161.0(1.7)
1103.2	119.6(1.2)	129.7(1.5)	142.5(1.8)	153.8(1.6)

Table 3.11

Dissociation Constant at Atmospheric Pressure

(mole l^{-1})

	Temperature (°C)			
	26.61	35.00	45.01	54.83
(a)				
Me_4NI	0.0028(0.0007)	0.0032(0.0007)	0.0029(0.0006)	0.0027(0.0005)
Et_4NI	0.0060(0.0004)	0.0062(0.0004)	0.0050(0.0004)	0.0047(0.0003)
$n\text{-}Pr_4NI$	0.0064(0.0009)	0.0058(0.0006)	0.0050(0.0006)	0.0039(0.0004)
(b)				
Me_4NI	0.0034(0.0006)	0.0031(0.0005)	0.0028(0.0004)	0.0024(0.0011)
Et_4NI	0.0079(0.0002)	0.0073(0.0003)	0.0062(0.0004)	0.0058(0.0004)
$n\text{-}Pr_4NI$	0.0080(0.0004)	0.0072(0.0004)	0.0061(0.0004)	0.0055(0.0005)
(c)				
Me_4NI	0.0031(0.0004)	0.0051(0.0006)	0.0028(0.0004)	0.0025(0.0007)
Et_4NI	0.0069(0.0005)	0.0068(0.0005)	0.0056(0.0003)	0.0052(0.0004)
$n\text{-}Pr_4NI$	0.0072(0.0006)	0.0065(0.0005)	0.0056(0.0004)	0.0047(0.0004)

Table 3.12

Dissociation Constant

(mole l^{-1})

Me_4NI Pressure (bar)	Temperature (°C) 26.61	35.00	45.01	54.83
1.0	0.0028(0.0007)	0.0032(0.0007)	0.0029(0.0006)	0.0027(0.0005)
137.9	0.0034(0.0009)	0.0038(0.0010)	0.0034(0.0008)	0.0032(0.0007)
275.8	0.0038(0.0011)	0.0044(0.0012)	0.0039(0.0009)	0.0037(0.0009)
413.7	0.0043(0.0013)	0.0053(0.0018)	0.0043(0.0011)	0.0042(0.0010)
551.6	0.0051(0.0017)	0.0052(0.0016)	0.0046(0.0012)	0.0042(0.0011)
689.5	0.0058(0.0021)	0.0057(0.0018)	0.0051(0.0015)	0.0045(0.0014)
827.4	0.0065(0.0025)	0.0060(0.0020)	0.0054(0.0016)	0.0125(0.0066)
965.3	0.0070(0.0027)	0.0064(0.0022)	0.0057(0.0017)	0.0051(0.0014)
1103.2	0.0073(0.0029)	0.0068(0.0025)	0.0059(0.0018)	0.0104(0.0055)
Et_4NI 1.0	0.0060(0.0004)	0.0062(0.0004)	0.0050(0.0004)	0.0047(0.0003)
137.9	0.0067(0.0005)	0.0069(0.0005)	0.0057(0.0004)	0.0054(0.0005)
275.8	0.0073(0.0006)	0.0076(0.0006)	0.0063(0.0005)	0.0060(0.0006)
413.7	0.0080(0.0007)	0.0081(0.0007)	0.0071(0.0006)	0.0065(0.0007)
551.6	0.0086(0.0007)	0.0083(0.0007)	0.0074(0.0010)	0.0070(0.0008)
689.5	0.0094(0.0008)	0.0088(0.0008)	0.0081(0.0008)	0.0078(0.0009)
827.4	0.0100(0.0009)	0.0093(0.0008)	0.0084(0.0009)	0.0082(0.0015)
965.3	0.0106(0.0011)	0.0096(0.0009)	0.0088(0.0010)	0.0082(0.0012)
1103.2	0.0111(0.0012)	0.0100(0.0010)	0.0090(0.0010)	0.0085(0.0014)

Table 3.12 (cont.)

Dissociation Constant

(mole l^{-1})

n-Pr_4NI

Pressure (bar)	Temperature (°C) 26.61	35.00	45.01	54.83
1.0	0.0064(0.0009)	0.0058(0.0006)	0.0050(0.0006)	0.0039(0.0004)
137.9	0.0072(0.0011)	0.0066(0.0008)	0.0057(0.0007)	0.0045(0.0006)
275.8	0.0078(0.0013)	0.0068(0.0011)	0.0056(0.0006)	0.0052(0.0006)
413.7	0.0084(0.0014)	0.0074(0.0013)	0.0066(0.0009)	0.0055(0.0007)
551.6	0.0089(0.0016)	0.0078(0.0014)	0.0065(0.0012)	0.0058(0.0008)
689.5	0.0093(0.0018)	0.0082(0.0016)	0.0068(0.0013)	0.0059(0.0008)
827.4	0.0098(0.0020)	0.0087(0.0017)	0.0071(0.0013)	0.0064(0.0009)
965.3	0.0102(0.0021)	0.0089(0.0019)	0.0073(0.0014)	0.0066(0.0010)
1103.2	0.0106(0.0023)	0.0092(0.0020)	0.0075(0.0015)	0.0067(0.0010)

Table 3.13

(a) Least-Mean-Square Fit of Equivalent Conductivity of Et_4NI to the Square Root of Concentration

atmospheric pressure cell data at 26.61°C

$$\Lambda = (209.95 \pm 0.375) - (1299 \pm 15)\, c^{\frac{1}{2}} \quad ; \quad E_{RMS} = 0.312$$

(b) Parameters Calculated in the Shedlovsky Treatment of Et_4NI for the Final Iteration

Pressure 1.0 bar				Temperature 26.61°C			Pressure 965.3 bar
Concentration (mole l^{-1})x10^4	Z (see text for units)	S(Z)	$y_\pm^2$	Concentration (mole l^{-1})x10^4	Z (see text for units)	S(Z)	$y_\pm^2$
11.25	0.102	1.107	0.902	12.19	0.094	1.098	0.910
9.729	0.095	1.100	0.908	10.54	0.088	1.092	0.915
8.770	0.091	1.095	0.913	9.505	0.084	1.087	0.920
3.341	0.059	1.061	0.943	3.621	0.054	1.055	0.949
3.292	0.058	1.060	0.944	3.567	0.053	1.055	0.949
1.068	0.034	1.035	0.967	1.158	0.031	1.032	0.970
				45.01°C			
10.94	0.102	1.108	0.900	11.97	0.094	1.099	0.909
9.463	0.096	1.101	0.906	10.35	0.088	1.092	0.915
8.531	0.092	1.096	0.911	9.328	0.084	1.088	0.919
3.250	0.060	1.061	0.942	3.554	0.054	1.055	0.948
3.202	0.060	1.061	0.942	3.501	0.053	1.055	0.949
1.039	0.035	1.036	0.966	1.136	0.031	1.032	0.970

table the effect of temperature and pressure on the various parameters can be noted.

To evaluate the computer program, the data obtained by Sears, Wilhoit, and Dawson (97) and Savedoff (98), were fitted and the results compared with those reported in their papers. The agreement obtained was within the error estimates of the program and the most probable precision (see section 8), for both the limiting equivalent conductivities and the dissociation constants. It was thought that this test, which produced results agreeing with two independent treatments, indicated that the Shedlovsky computer program developed in this work was reliable.

5. Thermodynamic Activation Parameters for Conductivity

A Volume of Activation

The experimental definition of the volume of activation for ionic conductivity, as used by Brummer and Hills (102), is

$$\Delta V_i^{\ddagger} = -RT\left(\frac{\partial \ln \lambda_i^{\circ}}{\partial P}\right)_T - \frac{2}{3} RT\beta \qquad (3.27)$$

where β is the isothermal solvent compressibility (calculated from the Tait equation and the results given for acetone in Appendix I)

λ_i° is the limiting equivalent ionic conductivity

R is the gas constant in ml bar deg^{-1} $mole^{-1}$

Calculations to obtain the pressure coefficient of conductivity were made on the combined cationic and anionic conductivities, which were the observed quantities. All the activation parameter calculations in the present section were done in this way since there are no transport numbers available for these salts in acetone. The effect of this

approximation will be discussed later.

In order to study the pressure coefficient of the interionic effect, equation (3.27) was applied to the equivalent conductivities measured at finite concentrations. The logarithms for a given temperature and concentration were fitted to a second-order polynomial in pressure, by the method of l. m. s., and the first derivative evaluated at the pressures of interest. This derivative was then used in equation (3.27) to obtain the volumes of activation. No weighting factors were used in these calculations. Tables 3.14, 3.15, and 3.16 record the results for the three salts studied.

The volumes of activation based on the limiting equivalent conductivity were calculated by the same procedure as those calculated at finite concentrations. Weighting factors were applied, however, as they were throughout the rest of the calculations wherever possible, in order to make use of the error estimates generated by the Shedlovsky program. This aspect of the calculations is discussed in section 7. The results are presented in Tables 3.17 and 3.18. The volumes in Table 3.18 are given without the compressibility correction, to indicate the magnitude and pressure and temperature variation of this term.

The results discussed in this section were obtained, with the exception of Tables 3.14, 3.15, and 3.16, by means of a computer program which utilized the same polynomial curve fitting subroutine program as the Shedlovsky treatment. This program has been listed in Appendix III. The equations, which are described later in this

Table 3.14

Volume of Activation for Conductivity of Me_4NI Corrected for Solvent Compressibility at Different Salt Concentrations (ml $mole^{-1}$)

Temperature (°C)	Pressure (bar)	Concentration at 1.0 bar and 26.61°C (mole l^{-1}) $\times 10^4$					
		4.468	4.201	2.807	2.170	1.946	1.724
26.61	1.0	8.77	8.64	9.27	9.71	9.69	10.19
	200	8.67	8.56	9.13	9.63	9.50	9.75
	400	8.41	7.03	8.83	9.39	9.16	9.35
	600	8.06	8.01	8.45	9.06	8.74	8.76
	800	7.67	7.64	8.01	8.68	8.26	8.12
	1000	7.24	7.24	7.54	8.27	7.73	7.65
35.00	1.0	8.19	8.42	9.03	9.15	9.33	9.46
	200	8.25	8.41	8.87	9.02	9.17	9.27
	400	8.12	8.22	8.53	8.71	8.83	8.90
	600	7.91	7.94	8.09	8.31	8.39	8.44
	800	7.63	7.60	7.60	7.84	7.90	7.92
	1000	7.32	7.22	7.07	7.34	7.36	7.36
45.01	1.0	8.51	8.86	9.38	9.52	9.42	9.71
	200	8.53	8.74	9.19	9.36	9.31	9.53
	400	8.31	8.38	8.76	8.97	8.97	9.11
	600	7.97	7.90	8.20	8.45	8.49	8.57
	800	7.56	7.33	7.58	7.86	7.96	7.95
	1000	7.10	6.74	7.00	8.22	7.38	7.29
54.83	1.0	8.33	8.53	9.07	9.63	9.55	9.81
	200	8.47	8.64	9.07	9.49	9.45	9.63
	400	8.29	8.42	8.75	9.03	9.02	9.13
	600	7.96	8.06	8.27	8.42	8.44	8.47
	800	7.53	7.60	7.70	7.71	7.76	7.72
	1000	7.08	7.11	7.10	6.97	7.06	6.91

Table 3.15

Volume of Activation for Conductivity of Et_4NI Corrected for Solvent Compressibility at Different Salt Concentrations (ml $mole^{-1}$)

Temperature (°C)	Pressure (bar)	Concentration at 1.0 bar and 26.61°C (mole l^{-1})					
		11.25	9.729	$x10^4$ 8.770	3.341	3.292	1.068
26.61	1.0	8.87	8.97	9.14	9.93	10.02	10.63
	200	8.78	8.87	9.01	9.72	9.77	10.28
	400	8.52	8.62	8.72	9.36	9.37	9.77
	600	8.19	8.28	8.34	8.91	8.88	9.17
	800	7.81	7.89	7.91	8.41	8.34	8.53
	1000	7.39	7.46	7.45	7.87	7.77	7.84
35.00	1.0	9.01	9.20	9.29	10.18	9.65	10.64
	200	8.86	9.05	9.10	9.86	9.42	10.22
	400	8.53	8.71	8.73	9.36	9.01	9.63
	600	8.11	8.28	8.27	8.77	8.51	8.93
	800	7.63	7.79	7.75	8.12	7.95	8.19
	1000	7.12	7.27	7.18	7.43	7.35	7.40
45.01	1.0	9.08	10.17	9.77	10.49	11.60	11.05
	200	9.00	9.79	9.51	10.19	11.04	10.62
	400	8.69	9.17	9.01	9.64	10.24	9.94
	600	8.25	8.43	8.39	8.97	9.31	9.14
	800	7.74	7.61	7.70	8.23	8.32	8.26
	1000	7.18	6.75	6.96	7.44	7.28	7.34
54.83	1.0	8.76	9.03	8.97	10.33	10.83	11.06
	200	8.85	9.11	9.04	10.18	10.58	10.72
	400	8.63	8.86	8.80	9.71	10.01	10.06
	600	8.25	8.47	8.40	9.09	9.29	9.25
	800	7.77	7.98	7.91	8.37	8.47	8.34
	1000	7.27	7.46	7.39	7.62	7.63	7.41

Table 3.16

Volume of Activation for Conductivity of n-Pr_4NI Corrected for Solvent Compressibility at Different Salt Concentrations (ml $mole^{-1}$)

Temperature (°C)	Pressure (bar)	Concentration at 1.0 bar and 26.61°C (mole l^{-1}) $\times 10^4$					
		10.67	8.118	5.783	3.647	1.697	0.8000
26.61	1.0	9.14	9.39	9.67	9.96	10.43	10.31
	200	9.00	9.17	9.42	9.65	10.05	10.02
	400	8.62	8.80	9.02	9.18	9.52	9.58
	600	8.20	8.34	8.53	8.63	8.91	9.06
	800	7.73	7.84	7.98	8.02	8.24	8.48
	1000	7.22	7.29	7.41	7.38	7.54	7.87
35.00	1.0	9.07	9.34	9.67	8.96	10.55	10.55
	200	8.93	9.17	9.45	8.95	10.18	10.17
	400	8.61	8.82	9.05	8.75	9.64	9.61
	600	8.19	8.37	8.56	8.46	8.99	8.95
	800	7.72	7.86	8.01	8.12	8.29	8.23
	1000	7.21	7.31	7.42	7.73	7.55	7.48
45.01	1.0	9.38	9.48	9.91	9.50	10.87	10.86
	200	9.22	9.34	9.70	9.30	10.49	10.45
	400	8.82	8.96	9.25	8.86	9.87	9.80
	600	8.29	8.45	8.67	8.30	9.13	9.02
	800	7.69	7.87	8.02	7.66	8.31	8.17
	1000	7.05	7.25	7.32	6.98	7.45	7.28
54.83	1.0	8.70	9.48	9.59	10.38	10.96	11.15
	200	8.85	9.42	9.56	10.21	10.68	10.79
	400	8.68	9.04	9.21	9.72	10.07	10.11
	600	8.37	8.52	8.71	9.08	9.32	9.29
	800	7.95	7.89	8.11	8.34	8.47	8.36
	1000	7.51	7.24	7.49	7.57	7.59	7.41

Table 3.17

Volume of Activation for Conductivity Corrected for Solvent Compressibility (ml $mole^{-1}$)

Pressure (bar)	Temperature (°C) 26.61	35.00	45.01	54.83
Me_4NI				
1.0	11.34(0.16)	10.67(0.25)	10.90(0.30)	11.13(2.26)
137.9	11.03(0.17)	10.40(0.28)	10.68(0.32)	11.15(2.74)
275.8	10.52(0.18)	10.03(0.31)	10.30(0.35)	10.99(3.23)
413.7	10.16(0.20)	9.59(0.34)	9.85(0.39)	10.72(3.73)
551.6	9.66(0.21)	9.11(0.38)	9.33(0.43)	10.38(4.24)
689.5	9.14(0.23)	8.60(0.41)	8.78(0.47)	10.00(4.75)
827.4	8.59(0.25)	8.06(0.45)	8.20(0.52)	9.58(5.26)
965.3	8.03(0.27)	7.51(0.49)	7.60(0.56)	9.15(5.77)
1103.2	7.45(0.29)	6.95(0.53)	6.99(0.61)	8.69(6.28)
Et_4NI				
1.0	10.95(0.14)	10.83(0.33)	11.98(0.33)	11.81(0.26)
137.9	10.71(0.15)	10.56(0.37)	11.60(0.36)	11.54(0.27)
275.8	10.37(0.15)	10.18(0.41)	11.08(0.41)	11.09(0.28)
413.7	9.98(0.16)	9.74(0.47)	10.46(0.45)	10.53(0.31)
551.6	9.55(0.18)	9.26(0.52)	9.80(0.50)	9.90(0.34)
689.5	9.10(0.19)	8.75(0.58)	9.09(0.56)	9.23(0.37)
827.4	8.62(0.21)	8.21(0.63)	8.36(0.61)	8.53(0.40)
965.3	8.13(0.22)	7.66(0.69)	7.61(0.66)	7.80(0.44)
1103.2	7.62(0.24)	7.10(0.75)	6.84(0.72)	7.05(0.47)

Table 3.17 (cont.)

Volume of Activation for Conductivity Corrected for Solvent Compressibility (ml $mole^{-1}$)

Pressure (bar)	Temperature (°C) 26.61	35.00	45.01	54.83
n-Pr_4NI				
1.0	10.90(0.20)	10.79(0.30)	11.27(0.39)	11.80(0.34)
137.9	10.60(0.22)	10.53(0.34)	10.96(0.43)	11.52(0.37)
275.8	10.21(0.24)	10.17(0.39)	10.50(0.49)	11.05(0.41)
413.7	9.76(0.27)	9.75(0.44)	9.96(0.55)	10.48(0.45)
551.6	9.27(0.30)	9.28(0.49)	9.37(0.62)	9.84(0.50)
689.5	8.76(0.33)	8.78(0.54)	8.73(0.69)	9.16(0.55)
827.4	8.23(0.35)	8.26(0.60)	8.07(0.76)	8.44(0.60)
965.3	7.68(0.39)	7.72(0.65)	7.39(0.83)	7.70(0.65)
1103.2	7.12(0.42)	7.17(0.71)	6.69(0.90)	6.95(0.71)

Table 3.18

Volume of Activation for Conductivity with No Correction for Solvent Compressibility

($ml\ mole^{-1}$)

	Temperature (°C)			
Pressure (bar)	26.61	35.00	45.01	54.83
Me_4NI				
1.0	13.43(0.10)	12.90(0.18)	13.50(0.21)	14.00(1.98)
137.9	12.79(0.12)	12.27(0.22)	12.81(0.25)	13.47(2.45)
275.8	12.15(0.14)	11.64(0.26)	12.11(0.30)	12.93(2.93)
413.7	11.51(0.16)	11.00(0.31)	11.41(0.35)	12.39(3.40)
551.6	10.86(0.19)	10.37(0.35)	10.71(0.40)	11.86(3.88)
689.5	10.22(0.21)	9.73(0.39)	10.02(0.45)	11.32(4.35)
827.4	9.58(0.23)	9.09(0.43)	9.32(0.49)	10.78(4.83)
965.3	8.93(0.25)	8.46(0.48)	8.62(0.54)	10.24(5.31)
1103.2	8.29(0.28)	7.82(0.52)	7.92(0.59)	9.70(5.78)
Et_4NI				
1.0	13.03(0.08)	13.06(0.25)	14.57(0.24)	14.73(0.15)
137.9	12.46(0.10)	12.43(0.31)	13.73(0.30)	13.90(0.19)
275.8	11.89(0.11)	11.79(0.37)	12.88(0.36)	13.06(0.23)
413.7	11.32(0.13)	11.16(0.43)	12.03(0.41)	12.23(0.26)
551.6	10.75(0.15)	10.52(0.49)	11.18(0.47)	11.39(0.30)
689.5	10.18(0.17)	9.88(0.55)	10.33(0.53)	10.55(0.34)
827.4	9.61(0.19)	9.25(0.61)	9.48(0.59)	9.72(0.38)
965.3	9.03(0.20)	8.61(0.67)	8.64(0.64)	8.88(0.42)
1103.2	8.46(0.22)	7.97(0.73)	7.78(0.70)	8.04(0.45)

Table 3.18 (cont.)

Volume of Activation for Conductivity with No Correction for Solvent Compressibility

(ml $mole^{-1}$)

Pressure (bar)	Temperature (°C) 26.61	35.00	45.01	54.83
n-Pr_4NI				
1.0	12.97(0.14)	13.02(0.23)	13.86(0.30)	14.72(0.24)
137.9	12.35(0.17)	12.41(0.29)	13.09(0.37)	13.88(0.29)
275.8	11.72(0.20)	11.73(0.35)	12.31(0.44)	13.03(0.35)
413.7	11.10(0.24)	11.16(0.40)	11.53(0.51)	12.18(0.41)
551.6	10.45(0.27)	10.54(0.46)	10.75(0.59)	11.33(0.46)
689.5	9.84(0.30)	9.91(0.52)	9.97(0.66)	10.48(0.52)
827.4	9.21(0.34)	9.29(0.58)	9.19(0.73)	9.63(0.58)
965.3	8.59(0.37)	8.67(0.64)	8.41(0.81)	8.78(0.63)
1103.2	7.96(0.40)	8.05(0.70)	7.63(0.88)	7.94(0.69)

section, were incorporated into this program, the appropriate values being inserted for the constants. The input to this program was such as to accept, with only a slight rearrangement, the output of the Shedlovsky program, Λ_o,$\Delta\Lambda_o$ (the error estimate in Λ_o), K_d, and ΔK_d (the error estimate in K_d). The Walden products were also calculated by this program.

B Energy of Activation at Constant Pressure

The energy of activation for conductivity at constant pressure may be defined by

$$E_P = RT^2 \left(\frac{\partial \ln \Lambda_o}{\partial T} \right)_P \qquad (3.28)$$

The logarithms of the limiting equivalent conductivities were fitted to a first-order polynomial in temperature by the l.m.s. method and the temperature coefficients used to evaluate E_P at different pressures. The computed results are reported in Table 3.19 for the three salts investigated. As is the case for all of the tables which report three results at atmospheric pressure, the first entry (a) refers to the data from the atmospheric pressure cells, the third entry refers to those from the high pressure cells, and the second entry refers to the combined results.

C Energy of Activation at Constant Volume

The energy of activation for conductivity at constant volume may be defined by

$$E_V = RT^2 \left(\frac{\partial \ln \Lambda_o}{\partial T} \right)_V \qquad (3.29)$$

Table 3.19

Energy of Activation at Constant Pressure for Conductivity

(kcal $mole^{-1}$)

Pressure (bar)	Me_4NI	Et_4NI	$n\text{-}Pr_4NI$
1.0 (a)	1.58(0.05)	1.59(0.02)	1.63(0.01)
1.0 (b)	1.49(0.04)	1.60(0.05)	1.67(0.02)
1.0 (c)	1.48(0.11)	1.59(0.08)	1.73(0.03)
137.9	1.46(0.08)	1.55(0.07)	1.69(0.04)
275.8	1.47(0.07)	1.56(0.06)	1.68(0.00)
413.7	1.49(0.07)	1.55(0.05)	1.67(0.02)
551.6	1.55(0.05)	1.55(0.02)	1.69(0.02)
689.5	1.60(0.03)	1.57(0.02)	1.71(0.02)
827.4	1.23(0.20)	1.60(0.04)	1.71(0.02)
965.3	1.65(0.01)	1.63(0.03)	1.73(0.03)
1103.2	1.41(0.15)	1.66(0.03)	1.75(0.03)

The logarithms of the limiting equivalent conductivities were first fitted to a third-order polynomial in the molal volume, at each of the four temperatures. Twelve volumes were then chosen over the range of pressure investigated, and the logarithms of Λ_o calculated for these volumes from the polynomial. These quantities were then fitted to a first-order polynomial in temperature for each one of the twelve volumes, and E_V was calculated using equation (3.29). Computed results are reported, for the three salts studied, in Table 3.20.

6. Thermodynamic Parameters for Ion-Pair Dissociation

A Gibbs Free Energy of Dissociation

The standard Gibbs free-energy change of dissociation was computed according to the equation

$$\Delta G_d^\circ = -RT \ln K_d \qquad (3.30)$$

where the superscript indicates that the quantity represents the standard change

These results are given in Table 3.21.

B Volume Change of Dissociation

The logarithms of the dissociation constants were fitted to a second-order polynomial in pressure by means of a l.m.s. method, and the first derivative evaluated at a series of pressures. These values were used in the equation below to calculate the volume changes of dissociation:

$$\Delta V_d^\circ = -RT \left(\frac{\partial \ln K_d}{\partial P}\right)_T - RT\beta \qquad (3.31)$$

Table 3.20

Energy of Activation at Constant Volume for Conductivity

(kcal mole^{-1})

Volume of Actone (ml mole $^{-1}$)	Me_4NI	Et_4NI	n-Pr_4NI
77.49	0.466(0.049)	0.523(0.132)	0.497(0.021)
76.30	0.377(0.068)	0.464(0.062)	0.506(0.015)
75.15	0.327(0.097)	0.424(0.056)	0.519(0.026)
74.22	0.308(0.104)	0.404(0.065)	0.532(0.029)
73.63	0.302(0.103)	0.399(0.068)	0.541(0.030)
72.76	0.301(0.096)	0.400(0.067)	0.557(0.030)
71.96	0.304(0.090)	0.411(0.062)	0.575(0.031)
71.17	0.307(0.093)	0.432(0.055)	0.594(0.034)
71.14	0.307(0.093)	0.434(0.054)	0.595(0.035)
70.42	0.308(0.106)	0.463(0.048)	0.615(0.041)
69.80	0.306(0.124)	0.496(0.045)	0.633(0.048)
69.06	0.297(0.150)	0.544(0.045)	0.658(0.060)

Table 3.21

Gibbs Free Energy of Dissociation

(kcal mole^{-1})

	Pressure (bar)	Temperature (°C) 26.61	35.00	45.01	54.83
Me_4NI	1.0 (a)	3.385(0.109)	3.539(0.103)	3.724(0.101)	3.938(0.291)
	1.0 (b)	3.434(0.083)	3.541(0.123)	3.724(0.096)	3.902(0.172)
	1.0 (c)	3.492(0.142)	3.523(0.135)	3.694(0.130)	3.861(0.124)
	137.9	3.393(0.155)	3.408(0.153)	3.592(0.145)	3.741(0.138)
	275.8	3.321(0.167)	3.325(0.166)	3.513(0.153)	3.645(0.150)
	413.7	3.241(0.178)	3.212(0.209)	3.445(0.164)	3.568(0.162)
	551.6	3.146(0.202)	3.215(0.184)	3.403(0.166)	3.560(0.168)
	689.5	3.068(0.216)	3.165(0.194)	3.336(0.181)	3.519(0.199)
	827.4	3.001(0.226)	3.132(0.199)	3.302(0.186)	4.359(3.440)
	965.3	2.956(0.232)	3.091(0.209)	3.267(0.192)	3.442(0.185)
	1103.2	2.931(0.233)	3.057(0.230)	3.242(0.194)	2.975(0.347)
Et_4NI	1.0 (a)	2.885(0.017)	3.009(0.023)	3.210(0.039)	3.361(0.042)
	1.0 (b)	2.967(0.040)	3.058(0.046)	3.279(0.035)	3.423(0.045)
	1.0 (c)	3.051(0.040)	3.116(0.044)	3.347(0.048)	3.491(0.046)
	137.9	2.981(0.046)	3.046(0.049)	3.267(0.048)	3.402(0.055)
	275.8	2.931(0.053)	2.990(0.051)	3.202(0.050)	3.336(0.065)
	413.7	2.874(0.048)	2.946(0.053)	3.124(0.055)	3.278(0.070)
	551.6	2.852(0.052)	2.934(0.052)	3.106(0.083)	3.233(0.077)
	689.5	2.782(0.051)	2.900(0.054)	3.047(0.063)	3.163(0.073)
	827.4	2.740(0.054)	2.866(0.055)	3.020(0.067)	3.132(0.123)
	965.3	2.708(0.059)	2.842(0.057)	2.996(0.069)	3.133(0.098)
	1103.2	2.679(0.062)	2.817(0.058)	2.975(0.073)	3.108(0.104)

Table 3.21 (cont.)

Gibbs Free Energy of Dissociation

(kcal mole^{-1})

	Pressure (bar)	Temperature (°C) 26.61	35.00	45.01	54.83
n-Pr_4NI	1.0 (a)	2.876(0.029)	3.020(0.034)	3.216(0.042)	3.386(0.061)
	1.0 (b)	2.934(0.050)	3.076(0.046)	3.278(0.045)	3.492(0.052)
	1.0 (c)	3.006(0.086)	3.145(0.066)	3.348(0.071)	3.608(0.061)
	137.9	2.935(0.091)	3.075(0.071)	3.271(0.075)	3.528(0.082
	275.8	2.890(0.098)	3.053(0.102)	3.276(0.065)	3.456(0.077)
	413.7	2.846(0.103)	3.002(0.107)	3.171(0.084)	3.392(0.081)
	551.6	2.814(0.108)	2.968(0.112)	3.180(0.114)	3.356(0.084)
	689.5	2.786(0.114)	2.936(0.117)	3.150(0.116)	3.347(0.087)
	827.4	2.755(0.119)	2.907(0.121)	3.129(0.120)	3.301(0.093)
	965.3	2.730(0.124)	2.889(0.127)	3.107(0.123)	3.280(0.098)
	1103.2	2.710(0.128)	2.872(0.131)	3.093(0.126)	3.265(0.100)

Results are given in Tables 3.22 where the solvent compressibility correction has been applied, and in 3.23, where it has not been applied.

C Enthalpy of Dissociation

The standard enthalpy of dissociation was calculated from the derivatives at the pressures for which the logarithm of the dissociation constant was fitted to a first-order polynomial in temperature. Use was made of the equation

$$\Delta H_d^\circ = RT^2 \left(\frac{\partial \ln K_d}{\partial T} \right)_P \qquad (3.32)$$

Results are presented in Table 3.24.

D Entropy of Dissociation

The standard entropy change of dissociation was calculated from the standard changes in the Gibbs free energy and the enthalpy of dissociation for all the conditions of temperature and pressure, according to the relation given below:

$$\Delta S_d^\circ = \frac{\Delta H_d^\circ - \Delta G_d^\circ}{T} \qquad (3.33)$$

Results for the three salts are presented in Table 3.25.

E Internal-Energy Change of Dissociation

The standard change in the internal energy of dissociation is defined by the equation

$$\Delta U_d^\circ = RT^2 \left(\frac{\partial \ln K_d}{\partial T} \right)_V \qquad (3.34)$$

Table 3.22

Volume of Dissociation Corrected for Solvent Compressibility

($ml\ mole^{-1}$)

	Temperature (°C)			
Pressure (bar)	26.61	35.00	45.01	54.85
Me_4NI				
1.0	-33.6(2.2)	-35.0(3.5)	-32.5(1.7)	-27.9(12.2)
137.9	-31.0(2.6)	-30.6(4.2)	-28.8(1.8)	-26.4(15.2)
275.8	-28.6(3.0)	-26.4(4.9)	-25.4(2.0)	-25.2(18.3)
413.7	-26.2(3.4)	-22.4(5.6)	-22.1(2.3)	-24.1(21.3)
551.6	-25.9(3.8)	-18.4(6.4)	-18.9(2.5)	-23.1(24.4)
689.5	-21.6(4.3)	-14.4(7.1)	-15.7(2.8)	-22.2(27.5)
827.4	-19.4(4.7)	-10.5(7.9)	-12.5(3.0)	-21.4(30.6)
965.3	-17.1(5.2)	- 6.6(8.7)	- 9.4(3.3)	-20.6(33.8)
1103.2	-14.9(5.6)	- 2.7(9.4)	- 6.4(3.6)	-19.8(36.9)
Et_4NI				
1.0	-22.8(1.0)	-20.8(2.1)	-29.2(1.8)	-30.9(1.9)
137.9	-21.0(1.0)	-18.6(2.4)	-25.7(2.0)	-27.0(2.1)
275.8	-19.2(1.1)	-16.5(2.8)	-22.3(2.2)	-23.4(2.3)
413.7	-17.5(1.2)	-14.5(3.1)	-19.1(2.5)	-20.0(2.6)
551.6	-15.9(1.3)	-12.6(3.5)	-15.9(2.8)	-16.7(2.9)
689.5	-14.3(1.4)	-10.7(3.9)	-12.8(3.0)	-13.4(3.2)
827.4	-12.7(1.5)	- 8.8(4.3)	- 9.8(3.3)	-10.2(3.5)
965.3	-11.2(1.7)	- 7.0(4.7)	- 6.8(3.6)	- 7.0(3.8)
1103.2	- 9.7(1.8)	- 5.2(5.1)	- 3.8(3.9)	- 3.8(4.2)

Table 5.22 (cont.)

Volume of Dissociation Corrected for Solvent Compressibility

($ml\ molo^{-1}$)

	Temperature (°C)			
Pressure (bar)	26.61	35.00	45.01	54.85
n-Pr_4NI				
1.0	-20.9(1.3)	-19.8(1.8)	-20.4(4.2)	-29.2(2.7)
137.9	-18.7(1.5)	-17.7(2.0)	-18.0(5.1)	-25.2(3.1)
275.8	-16.6(1.7)	-15.7(2.3)	-15.7(6.0)	-21.5(3.5)
413.7	-14.5(1.9)	-13.8(2.6)	-13.6(6.9)	-17.9(4.0)
551.6	-12.6(2.1)	-12.0(2.9)	-11.5(7.8)	-14.4(4.5)
689.5	-10.6(2.3)	-10.2(3.3)	- 9.5(8.7)	-11.0(5.0)
827.4	- 8.7(2.5)	- 8.5(3.6)	- 7.6(9.6)	- 7.7(5.5)
965.3	- 6.8(2.7)	- 6.8(3.9)	-5.6(10.6)	- 4.4(6.0)
1103.2	- 5.0(3.0)	- 5.1(4.3)	-3.7(11.5)	- 1.1(6.5)

Table 3.23

Volume of Dissociation with No Correction for Solvent Compressibility

($ml\ mole^{-1}$)

Pressure (bar)	Temperature (°C) 26.61	35.00	45.01	54.83
Me_4NI				
1.0	-30.5(1.8)	-31.7(3.0)	-28.7(1.1)	-23.5(11.6)
137.9	-28.4(2.2)	-27.8(3.8)	-25.6(1.4)	-22.9(14.8)
275.8	-26.3(2.7)	-24.0(4.6)	-22.7(1.7)	-22.3(17.6)
413.7	-24.2(3.2)	-20.3(5.3)	-19.8(2.0)	-21.6(20.9)
551.6	-22.1(3.6)	-16.6(6.2)	-16.9(2.3)	-20.9(24.1)
689.5	-20.0(4.1)	-12.7(6.9)	-13.9(2.5)	-20.3(27.2)
827.4	-17.9(4.5)	- 9.0(7.7)	-10.8(2.8)	-19.6(30.3)
965.3	-15.7(5.0)	- 5.2(8.6)	- 7.8(3.1)	-19.0(33.6)
1103.2	-13.6(5.5)	- 1.4(9.2)	- 5.0(3.4)	-18.3(36.7)
Et_4NI				
1.0	-19.7(0.5)	-17.5(1.6)	-25.3(1.2)	-26.6(1.2)
137.9	-18.4(0.7)	-15.8(2.1)	-22.5(1.6)	-23.4(1.6)
275.8	-16.9(0.8)	-14.1(2.5)	-19.6(1.9)	-20.5(1.9)
413.7	-15.5(0.9	-12.4(2.8)	-16.8(2.2)	-17.5(2.3)
551.6	-14.1(1.1)	-10.8(3.3)	-13.9(2.5)	-14.5(2.6)
689.5	-12.6(1.2)	- 9.0(3.7)	-11.0(2.7)	-11.4(2.9)
827.4	-11.2(1.4)	- 7.2(4.1)	- 8.2(3.0)	- 8.4(3.3)
965.3	- 9.9(1.5)	- 5.6(4.5)	- 5.3(3.4)	- 5.4(3.6)
1103.2	- 8.5(1.6)	- 3.9(5.0)	- 2.4(3.7)	- 2.3(4.0)

Table 3.23 (cont.)

Volume of Dissociation with No Correction for Solvent Compressibility

($ml\ mole^{-1}$)

Pressure (bar)	Temperature (°C) 26.61	35.00	45.01	54.83
n-Pr_4NI				
1.0	-17.8(0.9)	-16.5(1.3)	-16.5(3.7)	-24.9(2.1)
137.9	-16.1(1.2)	-14.9(1.7)	-14.8(4.7)	-21.7(2.6)
275.8	-14.3(1.4)	-13.3(2.0)	-13.0(5.6)	-18.5(3.1)
413.7	-12.5(1.6)	-11.7(2.4)	-11.3(6.6)	-15.3(3.7)
551.6	-10.8(1.9)	-10.2(2.6)	- 9.4(7.6)	-12.2(4.2)
689.5	- 8.9(2.1)	- 8.5(3.1)	- 7.6(8.4)	- 9.0(4.8)
827.4	- 7.3(2.3)	- 7.0(3.4)	- 5.9(9.4)	- 5.9(5.2)
965.3	- 5.5(2.6)	- 5.3(3.7)	- 4.0(10.4	- 2.7(5.8)
1103.2	- 3.8(2.8)	- 3.7(4.1)	- 2.3(11.3)	- 0.4(6.5)

Table 3.24

Enthalpy of Dissociation

(kcal mole^{-1})

Pressure (bar)	Me_4NI	Et_4NI	$n\text{-}Pr_4NI$
1.0 (a)	-2.25(0.14)	-2.21(0.24)	-2.56(0.13)
1.0 (b)	-1.43(0.26)	-2.10(0.44)	-2.96(0.22)
1.0 (c)	-0.69(0.66)	-1.87(0.59)	-3.48(0.44)
137.9	-0.62(0.71)	-1.76(0.58)	-3.34(0.46)
275.8	-0.47(0.74)	-1.65(0.62)	-2.92(0.37)
413.7	-0.64(0.94)	-1.49(0.44)	-2.87(0.26)
551.6	-1.49(0.44)	-1.52(0.22)	-2.93(0.14)
689.5	-1.82(0.34)	-1.34(0.13)	-3.19(0.12)
827.4	-2.05(0.90)	-1.63(0.19)	-3.06(0.21)
965.3	-2.25(0.09)	-1.87(0.10)	-3.11(0.18)
1103.2	0.66(2.57)	-1.98(0.15)	-3.17(0.21)

Table 3.25

Entropy of Dissociation

(cal deg^{-1} $mole^{-1}$)

	Pressure (bar)	Temperature (°C) 26.61	35.00	45.01	54.83
Me_4NI	1.0 (a)	-18.8(0.8)	-18.8(0.8)	-18.8(0.8)	-18.9(1.3)
	1.0 (b)	-16.2(1.1)	-16.1(1.2)	-16.2(1.1)	-16.3(1.3)
	1.0 (c)	-14.0(2.7)	-13.7(2.6)	-13.8(2.5)	-13.9(2.4)
	137.9	-13.4(2.9)	-13.1(2.8)	-13.2(2.7)	-13.3(2.6)
	275.8	-12.7(3.0)	-12.3(2.9)	-12.5(2.8)	-12.6(2.7)
	413.7	-12.9(3.7)	-12.5(3.7)	-12.9(3.5)	-12.8(3.3)
	551.6	-15.5(2.1)	-15.3(2.0)	-15.4(1.9)	-15.4(1.8)
	689.5	-16.3(1.9)	-16.2(1.7)	-16.2(1.7)	-16.3(1.7)
	827.4	-16.8(3.7)	-16.7(3.6)	-16.8(3.4)	-19.5(13.2)
	965.3	-17.4(1.1)	-17.3(1.0)	-17.3(0.9)	-17.3(0.8)
	1103.2	- 7.6(9.4)	- 7.8(9.1)	- 8.1(8.7)	- 7.0(8.9)
Et_4NI	1.0 (a)	-17.0(0.9)	-16.9(0.9)	-17.0(0.9)	-17.0(0.9)
	1.0 (b)	-16.8(1.6)	-16.7(1.6)	-16.8(1.5)	-16.8(1.5)
	1.0 (c)	-16.3(2.1)	-16.1(2.1)	-16.3(2.0)	-16.3(1.9)
	137.9	-15.8(2.1)	-15.5(2.0)	-15.8(2.0)	-15.7(1.9)
	275.8	-15.3(2.2)	-15.0(2.2)	-15.2(2.1)	-15.2(2.1)
	413.7	-14.6(1.6)	-14.3(1.6)	-14.5(1.6)	-14.5(1.6)
	551.6	-14.5(0.9)	-14.4(0.9)	-14.5(0.9)	-14.5(0.9)
	689.5	-13.7(0.6)	-13.7(0.6)	-13.8(0.6)	-13.7(0.6)
	827.4	-14.6(0.8)	-14.6(0.8)	-14.6(0.8)	-14.6(0.9)
	965.3	-15.2(0.5)	-15.3(0.5)	-15.3(0.5)	-15.2(0.6)
	1103.2	-15.5(0.7)	-15.5(0.7)	-15.5(0.7)	-15.5(0.8)

Table 3.25 (Cont.)

Entropy of Dissociation

($cal\ deg^{-1}\ mole^{-1}$)

Temperature (^{o}C)

Pressure (bar)	26.61	35.00	45.01	54.83
n-Pr_4NI				
1.0 (a)	-18.1(0.5)	-18.1(0.5)	-18.2(0.5)	-18.1(0.6)
1.0 (b)	-19.7(0.9)	-19.6(0.9)	-19.6(0.8)	-19.7(0.8)
1.0 (c)	-21.6(1.7)	-21.5(1.6)	-21.5(1.6)	-21.6(1.5)
137.9	-20.9(1.8)	-20.8(1.7)	-20.8(1.7)	-20.9(1.6)
275.8	-19.4(1.6)	-19.4(1.5)	-19.5(1.4)	-19.4(1.4)
413.7	-19.1(1.2)	-19.1(1.2)	-19.0(1.1)	-19.1(1.0)
551.6	-19.2(0.8)	-19.2(0.8)	-19.2(0.8)	-19.2(0.7)
689.5	-20.0(0.8)	-20.0(0.8)	-19.9(0.7)	-19.9(0.6)
827.4	-19.4(1.1)	-19.4(1.1)	-19.5(1.0)	-19.4(0.9)
965.3	-19.5(1.0)	-19.5(1.0)	-19.5(1.0)	-19.5(0.9)
1103.2	-19.6(1.1)	-19.6(1.1)	-19.7(1.0)	-19.6(0.9)

The logarithms of the dissociation constants were first fitted to a third-order polynomial in the molal volume at each of the four temperatures. Twelve volumes were then chosen over the range of pressure investigated, and the logarithms of K_d calculated for these volumes from the polynomial. These quantities were then fitted to a first-order polynomial in temperature for each one of the twelve volumes and ΔU_d^o was calculated using equation (3.34). Computed results are reported for the three salts studied in Table 3.26.

7. Errors

In almost all of the results presented in the tables of this chapter, an error estimate is given in brackets. These estimates represent the relative uncertainty of the results of a given calculation. The equations upon which they are based, have been incorporated into the computer programs. The goodness of fit of polynomials to any of the sets of data fitted in the computer programs was estimated by the subroutine from the formula given below:

$$E_{RMS} = \left[\frac{\sum_{i=1}^{N} (W_i R_i^2)}{N - K} \right]^{\frac{1}{2}} \qquad (3.35)$$

where R_i is the residual at the ith point

W_i is the weight associated with the ith point

N is the number of points

K is the number of coefficients (for example K is four for a third-degree polynomial)

Table 3.26.

Internal-Energy Change of Dissociation at Constant Volume

(kcal mole^{-1})

Volume of Acetone (ml mole^{-1})	Me_4NI	Et_4NI	$n\text{-}Pr_4NI$
77.49	-0.14(2.30)	0.27(0.43)	-0.21(1.05)
76.30	1.48(0.70)	0.10(0.28)	-0.78(0.62)
75.15	1.92(0.35)	0.06(0.56)	-1.20(0.37)
74.22	1.74(0.86)	0.07(0.62)	-1.46(0.26)
73.63	1.49(1.05)	0.07(0.60)	-1.59(0.21)
72.76	1.07(1.14)	0.05(0.51)	-1.77(0.17)
71.96	0.76(1.02)	-0.01(0.39)	-1.91(0.14)
71.17	0.67(0.75)	-0.14(0.26)	-2.04(0.14)
71.14	0.67(0.73)	-0.15(0.26)	-2.05(0.14)
70.42	0.91(0.55)	-0.35(0.16)	-2.18(0.15)
69.80	1.42(0.89)	-0.60(0.11)	-2.30(0.18)
69.06	2.52(1.81)	-1.01(0.10)	-2.47(0.26)

The standard error in each coefficient was estimated by the equation below.

$$(\Delta a_i)_{RMS} = A_{ii}^{\frac{1}{2}} E_{RMS} \qquad (3.36)$$

where $1 \leq i \leq K$ and A_{ii} is the ith diagonal element of the inverse of the matrix of the normal equations.

Where applicable, weighting factors, based on the error estimates of the limiting equivalent conductivity and the dissociation constants generated by the Shedlovsky program, were used. In the curve-fitting by the subroutine, a convention according to equation (3.36) was adopted:

$$W_i = \left(\frac{1}{\Delta Y_i}\right)^2 \qquad (3.37)$$

where W_i is the weighting factor for the ith point

Y_i is the ith dependent variable in the set fitted

ΔY_i is the error estimate in the ith Y above

This convention is similar to that suggested by Young (103).

As an example of how the error estimate was obtained, the error equation for the volume of activation for conductivity will be derived. This volume parameter was obtained from two separate l.m.s. fittings. The first kind was in the Shedlovsky program, to obtain sets of Λ_o for each temperature at nine pressures. Each of these fits resulted in a standard error, defined by equation (3.36), for each coefficient of the polynomial fitted. The error in the equivalent conductivity at infinite dilution, $\Delta\Lambda_o$, was obtained directly

from the standard error in the intercept. This standard error was then used to weight the dependent variable, $\ln\Lambda_o$, in the second-order polynomial in pressure which was then fitted:

$$W_i = \left(\frac{\Lambda_o}{\Delta\Lambda_o}\right)^2 \tag{3.38}$$

The result of this curve fitting was the polynomial

$$\ln\Lambda_o = a_o + a_1 P + a_2 P^2 \tag{3.39}$$

where the standard errors in the coefficients are Δa_o, Δa_1, and Δa_2. The coefficient of $\ln\Lambda_o$ with respect to pressure was obtained by differentiating equation (3.38):

$$\left(\frac{\partial \ln\Lambda_o}{\partial P}\right)_T = a_1 + 2 a_2 P \tag{3.40}$$

The error in this slope was estimated as follows:

$$\Delta\left(\frac{\partial \ln\Lambda_o}{\partial P}\right)_T = \Delta a_1 + 2\Delta a_2 P + 2 a_2 \Delta P \tag{3.41}$$

The volume of activation was calculated by substituting the slope given by equation (3.40) into equation (3.27). The error in the volume of activation was given by the equation

$$\Delta(\Delta V^{\ddagger}) = RT\Delta\left(\frac{\partial \ln\Lambda_o}{\partial P}\right)_T + \frac{2}{3} RT\,\Delta\beta \tag{3.42}$$

The error in the compressibility was estimated from the errors in the experimental Tait constants as described in Appendix I. Error estimates in other parameters were derived from similar equations.

The error estimates themselves represent the maximum possible estimated error since no factor was used to convert them to a probable error, and positive terms were always taken in the error equations. The curve fitting procedure results in calculated values for the fitted parameter which are more reliable than any of the individual measurements which go into the data set fitted by the curve. This statement is confirmed by a result derived by Young (103),

$$\sigma_m = \sigma / N^{\frac{1}{2}} \qquad (3.43)$$

where σ_m is the standard deviation of the mean

σ is the standard deviation for a set of N points.

This standard deviation of the mean is usually described as the precision of the mean. Therefore, to convert error estimates given in tables to the most probable precision of the measurements, equation (3.43) is applied and the result multiplied by 0.674. To illustrate this with some examples, the volume of activation error calculated by equation (3.42), would be reduced by the factor 0.674/3; the energies of activation and enthalpies of dissociation errors would be reduced by a factor of 0.674/2; the limiting equivalent conductivities errors would be reduced by a factor of $0.674/6^{\frac{1}{2}}$, $0.674/8^{\frac{1}{2}}$, or $0.674/14^{\frac{1}{2}}$, depending on whether they were based on the high-pressure cell data, the atmospheric cell data, or the combined data respectively; the errors in the dissociation constant would be reduced by the same factors as those in the limiting equivalent conductivity. These factors should be considered if the absolute reliability of a

given number is being considered. Comparisons within the data obtained in this work can be made by using the program error estimates in the tables as a guide to the relative precision of the data.

CHAPTER 4

DISCUSSION

1. Conductivity

A Summary of Results

Table 4.1 summarizes the conductivity results presented in Chapter 3. The conductivity of Me_4NI, Et_4NI, and $n\text{-}Pr_4NI$ in acetone has been found to have the following main features:

(i) The limiting equivalent conductivity decreases with the size of the cation, increases with temperature, and decreases with pressure (Tables 3.9 and 3.10). Both the viscosity and the dielectric constant of acetone decrease with temperature and increase with pressure (Tables 3.2 and 3.3).

(ii) The Walden product, $\Lambda_o \eta_o$, tends to decrease with temperature and to increase with pressure (Tables 4.2 and 4.3).

(iii) The energy of activation at constant pressure is greater than the energy of activation at constant volume by about 1 kcal $mole^{-1}$ (Tables 3.19 and 3.20). Both quantities increase with the size of the cation. The energy of activation at constant volume increases with decrease in the volume for $n\text{-}Pr_4NI$ which has the largest cation, but decreases for the other two salts (Table 3.20). The energy of activation at constant pressure is independent of the pressure within the precision of the measurements (Table 3.19).

(iv) The volumes of activation are all positive, and within the precision of the measurements are independent of the cation under all conditions of temperature and pressure studied. It is also independent of temperature, but decreases from about 11 to 7 ml $mole^{-1}$ when the pressure is increased

Table 4.1

Qualitative Summary of the Conductivity Results

Parameter	Increase in Cation size	Pressure	Temperature	Volume
Λ_o	d	d	i	n.a.
$\Lambda_o \eta_o$	d	i	d	n.a.
E_P	i	n.c.	n.a.	n.a.
E_V	i	n.a.	n.a.	d
$\Delta V^{\ddagger}$	n.c.	d	n.c.	d

i increase

d decrease

n.c. no change

n.a. not applicable

Table 4.2

Walden Product at Atmospheric Pressure

($g\ cm\ \Omega^{-1} sec^{-1} mole^{-1}$)

	Temperature (°C)			
	26.61	35.00	45.01	54.83
(a)				
Me_4NI	0.633(0.012)	0.614(0.009)	0.615(0.009)	0.609(0.009)
Et_4NI	0.615(0.003)	0.607(0.003)	0.615(0.004)	0.603(0.004)
$\underline{n}\text{-}Pr_4NI$	0.566(0.005)	0.565(0.004)	0.568(0.005)	0.568(0.005)
(b)				
Me_4NI	0.629(0.007)	0.629(0.007)	0.627(0.007)	0.611(0.022)
Et_4NI	0.610(0.001)	0.608(0.002)	0.607(0.003)	0.601(0.003)
$\underline{n}\text{-}Pr_4NI$	0.564(0.002)	0.563(0.002)	0.563(0.003)	0.558(0.004)
(c)				
Me_4NI	0.631(0.006)	0.623(0.009)	0.623(0.007)	0.610(0.013)
Et_4NI	0.613(0.003)	0.608(0.003)	0.611(0.003)	0.602(0.004)
$\underline{n}\text{-}Pr_4NI$	0.565(0.003)	0.564(0.003)	0.565(0.003)	0.563(0.004)

Table 4.3

Walden Product

($g\ cm\Omega^{-1}sec^{-1}mole^{-1}$)

	Pressure (bar)	Temperature (°C) 26.61	35.00	45.01	54.83
Me_4NI	1.0	0.633(0.012)	0.614(0.009)	0.615(0.009)	0.609(0.009)
	137.9	0.648(0.012)	0.630(0.010)	0.627(0.009)	0.617(0.009)
	275.8	0.665(0.012)	0.646(0.010)	0.641(0.009)	0.630(0.009)
	413.7	0.676(0.012)	0.657(0.011)	0.654(0.010)	0.641(0.009)
	551.6	0.684(0.012)	0.671(0.010)	0.665(0.009)	0.655(0.010)
	689.5	0.685(0.011)	0.676(0.010)	0.672(0.010)	0.664(0.011)
	827.4	0.687(0.011)	0.683(0.010)	0.679(0.010)	0.634(0.008)
	965.3	0.689(0.011)	0.685(0.010)	0.682(0.010)	0.676(0.010)
	1103.2	0.690(0.010)	0.689(0.010)	0.686(0.009)	0.652(0.009)
Et_4NI	1.0	0.615(0.003)	0.607(0.003)	0.615(0.004)	0.603(0.004)
	137.9	0.633(0.004)	0.621(0.004)	0.623(0.004)	0.612(0.004)
	275.8	0.648(0.004)	0.636(0.004)	0.636(0.004)	0.623(0.005)
	413.7	0.659(0.004)	0.648(0.004)	0.644(0.004)	0.633(0.005)
	551.6	0.669(0.004)	0.660(0.004)	0.654(0.006)	0.642(0.006)
	689.5	0.671(0.003)	0.666(0.004)	0.659(0.004)	0.646(0.005)
	827.4	0.674(0.003)	0.672(0.004)	0.666(0.005)	0.651(0.008)
	965.3	0.673(0.004)	0.673(0.004)	0.669(0.005)	0.659(0.007)
	1103.2	0.674(0.004)	0.675(0.004)	0.671(0.005)	0.662(0.007)

Table 4.3 (cont.)

Walden Product

(g cm Ω^{-1} sec^{-1} $mole^{-1}$)

Pressure (bar) / n-Pr_4NI	Temperature (°C) 26.61	35.00	45.01	54.83
1.0	0.566(0.005)	0.565(0.004)	0.568(0.005)	0.568(0.005)
137.9	0.580(0.006)	0.577(0.004)	0.577(0.005)	0.575(0.006)
275.8	0.595(0.006)	0.594(0.006)	0.591(0.004)	0.585(0.005)
413.7	0.607(0.006)	0.605(0.007)	0.599(0.005)	0.594(0.006)
551.6	0.616(0.006)	0.614(0.007)	0.613(0.008)	0.603(0.006)
689.5	0.619(0.006)	0.620(0.007)	0.618(0.008)	0.610(0.006)
827.4	0.624(0.006)	0.625(0.007)	0.624(0.008)	0.616(0.006)
965.3	0.625(0.006)	0.626(0.007)	0.628(0.008)	0.620(0.006)
1103.2	0.626(0.007)	0.628(0.007)	0.631(0.008)	0.623(0.007)

from atmospheric to 1.1 kbar (Tables 3.17 and 3.18).

B Walden's Rule and the Limiting Equivalent Conductivity

Walden (104) originally proposed the empirical equation

$$\Lambda_o \eta_o = \text{constant} \qquad (4.1)$$

where Λ_o is the limiting equivalent conductivity for a given condition of temperature and pressure

η_o is the viscosity of the solvent under identical conditions

The Walden product has been calculated by computer, according to equation (4.1), and the results are reported in Tables 4.2 and 4.3. Table 4.2 has been divided into parts; (a) high-pressure cell results at atmospheric pressure, (b) atmospheric-cell results, and (c) the results obtained from a Shedlovsky treatment of the combined (a) and (b) data. Pressure is seen to bring about an increase in the Walden product in all cases.

The effect of pressure in bringing about an increase in the Walden products of Me_4NBr, NaBr, n-Bu_4NBr, and n-Bu_4NBPh_4 in methanol was found by Skinner and Fuoss (105) to become less in the series of salts from Me_4NBr where the increase was approximately 10% for about 1 kbar, to n-Bu_4NBPh_4 where no pressure effect was detected. Skinner and Fuoss conclude that the pressure dependence of $\Lambda_o \eta_o$ for the first three salts above must be mostly a property of the bromide ions, since the Walden product for n-Bu_4NBPh_4 is independent of pressure. However, this conclusion is based on results obtained at one temperature only, 31°C. If the increase in the Walden product was primarily a property of the anion, then the behaviour of the Walden product as a function of temperature at different pressures would be the same for salts with different cations but a common anion.

However, Table 4.3 indicates that in acetone the decrease in the Walden product accompanying a 30°C increase in the temperature is accentuated by compression to a greater extent for the smaller cation, Me_4N^+, than for $n\text{-}Pr_4N^+$. The conductivity work of Sears, Wilhoit, and Dawson (97) in acetone solutions at atmospheric pressure indicated that the average Walden product for $n\text{-}Bu_4NI$, an iodide salt with a larger cation in the same series of salts studied here, was 0.545±0.001 at temperatures from 25° to -50°C. It follows from these considerations, that the ionic radius is one of the properties of a salt which determines whether or not its conductivity behaviour as a function of temperature and pressure can be understood solely in terms of the variation of the viscosity of the solvent.

To illustrate the relationship which exists between the ionic radius and the limiting equivalent conductivity, Figure 4.1 has been constructed from the conductivity data obtained in the present work and those taken from the tabulation of literature ionic conductivities provided in Table 4.4(a). The ionic radii chosen for the tetraalkylammonium ions are those estimated by Robinson and Stokes (106) from molecular volumes or models; the other ionic radii, with the exception of the ClO_4^-, picrate (Pi^-), and NO_3^- ions were taken from Pauling (28). The ClO_4^- and Pi^- radii were taken to be the van der Waals radii and the NO_3^- radius was taken to be the crystallographic radius. These values were obtained from a critical compilation of ionic radii estimated by various methods described by Stern and Amis (107). The points can be well represented by two straight lines A and B. The vertical line which divides A and B corresponds to the radius of

Figure 4.1. Walden products in acetone plotted as a function of ionic radii (a) present work

(b) Savedoff (98)

(c) Sears, Wilhoit, and Dawson (97)

All unmarked data are from Reynolds and Kraus (108)

Vertical lines: C, corresponds to the radius of the acetone molecule, 2.8 Å

D, corresponds to the critical ionic radius, 2.36 Å, (see text)

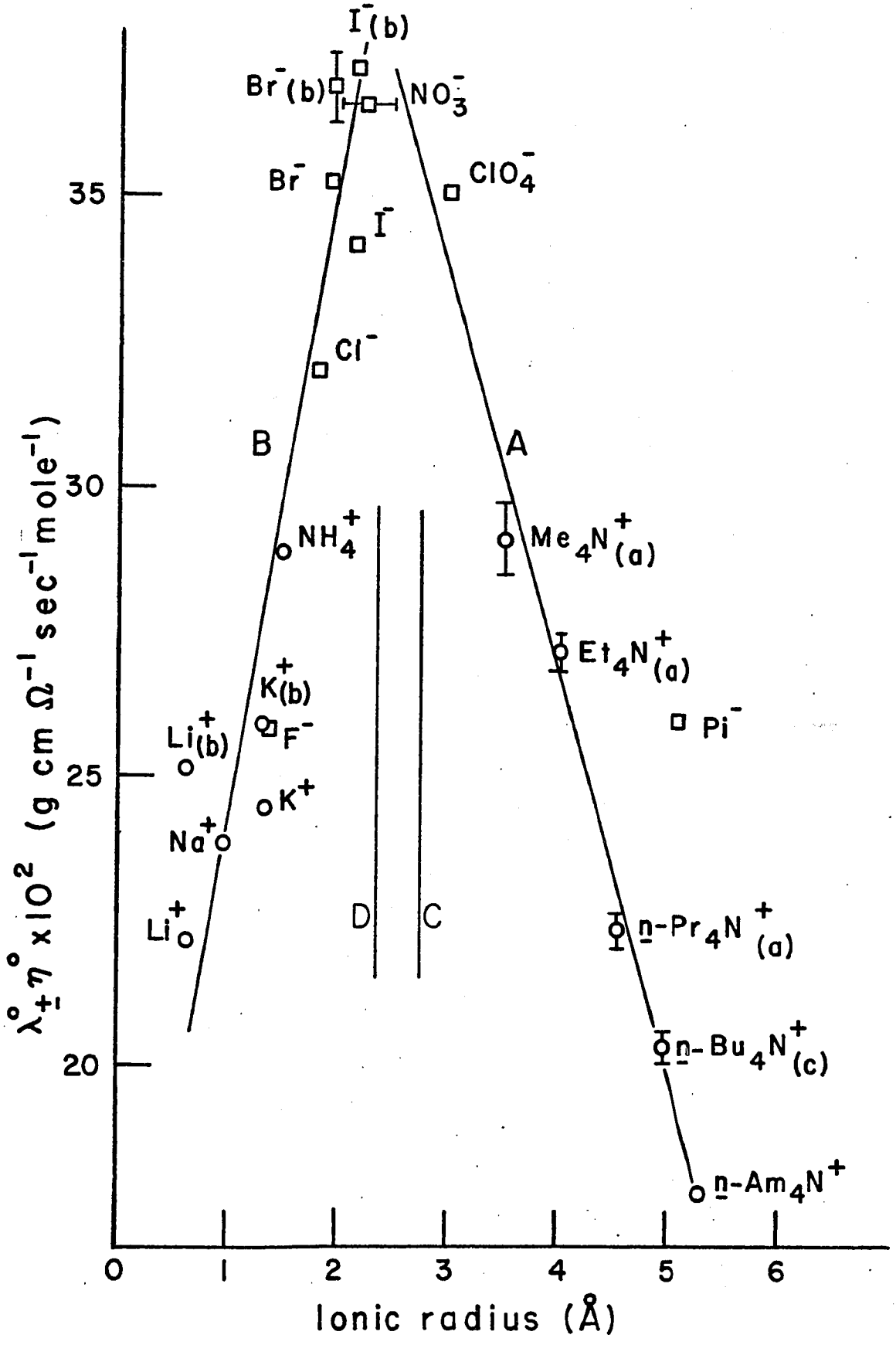
$I^-_{(b)}$
$Br^-_{(b)}$
NO_3^-
Br^-
ClO_4^-
I^-
Cl^-
B
A
NH_4^+
$Me_4N^+_{(a)}$
$Et_4N^+_{(a)}$
$K^+_{(b)}$
$Li^+_{(b)}$
F^-
Pi^-
K^+
Na^+
Li^+
D
C
n-$Pr_4N^+_{(a)}$
n-$Bu_4N^+_{(c)}$
n-Am_4N^+
35
30
25
20
0
1
2
3
4
5
6
$\lambda^\circ_\pm \eta^\circ \times 10^2$ (g cm Ω^{-1} sec^{-1} $mole^{-1}$)
Ionic radius (Å)

Table 4.4(a)

Conductivity Parameters in Acetone at Atmospheric Pressure and 25°C

Salt	Λ_o ($cm^2\Omega^{-1}mole^{-1}$)	λ^o_+	λ^o_-	$K_d \times 10^3$ (mole l^{-1})	Ion Size (Å)	Reference
n-Bu_4NFBPh_3	132.4	67.1	67.1	19.7	6.11_a	Reynolds and Kraus (108)
n-Bu_4NPi	152.4	67.1	85.3	22.3	6.75	
n-Bu_4NClO_4	182.4	67.1	115.3	9.58	4.45	
n-Bu_4NNO_3	187.2	67.1	120.1	5.46	3.82	
n-Bu_4NBr	183.0	67.1	115.9	3.29	3.41	
n-Bu_4NI	179.4	67.1	112.3	6.48	3.98	
Et_4NPi	176.5	91.2	85.3	17.5	5.69	
Me_4NFBPh_3	165.1	98.0	67.1	6.93	4.05	
Me_4NF	183	98.0	85	0.77	2.69	
LiPi	158.1	72.8	85.3	1.03	2.80	
NaPi	163.7	78.4	85.3	1.35	2.92	
KPi	165.9	80.6	85.3	3.43	3.45	
KI	192.8	80.5	112.3	8.02	4.22	
KCNS	201.6	80.5	121.0	3.83	3.52	

Table 4.4(a) (cont.)

Salt		Λ_o	λ_+^o	λ_-^o	$K_d \times 10^3$	Ion size		Reference
		($cm^2 \Omega^{-1} mole^{-1}$)			(mole l^{-1})	(Å)		
NH_4Pi		180.2	94.9	85.3	1.11	2.84_a		McDowell and Kraus
Me_4NPi		183.1	97.8	85.3	11.2	4.69		(109)
$\underline{n}\text{-}Pr_4NI$		190.6	78.3	112.3	4.98	3.74		
$\underline{n}\text{-}Am_4NBr$		174.4	58.5	115.9	4.25	3.60		
Octd.$\underline{n}\text{-}Bu_3NI$		163.6	51.3	112.3	5.99	3.90		
$Octd_2.\underline{n}\text{-}Bu_2NI$		157.2	44.9	112.3	6.77	4.03		
$\underline{n}\text{-}Bu_4NCl$		172.3	67.1	105.2	2.28	3.19		
$\underline{n}\text{-}Bu_4NPi$	(108)$_c$	152.34(0.08)			$59(14)_e$	9.10	$4.6(0.2)_b$	Evans, Zawoyski,
$\underline{n}\text{-}Bu_4NClO_4$	(108)	182.8(0.1)			12.5(0.6)	4.89(0.1)	5.8(0.2)	and Kay (110)
$\underline{n}\text{-}Bu_4NNO_3$	(108)	187.11(0.01)			6.99(0.02)	4.06(0.00)	4.96(0.02)	
$\underline{n}\text{-}Bu_4Br$	(108)	183.2(0.1)			3.79(0.05)	3.52(0.01)	5.4(0.2)	
$\underline{n}\text{-}Bu_4NI$	(108)	180.3(0.2)			6.99(0.28)	4.06(0.04)	6.1(0.3)	
Et_4NPi	(108)	176.65(0.03)			22.2(0.9)	6.7(0.3)	6.3(0.1)	
Me_4NF	(109)	182.7(0.03)			0.877(0.003)	2.75(0.00)	0.8(0.5)	
LiPi	(108)	157.7(0.2)			1.22(0.1)	2.87(0.03)	1.5(0.1)	

Table 4.4(a) (cont.)

Salt	Λ_o ($cm^2 \Omega^{-1} mole^{-1}$)	$K_d \times 10^3$ (mole l^{-1})	Ion size (Å)		Reference
NaPi	(108) 163.5(0.2)	1.47(0.02)	2.96(0.00)	5.4(0.3)[b]	Evans, Zawoyski,
KPi	(108) 166.0(0.1)	4.10(0.08)	3.58(0.01)	5.0(0.2)	and Kay (110)
Me_4NPi	(109) 183.4(0.1)	14.9(0.2)	5.25(0.04)	5.8(0.1)	
$n\text{-}Pr_4NI$	(109) 190.72(0.03)	6.17(0.25)	3.94(0.03)	5.2(0.6)	
$n\text{-}Am_4NBr$	(109) 174.7(0.1)	4.54(0.37)	3.65(0.08)	7(1)	
$n\text{-}Pr_4NPi$	(111) 156.2(0.1)	37(8)[e]	9.10	5.2(0.4)	
NaI	(111) 183.6(0.2)	5.65(0.44)	3.85(0.05)	14(1)	
KCNS 25°C	202.2	3.4	3.39		Sears, Wilhoit,
20°C	191.6	3.8	3.42		and Dawson (97)
10°C	173.7	4.2	3.44		
0°C	154.4	5.2	3.51		
-10°C	138.1	6.0	3.58		
-20°C	122.2	6.8	3.63		
-30°C	106.7	8.5	3.80		
-40°C	92.3	9.6	3.89		
-50°C	78.1	10.9	4.00		

Table 4.4(a) (cont.)

Salt		Λ_o ($cm^2 \Omega^{-1} mole^{-1}$)	$K_d \times 10^3$ (mole l^{-1})	Ion size (Å)		Reference
n-Bu_4NI	25°C	180.2	6.1	3.85_a		Sears, Wilhoit,
	20°C	171.2	6.8	3.90		and Dawson (97)
	10°C	155.2	7.7	3.95		
	0°C	139.3	8.5	3.98		
	-10°C	124.7	9.6	4.04		
	-20°C	110.1	10.8	4.11		
	-30°C	96.4	11.8	4.19		
	-40°C	82.8	13.6	4.34		
	-50°C	69.8	15.5	4.50		
LiCl		214(4)	0.0033 (0.0001)	1.60(0.00)	2.17_d	Savedoff (98)
LiBr		194(3)	0.219(0.007)	2.30(0.01)	3.25	
LiI		195.0(0.2)	6.91(0.16)	4.05(0.02)	5.50	
Li p-toluene-sulphonate		172(2.5)	0.0096 (0.0003)	1.71(0.01)		
KI		197.52(0.08)	5.57(0.03)	3.84(0.00)		
n-Bu_4NCl		188(2)	1.66(0.1)	3.02(0.03)		
n-Bu_4N p-toluene-sulphonate		151.6(0.2)	2.46(0.03)	3.23(0.01)		

Table 4.4(a) (cont.)

a. ion size parameter obtained by fitting the dissociation constant to the Fuoss equation

b. ion size parameter from the Fuoss-Onsager conductance theory

c. recalculated data from the references indicated according to the Fuoss-Onsager treatment

d. ion size parameter calculated from the Denison-Ramsey equation

e. the maximum K_d predicted by the Fuoss equation is 26.0×10^{-3} corresponding to an ion size parameter of 9.10Å

Table 4.4(b)

Stokes Law Ionic Radius at 26.61°C and Atmospheric Pressure

(Å)

	Me_4NI	Et_4NI	$n\text{-}Pr_4NI$
Cationic	2.80(0.05)	3.00(0.01)	3.54(0.02)
Anionic	2.44(0.04)	2.44(0.01)	2.47(0.02)
Sum	5.24(0.09)	5.44(0.02)	6.01(0.04)
Sum of crystallographic radii	5.63	6.16	6.68

the acetone molecule, 2.8 Å, estimated by Zeidler (26). The maximum in the limiting equivalent conductivity at about 2.5 Å is a striking illustration of the size factor in determining the extent of solvation and, therefore, the transport behaviour of ions. Line A includes the large ions which presumably interact only weakly with the acetone dipoles because of their low surface charge density. The conductivity decreases almost linearly with increasing radius except for Me_4N^+ which falls below curve A; Me_4N^+ interacts more strongly with the acetone dipoles than the other tetraalkylammonium ions. Ions with smaller radii than about 2.3 Å, which are represented by line B, have decreasing limiting equivalent conductivities as the ionic radius decreases. This indicates that these ions interact strongly with the acetone dipoles producing solvodynamic entities for which effective radii are identical to ions having the same Walden product on line A. For example, the solvated Li^+ ion has approximately the same effective hydrodynamic radius as the $n\text{-}Pr_4N^+$ ion, which is not solvated.

Nightingale (112), in constructing a plot of the crystal radii versus the hydrated radii of ions in water, found a broad minimum at about 2.5 Å. This minimum corresponds to a maximum in the Walden product. There is also a break in this curve at about 1.3 Å which roughly corresponds to the radius of a water molecule. The interpretation of this feature of such plots is that when the radius of an ion approaches the same value as the radius of the solvent molecules, ionic transport can more easily occur by the same mechanism as that of the self-diffusion of the solvent.

If a simple ion-dipole interaction is assumed to hold between an ion and an acetone molecule, for example the ClO_4^- or NO_3^- ions which

have approximately the same radius as acetone, it is possible to calculate the ionic radius below which the ion-dipole interaction energy is greater than the heat of vaporization at 25°C. Following the procedure given by Gurney (113) and taking the heat of vaporization to be 7.403 kcal mole^{-1} as calculated from the measurements of Pennington and Kobe (114) for 25°C, the critical ionic radius can be estimated. The distance r between the center of the ion and the center of the dipole when the dipole axis is oriented along the line joining the centers of the ion and the dipole is given by

$$r = (\mu e / \Delta H_v)^{\frac{1}{2}} \qquad (4.2)$$

$$= \left\{ \frac{4.80\times10^{-10} \times 2.85\times10^{-18} \times 6.024\times10^{23} \times 10^{16}}{7.403\times10^{3} \times 4.184\times10^{7}} \right\}^{\frac{1}{2}}$$

$$= 5.16 \text{ Å}$$

where e is the electronic charge

μ is the dipole moment of acetone

ΔH_v is the heat of vaporization of acetone at 25°C

The radius of an acetone molecule is about 2.8 Å; therefore, when ions have a radius of about 5.16-2.8 = 2.36 Å or less at 25°C and atmospheric pressure, solvation by acetone molecules can be expected. In a similar calculation, Nightingale (112) interpreted the broad minimum in the plot of the hydrated radii of aqueous ions against their crystal radii to indicate the strong hydration of ions with radii less than about 2.3 Å.

Before interpreting the pressure dependence of the Walden products in terms of the above analysis, it is useful to review a conclusion reached by Gopal and Rizvi (115), also supported by Nightingale (112), that the solvated volume of an ion increases with temperature to a greater extent for ions which have minimal solvation at low temperatures.

This effect in aqueous media is due to the thermal disruption of the water structure at high temperatures. This permits a greater hydration of these ions at high temperature, because at low temperature the ion-solvent interaction is too weak with respect to the solvent-solvent interaction to bind the water molecules to the ions. The Walden product of ions near the maximum in Figure 4.1 would therefore be expected to decrease with temperature. This result was found by Nightingale (112) for those ions in aqueous solution near the minimum in the plot alluded to above. The broadness of the minimum in this plot for water is related to the wide range of possible interaction energies between water molecules, as was discussed in Chapter 1. In acetone, the primary intermolecular interactions are the dipole-dipole forces which have an inverse cube dependence on the separation of the interacting dipoles. The probability distribution curve of intermolecular energies is probably much narrower than in water, so that the extent of solvation, and hence the mobility, is strongly dependent on the ionic radius; the maximum in Figure 4.1 is thus quite sharp.

The effect of pressure on the Walden product will also be a strong function of the ionic radius. In the paper discussed above, by Skinner and Fuoss (105), an increase was observed in the Walden product of n-Bu_4NBr with pressure but not in that of n-Bu_4NBPh_4. This is probably due to the fact that although the n-Bu_4N^+ ion is not solvated in either salt, and increasing the pressure has little effect on the degree of its solvation, the Br^- ion is somewhat solvated at atmospheric pressure and the extent of its solvation is decreased by pressure. This would not be the case for the BPh_4^- anion which would be expected to remain unsolvated

at all pressures because of its large size. Since an increase with pressure in the Walden products was observed for the three salts investigated in acetone, the extent of interaction of these ions with the solvent must be decreased relative to the solvent-solvent interactions by compression. A clearer analysis of this interaction can be obtained by a consideration of conductivity as a process of ions moving between equilibrium positions of low free energy by a jump mechanism.

The above discussion could be extended if transport numbers in acetone were available at other than 25°C and atmospheric pressure. On the assumption that the transport numbers of $\underline{n}$-Bu_4NBPh_4 are not a function of pressure, Skinner and Fuoss (105) have interpreted the variation of the Walden product with pressure in terms of the dielectric relaxation of the solvent. The Stokes radius was found to decrease with increasing pressure, or increasing dielectric constant, for all the ions treated by this theory except for $\underline{n}$-Bu_4N^+ and BPh_4^-. The Stokes radii of these ions were independent of pressure. However, these results are not thought to be conclusive, especially for Na^+ and Br^-, since the points extrapolated to a negative radius for $\epsilon^{-1} \rightarrow 0$ (very high pressure).

The decrease in the Stokes radii with pressure is the opposite to that expected from electrostriction considerations. Ions might be expected to cause greater compression of solvent at high pressures where the lower volume of the system is energetically more favorable. However, to counter this effect the attractive intermolecular forces between acetone molecules are enhanced by pressure (Apendix I). It therefore becomes more difficult for acetone molecules to be removed from the bulk solvent into the

solvation spheres of the ions. Since the Walden products increase with pressure (decrease with temperature), a decrease in the extent of solvation of the ions with pressure (increased solvation with temperature) is suggested. However, it would appear that the many assumptions involved in the dielectric relaxation treatment make the results obtained quite uncertain.

The Stokes-law ionic radii were calculated from the Walden products at 26.61°C and atmospheric pressure, on the basis of the transport numbers estimated by Reynolds and Kraus (108), using the equation given by Robinson and Stokes (116):

$$r_i = \frac{0.820}{\lambda_i^\circ \eta^\circ} \qquad (4.5)$$

where r_i is the Stokes radius of the ion in Å

The results are shown in Table 4.4(b). The Stokes radii increase with the size of the cations estimated by Robinson and Stokes (116): Me_4N^+, 3.47 Å; Et_4N^+, 4.00 Å; and $\underline{n}\text{-}Pr_4N^+$, 4.52 Å. However, the Stokes radii in acetone are all less than the estimates of the radii of the cations. The average Stokes radius obtained for I^- of 2.45±0.04Å is in good agreement with both Savedoff (98), 2.40 Å, and Hughes and Hartley (117), 2.36 Å. The Stokes radius of I^- is greater than the crystal radius given by Gourary and Adrian (118) of 2.05 Å or by Pauling (28) of 2.16 Å.

From these considerations it can be concluded that there is not a permanent primary solvation shell which accompanies these ions as they move through the solution. If this were the case, the Stokes radius would be expected to be much larger than the crystal radius as it is, for example, for Li^+. The crystal radius of Li^+ is 0.60 Å according to

Pauling (28), compared to the Stokes radius measured in acetone by Savedoff (98) of 3.16 Å.

C Energy of Activation for Conductivity at Constant Volume, E_V, and at Constant Pressure, E_p, and the Pressure Coefficient of Conductivity

In a conductivity study of several salts in N,N-dimethylformamide (D.M.F.) which encompassed a range of temperatures and pressures similar to that employed here, Brummer (119) has discussed the interpretation of E_V and E_p with a view to gaining an understanding of limiting equivalent conductivity. The analysis was based on the activated-complex theory of conductivity proposed by Stearn and Eyring (120), in which it is assumed that migration of an ion occurs by a discrete jump over a free-energy barrier to transport between positions of equilibrium in the liquid. Brummer has made a careful review of equations similar to that of Stearn and Eyring (120). Two slightly different approaches are given by Glasstone, Laidler, and Eyring (121). The second treatment, which has been applied to proton transfer in hydroxylic solvents in this theoretical derivation, has been generalized by Bockris, Kitchener, Ignatowicz, and Tomlinson (122). In connection with the electric conductance of simple molten electrolytes, Bockris, Crook, Bloom, and Richards (123) have elaborated a theory which separates the process of the ion jumping between equilibrium positions and the formation of a hole in the liquid. These aspects will be discussed further in connection with the difference between E_V and E_p. In this discussion, the equation adopted by Brummer (124) and Brummer and Hills (125), which differs from the treatment of viscosity and diffusion given by Glasstone, Laidler, and Eyring (126) by a factor of six in the denominator of

the pre-exponent, will be employed. The limiting equivalent ionic conductivity is therefore assumed to be given by the equation

$$\lambda_i^o = \frac{z\,e\,F}{6\,h}\,L^2 \exp(-\bar{\mu}_o^{\ddagger}/RT) \qquad (4.4)$$

where ze is the charge of the ion

F is the Faraday constant

h is Planck's constant

L is the jump distance between equilibrium positions

$\bar{\mu}^{\ddagger}_o$ is the change in chemical potential for the ion to reach the saddle point or col of the free-energy barrier

the transmission coefficient is assumed to be unity

This equation can also be written as

$$\lambda_i^o = \frac{z\,e\,F}{6\,h}\,L^2 \exp(\Delta\bar{S}_o^{\ddagger}/R) \exp(-\Delta\bar{H}_o^{\ddagger}/RT) \qquad (4.5)$$

where $\Delta\bar{S}_o^{\ddagger}$ and $\Delta\bar{H}_o^{\ddagger}$ are the partial molar standard entropy and enthalpy of conductivity respectively

On differentiating equation (4.5) with respect to temperature, first at constant pressure then at constant volume, the following results are obtained;

$$RT^2\left(\frac{\partial \ln \lambda_i^o}{\partial T}\right)_P = 2RT^2\left(\frac{\partial \ln L}{\partial T}\right)_P + (\Delta\bar{H}_o^{\ddagger})_P = E_P \qquad (4.6)$$

$$RT^2\left(\frac{\partial \ln \lambda_i^o}{\partial T}\right)_V = 2RT^2\left(\frac{\partial \ln L}{\partial T}\right)_V + (\Delta\bar{U}_o^{\ddagger})_V = E_V \qquad (4.7)$$

where $(\Delta\bar{U}_o^{\ddagger})_V$ is the partial molar standard internal energy of activation for conductivity at constant volume,

the other quantities have been defined previously

Equation (4.7) can be further simplified if it is assumed that

$\left(\frac{\partial \ln L}{\partial T}\right)_V$ is approximately zero, so that E_V is identified with $(\Delta \bar{U}_o^{\ddagger})_V$. E_P, however, is a more complex function involving the isobaric coefficient of expansion of the solvent as well as the enthalpy term $(\Delta \bar{H}_o^{\ddagger})_P$:

$$E_P = (2/3)\ R\ T^2 \alpha + (\Delta \bar{H}_o^{\ddagger})_P \qquad (4.8)$$

since $\left(\frac{\partial \ln L}{\partial T}\right)_P = (1/3)\left(\frac{\partial \ln V}{\partial T}\right)_P$

$$= \frac{\alpha}{3} \qquad (4.9)$$

It has been shown by Brummer and Hills (125) and Evans and Polanyi (127) that E_P and E_V are related as follows:

$$E_P - E_V = (\pi + P)\ \Delta \bar{V}_o^{\ddagger} + (2/3)\ R\ T^2 \alpha \qquad (4.10)$$

$$= (\pi + P)((\Delta \bar{V}_o^{\ddagger}) + (2/3)\ R\ T \beta)$$

where $\left(\frac{\partial U}{\partial V}\right)_T$ is the internal pressure of the solvent π

$\Delta \bar{V}_o^{\ddagger}$ is the partial molar standard volume of activation for conductivity

When equation (4.5) is differentiated with respect to pressure at constant temperature, the partial molar standard volume of activation is defined as shown earlier in equation (3.27):

$$-R\ T\left(\frac{\partial \ln \lambda_i^o}{\partial P}\right)_T = -2\ R\ T\left(\frac{\partial \ln L}{\partial P}\right)_T + \Delta \bar{V}_o^{\ddagger} \qquad (4.11)$$

Since $\left(\frac{\partial \ln L}{\partial P}\right)_T = (1/3)\left(\frac{\partial \ln V}{\partial P}\right)_T$

$$= -\frac{\beta}{3} \qquad (4.12)$$

where β is the isothermal compressibility of the solvent, equation (4.11) can be written as

$$\Delta \bar{V}_o^{\ddagger} = -R\ T\left(\frac{\partial \ln \lambda_i^o}{\partial P}\right)_T - (2/3)\ R\ T \beta \qquad (4.13)$$

Equations (4.6), (4.7), (4.8), (4.10), and (4.13) constitute the theoretical framework within which the calculations of Chapter 3 have been carried out.

It is clear from the number of authors who have recently commented on the differences observed in the constant-pressure and constant-volume parameters of the transport, chemical equilibria, and chemical reaction studies in the liquid phase, that interest is returning to an aspect of the study of liquids which has been somewhat neglected over the past two decades (121,128,129,130,131,132,71,133,134,127,135). In some instances it has been found that the constant-volume parameters are simpler than the corresponding constant-pressure parameters. For example, Newitt and Weissenberg (133), in a study of the kinetics of the association of cyclopentadiene, found that the Arrhenius activation energy at constant volume, E_V, and the pre-exponent, A_V, were constant up to 3000 atmospheres, whereas the corresponding constant-pressure parameters, E_P and A_P, increased markedly. Qualitatively, it is to be expected that if the temperature coefficient for a process is to constitute a meaningful basis for the calculation of the energy required for that process to occur, the environment for that process should not vary with change in temperature. At constant volume, the intermolecular distances remain essentially unchanged as the temperature is varied; the energy of activation at constant volume on this basis is representative of the process itself and does not contain a term which depends on the variation in the intermolecular potential between the solvent molecules. This view has been put forward for diffusion in liquids by Nagarajan and Bockris (131) and for liquid viscosity by Bondi (130). It is most important, however, to recognize that the simplicity of constant-volume

parameters over constant-pressure parameters requires that the solvent has no temperature-sensitive structure. It has been shown in the compressibility study of acetone (see Appendix I), that the heat capacity of acetone at constant volume is a function of temperature, especially at small volumes. In acetone, therefore, the constant-volume parameters may not have this simple and more direct interpretation. Related to this consideration is that the nature of the mobile ionic species may be a function of temperature at constant volume as well as at constant pressure. Solvent molecules are less bound to each other by dipole-dipole interactions as the temperature is raised at constant volume or at constant pressure. Solvent molecules are, therefore, more easily bound to the ions at high temperatures, an effect which causes curvature in the Arrhenius plots at either constant pressure or constant volume.

D The Hole Theory of Liquids and Transport Properties

The differences between constant-volume and constant-pressure parameters can be given a physical interpretation in terms of the hole model of liquids. It is first necessary to justify the application of a hole theory to liquids in general and to acetone in particular. Hildebrand and Scott (136) have presented several arguments against the reality of holes of a molecular size or the use of the concept of free volume to calculate thermodynamic properties of liquids, stressing that "all liquids with fairly symmetrical molecules possess equal amounts of configurational entropy under the conditions of comparison, a situation quite unlikely to exist if the molecular disorder in them were less than maximum". However, there need be no postulate of a pseudo-lattice structural model of the liquid state for a theory of holes to be developed. Bockris and

Richards (137), on the basis of an earlier treatment of a hole theory of liquids by Fürth (138), suggested that the holes have sizes that are thermally distributed and that they arise from density fluctuations in the liquid. Brummer (119) has suggested that the view of Watts, Alder, and Hildebrand (139), that movement of a molecule occurs by a weakening of the cage surrounding the molecule, differs only semantically from a hole model of the liquid where a hole is supposed to arise near a molecule by a density fluctuation. However, there is more than a semantic difference between the two views. Hildebrand and Scott (136) strongly support the views of Alder and Wainwright (140) which are based on the computed trajectories of hard-sphere molecules in which diffusion is found to occur by a process of random walk with very small steps. Nagarajan and Bockris (131), in studies of the self-diffusion in molten salts at constant volume, do not support a micro-jump model such as that described above, or the model of Swalin (141) in which small random movements of about 0.1 Å of the diffusing species occurs. Their observations can be best interpreted in terms of a hole model of the liquid. They suggest that a liquid containing no holes of the size of the diffusing particles should be considered for the sake of argument. Since the diffusing particle must open a hole of its own size when it moves in such a liquid, the energy of activation at constant volume would have to contain the energy of hole formation as well as the energy of activation for jumping. However, their results indicate that the energy of activation at constant volume is much less than the energy of activation at constant pressure (E_V is about 15-20% of E_P). This indicates that E_V does not contain the energy of hole formation. This relation between E_V and E_P is observed for conductivity in acetone as can

be seen in Tables 3.19 and 3.20. These observations lend strong support to the important part that holes in the liquid must play in the mechanism of transport. They also support a hole model of the liquid state. Before outlining a quantitative theory of a hole mechanism of transport, it is thought that further evidence for the hole theory of liquids of simple organic molecules such as acetone ought to be presented.

The temperature dependence of the viscosity of liquids well above their melting points is adequately described by the Arrhenius equation. However, near the melting point or at high pressure this equation does not hold in its simple form. An equation in which $\exp(E_{act}/RT)$ is replaced by $\exp(E_{act}/R(T-T_o))$, where T_o is a constant, has been found by Angell (142) to represent the viscosity results more accurately. In connection with the effect of volume on the temperature dependence of the viscosity of associated liquids or of van der Waals liquids at small volume, Bridgman (143) has reported that the viscosity varies markedly with temperature at constant volume. The nature of this temperature dependence of viscosity was not stated, except that the nature of the dependence was indicated to be a function of the volume. Contrary to the view of Hildebrand and Scott (136), these observations are thought to be best interpreted by a model of the liquid state which emphasizes the importance of free volume. In the non-Arrhenius region, according to Angell (7,142) and Davies and Matheson (144), a free-volume parameter should be considered. Free volume, v_f, is defined as the expansion volume $(v-v_o)$ where v is the specific volume of the liquid at temperature T and v_o is the specific volume of the liquid at temperature T_o at which the mobility of the molecules is effectively zero. Angell (7) suggests that T_o

corresponds to the theoretical glass transition temperature where $v_f \rightarrow 0$ and, therefore, $\Lambda_o \rightarrow 0$, $D \rightarrow 0$, and $\eta \rightarrow \infty$. In the liquid range of a substance, a discontinuity often occurs in the temperature dependence of the viscosity which divides Arrhenius behaviour from non-Arrhenius behaviour. According to Davies and Matheson (144), the temperature at which such a discontinuity is found should correspond to a second-order thermodynamic transition. In the temperature range investigated in acetone at atmospheric pressure, the behaviour of the viscosity is Arrhenius. However, in a compressed condition in this temperature range, acetone shows some evidence that the heat capacity at constant volume, as a function of temperature, goes through a minimum (see Appendix I). This effect would constitute a second-order thermodynamic transition. It is, therefore, thought that at high pressures a free-volume theory should describe the transport properties observed in acetone.

The physical model treated by Davies and Matheson (144) involves restriction of rotational modes of freedom as the amount of free volume is reduced. In the Arrhenius region the molecules have sufficient rotational freedom to reorientate several times between translational jumps. However, in the non-Arrhenius region, reorientation between translational jumps is hindered because one or more rotational degrees of freedom are lost. A molecule may possess sufficient energy to jump, but may not be capable of jumping. It may lose the ability to reorientate itself in order to move into a position where surrounding molecules have momentarily opened up sufficient free volume. The viscosity of liquids at high pressures has been treated by a free-volume formulation by Matheson (145).

Angell (7) states that measurements of the effect of pressure

on relaxation properties have not been in accord with free-volume model predictions. This assertion was based on a statement by Brummer (119) that his conductivity results did not support the Cohen and Turnbull (146) free-volume theory. According to Cohen and Turnbull, the diffusion coefficient, D, for free-volume-limited transport should vary as $T^{\frac{1}{2}}$ at constant volume. The Nernst-Einstein equation (147)

$$\lambda_i^o = \frac{F^2}{RT} z_i D_i^o \qquad (4.14)$$

where λ_i^o is the limiting equivalent ionic conductivity

D_i^o is the limiting ionic diffusion coefficient

z_i is the charge of ionic species i

F is the Faraday constant

relates the diffusion coefficient and the limiting equivalent conductivity for cases where the moving species translate under identical local conditions ($\lambda_+^o = \lambda_-^o$). On the assumption that this equation holds, Λ_o should be a linear function of $T^{-\frac{1}{2}}$ at constant volume, under conditions where the process is free-volume-limited. Brummer (119) states, for several salts in D.M.F., that Λ_o increases with temperature rather more rapidly than with $T^{-\frac{1}{2}}$. However, when these data were plotted in Figure 4.2 at several volumes, they appeared to be quite linear except possibly at high volumes where the process would not be expected to be free-volume-limited. A similar plot of the results in acetone is shown in Figure 4.3. Particularly for Et_4NI and $n\text{-}Pr_4NI$, it can be seen that the curvature present at large volume disappears at smaller volumes. The Me_4NI results, plotted in Figure 4.4, do not show this trend. A plot of Λ_o against $T^{\frac{1}{2}}$ at constant pressure, in Figure 4.4, indicates that Me_4NI behaves differently from the other two salts. This is

Figure 4.2. Test of free-volume theory with the high-pressure conductivity data of Brummer (119) in N,N-dimethylformamide.

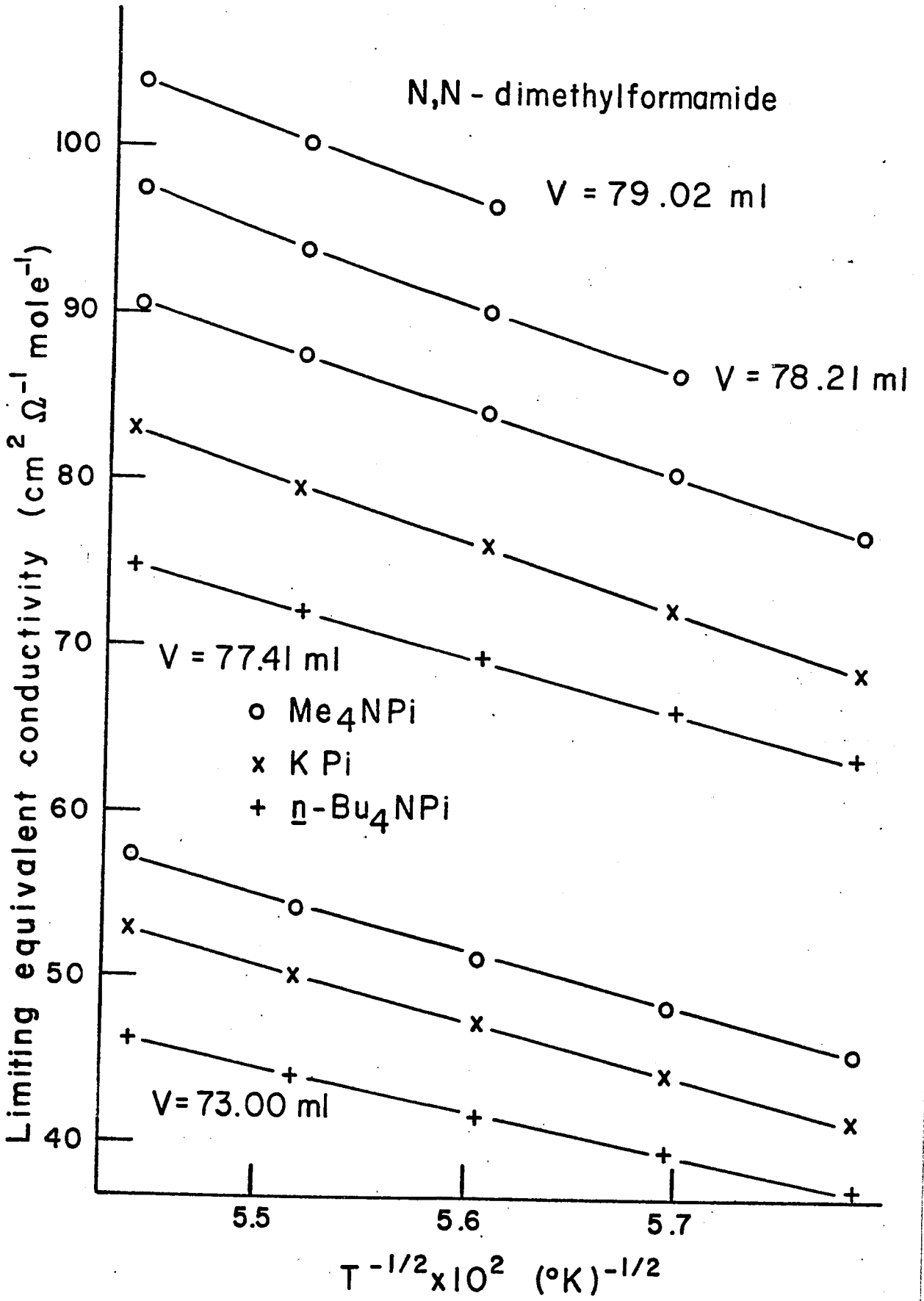
N,N - dimethylformamide
V = 79.02 ml
V = 78.21 ml
V = 77.41 ml
V = 73.00 ml
o Me4NPi
x K Pi
+ n-Bu4NPi
Limiting equivalent conductivity (cm2 Ω-1 mole-1)
100
90
80
70
60
50
40
5.5
5.6
5.7
T-1/2 x 10^2 (°K)-1/2

Figure 4.3. Test of free-volume theory with high-pressure conductivity data in acetone.

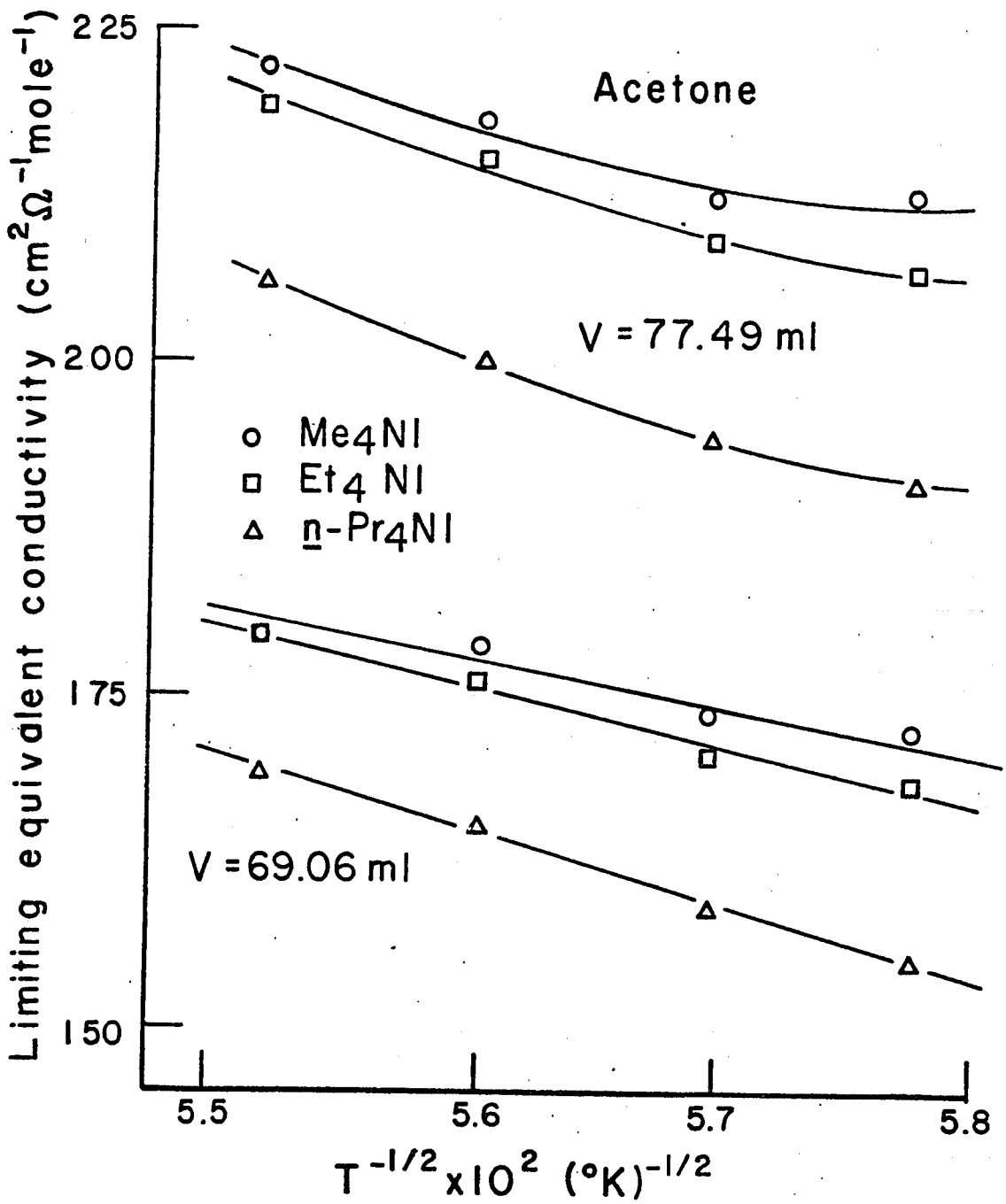
Acetone
V = 77.49 ml
V = 69.06 ml
o Me4NI
□ Et4 NI
△ n-Pr4NI
225
200
175
150
5.5
5.6
5.7
5.8
Limiting equivalent conductivity (cm²Ω⁻¹mole⁻¹)
T⁻¹/² x10² (°K)⁻¹/²

Figure 4.4. Λ_o plotted against $T^{+\frac{1}{2}}$ at two pressures.

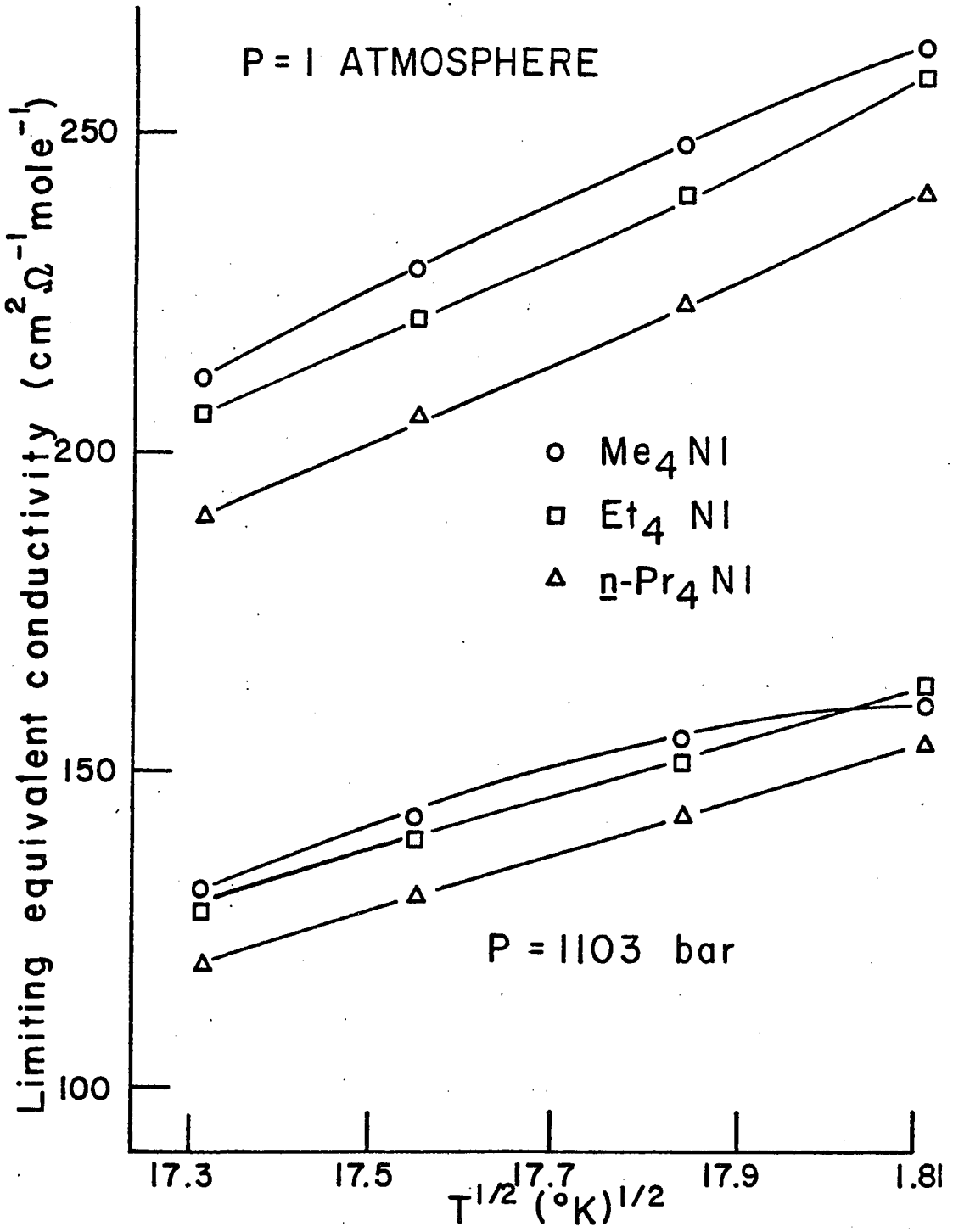
P = 1 ATMOSPHERE
P = 1103 bar
o Me4 NI
□ Et4 NI
△ n-Pr4 NI
Limiting equivalent conductivity (cm2Ω-1mole-1)
250
200
150
100
17.3
17.5
17.7
17.9
1.81
T1/2 (°K)1/2

thought to be a result of the temperature-dependent solvation effect discussed above. A hole model of conductance will be used to interpret the observations in acetone.

The free energy of activation for conductivity at constant pressure, E_p, is assumed to contain a partial free-energy term for hole formation, $\Delta\bar{G}_h$, as well as a partial free energy of activation for jumping, $\Delta\bar{G}_j^{\ddagger}$, in the theory of conductivity outlined below. Application of the equation given by Nagarajan and Bockris (131) for diffusion in fused salts gives the following conductance equation which refers to constant-pressure conditions:

$$\Lambda_o = \text{constant} \times \exp\left[(\Delta\bar{S}_h + \Delta\bar{S}_j^{\ddagger})/R \right] \exp\left[-(\Delta\bar{H}_h + \Delta\bar{H}_j^{\ddagger})/RT \right] \qquad (4.15)$$

where the subscripts h and j refer to parameters of hole formation and jump respectively

This equation is based on the concept developed by Frenkel (148) for crystal defects. The number of holes per mole of liquid, N_h, in equilibrium with the number of molecules per mole of liquid is given by the relationship

$$N_h/N = \exp(-\Delta\bar{G}_h/RT) \qquad (4.16)$$

To obtain equation (4.15), equation (4.16) has been combined with a probability factor, $\exp(-\Delta\bar{G}_j^{\ddagger}/RT)$, which predicts the probability of a collision between a hole and an ion, that is the probability for a jump to take place. Comparison of equations (4.15) and (3.28) gives

$$E_P = (\Delta\bar{H}_h)_P + (\Delta\bar{H}_j^{\ddagger})_P \qquad (4.17)$$

In the formulation by Nagarajan and Bockris (131), $(\Delta\bar{H}_j^{\ddagger})_P$ is written as an energy of activation for jumping, but it is preferable to write it as an enthalpy of activation following Brummer (124).

Further, for constant-volume conditions, the enthalpy function becomes an internal-energy function, so that comparing equations (4.15) and (3.29) the following relationship can be written

$$E_V = (\Delta\bar{U}_h)_V + (\Delta\bar{U}_j^{\ddagger})_V \qquad (4.18)$$

In order to identify E_V with an energy associated solely with the jump process in liquid transport, it must be demonstrated that $(\Delta\bar{U}_h)_V$ is negligible compared to $(\Delta\bar{U}_j^{\ddagger})_V$. This point has been considered for the case of fused salts by Nagarajan and Bockris (131) in the following way. They assume that change in the volume of a liquid with temperature is largely a result of an increase in the free volume or the total volume of holes:

$$V_{T_2} - V_{T_1} = (N_h v_h)_{T_2} - (N_h v_h)_{T_1} \qquad (4.19)$$

where v_h represents the most probable volume of the holes

N_h is given by equation (4.16)

T_1 and T_2 are two temperatures, $T_2 > T_1$

It is assumed that v_h is independent of temperature at constant volume. Combining equations (4.19) and (4.16) and noting that $V_{T_2} - V_{T_1}$ is zero at constant volume gives

$$\exp(-\Delta\bar{G}_h/RT_2) - \exp(-\Delta\bar{G}_h/RT_1) = 0 \qquad (4.20)$$

This equation implies that the change of $\exp(-\Delta\bar{G}_h/RT)$ with temperature at constant volume is zero. This is the same as saying that $(\Delta\bar{U}_h)_V$ is zero, which is the point in question. Therefore, if we assume that the most probable volume of holes is not affected by a variation in the temperature at constant volume, the energy of activation at constant volume, E_V, may be equated to $(\Delta\bar{U}_j^{\ddagger})_V$. The two quantities $(\Delta\bar{H}_j^{\ddagger})_P$ and $(\Delta\bar{U}_j^{\ddagger})_V$ are identical if the movement of an ion into a hole is not accompanied by a volume change. This problem is discussed in connection

with the volume of activation parameter associated with conductivity. A hole theory of liquids based on density fluctuations in the liquid has been used by Bockris and Richards (137) to derive an equation which gives a rough correlation between the melting point, T_m, at atmospheric pressure and $\Delta \bar{H}_h$ for the viscous flow of a wide variety of liquid gases, hydrocarbons, simple organic liquids, and fused salts:

$$(\Delta \bar{H}_h)_P \doteq 3.74\ R\ T_m \qquad (4.21)$$

The predicted enthalpy of hole formation in acetone is 1.32 kcal mole^{-1}. The differences $E_P - E_V$ at atmospheric pressure, based on the results in Tables 3.19 and 3.20, are 1.16, 1.17, and 1.21 kcal mole^{-1} for Me_4NI, Et_4NI, and $n\text{-}Pr_4NI$ respectively. The constancy of this number for the three salts suggests that the same process is being measured for each salt and that this is indeed the enthalpy of hole formation in equation (4.17), $(\Delta \bar{H}_h)_P$. The results of Howard (149) in methanol solutions also tend to support the view that $E_P - E_V$ is nearly independent of the ionic species as would be expected if it represented the energy of hole formation.

If the trends in E_V are studied in Table 3.20, the usual increase with decreasing volume is found for $n\text{-}Pr_4NI$ and Et_4NI. This increase in E_V is associated with the enhanced solvent-solvent interactions present when the solvent is more densely packed. In contrast to the results reported by Brummer (119), which indicated that E_V was inversely proportional to the ion size, it was found that E_V increased with the ion size. The Me_4NI results appear to show a decrease in E_V with compression. This observation suggests that condition-variable solvation effects associated with smaller ions, which are near the peak of plots such as that in Figure 4.1, would somewhat limit the applicability of the simple hole theory. However, in keeping with the interpretation outlined above of

the increase in the Walden products with pressure, the decrease in E_V with pressure could also be interpreted as a lessening with pressure, of the solvation binding, relative to the solvent-solvent interaction, such that the energy of activation for the jump process is reduced. From the results of E_V as a function of volume reported by Brummer (119), particularly for KPi, where the solvation should be most important, there appears to be some indication of a minimum in E_V at the higher volume side of the plot.

The pre-exponents of the isochoric plots between $\ln\Lambda_o$ and T^{-1} have been plotted against the volume in Figure 4.5. The pre-exponent decreases with decreasing volume throughout the range of volumes studied, except for Et_4NI, which shows evidence of a minimum at about 71 ml. The results presented by Brummer (119) indicate that such minima are present in all of the salts he studied in D.M.F. As is indicated in equation (4.5), there are two unknowns in the pre-exponent, L, the jump distance, and $\Delta\bar{S}_o^{\ddagger}$, the partial molar entropy of activation. Brummer (119) has discussed the problem of estimating the pre-exponent. A transmission factor included in this term has been assumed to be unity. Estimates of the jump distance, L, have been made by Brummer from the equation

$$L = (V/N)^{1/3} \qquad (4.22)$$

where V is the molar volume of the liquid

N is Avogadro's number

With the L parameter calculated from equation (4.22), Brummer found that the calculated entropies, when plotted against the volume, paralleled the pre-exponent v.s. volume curves. The entropies were negative and had values from 7.5 to 6.5 e.u. Negative entropies of activation indicate that the activated state is more ordered than the initial state.

Figure 4.5. Semi-logarithmic plot of the pre-exponent of the isochoric plots of $\ln\Lambda_o$ versus T^{-1} against the volume

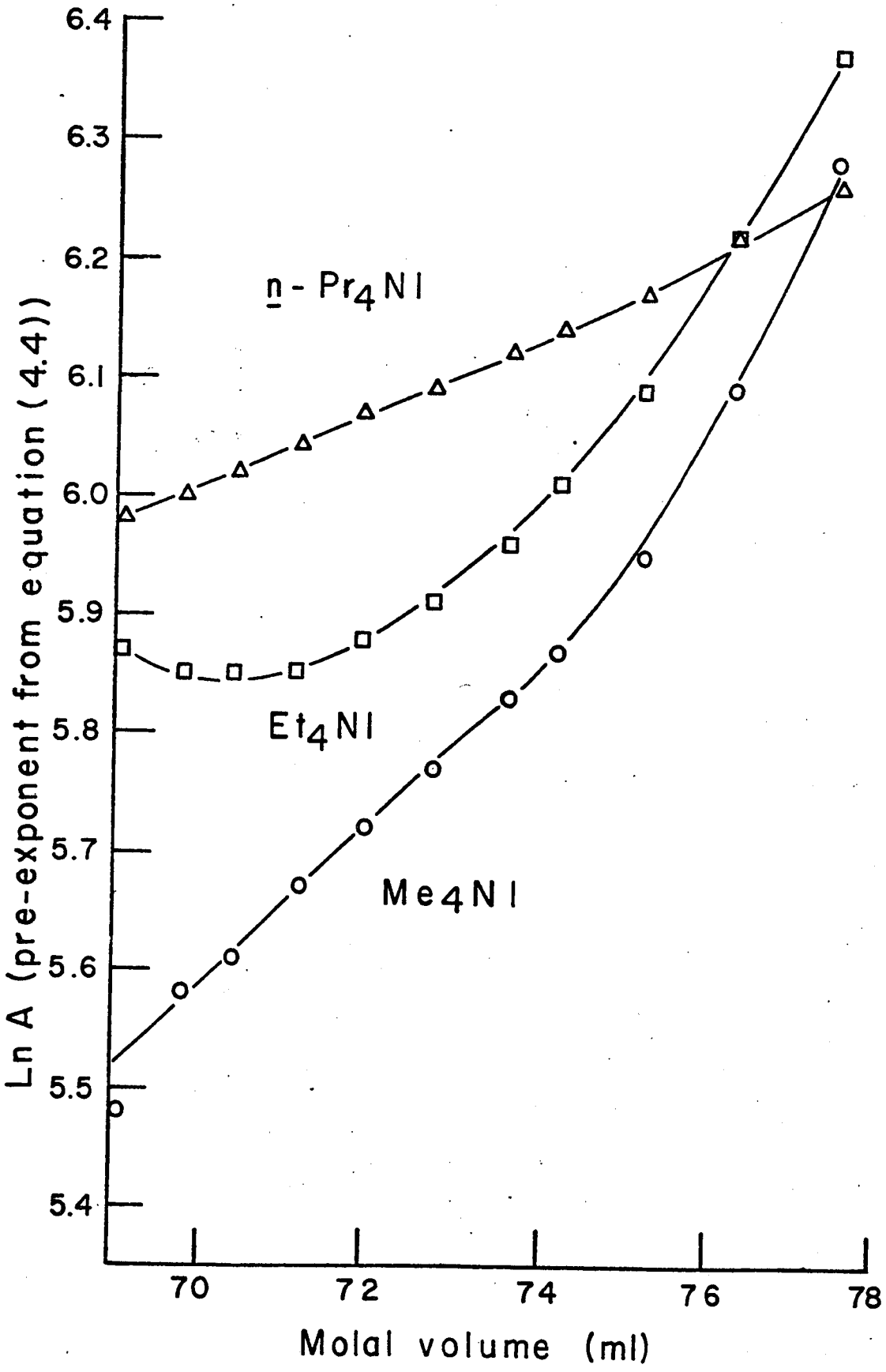
6.4
6.3
6.2
6.1
6.0
5.9
5.8
5.7
5.6
5.5
5.4
Ln A (pre-exponent from equation (4.4))
n - Pr4NI
Et4NI
Me4NI
70
72
74
76
78
Molal volume (ml)

Equation (4.22) is not thought to give an adequate estimate of the volume dependence of L, especially since there are indications, from the volume dependence of the pre-exponent, that L may not be a monotonic function of the solvent volume. In a study of n.m.r. spin-lattice relaxation times of protons and deuterons by pulse methods in mixtures of proton-containing and fully deuterated acetone molecules in the liquid state, Zeidler (26) has estimated the self-diffusion coefficient of acetone. Molecular-kinetic processes in the liquid were discussed and the reorientation time, the jump-time, and the mean jumping distance were calculated. If this mean jump distance, estimated for acetone at 25°C and atmospheric pressure to be 10.5 Å, is taken to be equivalent to the ionic jump distance, L, then $\Delta\bar{S}_o^{\ddagger}$ is estimated to be -8.7 e.u. from the pre-exponent of equation (4.5). This jump distance is slightly less than two molecular diameters, which certainly does not support the micro-jump mechanism of transport in liquids. In order to interpret a negative entropy of activation in conjunction with the positive volumes of activation observed (see Tables 3.14-3.18), the volume of activation measured is considered to be largely determined by the volume of hole formation in the liquid, which is a quantity that is independent of the species being studied. This idea will be developed further in the next section. In acetone, in contrast to the findings of Brummer (119), over most of the volume range studied the entropy of activation is more negative for the smaller ions. This observation is taken to indicate (i) the greater ordering influence of the ions with larger charge to surface area ratios, and (ii) that larger ions produce a greater degree of disruption in the solvent when the jump occurs. The reversal of the ion-size trend observed

by Brunner (119) is probably due to the solvation of K^+ and Me_4N^+. The presence of solvation effects in the case of K^+ is indicated by the decrease in Λ_o in the order Me_4N^+, K^+, and $n\text{-}Bu_4N^+$.

McCall, Douglas, and Anderson (150) have used n.m.r. spin-echo techniques to measure the pressure and temperature dependence of self-diffusion in acetone. The energy of activation at constant pressure was 2.03 kcal $mole^{-1}$ for the self-diffusion of acetone. This value was found to be independant of temperature to within 5-10%. The energy of activation for self-diffusion at constant volume was 1.00 kcal $mole^{-1}$. Within the experimental errors of these two energies, the difference, 1.03 kcal $mole^{-1}$, is close to the predicted enthalpy of hole formation of 1.32 kcal $mole^{-1}$. This is the same result found in the acetone conductivity work. Such a close similarity in these values suggests a common mechanism to both ionic conductivity and self-diffusion in acetone.

The importance of the ionic size in connection with the limiting equivalent conductivity has been emphasized in the discussion of Figure 4.1. Cohen and Turnbull (146) have made a similar correlation between the size of a diffusing species with respect to the solvent molecules and the rate of diffusive transport. If the species is smaller than, or about the same size as the solvent, but larger than the average hole size, then the diffusion process is controlled by the rate of self-diffusion of the solvent and such species will diffuse at the same rate as the solvent. This condition corresponds to that of ions with radii approaching that of the solvent molecule. In Figure 4.1, such ions have a maximum ionic mobility. Smaller ions do not have a higher mobility, because they are solvated. Larger species than the solvent molecules diffuse

more slowly and, therefore, larger ions or ion-solvent complexes also have lower mobilities.

Calculations have been made by Mackenzie (151) on the ratio of the energy of activation for viscosity of liquid acetone at constant volume to the energy at constant pressure; this ratio increases with decreasing volume from 0.2 to 0.6. This increase is a result of an increase in E_V with decrease in volume. He suggests that E_P is the energy of activation for jumping plus the energy of hole formation. In addition, on the basis of a review of the viscosity data for many liquids, he concluded that, in general, E_V is always much less than E_P, except at very high pressures. The energy of activation for viscosity at constant volume for acetone is about 0.5 kcal $mole^{-1}$, whereas at constant pressure this energy is 1.70 kcal $mole^{-1}$. These activation energies closely resemble those obtained for conductivity in acetone recorded in Tables 3.19 and 3.20. In addition, the difference between E_P and E_V for viscosity, 1.2 kcal $mole^{-1}$, is approximately equal to the energy of hole formation, 1.32 kcal $mole^{-1}$. Viscosity as well as self-diffusion appear to depend on the same molecular processes as conductivity in dilute solution. The nature of this fundamental process seems to be closely related to the amount of free volume in the system.

E Volume of Activation for Conductivity

The volume of activation was calculated with and without a correction for the solvent compressibility as shown in Tables 3.17 and 3.18. It can be seen that the volume of activation is more positive by about 20% when no correction for solvent compressibility is applied. It is possible to compare the volumes of activation for self-diffusion

and viscosity taken from the literature with the volumes of activation for conductivity by using the values which have not been corrected for the solvent compressibility. The decrease in $\Delta\bar{V}_o^{\ddagger}$ with pressure is similar to the decreases observed by Brummer (119) in D.M.F., by Brummer and Hills (125) in methanol and nitrobenzene, and by Howard (149) in methanol solutions. This decrease is related to the reduced free volume in the solvent at high pressures.

The most striking observation in connection with the volumes of activation is their independence, within the experimental error of about 1-2%, from the ionic species (see Figure 4.6). This observation confirms the results of Brummer (119), using D.M.F., that the volumes of activation of n-Bu_4NPi, Me_4NPi, FPi, KPi, and KBr over a 10% range of volume, differ by less than 10%. Neglecting KBr in this comparison, the volumes of activation are found to be identical to within about 5%. The effect of different sized anions on $\Delta\bar{V}_o^{\ddagger}$ is of the same order of magnitude as the effect that different sized cations have on $\Delta\bar{V}_o^{\ddagger}$. KBr and KPi have $\Delta\bar{V}_o^{\ddagger}$ values which differ by about 4% at high volumes and become almost identical when the system is compressed by 10%. This independence of $\Delta\bar{V}_o^{\ddagger}$ from the nature of the ionic species has also been observed by Brummer and Hills (125) in methanol and nitrobenzene solutions.

This behaviour can be related to the dual nature of the proposed mechanism for transport in liquids. The pressure derivative of equation (4.15) gives the partial derivatives of the free energy of activation for jumping, $\left(\frac{\partial\Delta\bar{F}_j^{\ddagger}}{\partial P}\right)_T$, and the partial derivative of the free energy of hole formation, $\left(\frac{\partial\Delta\bar{F}_h}{\partial P}\right)_T$; $\Delta\bar{V}_j^{\ddagger}$, the volume change associated with the jump process, and $\Delta\bar{V}_h$, the most probable volume of the holes in the liquid, are derived from their respective differentials.

Figure 4.6. Volume of activation for conductivity, corrected for solvent compressibility, plotted against specific volume of acetone.

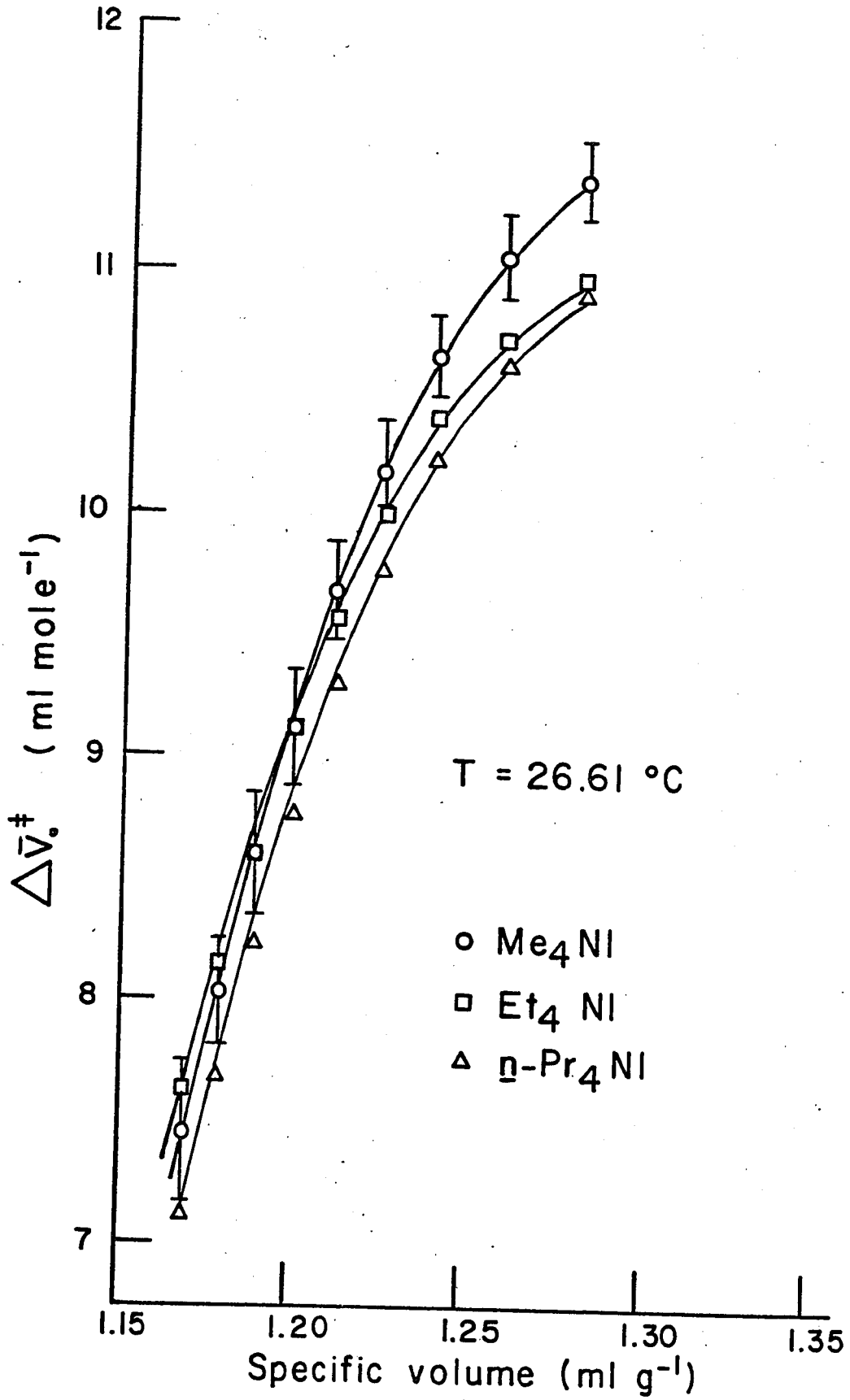
12
11
10
9
8
7
$\Delta\bar{V}_o^{\ddagger}$ (ml mole^{-1})
T = 26.61 °C
o Me_4NI
□ Et_4 NI
△ n-Pr_4NI
1.15
1.20
1.25
1.30
1.35
Specific volume (ml g^{-1})

$$\Delta\bar{V}_o^{\ddagger} = \Delta\bar{V}_j^{\ddagger} + \Delta\bar{V}_h \qquad (4.23)$$

The volume of activation for jumping can be understood in terms of the equation (133)

$$\Delta\bar{V}_j^{\ddagger} = (\bar{V}_i^{\ddagger} + \bar{V}_h^{\ddagger}) - (\bar{V}_i + \bar{V}_h) \qquad (4.24)$$

where $\bar{V}_i$ and $\bar{V}_i^{\ddagger}$ are the partial molar volumes of the ions before jumping and at the free-energy col respectively

$\bar{V}_h$ and $\bar{V}_h^{\ddagger}$ are the most probable volumes of the holes without and with an ion at the col in the free-energy surface

The term $\Delta\bar{V}_j^{\ddagger}$, therefore, can be seen to be the result of distortion of the holes when the ion jumps. This distortion volume is likely to be small. In fact, since the other term, $\Delta\bar{V}_h$, in equation (4.23), is independent of the ionic species at infinite dilution, the small differences observed in $\Delta\bar{V}_o^{\ddagger}$, of about 10%, indicate that if there is a large distortion volume, it is largely independent of the charge-to-volume ratio of the ions.

The most probable volume of holes in a liquid has been theoretically derived by Fürth (138). The model considers the holes to be analogous to clusters of molecules which are found in a dense gas or vapour. Holes are formed by the action of irregular thermal movement and according to Fürth "perform a kind of Brownian movement". The sizes of the holes are variable, with larger holes becoming more frequent at higher temperatures and volumes. The solvent surrounding the holes is considered to be a continuum which has the same surface tension as the bulk liquid. Inside the holes, the vapour pressure is assumed to be the same as the macroscopic value corresponding to that temperature. Following this model, Fürth derived the equation

$$7\,k\,T = 3\,(P - p_o)\,v + 9.20\sigma v^{2/3} \qquad (4.25)$$

where v is the average volume of a hole

P is the external pressure

p_o is the vapour pressure of the liquid at temperature, T, and pressure, P

σ is the surface tension of the liquid

From atmospheric pressure to about 1 Kbar, for normal organic liquids the first term on the right side of equation (4.25) is much less than the second term. Therefore, the equation can be written as

$$v_o \doteq 0.68 \, (kT/\sigma)^{3/2} \qquad (4.26)$$

This is the rigorous equation when p_o is equal to the atmospheric pressure, that is at the boiling point or, in general, when p_o equals the external pressure. When the external pressure is greater than p_o, the volume calculated by the use of equation (4.25) is slightly less than v_o. The most probable molar volume of holes is, therefore, approximately given by the equation

$$\Delta V_h \doteq N v_o \qquad (4.27)$$

where N is Avogadro's number. A test of this simple theory is to compare ΔV_h, assuming that $\Delta \bar{V}_j^{\ddagger}$ is small compared to ΔV_h calculated by equation (4.27), with the measured volumes of activation for conductivity, self-diffusion, and viscosity. This comparison is made in Table 4.5. The agreement between ΔV_h and $\Delta \bar{V}_{\Lambda^o}^{\ddagger}$, $\Delta V_D^{\ddagger}$, and $\Delta V_\eta^{\ddagger}$ for D.M.F., nitrobenzene, benzene, cyclohexane, and nitromethane is very good. The volumes of activation for isopentane show fair agreement. However, the liquids acetone, methanol, and water have volumes of activation for transport which are much smaller than the estimated ΔV_h values from equation (4.27). This lack of agreement can be interpreted in terms of the following ideas.

Table 4.5

Comparison Between the Volume of Activation for Conductivity, Self-diffucion, and Viscosity and the Average Volume of Holes Estimated by Fürth's Equation

Liquid	Dielectric constant (25°C)	Surface tension (27°C) (dyne cm^{-1})	$(\Delta v_h)_{av.}$	$\Delta \bar{v}^{\ddagger}_{\Lambda_o}$ (ml $mole^{-1}$)	$\Delta v^{\ddagger}_{D}$	$\Delta v^{\ddagger}_{\eta}$
acetone	20.7	23.2	30	13_a	13.0_b	15.9_b
methanol	32.63	21.7	34	7_c		8_d
water	78.54	71.2	6	-2_e	0.0	1.3
N,N-dimethylformamide	36.7	35.2_f	16	11_g		
nitrobenzene	34.82	42.2	13	15_e		
benzene	2.274	28.0	23		20.0	20.4
cyclohexane	2.015	25.3	27		28	30.8
nitromethane	39.5	35.5	16		13.6	
isopentane	2	15.8	50		34	23.8

References

a. present work

b. McCall, Douglas, and Anderson (150) except for methanol

c. Howard (149)

d. Bondi (130)

e. Hills (71)

f. Blankenship and Clampitt (152)

g. Brummer (119)

The volume of activation for jumping may be negative, such that $\Delta\bar{V}_o^{\ddagger}$ is reduced to a value much less than ΔV_h in these liquids. This interpretation is commonly made to explain the negative volumes of activation for conductivity in water (see Horne, Courant, and Johnson (153)). A negative $\Delta\bar{V}_j^{\ddagger}$ implies that the short-range liquid structure in the environment of the ion is destroyed when the ion jumps. This explanation correctly correlates the negative entropies of activation with negative volume changes on jumping, if it is assumed that there is more dense packing around the ion at the col, resulting in an increase in order in the activated over the initial state. A second possibility is that the model upon which equation (4.27) is based is not adequate to treat highly polar solvents and that the bulk liquid surface tension is not a good parameter for estimating the volume of holes when the liquid possesses more than a minimum of short-range order. The significant result is that the similarities in the volumes of activation for ionic conductivity at high dilution, self-diffusion, and viscosity in a wide range of liquids indicate that these processes are related in a fundamental way. The mechanism of transport appears to involve the formation of holes as a separate process from the movement of the mobile species.

At finite concentrations, the effect of different ionic species on the activation parameters of conductivity is more pronounced. Tables 3.14, 3.15, and 3.16 indicate that the volume of activation for conductance increases linearly to its limiting value at infinite dilution. The slope becomes progressively less negative at higher pressures. The salt with the smallest cation has the most negative slope with concentration, the increase in $\Delta\bar{V}^{\ddagger}$ being about 3 ml for a decrease from (5 to 0)$\times 10^{-4}$ mole l^{-1} for Me_4NI. This variation can be correlated with

the effect that added colutes have on the surface tension in liquids, in view of equation (4.26). The addition of about 6.5 moles % (approximately a 1 molar solution) of NaI to acetone increases the surface tension from 24.0 to 25.12 dynes cm^{-1}. This is clearly not a large enough change to explain the strong concentration dependence of $\Delta\bar{V}^{\ddagger}$, especially at low concentrations, although it is in the correct direction. The smallest ions show the strongest dependence on the concentration, suggesting that the explanation for this effect should involve electrostriction. Concentration-dependence studies of the compressibility of these salts in acetone or like solvents would help in the understanding of this effect.

Equation (4.10), which relates the difference in E_p and E_V to $\Delta\bar{V}_o^{\ddagger}$, suggests that the major expenditure of energy in the jump of an ion is the work done in the change in volume, $\Delta\bar{V}_o^{\ddagger}$, against the internal pressure of the liquid, π. The internal pressure of acetone was calculated from the isothermal compressibility of acetone and is reported in Appendix I. Combining the experimental values of π and β for 40°C and atmospheric pressure with the average measured difference $E_p - E_V$ of 1.18 kcal $mole^{-1}$ at atmospheric pressure, the value of $\Delta\bar{V}_o^{\ddagger}$ predicted by equation (4.10) is 12 ml $mole^{-1}$. This is in excellent agreement with the experimental activation volumes of Table 3.17. Therefore, the pressure dependence of the limiting equivalent conductivity is seen to be largely a volume property of the solvent. This follows because the internal pressure is the rate of change of the internal energy of the liquid with volume at constant temperature. The internal-pressure function, therefore, relates the intermolecular solvent forces to the volume. That this agreement is so satisfactory suggests that the activated-complex theory gives an

adequate account of the limiting equivalent conductivity. The agreement between the calculated and the experimental $\Delta \bar{V}_o^{\ddagger}$ for acetone, using the internal-pressure correlation, is better than the treatment involving the surface tension. This probably reflects the failure of the simple assumptions, upon which the hole theory is based, to adequately represent a dipolar liquid. The internal-pressure function is more characteristic than the surface tension of the intermolecular forces which determine the energetics of hole formation.

F Summary of Conclusions

1. There is a sharp maximum in the correlation between ionic radius and limiting ionic equivalent conductivity in acetone solution at a radius close to the acetone molecular radius. This value has a significance in terms of the ion-dipole and dipole-dipole forces in the solution. For ions with radii which are greater than the radius at this break, the ionic equivalent conductivity decreases with increasing ion size. For ions with radii less than this value, increasing solvation of the ions with decreasing radius brings about a decrease in the ionic equivalent conductivity.

2. An increase observed in the Walden product with pressure is a result of a decrease in the extent of ionic solvation at high pressure.

3. None of the quaternary ammonium ions studied is accompanied by a primary solvation layer when it moves in the solution, whereas the Li^+ ion moves in acetone with its primary solvation shell intact.

4. The energies of activation for conductivity at constant pressure and at constant volume observed in acetone solution are consistent with predictions of the hole theory of liquid structure and transport processes in liquids.

5. The volume of activation for conductivity, which is found experimentally to be almost independent of the ionic species, is closely related to the distribution of free volume in the liquid. The distortion volume change accompanying the jump process is small compared to the most probable volume of holes.

6. Activated-complex theory offers a convenient framework in terms of which the temperature and pressure coefficients of conductivity can be interpreted. However, maximum insight into the mechanism of ionic conductivity is obtained at the present time when hydrodynamic and activated-complex theory are both used. There is a lack of a large body of data from pressure and temperature studies of conductivity into which the results of a single investigation can be fitted, but the conductivity results at 25°C and atmospheric pressure are extensive for many solvents.

2. Ion-Pair Dissociation

A Summary of Results

Table 4.6 summarizes the ion-pair dissociation results presented in detail in Chapter 3. The ion-pair dissociation behaviour of the three tetraalkylammonium halides studied has the following general features:

(i) All of the K_d values increase with pressure and decrease with temperature (Tables 3.11 and 3.12).

(ii) The K_d values increase in the order $Me_4NI < Et_4NI \doteq n\text{-}Pr_4NI$ (Tables 3.11 and 3.12).

(iii) The ΔG_d° values are about 3 kcal mole^{-1}; they decrease with pressure and increase with temperature (Table 3.21).

Table 4.6

Qualitative Summary of Ion-Pair Dissociation Results

Parameter	Increase in Cation size	Pressure	Temperature	Volume
K_d	i	i	d	d
ΔG_d^o	d	d	i	i
ΔH_d^o	d	n.c.	n.a.	n.c.
ΔS_d^o	d	i	n.c.	i
ΔU_d^o	d	d	n.a.	d
ΔV_d^o	i	i	d	i

i increase

d decrease

n.c. no change

n.a. not applicable

(iv) The ΔG_d° values decrease in the order $Me_4NI > Et_4NI \doteq \underline{n}\text{-}Pr_4NI$ (Table 3.21).

(v) The ΔH_d° values are negative (the dissociation process is exothermic), the values being about -2 kcal mole^{-1} (Table 3.24).

(vi) The ΔH_d° values do not show any significant change with pressure, but tend to become more negative in the order $Me_4NI < Et_4NI < \underline{n}\text{-}Pr_4NI$ (Table 3.24).

(vii) The ΔS_d° values are strongly negative and are independent of the temperature; they become more negative in the order $Me_4NI < Et_4NI < \underline{n}\text{-}Pr_4NI$ (Table 3.25).

(viii) The ΔS_d° values for Me_4NI and Et_4NI become significantly larger (less negative) as the pressure increases, whereas the ΔS_d° values for $\underline{n}\text{-}Pr_4NI$ show little or no increase with pressure (Table 3.25).

(ix) The ΔV_d° values are all strongly negative. They tend to become more negative as the temperature increases. The ΔV_d° values vary with the salt in the order $Me_4NI < Et_4NI < \underline{n}\text{-}Pr_4NI$ (Tables 3.22 and 3.23).

(x) The ΔV_d° values all become significantly larger (less negative) as the pressure increases (Tables 3.22 and 3.23).

(xi) The $(\Delta H_d^\circ)_V$ values decrease with decreasing volume and are increasingly negative in the order $Me_4NI < Et_4NI < \underline{n}\text{-}Pr_4NI$ (Table 3.26).

B General Discussion

A comparison of the K_d values obtained with the literature is only possible for $\underline{n}\text{-}Pr_4NI$ at 25°C and atmospheric pressure. This value is given in Table 4.4(a) and the agreement is within the experimental error limits.

The negative ΔV_d° and ΔS_d° values indicate that there is considerably more solvation in the dissociated than in the ion-pair state. The variation of ΔV_d° with the salt (point (ix) above) suggests that there is more ionic solvation in the case of the smaller cations.

The small K_d values and positive ΔG_d° values are largely due to the strongly negative ΔS_d° values; the dissociated state is one of low entropy, and is reached only with difficulty. The solvation of the ions causes their enthalpy to be low, so that the ΔH_d° values are negative; the enthalpy effect is, however, offset by the entropy effect.

The pressure effects on K_d reflect negative ΔV_d° values. The fact that ΔS_d° values become less negative as pressure increases (point (viii)) reflects the greater difficulty that the field of the ion has in orienting solvent dipoles when the solvent is compressed. The decrease in the volume change ΔV_d° with pressure is also related to this effect.

The effect of variation of the temperature and pressure on ion-pair dissociation in water has been investigated for $\left[Co(III)(NH_3)_6\right](SO_4)^+$ going to $\left[Co(III)(NH_3)_6\right]^{+3}$ and SO_4^{-2} by Shimizu, Takizawa, and Osugi (154). They reported that at 25°C ΔV_d° went from a value of -2.0 to -12 ml mole^{-1} for a rise from 1 to 600 kg cm^{-2} in the pressure. This decrease in ΔV_d° with pressure was not observed at 40°C, where an increase in ΔV_d° with pressure, similar to that observed in acetone, was found. The entropy of dissociation was found to be strongly negative and to increase (become less negative) with pressure. The enthalpy of dissociation showed complicated temperature and pressure dependence. At 25°C, ΔH_d° was negative at all pressures, while it was found to become positive at 40°C and 600 kg cm^{-2}.

Osugi, Shimizu, and Takizawa, (155) found that the pressure dependence of the dissociation in water of $\left[Co(III)(NH_3)_6\right] Cl^{+2}$, to give $\left[Co(III)(NH_3)_6\right]^{+3}$ and Cl^-, gave a positive volume change at low pressures, the values becoming negative at higher pressures. These anomalous results in aqueous solutions are attributed to the structural effects.

Fisher and Davis (156) have studied the pressure dependence of the dissociation of $MnSO_4$ in aqueous solutions, and have found that ΔV_d^o increases from about -7 to -5 ml mole^{-1} for an increase of 2000 atmospheres in the pressure. The pressure and temperature dependence of the thermodynamic parameters of ion-pair formation in water are not the same as those found in acetone, but the entropy and volume changes observed are generally negative and show in most cases the same pressure dependence, although to a lesser extent, as has been observed in acetone.

C Variation of K_d with Changes in the Ionic Radius

It is not possible to give an adequate interpretation of the different K_d values solely in terms of the electrostatic interactions between the cation and the anion using the crystallographic radii. This can be inferred from the solvation effects observed in the ionic-radius dependence of the limiting equivalent conductivity. When the ionic radius falls below a certain radius, the value of which will depend on the temperature and pressure of the solvent, the ion becomes solvated and the effective charge to volume ratio is reduced. If the counter-ion can not displace the molecules in the solvation sheath, then the observed K_d will be greater than predicted on the basis of an electrostatic theory using the crystallographic radii. Of particular interest in this regard

are the lithium halides, whose conductivities have been studied by Savedoff (98). There is a 2000-fold increase in the dissociation constant in going from LiCl to LiI. This increase is far larger than that predicted by the electrostatic theory based on the increase in the anionic radii from Cl^- to I^-. These results suggest that there is a drastic difference in the ion pair formed between Li^+ and Cl^- from that formed between Li^+ and I^-. Furthermore, the enthalpy of dissociation for LiCl ion pairs is much more negative than that for either LiBr or LiI ion pairs (see Table 1.1). This is a result of the extreme sensitivity of the nature of the ion pair to the ionic radii of the ions.

Four classes of ion pairs were defined by Griffiths and Symons (157) in connection with the study of ionic interactions by ultraviolet spectroscopy: (i) Complexes: two or more ions, in contact, held together by covalent bonds; (ii) Contact ion pairs: ions, in contact, but with no covalent bonding between them; (iii) Solvent-shared ion pairs: pairs of ions, linked electrostatically, by a single (oriented) solvent molecule; and (iv) Solvent-separated ion pairs: pairs of ions, linked electrostatically, but separated by more than one solvent molecule. They used the general term "ion pairs" to include classes (ii), (iii), and (iv) when a distinction between them can not be made. In benzene and carbon tetrachloride an absorption band was found that was relatively independent of solvent. This band, found in solutions of quaternary ammonium iodides, was identified as being due to the presence of contact ion pairs (class (ii)). Temperature independence, and a shift to higher frequency as the alkyl group in the tetraalkylammonium cation was reduced in size, were two features of this band not found in

more polar solvents. In the contact ion pairs it was suggested that the electron is transferred from the iodide to the cation, where it is held in an expanded orbital similar to the electron in metal-ammonia solutions. This kind of orbital explains the frequency dependence of the absorption band on the radius of the cation.

In dioxane and 1,2-dimethoxyethane, a new band was found when excess tetraalkylammonium cations (Et_4N^+, $n\text{-}Pr_4N^+$, and $n\text{-}Bu_4N^+$) were added to iodide solutions. This observation was not made in benzene or carbon tetrachloride. The new band was found to be sensitive to temperature only in 1,2-dimethoxyethane. On the basis of these observations, the main band in dioxane and the new band in 1,2-dimethoxyethane were ascribed to solvent-separated ion pairs. The peak due to solvated iodide ions is quite temperature-sensitive in polar solvents, so that band sensitivity to temperature is thought to be a good criterion of ion-pair formation of class (iii) or (iv). Solvents such as acetone are predicted to form solvent-separated ion pairs of class (iv), the class of ion pairs thought to be the most common in solvents of low bulk dielectric constants but large dipole moments. In solvent-shared ion pairs, the electron is thought to be transferred to a shared, field-oriented, and polarized solvent molecule. The solvent shell surrounding the ion pair is distorted from spherical to axial symmetry. The most important result of this work, in terms of the present studies, is that it was suggested that a solvent such as acetone should contain ion pairs of two classes, class (iii) and class (iv).

Recently, Griffiths and Scarrow (158) have presented spectroscopic evidence that ion-pair interactions are important in acetone

solutions of a series of alkylammonium bromides. The $\left[Br^{-} : Ni^{+2}\right]$ ratio for conversion of $NiBr_2$ to $NiBr_4^{-2}$ was found to be quite sensitive to the radius of the cation used in the salt to supply the bromide ions.

The sensitivity, with respect to pressure and temperature, of the ultra-violet spectrum of iodide ions in various organic solvents has been studied by Griffiths and Wijayanayake (159) up to about 200 bar pressure and 300°C. It was found that the charge transfer to solvent spectrum was sensitive to the temperature and pressure. Solvents with dielectric constants greater than 23 are expected to contain only solvent-separated ion pairs. From dielectric constants of 23 down to 11 solvents are expected to contain solvent-shared ion pairs as well. It is most interesting, therefore, that the dielectric constant of acetone increases from about 20 to 23 at 26.6°C when the pressure is raised from one atmosphere to 1.1 kbar.

The solvation of the iodide ion in acetone is expected to be symmetrical, even in the ion paired state, if the dielectric constant is such as to prohibit the formation of solvent-shared ion pairs. The measured values of the temperature dependence of the absorption maximum position over a wide temperature range agree with the correlation predicted for pure solvation. When the dielectric constant is less than about 20 (in acetone this corresponds to low pressures and temperatures greater than 35°C, see Table 3.2) the spectrum becomes cation-dependent. This is interpreted as an indication of the formation of solvent-shared ion pairs. On the basis of a study of band shapes, the excited orbital of iodide in these ion pairs is concluded to be ellipsoidal. The temperature

dependence of the solvent-shared ion-pair absorption is greatly reduced from that of solvent-separated ion pairs.

The spectroscopic evidence presented above indicates that the separation of the cation and the anion in an ion pair (or in other words, the class of ion pair formed) depends critically on the solvent and the temperature and pressure conditions of the experiment. Acetone, because of the variation of its dielectric constant over the present range of temperature and pressure (Table 3.2), should contain solvent-shared ion pairs at the higher temperatures and lower pressures, and solvent-separated ion pairs at the lower temperatures and higher pressures. Because of the nature of the charge transfer in these two classes of ion pairs, a difference in the extent of electrostriction of the solvent is predicted. In a solvent-shared ion pair, the residual charge on the ions is thought to be negligible. This implies that two full charges are developed on the dissociation of a neutral ion pair for class (iii) ion pairs, with a large electrostriction of solvent to be expected. Tables 3.22 and 3.23 indicate that a large negative volume change results under the dielectric conditions thought to favour solvent-shared ion pairs. Solvent-separated ion pairs, however, do not result in a charge neutralization, since the electron of the anion is transfered only to the solvent. This implies that there is only a small increase in the charge developed when a class (iv) ion-pair dissociates. The increased electrostriction of the solvent that results from the dissociation of this kind of ion pair should be small. Tables 3.22 and 3.23 indicate that a small negative volume change is found under conditions thought

to favour class (iv) ion-pair formation.

The values of the dissociation constants themselves also support this explanation involving two classes of ion pairs. At low pressures, the salt with the largest cation, n-Pr_4NI, is most dissociated (see summary point (ii) above). However, at high pressure, the dissociation constants approach one another in value. The radius of the cation is less important under these conditions, a characteristic of class (iv) ion pairs.

The internal-energy change at constant volume, shown in Table 3.26, indicates that there is a significant difference in the volume dependence of this function for the three salts investigated. $(\Delta U_d^\circ)_V$ decreases with decreasing volume in each case. The trend is not well delineated for Me_4NI, but is very definite for Et_4NI and n-Pr_4NI. Work must be done to separate the ions forming an ion pair, which implies that $(\Delta U_d^\circ)_V$ should be positive. At large volumes, $(\Delta U_d^\circ)_V$ is either positive, or small and negative, for the three salts studied. This suggests that the dominant interaction in the ion pair under these conditions is the electrostatic interaction between the two ions. When the solvent is compressed, $(\Delta U_d^\circ)_V$ decreases, indicating that the stability of the free ions is enhanced by ion-solvent interactions at small volumes. These results suggest that a negative $(\Delta U_d^\circ)_V$ could be used as a diagnostic test to indicate the formation of solvent-separated ion pairs.

D Fuoss Theory of Ion-Pair Dissociation

In the theory developed by Fuoss (160) the cations are represented by charged spheres of radius 'a' in a continuum having the bulk dielectric constant of the solvent. Ion pairs are said to be present

when anions, considered to be charged point masses, are a distance $r \leq a$ from the center of a cation. The equation, using the molarity scale of concentration, that has been derived on the basis of this model by Fuoss, is

$$K_F = 3000/\ 4\pi N a^3 \exp (b)$$

where $$b = |z_1 z_2|\ e^2/(\epsilon kT\ a) \qquad (4.28)$$

In these equations

N is Avogadro's number

a is the ion-size parameter

z_1 and z_2 are the number of charges on the cations and anions

e is the electronic charge

ϵ is the dielectric constant

k is the Boltzmann's constant

T is the temperature, ^oK

It has been pointed out by Robinson and Stokes (78) that, for a given salt, the temperature dependence of K_F, the dissociation constant predicted by the Fuoss equation (4.28), reduces to the form

$$\ln K_F = A - B/(\epsilon T) \qquad (4.29)$$

where $A = \ln (3000/4\pi N a^3)$

$B = |z_1 z_2| e^2/(k a)$.

Hamann, Pearce, and Strauss (161) have derived the following equation which is based on the pressure dependence of $\ln K_F$ predicted from the Fuoss equation:

$$\left(\frac{\partial \ln K_F}{\partial P}\right)_T = -\left(\frac{\partial b}{\partial \epsilon}\right)_T \left(\frac{\partial \epsilon}{\partial P}\right)_T \qquad (4.30)$$

This equation holds if the contact distance is not a function of the pressure. Rearranging this equation, substituting for b, and combining with equation (3.31), gives a theoretical equation for ΔV_d^o:

$$\Delta V_d^o = -\frac{N z_1 z_2 e^2}{a \epsilon} \left(\frac{\partial \epsilon}{\partial P}\right)_T + RT\beta \qquad (4.31)$$

The enthalpy of dissociation can be calculated from the Fuoss theory by taking the temperature derivative of $\ln K_F$, defined by equation (4.29) at constant pressure, and assuming that the ion-size parameter is independent of temperature:

$$\left(\frac{\partial \ln K_F}{\partial T}\right)_P = \frac{B}{T\epsilon^2}\left(\frac{\partial \epsilon}{\partial T}\right)_P + \frac{B}{\epsilon T^2} \qquad (4.32)$$

Substituting the result above, for the derivative in equation (3.32), ΔH_d^o is derived in terms of the Fuoss theory to give

$$\Delta H_d^o = \frac{T N |z_1 z_2| e^2}{a \epsilon^2}\left(\frac{\partial \epsilon}{\partial T}\right)_P + \frac{N |z_1 z_2| e^2}{\epsilon a} \qquad (4.33)$$

A computer program was written which calculated the dissociation constants from equation (4.29) for values of the ion-size parameter from 0.05 to 10.00 Å, for the thirty-six conditions of temperature and pressure studied. This program is listed in Appendix III. Calculations to obtain the dissociation constants at 25°C and atmospheric pressure for ion-size parameters from 0.05 to 20.00 Å were also completed. Similar calculations were done at the nine temperatures from 25 to -50°C which were used in the work of Sears, Milhoit, and Dawson (97). The ion-size parameters required to fit the experimental dissociation constants from the literature are shown in Table 4.4. The dependence of $\log_{10} K_F$ on the ion-size parameter is shown graphically for three representative conditions in Figure 4.7. The ion-size parameters which

Figure 4.7. Logarithm of the dissociation constant calculated from the Fuoss equation plotted against the ion-size parameter.

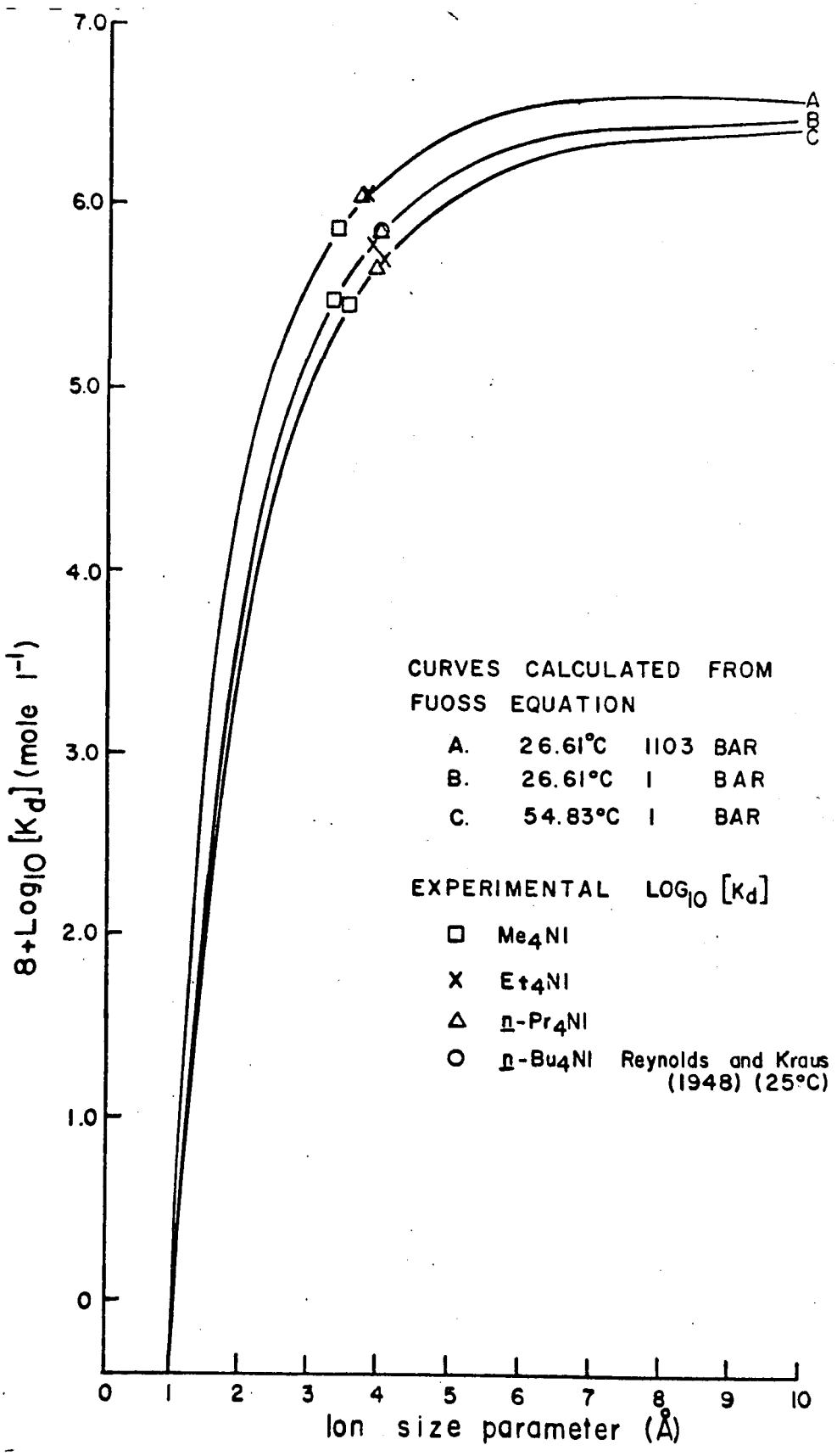
7.0
6.0
5.0
4.0
3.0
2.0
1.0
0
8+Log10 [Kd] (mole l-1)
A
B
C
CURVES CALCULATED FROM FUOSS EQUATION
A. 26.61°C 1103 BAR
B. 26.61°C 1 BAR
C. 54.83°C 1 BAR
EXPERIMENTAL LOG10 [Kd]
Me4NI
Et4NI
n-Pr4NI
n-Bu4NI Reynolds and Kraus (1948) (25°C)
0 1 2 3 4 5 6 7 8 9 10
Ion size parameter (Å)

best fit the experimental dissociation constants obtained in the present work are shown in Table 4.7. The ion-size parameter for the atmospheric-pressure data for each temperature was obtained in the same way, and is shown in Table 4.8. The four parts of this table correspond to (a) the high-pressure cells, (b) the atmospheric-pressure cells, (c) the combined data from (a) and (b), and (d) the average ion-size parameter from (a), (b), and (c) with the standard deviation. The results obtained for the ion-size parameter at the nine pressures were averaged for each temperature and the values are shown in Table 4.9. The uncertainties in these averaged quantities are the standard deviations calculated in the usual way.

The experimental volumes of dissociation and enthalpies of dissociation were used in conjunction with equations (4.31) and (4.33) to compute the ion-size parameters associated with these pressure and temperature derivatives. The results are presented in Tables 4.10 and 4.11. The average values are shown in Table 4.12.

Figure 4.7, showing the dependence of K_F on the ion-size parameter, indicates that a maximum in K_F occurs at about 7 or 8 Å for the pressure conditions where there is a higher dielectric constant. This is an artifact of the treatment and does not correspond to a real decrease in K_d, which must increase continuously with the ionic radius for large ions.

The calculated ion-size parameters, given in Tables 4.7 and 4.8, show a decrease with pressure which is least pronounced for Me_4NI. The temperature dependence of the ion-size parameter is little effected by pressure, and except for a slight increase with temperature for Me_4NI,

Table 4.7

Ion Size Parameter Calculated from the Fuoss Equation

(Å)

	Pressure (bar)	Temperature. (°C) 26.61	35.00	45.01	54.83
Me_4NI	1.0	3.27	3.41	3.50	3.51
	137.9	3.27	3.42	3.42	3.48
	275.8	3.27	3.42	3.40	3.47
	413.7	3.27	3.46	3.37	3.45
	551.6	3.31	3.38	3.33	3.37
	689.5	3.34	3.37	3.33	3.33
	827.4	3.36	3.35	3.30	(2.53)
	965.3	3.36	3.33	3.28	3.28
	1103.2	3.33	3.31	3.26	(3.84)
Et_4NI	1.0	3.84	3.95	3.88	3.96
	137.9	3.82	3.92	3.83	3.91
	275.8	3.78	3.89	3.79	3.86
	413.7	3.78	3.85	3.80	3.82
	551.6	3.75	3.77	3.72	3.78
	689.5	3.75	3.75	3.72	3.78
	827.4	3.75	3.72	3.68	3.75
	965.3	3.74	3.68	3.64	3.67
	1103.2	3.71	3.67	3.60	3.63

Table 4.7 (cont.)

Ion Size Parameter Calculated from the Fuoss Equation

(Å)

	Temperature (°C)			
Pressure (bar)	26.61	35.00	45.01	54.83
$n\text{-}Pr_4NI$				
1.0	3.91	3.90	3.88	3.82
137.9	3.89	3.87	3.82	3.75
275.8	3.85	3.79	3.69	3.73
413.7	3.83	3.75	3.72	3.67
551.6	3.79	3.72	3.61	3.62
689.5	3.75	3.68	3.57	3.54
827.4	3.72	3.65	3.51	3.52
965.3	3.70	3.62	3.48	3.48
1103.2	3.65	3.57	3.43	3.44

Table 4.8

Ion Size Parameter Calculated from the Fuoss Equation at Atmospheric Pressure (Å)

	Temperature (°C)			
(a)	26.61	35.00	45.01	54.83
Me_4NI	3.27	3.41	3.50	3.51
Et_4NI	3.84	3.95	3.88	3.96
$\underline{n}$-Pr_4NI	3.91	3.90	3.88	3.82
(b)				
Me_4NI	3.39	3.40	3.41	3.45
Et_4NI	4.13	4.14	4.09	4.17
$\underline{n}$-Pr_4NI	4.15	4.12	4.03	4.14
(c)				
Me_4NI	3.34	3.40	3.41	3.42
Et_4NI	3.97	4.05	3.98	4.08
$\underline{n}$-Pr_4NI	4.04	4.02	3.98	3.98
(d)				
Me_4NI	3.33(0.05)	3.40(0.01)	3.44(0.04)	3.46(0.04)
Et_4NI	3.98(0.12)	4.05(0.08)	3.98(0.09)	4.07(0.09)
$\underline{n}$-Pr_4NI	4.03(0.10)	4.01(0.09)	3.97(0.06)	3.98(0.13)

Table 4.9

Average Ion-Size Parameter for Nine Pressures Calculated from the Fuoss Equation Results of Table 4.7

(Å)

	Temperature (°C)			
	26.61	35.00	45.01	54.83
Me_4NI	3.33(0.04)	3.38(0.05)	3.35(0.07)	3.36(1.04)
Et_4NI	3.75(0.04)	3.80(0.10)	3.74(0.09)	3.79(0.11)
$n\text{-}Pr_4NI$	3.79(0.08)	3.73(0.10)	3.63(0.15)	3.62(0.12)

Table 4.10

Ion Size Parameter Calculated from the Experimental Volumes of Dissociation and the Pressure Derivative of the Fuoss Equation

(Å)

Pressure (bar)	Temperature (°C) 26.61	35.00	45.01	54.83
Me_4NI				
1.0	2.61	2.76	3.44	4.49
137.9	2.55	2.82	3.45	4.21
275.8	2.50	2.91	3.48	3.93
413.7	2.44	3.06	3.53	3.62
551.6	2.40	3.29	3.62	3.30
689.5	2.35	3.65	3.76	2.97
827.4	2.30	4.27	4.00	2.63
965.3	2.25	5.54	4.40	2.28
1103.2	2.21	9.35	5.16	1.92
Et_4NI				
1.0	3.69	4.36	3.78	4.11
137.9	3.64	4.39	3.82	4.13
275.8	3.59	4.44	3.90	4.19
413.7	3.53	4.51	4.02	4.28
551.6	3.48	4.61	4.20	4.43
689.5	3.42	4.75	4.49	4.68
827.4	3.37	4.97	4.96	5.10
965.3	3.31	5.30	5.81	5.88
1103.2	3.26	5.85	7.73	7.67

Table 4.10 (cont.)

Ion Size Parameter Calculated from the Experimental Volumes of Dissociation and the Pressure Derivative of the Fuoss Equation

(Å)

	Pressure (bar)	Temperature (°C) 26.61	35.00	45.01	54.83
n-Pr_4NI	1.0	3.98	4.56	5.15	4.31
	137.9	4.02	4.60	5.22	4.38
	275.8	4.08	4.64	5.31	4.52
	413.7	4.17	4.71	5.42	4.71
	551.6	4.28	4.81	5.58	5.02
	689.5	4.45	4.94	5.81	5.53
	827.4	4.70	5.14	6.16	6.44
	965.3	5.10	5.45	6.74	8.46
	1103.2	5.76	5.96	7.80	15.9

Table 4.11

Ion Size Parameter Calculated from the Experimental Enthalpy of Dissociation and the Temperature Derivative of the Fuoss Equation

(Å)

	Pressure (bar)	Temperature (°C) 26.61	35.00	45.01	54.83
Me_4NI	1.0	8.55	11.9	16.6	22.4
	137.9	8.00	11.0	15.2	20.2
	275.8	9.07	12.7	17.8	23.8
	413.7	5.74	8.30	11.8	16.0
	551.6	2.15	3.20	4.60	6.31
	689.5	1.53	2.38	3.52	4.91
	827.4	1.21	1.98	2.99	4.24
	965.3	-0.96	1.64	2.56	3.70
	1103.2	-2.84	-5.13	-8.19	-12.0
Et_4NI	1.0	3.19	4.42	6.20	8.36
	137.9	2.84	3.90	5.39	7.18
	275.8	2.60	3.66	5.10	6.84
	413.7	2.48	3.59	5.09	6.92
	551.6	2.11	3.15	4.53	6.22
	689.5	2.09	3.26	4.82	6.73
	827.4	1.52	2.47	3.74	5.30
	965.3	1.16	1.99	3.10	4.47
	1103.2	0.96	1.73	2.77	4.05

Table 4.11 (cont.)

Ion Size Parameter Calculated from the Experimental Enthalpy of Dissociation and the Temperature Derivative of the Fuoss Equation

(Å)

	Temperature (°C)			
Pressure (bar)	26.61	35.00	45.01	54.83
n-Pr_4NI				
1.0	1.69	2.35	3.30	4.45
137.9	1.48	2.04	2.82	3.75
275.8	1.46	2.05	2.87	3.85
413.7	1.28	1.85	2.62	3.55
551.6	1.09	1.62	2.34	3.21
689.5	0.87	1.36	2.01	2.81
827.4	0.81	1.31	1.98	2.81
965.3	0.69	1.19	1.85	2.67
1103.2	0.60	1.07	1.72	2.51

Table 4.12

Average Ion Size Parameter Calculated at Several Temperatures

(Å)

(a) Values based on the experimental volumes of dissociation and the pressure derivative of the Fuoss equation

	Temperature (°C)			
	26.61	35.00	45.01	54.83
Me_4NI	2.40 (0.13)	4.18 (2.01)	3.87 (0.55)	3.26 (0.83)
Et_4NI	3.48 (0.14)	4.80 (0.47)	4.75 (1.22)	4.94 (1.11)
$\underline{n}$-Pr_4NI	4.50 (0.56)	4.98 (0.44)	5.91 (0.82)	6.59 (3.55)

(b) Values based on the experimental enthalpy of dissociation and the temperature derivative of the Fuoss equation

	Temperature (°C)			
	26.61	35.00	45.01	54.83
Me_4NI	3.82 (4.09)	5.33 (5.64)	7.43 (8.04)	9.96 (10.96)
Et_4NI	2.11 (0.72)	3.13 (0.85)	4.53 (1.06)	6.23 (1.30)
$\underline{n}$-Pr_4NI	1.11 (0.47)	1.65 (0.42)	2.39 (0.51)	3.29 (0.61)

the ion-size parameter is not a strong function of temperature. The decrease in the ion-size parameter with the pressure can be seen by comparing the average values recorded in Table 4.9 with the average atmospheric values recorded in Table 4.8(d). This decrease does not support the postulate in which two classes of ion pairs are used to explain the pressure dependence of ΔV_d^o. An increase in the ion-size parameter would be the trend expected.

The results calculated from the experimental volumes of dissociation are more plausible in terms of the concept of two classes of ion pairs. Except for Me_4NI at 26.61°C and at 54.85°C (a temperature where the Me_4NI results were less precise) and Et_4NI at 26.61°C, the ion-size parameters increase with pressure, in keeping with the pressure dependance of the two classes of ion pairs discussed above. It could be concluded that the low-temperature results for Me_4NI and Et_4NI indicate that solvent-shared ion pairs are present even at high pressures under these conditions. This would be a very tentative conclusion, however, because of the approximations involved in equation (4.31).

The ion-pair parameters calculated from equation (4.33) are shown in Table 4.11 to decrease markedly with pressure. This is a result of the neglect of the term containing the variation of the ion-size parameter with temperature. The coefficient $\left(\frac{\partial \ln a}{\partial T}\right)_p$ is small, but the factor associated with this term is large. This term can not be neglected, and the ΔH_d^o values can therefore not be used to calculate meaningful ion-size parameters. In this connection, Hamann, Pearce, and Strauss (161) are perhaps making a poor assumption in assuming that the

ion-size parameter is independent of the pressure.

The average values of the ion-size parameter shown in Table 4.12 are seen to increase with the ion size. This is expected when the ion-size parameter is calculated from ΔV_d^o. However, the ion-size parameter calculated from ΔH_d^o decreases with the ion size. This latter observation is another indication that the temperature variation of the ion-size parameter can not be neglected in equation (4.33).

The model upon which equation (4.28) rests is quite crude and it is therefore not unexpected that physically unreasonable ionic separations are found. For example, the sum of the Stokes radii for $n\text{-}Pr_4NI$ is 6.01±0.04 Å, the Fuoss-Onsager conductance equation predicts an ion-size parameter of 5.2±0.6 Å, while the sum of the crystallographic radii is 6.68 Å. A comparison of these values, which refer to 26.6°C, to the ion-size parameters calculated by equation (4.28), shows that the Fuoss equation predicts separations that are too small to be physically realistic.

E Summary of Conclusions

1. Solvation of the free ions determines the sign and magnitude of the thermodynamic parameters of ion-pair dissociation in acetone.

2. Theories of ion-pair formation advanced on the basis of spectroscopic observations are consistent with the results obtained in the present work.

3. Acetone solutions are thought to contain solvent-shared and solvent-separated ion pairs; the proportion of each class present depends on the conditions of temperature and pressure.

4. The ion-size parameters calculated by continuous dielectric theory are generally a function of pressure and temperature and have smaller values than would be expected from other considerations.

APPENDIX I

INTRODUCTION

For the interpretation of kinetic results obtained over a range of temperature and pressure it is necessary to have precise information about the effects of pressure and temperature on the volume of the pure solvent. The present work provides such information for liquid acetone.

The isothermal compressibility of acetone was measured in the pioneering work of Amagat and Bridgman (162,163,164), but the results are not sufficiently precise to be useful in kinetic studies. More precise measurements were made by Newitt and Weale (165), for pressures up to 1 kilobar but one temperature only (25°C). For this work the information was needed over a range of temperatures, and measurements have been made at 26.6°, 35.0°, 45.0° and 54.8°C (the normal boiling point of acetone is 56.2°C).

Velocity of sound measurements have been recorded in the literature over a range of temperatures at atmospheric pressure. Fryer, Hubbard, and Andrews (166), Staveley, Tupman and Hart (167), Staveley and Parham (168) and Low and Moelwyn-Hughes (169) calculated the isothermal compressibility from the adiabatic compressibility and the heat capacity at constant pressure. Such a procedure, however, does not reveal the pressure dependence of the compressibility, a quantity that is necessary for estimating the variation with pressure of the thermodynamic properties of the liquid.

EXPERIMENTAL

Comparative measurements of the compression of acetone relative to water were made using the apparatus shown diagrammatically in Figure I.1. The isothermal compressibilities of water at the temperatures and pressures

Figure I.1. Compressibility apparatus.

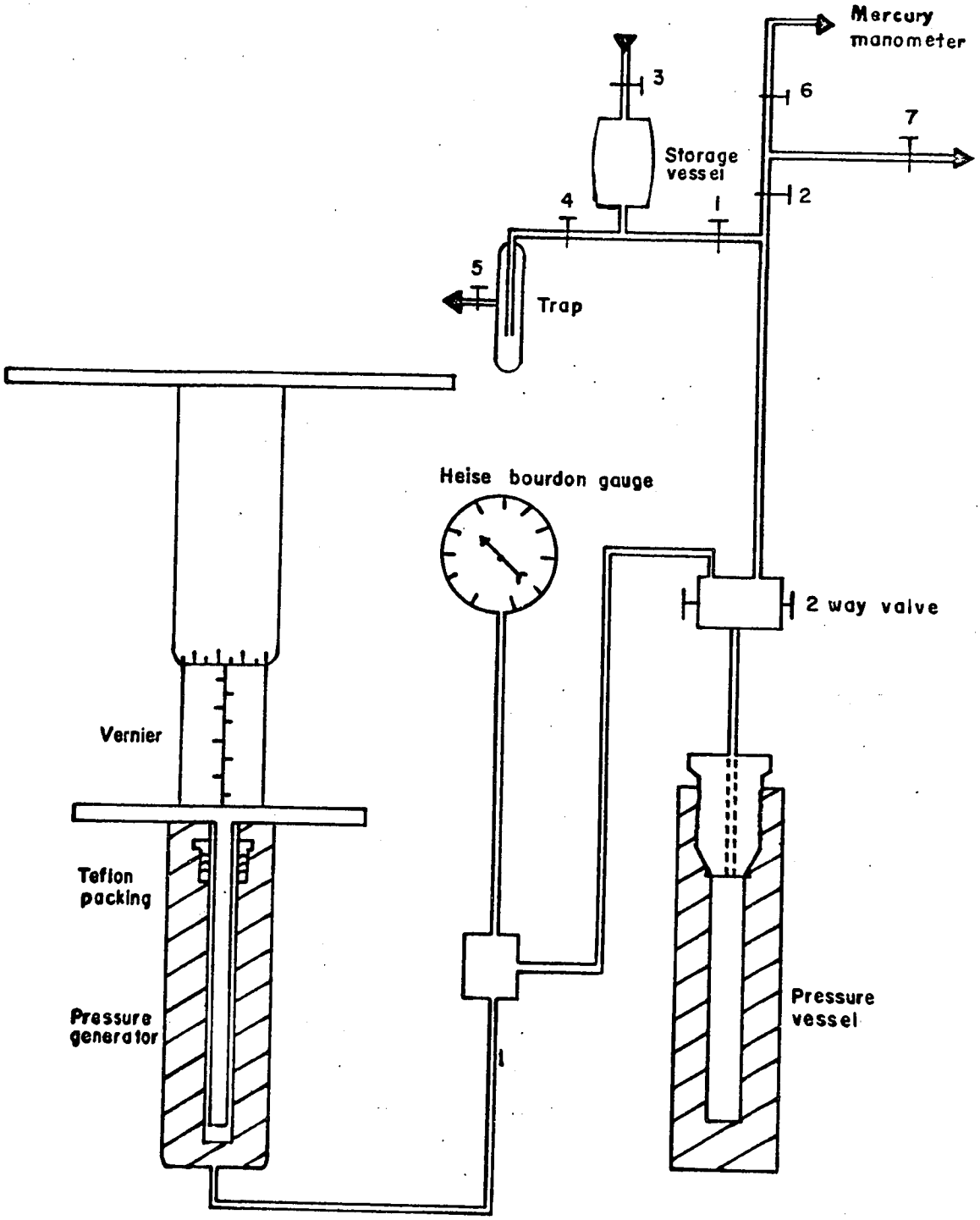
Mercury manometer
3
6
7
Storage vessel
4
1
2
5
Trap
Heise bourdon gauge
2 way valve
Vernier
Teflon packing
Pressure generator
Pressure vessel

required were calculated from the work of Kell and Whalley (170). The isothermal compressibility of acetone was then calculated at the four temperatures mentioned and at a series of pressures up to 1.1 kilobar.

Liquid was introduced into the evacuated high pressure system by means of the inlet system shown in Figure I.1. Gas-free, twice distilled water was used for the reference liquid. A single lot of Baker Analyzed Reagent acetone was used for all of the acetone compressions. The acetone had the following properties at 25°C: specific conductivity, 2×10^{-7} Ω^{-1} cm^{-1}, density (determined pycnometrically), 0.7852 ± 0.0003 g ml^{-1}: and refractive index for sodium D light, 1.3559 ± 0.0002.

The compression was measured on a vernier scale attached to an 11 cm^3 pressure generator. The pressure vessel of approximately 100 cm^3 capacity and the pressure generator were obtained from the High Pressure Equipment Co., Erie, Penn., U.S.A. Pressure was measured with a 16 inch bourdon tube gauge obtained from the Heise Bourdon Tube Co., Inc., Newton, Conn., U.S.A. (see Figure I.2 for photograph of apparatus).

Temperature control to ± 0.02°C was maintained by immersing all of the apparatus, with the exception of the bourdon gauge, in a 30 gallon oil thermostat. Four Beckmann thermometers calibrated in the Division of Applied Physics, National Research Council, Ottawa, were used to measure the temperature. Control of temperature variation due to the heat of compression was aided by a thermocouple inserted into a well in the pressure vessel.

RESULTS AND DISCUSSION

The results were fitted to the Tait equation

$$-\frac{1}{v^0}\left(\frac{\partial v}{\partial p}\right)_T = \frac{C}{B + p} \qquad (I.1)$$

Figure I.2. Photograph of the compressibility apparatus.

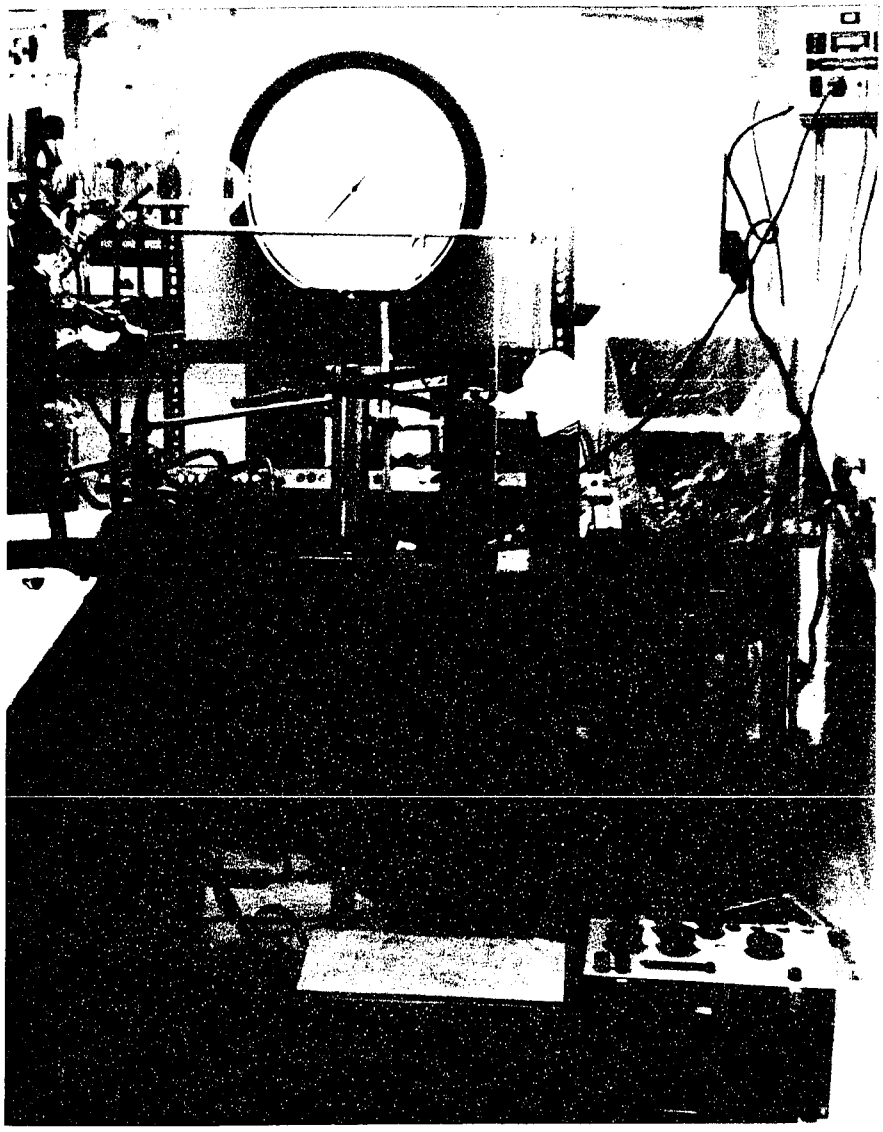

which relates the isothermal compressibility, β_T, equal to $-1/V^o\ (\partial V/\partial P)_T$, to the pressure P; V^o is the volume at atmospheric pressure, and B and C are two constants of which the former is generally dependant on temperature and the latter not. The applicability of the equation is shown in Figure I.3, in which β_T^{-1} is plotted against the pressure; the points at each temperature lie very close to a straight line. The lines are parallel, showing that C is independent of temperature.

The values of B and C obtained in a least-square fit to the equation done using an I.B.M. 1620 computer, are shown in Table I.1. The variations in C are seen to be insignificant within the experimental error. The variation of B with temperature was expressed by fitting B to a three-term polynomial in temperature; this was again done on the computer and the result is

$$B = \left[755.7 - 5.124(t - 25.00) - 0.0388\ (t-25.00)^2\right] \pm 13 \text{ bar} \qquad (I.2)$$

where t is the temperature in degrees C.

The compression, k, is defined as

$$k = \frac{V^o - V}{V^o} \qquad (I.3)$$

From the integrated form of the Tait equation

$$k = 2.303\ C \log_{10}\left[\frac{B+P}{B+P^o}\right] \qquad (I.4)$$

where P^o indicates atmospheric pressure. The isothermal compressibilities, the compressions and the volumes agreed satisfactorily with earlier measurements where comparisons could be made; this is shown in Tables I.2 and I.3.

Figure I.3. Compressibility data plotted according to the Tait equation at four temperatures.

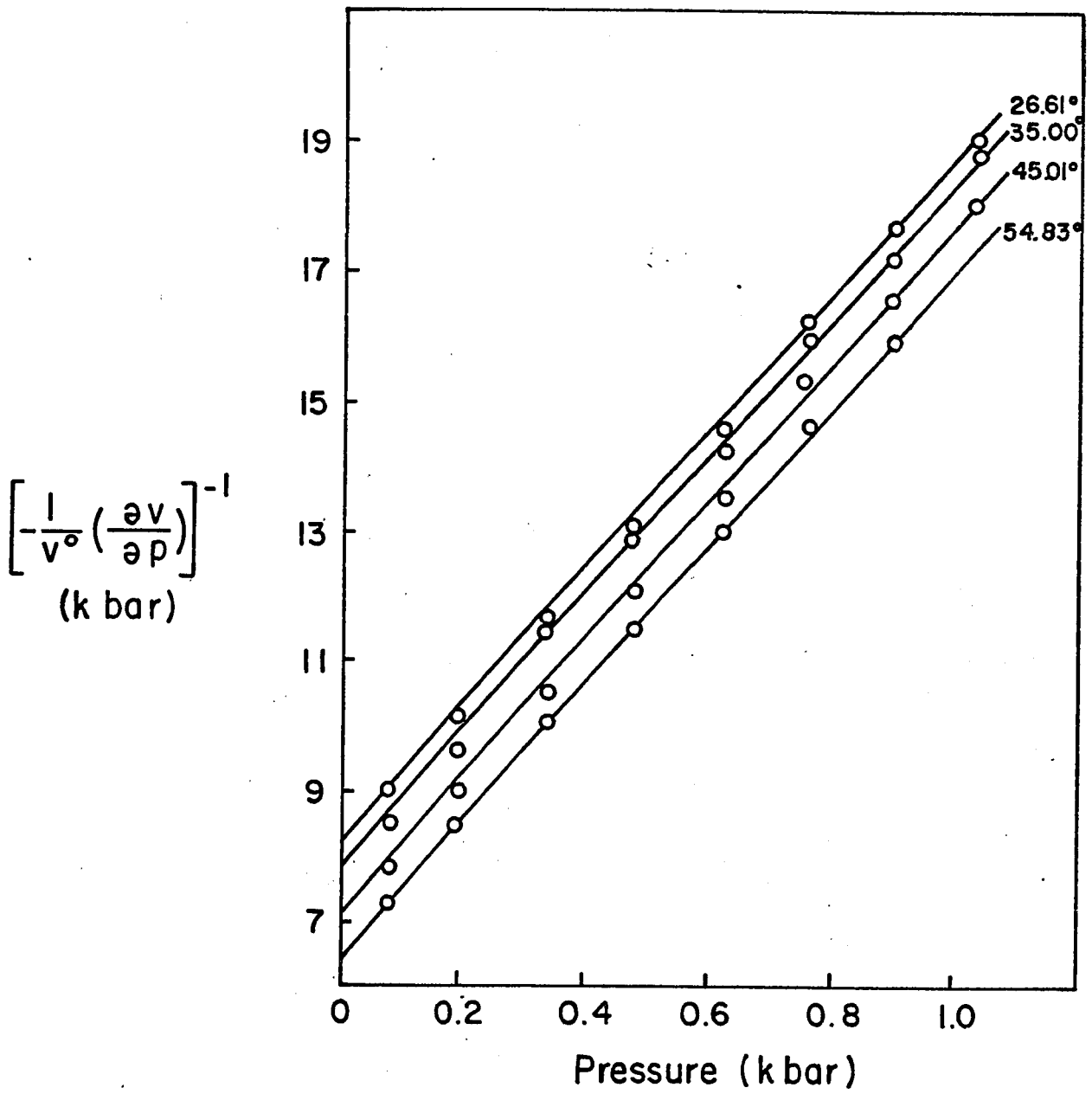
$\left[-\frac{1}{v^\circ}\left(\frac{\partial v}{\partial p}\right)\right]^{-1}$
(k bar)
19
17
15
13
11
9
7
0
0.2
0.4
0.6
0.8
1.0
Pressure (k bar)
26.61°
35.00°
45.01°
54.83°

Table I.1

Constants Obtained by a Least-Mean-Square Fit of Compressibility Data to the Tait Equation

T (°C)	26.61	35.00	45.01	54.83
B (bars)	745(14)	710(14)	627(14)	572(14)
C x 10^4	931(11)	927(11)	920(10)	916(11)

Table I.2

Compressions and Specific Volumes of Acetone Obtained by Various Workers at 26.61°C

Pressure	Compression x 10^2			Specific Volume (ml g^{-1})		
(atmospheres)	present work	Newitt and Weale (165)	Bridgman (164)	present work	Newitt and Weale (165)	Bridgman (164)
400	4.04(0.15)	4.10(0.04)		1.22619	1.2254	
500	4.82(0.16)	4.90(0.05)	4.72	1.21615	1.2151	1.2174
600	5.55(0.17)	5.69(0.06)		1.20691	1.2051	
700	6.22(0.18)	6.42(0.06)		1.19828	1.1957	
800	6.85(0.19)	7.00(0.07)		1.19027	1.1883	
900	7.44(0.20)	7.63(0.08)		1.18276	1.1795	
1000	7.99(0.22)	8.22(0.05)	7.65	1.17569	1.1727	1.1800

Table I.3

Isothermal Compressibilty of Acetone at Atmospheric Pressure

(atmosphere^{-1} x 10^6)

T (°C)	present work	Newitt and Weale (165)	Staveley and Parham (168)	Fryer, Hubbard, and Andrews (166)
26.61	126.8(1.4)			
35.00	132.4(1.4)			
45.01	148.2(1.7)			
54.83	162.6(1.9)			
20.0	119.8(2.8)		124.5(7.4)	129.2
25.0	123.9(3.0)	125.7(0.5)		
30.0	128.2(3.1)		136.2(8.2)	
40.0	139.5(3.6)		148.3(9.0)	158.2
50.0	154.9(4.3)		162.3(9.3)	

From equations (I.3) and (I.4) it can be shown that

$$\left(\frac{\partial V}{\partial T}\right)_P = \left(\frac{\partial V^\circ}{\partial T}\right)_{P^\circ} (1 - k^\circ) + \alpha V^\circ \left\{ \frac{(P - P^\circ)}{(B+P)\ (B+P^\circ)} \left(\frac{dB}{dT}\right) \right\} \qquad (I.5)$$

The superscript zeros denote quantities at atmospheric pressure. The quantity on the left-hand side divided by V° is the isobaric expansivity, α:

$$\alpha = \frac{1}{V^\circ} \left(\frac{\partial V}{\partial T}\right)_P \qquad (I.6)$$

Since

$$\left(\frac{\partial V}{\partial T}\right)_P = -\left(\frac{\partial V}{\partial P}\right)_T \left(\frac{\partial P}{\partial T}\right)_V \qquad (I.7)$$

it follows that the thermal-pressure coefficient $\left(\frac{\partial P}{\partial T}\right)_V$ is given by

$$\left(\frac{\partial P}{\partial T}\right)_V = \frac{\alpha}{\beta} \qquad (I.8)$$

The internal pressure of a liquid, π, is defined as $\left(\frac{\partial U}{\partial V}\right)_T$, where U is the internal energy, it is given by

$$\pi = \left(\frac{\partial U}{\partial V}\right)_T = T\left(\frac{\partial P}{\partial T}\right)_V - P \qquad (I.9)$$

It can therefore be readily calculated using equation (I.8).

The work of Gibson and co-workers (171,172) has suggested the following interpretation of the variation of the internal pressure of liquids with the volume and the temperature. The internal energy is divided into a contribution, U(T), which depends on temperature but not on volume, an attractive energy, U_a, and a repulsive energy, U_r:

$$U = U(T) + U_a + U_r \qquad (I.10)$$

Differentiation at constant temperature with respect to volume gives

$$\pi = \left(\frac{\partial U}{\partial V}\right)_T = \left(\frac{\partial U_a}{\partial V}\right)_T + \left(\frac{\partial U_r}{\partial V}\right)_T \qquad (I.11)$$

$$= \pi_a + \pi_r \qquad (I.12)$$

where $\pi_a = \left(\frac{\partial U_a}{\partial V}\right)_T$ is the attractive component of the internal pressure and $\pi_r = \left(\frac{\partial U_r}{\partial V}\right)_T$ is the repulsive component.

If the shape of the intermolecular potential function for molecules in a liquid is considered, the attractive pressure π_a will be seen to be positive while the repulsive pressure π_r is negative. Further, the function π_a is not a strong function of intermolecular separation while π_r is quite sensitive to small variations in this distance. If the temperature is raised at constant volume, the average separation of the molecules remains constant, but the probability distribution function of molecules about a given molecule varies with temperature. This variation is in part due to the compressions of molecules undergoing collision with each other; as the kinetic energy of the molecules is increased the intermolecular separation corresponding to the collision diameter decreases, resulting in a shift of the probability distributions to smaller separations. Since this postulated effect does not involve hindered rotations, but interpenetration of molecules, it was called "hindered translation" by Gibson and Loeffler (171). The repulsive term π_r thus becomes more negative as the temperature is raised at constant volume, while π_a changes very slightly. The theory of hindered translation predicts that, because of an increase in repulsive energy, the internal pressure decreases with increasing temperature at constant volume. This point of view was first put forward for carbon tetrachloride,

a non-polar substance; this effect will be important in the case of acetone but the effect of association must also be considered.

As is suggested by the results obtained by Gibson and Loeffler (172) on several liquids, it is a useful hypothesis to assume that π_r can be equated to $(B + P)$, where B is the constant in the Tait equation:

$$\pi_r = \left(\frac{\partial U_r}{\partial V}\right)_T = -(B + P) \qquad \text{(I.13)}$$

Equations (I.12) and (I.9) then lead to

$$\pi_a = \left(\frac{\partial U_a}{\partial V}\right)_T = T\left(\frac{\partial P}{\partial T}\right)_V + B \qquad \text{(I.14)}$$

Equations (I.13) and (I.14) now allow π_a and π_r to be calculated for acetone from the results obtained in the present work.

Figure I.4 shows the internal pressure, π, calculated using equation (I.9) plotted against the molal volume. As predicted by the theory of hindered translation, the value of π does become more negative at constant volume as the temperature is raised. However, in contrast to the situation with carbon tetrachloride, the magnitude of the change depends considerably on the volume.

Figure I.5 shows a double-logarithmic plot of attractive pressure against the molal volume. For carbon tetrachloride the curves are the same for all temperatures (171); the present work shows a strong temperature effect for acetone.

Table I.4 shows values at different molal volumes for the temperature coefficients (at constant volume) of the total internal pressure and the repulsive pressure π_r ($-(B + P)$). It is to be seen

Figure I.4. Plot of internal pressure, π, against molal volume of acetone at four temperatures.

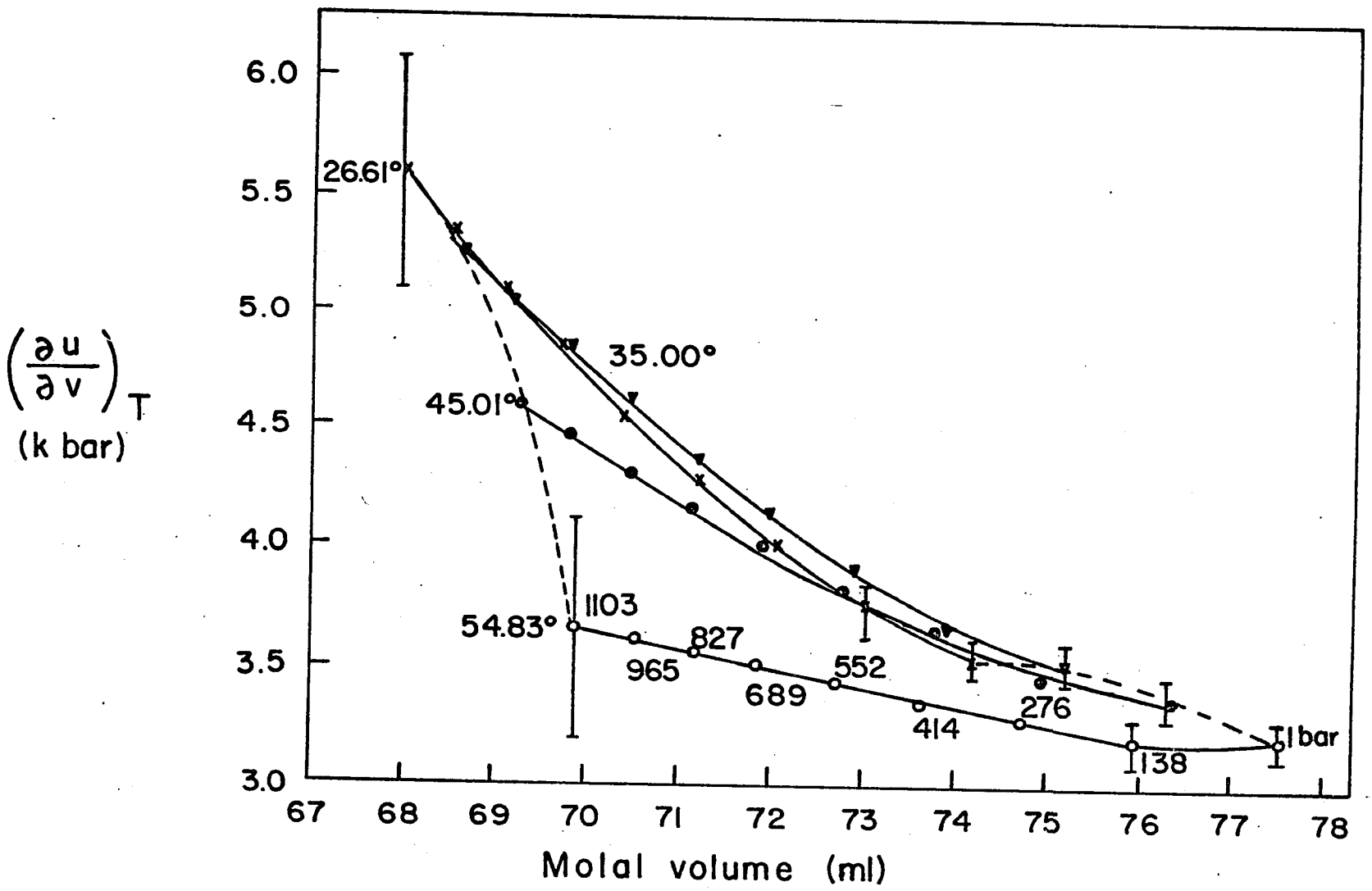
$\left(\frac{\partial u}{\partial v}\right)_T$
(k bar)
6.0
5.5
5.0
4.5
4.0
3.5
3.0
26.61°
35.00°
45.01°
54.83°
1103
827
965
552
689
414
276
138
1 bar
67
68
69
70
71
72
73
74
75
76
77
78
Molal volume (ml)

Figure I.5. Plot of $\log_{10} \pi_a$ against $\log_{10}$(molal volume)

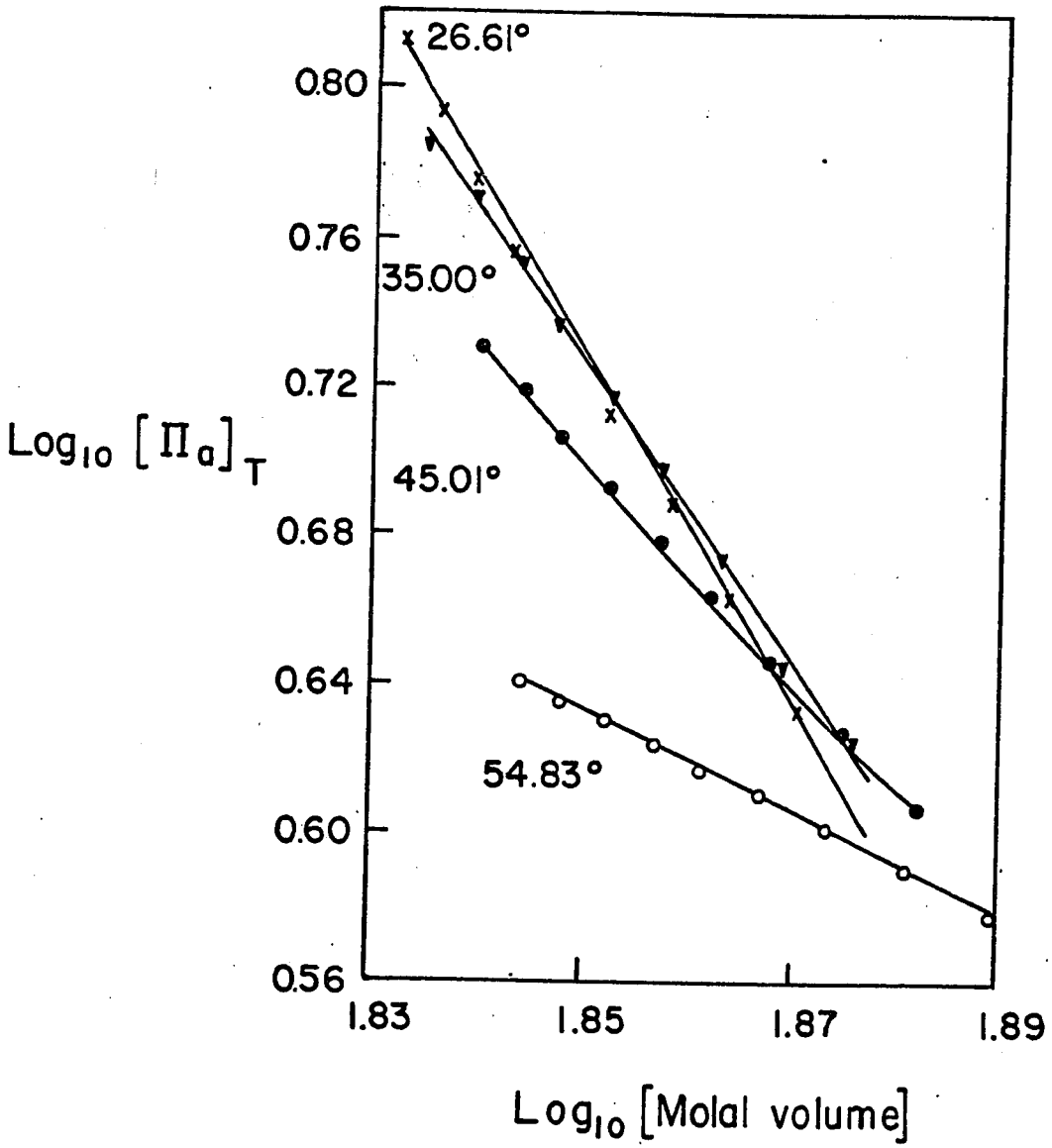
26.61°
35.00°
45.01°
54.83°
0.80
0.76
0.72
0.68
0.64
0.60
0.56
1.83
1.85
1.87
1.89
Log10 [Πa]T
Log10 [Molal volume]

Table I.4

Least-Mean-Square Estimates of Slopes of π and π_r with respect to Temperature at Several Volumes

Volume (ml mole^{-1})	$\left(\frac{\partial \pi}{\partial T}\right)_V$ (bar deg^{-1})	$\left(\frac{\partial (B + P)}{\partial T}\right)_V$ (bar deg^{-1})
75	-3.7(3.0)	9.5(0.2)
74	-2.4(3.0)	9.6(0.3)
73	-12(3)	8.5(0.3)
72	-22(4)	7.4(0.3)
71	-31(4)	6.3(0.4)
70	-41(4)	5.1(0.4)

that the decreases of π with T are not equal to the increases of π_r, as they are for a normal liquid such as carbon tetrachloride (171). Table I.5, the values in which are derived from Figure I.5, shows, at different temperatures, the variation (at constant temperature) of $\log_{10} \pi_a$ with $\log_{10} V$. Again the behaviour is different from that of carbon tetrachloride, where these slopes are independent of temperature. The attractive pressure π_a must, for acetone, be expressed as a function of volume and temperature; Figure I5 and Table I.5 show that if π_a is expressed as

$$\pi_a = bV^{-n} \qquad \text{(I.15)}$$

the exponent n is temperature-dependent.

Heat Capacities

It is also possible, using the present data, to derive information about the heat capacity of acetone at constant volume, and its variation with temperature, pressure, and molal volume. The temperature dependence of C_p for acetone, at atmospheric pressure, has been measured by Staveley and Parker (168) and by Low and Moelwyn-Hughes (169), with good agreement where the temperatures overlap. Values of C_p at pressures other than atmospheric were calculated using the present results and the relationship

$$\left(\frac{\partial C_p}{\partial P}\right)_T = -T\left(\frac{\partial^2 V}{\partial T^2}\right)_P \qquad \text{(I.16)}$$

The results for the variation of volume with temperature at constant pressure were fitted to the polynomial

$$\left(\frac{\partial V}{\partial T}\right)_P = a_0 + a_1 T + a_2 T^2 \qquad \text{(I.17)}$$

Table I.5

Least-Mean-Square Estimate of the Exponent, m, in Equation (I.15) at Four Temperatures

T (°C)	$\left(\frac{\partial \log_{10}(\pi_a)_T}{\partial \log_{10} V}\right)_V$
26.61	-4.64(0.02)
35.00	-4.14(0.02)
45.01	-2.93(0.01)
54.83	-1.38(0.01)

so that the second derivative used in equation (I.16) is $a_1 + 2a_2T$. Values of C_P at different pressures and temperatures were thus calculated making use of the present data. The results at a given temperature were fitted to the polynomial

$$\left(\frac{\partial C_P}{\partial P}\right)_T = b_o + b_1 P + b_2 P^2 \qquad (I.18)$$

Equation (I.18) was integrated at each temperature and, with the use of the appropriate value of C_P at atmospheric pressure, C_P was calculated at different pressures and temperatures by the use of the thermodynamic equation

$$C_P - C_V = TV\alpha \left(\frac{\partial P}{\partial T}\right)_V \qquad (I.19)$$

together with the data obtained in the present work. The results are shown in Figure I.6 in the form of C_V values plotted against the molal volume, at the four temperatures. Since a second derivative has to be used in the calculation of $\left(\frac{\partial C_P}{\partial P}\right)_T$, the errors in the individual C_V values are fairly large; the relative errors are only 1 to 2 percent, however.

With normal liquids such as carbon tetrachloride C_V increases when the liquid is compressed at constant temperature. In the present work this is indeed found at the higher temperatures (Figure I.6). All of the slopes, $\left(\frac{\partial C_V}{\partial V}\right)_T$, become less negative as the volume is increased. At the lowest temperature the slopes are much less negative, over the entire volume range, than is usually the case with a normal liquid such as carbon tetrachloride.

This behaviour is consistent with there being, particularly at the lower temperatures, some associative interactions leading to short-range ordering in the liquid. Thus, in the case of water, where these

Figure I.6. Plot of heat capacity, C_V, against molal volume at four temperatures.

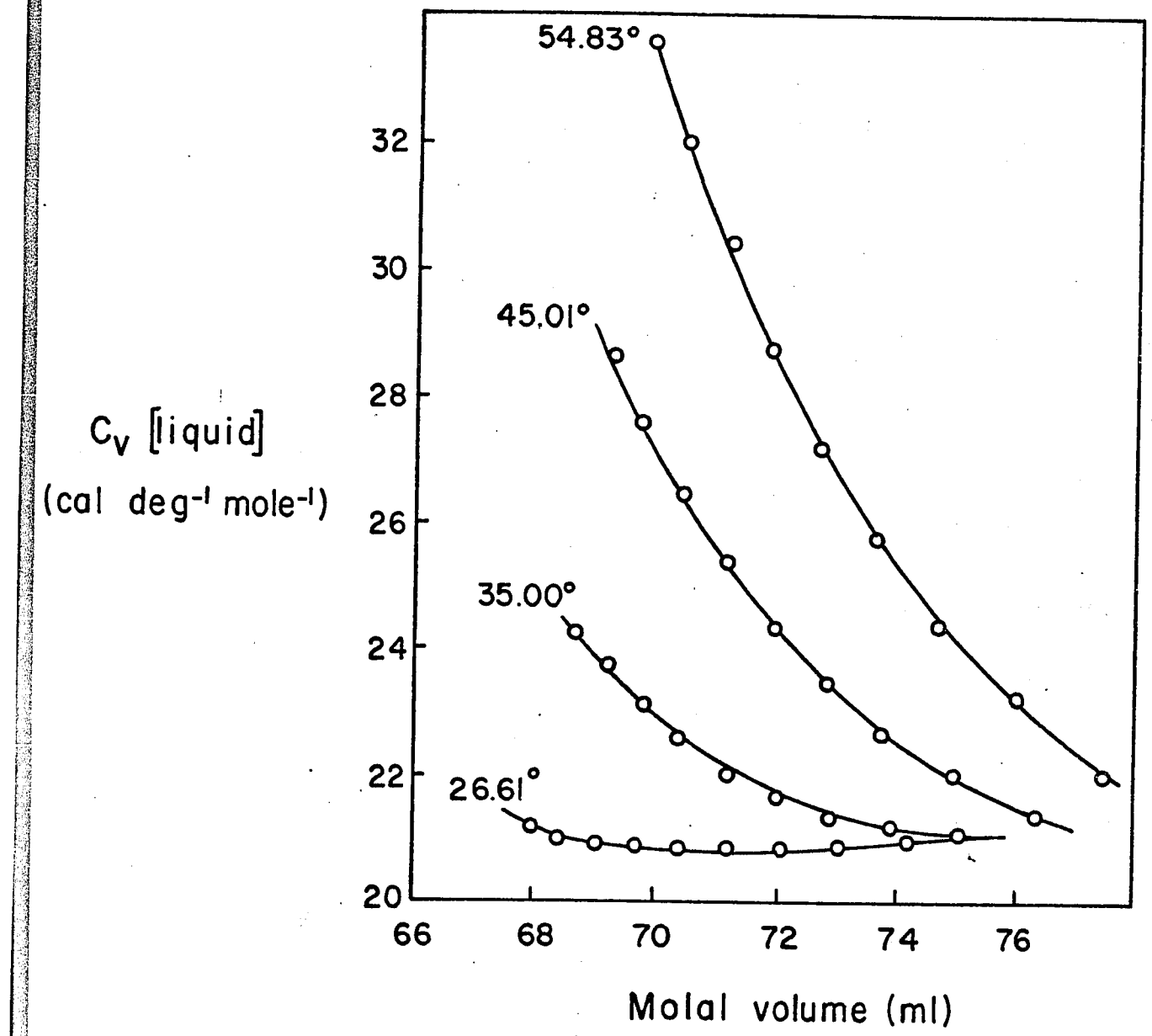
54.83°
45.01°
35.00°
26.61°
32
30
28
26
24
22
20
66
68
70
72
74
76
C_v [liquid]
(cal deg^{-1} mole^{-1})
Molal volume (ml)

interactions are known to be strong, the heat capacity C_v of water actually increases rather than decreases with increasing molal volume (171, 173, 174). The general tendency of the slopes in Figure I.6 to become less negative as the temperature is lowered can therefore be explained on the hypothesis that ordering is becoming more important at the lower temperatures. This ordering is attributed to dipole-dipole interactions coupled with the packing patterns favored by the shapes of the molecules.

GENERAL DISCUSSION

Some evidence for a change in the degree of association present in liquid acetone, especially at a temperature close to 25°C, has been obtained by Cole (175) from dielectric constant measurements. These results indicate that the Kirkwood correlation factor, g, the structural factor, passed through a maximum close to 25°C. The value of g obtained was close to 1.21 over the whole liquid range indicating consociation of dipoles.

The effect of pressure on the dielectric constant was investigated by Jacobs and Lawson (176) on the basis of older experimental data. The calculations indicate that the effect of pressure on the dielectric constant of acetone is similar to the effect of pressure on that of water. This is taken as further evidence of the importance of structure in acetone.

Pressure has a positive effect on the heat capacity of normal liquids such as carbon tetrachloride, as mentioned earlier. Since higher temperatures tend to destroy any short range order, compression should produce evidence of a normal pressure effect on the heat capacity at higher temperatures. The normal behaviour will therefore predominate in the higher isotherms and such is found to be the case at 55°, 45° and

55°C. The magnitude of this variation brought about by compression is large, but such variations in C_T for acetone have been indicated by the earlier work of Bridgman (164).

A paper by Low and Moelwyn-Hughes (169) was referred to in connection with C_p. These workers have calculated the dependence of the heat capacity C_T of acetone on volume from -20 to +35°C. The pressure dependence of the compressibility and expansivity which they adopted, however, was based on the work of Bridgman and Amagat (162, 163, 164) which is not of a sufficiently high degree of accuracy to give reliable heat capacity pressure dependence. The heat capacity increases on compression at 35°C according to them, at about the same rate as has been calculated in the present work. They report a slight reduction in the rate of increase in C_T with compression as the temperature is raised; this, however, is not borne out by our results.

The heat capacity can be separated into the contributions due to different forms of molecular motion as suggested by Harrison and Moelwyn-Hughes (173). Such an analysis predicts a structural contribution at atmospheric pressure of close to 2R. Since the structural contribution for water is about 3R, an association effect is suggested. The temperature variation of the structural contribution to C_V is small, but a slight decrease is apparent above 25°C.

APPENDIX II

Primary Data

(a) Resistance extrapolated to infinite frequency (Ω)

High-pressure cells

Me_4NI

	Pressure (bar)	Temperature (°C) 26.61	35.00	45.01	54.83
1.	1.0	3761.42	3609.73	3380.16	3215.91
	137.9	3925.82	3740.72	3517.16	3339.76
	275.8	4098.67	3893.16	3659.31	3462.90
	413.7	4272.35	4054.95	3800.44	3592.94
	551.6	4450.40	4215.85	3949.87	3725.13
	689.5	4639.95	4379.94	4091.11	3854.16
	827.4	4827.93	4548.38	4241.66	4058.53
	965.3	5009.49	4716.41	4395.73	4135.13
	1103.2	5203.07	4883.40	4552.08	4308.60
2.					
	1.0	3815.01	3657.84	3429.23	3260.06
	137.9	3984.70	3798.79	3571.41	3388.46
	275.8	4159.99	3957.49	3716.40	3515.69
	413.7	4335.92	4123.46	3862.03	3649.41
	551.6	4513.37	4288.01	4014.82	3785.47
	689.5	4702.66	4457.23	4160.15	3925.54
	827.4	4890.64	4629.12	4312.79	4124.64
	965.3	5075.78	4801.15	4471.47	4207.72
	1103.2	5274.97	4971.35	4628.45	4407.88
4.					
	1.0	5940.18	5707.85	5336.17	5054.62
	137.9	6222.78	5944.54	5573.98	5273.26
	275.8	6512.60	6203.74	5814.26	5485.88
	413.7	6805.75	6475.58	6054.14	5708.81
	551.6	7103.13	6745.01	6304.83	5914.12
	689.5	7425.14	7018.97	6541.92	6137.25
	827.4	7746.10	7298.21	6788.83	6538.14
	965.3	8046.65	7575.50	7047.68	6598.89
	1103.2	8365.94	7850.36	7301.08	6956.86
5.					
	1.0	7780.55	7486.95	6983.30	6617.02
	137.9	8170.41	7811.22	7310.15	6919.54
	275.8	8566.31	8165.42	7637.45	7211.48
	413.7	8966.45	8527.48	7961.73	7514.15
	551.6	9377.01	8888.17	8295.38	7796.41
	689.5	9813.86	9254.31	8613.46	8105.74
	827.4	10237.9	9622.86	8944.08	8681.76
	965.3	10638.8	9995.64	9281.81	8701.25
	1103.2	11062.4	10362.4	9619.38	9221.21
6.					
	1.0	8841.63	8562.53	7998.75	7591.36
	137.9	9292.99	8947.26	8380.45	7946.01
	275.8	9743.75	9360.23	8760.34	8286.31
	413.7	10200.5	9778.65	9134.63	8634.01
	551.6	10664.6	10196.9	9520.11	8954.81
	689.5	11164.8	10620.6	9888.05	9269.27
	827.4	11661.0	11047.6	10268.5	10030.2
	965.3	12131.3	11475.9	10661.0	10003.5
	1103.2	12629.8	11899.2	11048.3	10636.6

Me_4NI (cont.)		Temperature (°C)		
7. Pressure (bar)	26.61	35.00	45.01	54.83
1.0	9015.25	8677.83	8106.79	7681.12
137.9	9487.01	9076.76	8497.26	8046.05
275.8	9957.87	9499.86	8885.15	8397.22
413.7	10442.9	9927.95	9267.60	8752.33
551.6	10949.0	10356.2	9659.88	9078.27
689.5	11457.6	10789.3	10039.9	9424.45
827.4	11944.0	11222.5	10429.3	10174.7
965.3	12415.3	11660.8	10827.5	10143.1
1103.2	12908.2	12091.0	11224.9	10797.7
Et_4NI				
1. 1.0	1839.82	1745.99	1643.10	1577.69(1586.69)
137.9	1917.61	1824.73	1722.19	1642.45
275.8	2008.38	1905.76	1797.11	1711.21
413.7	2099.49	1992.07	1872.85	1780.52
551.6	2187.83	2077.08	1949.43	1852.34
689.5	2283.86	2158.96	2025.77	1922.18
827.4	2376.94	2240.61	2102.70	1999.61
965.3	2471.89	2327.50	2182.29	2069.42
1103.2	2568.70	2417.73	2261.13	2141.37
2.				
1.0	1537.42	1482.75	1371.65	1312.01(1311.57)
137.9	1601.71	1547.22	1434.11	1362.93
275.8	1676.48	1590.15	1494.08	1417.47
413.7	1751.64	1660.22	1555.26	1472.17
551.6	1825.29	1729.52	1617.90	1529.53
689.5	1903.13	1796.72	1679.70	1585.27
827.4	1980.09	1863.01	1743.26	1646.74
965.3	2058.97	1934.85	1807.46	1702.70
1103.2	2138.27	2007.77	1872.32	1760.23
4.				
1.0	2112.84	2005.60	1882.59	1795.98(1795.98)
137.9	2204.85	2097.77	1971.90	1871.11
275.8	2310.68	2191.73	2057.59	1949.37
413.7	2416.81	2290.83	2144.42	2027.33
551.6	2520.86	2388.53	2232.91	2108.23
689.5	2630.84	2483.51	2319.98	2187.11
827.4	2738.83	2576.35	2409.43	2273.39
965.3	2849.82	2677.15	2499.55	2352.31
1103.2	2961.73	2779.95	2590.57	2432.90
6.				
1.0	5396.37	5144.15	4805.61	4565.38(4570.38)
137.9	5665.11	5409.08	5065.09	4786.56
275.8	5958.14	5675.51	5312.32	5012.69
413.7	6253.15	5951.21	5555.70	5235.06
551.6	6538.59	6221.98	5800.67	5461.28
689.5	6844.59	6484.36	6044.20	5683.63
827.4	7148.16	6744.65	6288.63	5920.35
965.3	7456.73	7019.62	6536.15	6139.97
1103.2	7765.74	7299.95	6783.46	6363.05

Et_4NI (cont.)	Temperature (°C)			
7. Pressure (bar)	26.61	35.00	45.01	54.83
1.0	4940.11	4698.69	4388.31	4179.04
137.9	5186.80	4940.17	4622.83	4389.07
275.8	5457.54	5182.31	4848.62	4601.86
413.7	5727.07	5433.10	5070.85	4810.33
551.6	5990.07	5680.78	5295.23	5023.77
689.5	6269.17	5920.37	5517.16	5231.09
827.4	6544.34	6155.73	5740.64	5452.26
965.3	6824.04	6407.93	5965.52	5656.59
1103.2	7102.68	6662.09	6191.39	5863.97
8.				
1.0	14889.3	14167.3	13130.0	12433.2
137.9	15662.2	14932.5	13893.4	13075.5
275.8	16518.8	15698.6	14600.6	13723.9
413.7	17389.8	16485.3	15291.3	14350.8
551.6	18214.3	17260.6	15979.1	14987.9
689.5	19112.6	17994.8	16662.4	15693.5
827.4	19967.3	18721.0	17338.4	16261.7
965.3	20814.1	19481.9	18023.4	16860.2
1103.2	21675.8	20272.0	18702.4	17469.2
$n\text{-}Pr_4NI$				
1. 1.0	1841.18	1744.98	1644.78	1574.77
137.9	1924.98	1826.08	1716.57	1639.91
275.8	2014.93	1908.24	1792.23	1706.02
413.7	2102.03	1987.02	1867.08	1776.23
551.6	2195.08	2071.48	1944.68	1847.02
689.5	2289.59	2153.08	2021.72	1918.18
827.4	2377.38	2235.17	2099.98	1989.32
965.3	2470.78	2324.78	2174.47	2059.92
1103.2	2567.14	2411.99	2254.32	2133.28
2.				
1.0	2220.73	2102.38	1978.93	1880.92
137.9	2325.08	2204.03	2067.02	1960.66
275.8	2437.52	2306.12	2160.51	2040.56
413.7	2545.32	2404.52	2251.22	2126.21
551.6	2660.68	2508.62	2346.36	2211.41
689.5	2777.12	2609.71	2439.65	2297.20
827.4	2885.21	2710.56	2534.76	2382.44
965.3	3000.52	2821.16	2624.50	2468.45
1103.2	3118.11	2928.20	2721.44	2555.04
4.				
1.0	3325.45	3144.35	2952.98	2799.11
137.9	3489.30	3303.24	3092.82	2926.75
275.8	3662.59	3462.23	3239.17	3054.10
413.7	3829.33	3613.58	3380.56	3186.70
551.6	4006.28	3774.07	3527.86	3318.54
689.5	4185.12	3930.06	3668.93	3451.44
827.4	4352.51	4086.25	3814.93	3583.42
965.3	4529.61	4255.05	3955.03	3716.17
1103.2	4710.44	4419.24	4103.52	3849.37

n-Pr_4NI (cont.)

	Pressure (bar)	Temperature (°C) 26.61	35.00	45.01	54.83
6.	1.0	5314.68	5076.81	4760.42	4504.59
	137.9	5590.56	5345.60	5002.20	4727.32
	275.8	5872.62	5530.07	5247.84	4947.31
	413.7	6146.53	5782.63	5486.17	5170.28
	551.6	6433.09	6043.69	5622.76	5393.06
	689.5	6721.45	6296.29	5857.76	5615.29
	827.4	6993.56	6550.74	6092.27	5837.12
	965.3	7279.50	6820.05	6318.17	6057.95
	1103.2	7571.22	7083.66	6555.47	6280.34
7.					
	1.0	10054.6	9467.25	8840.62	8322.58
	137.9	10602.0	9996.44	9314.54	8764.04
	275.8	11162.1	10509.7	9794.91	9192.31
	413.7	11703.4	11010.8	10255.9	9624.17
	551.6	12268.3	11525.9	10715.7	10049.9
	689.5	12838.7	12024.9	11180.1	10474.3
	827.4	13370.6	12522.5	11641.6	10894.6
	965.3	13932.0	13054.4	12082.5	11312.4
	1103.2	14502.6	13570.1	12547.7	11731.2
8.					
	1.0	21348.0	20034.3	18583.9	17382.2
	137.9	22536.4	21169.4	19602.2	18322.8
	275.8	23732.4	22215.4	20614.4	19230.1
	413.7	24896.1	23283.8	21587.0	20134.6
	551.6	26089.1	24366.1	22486.0	21020.6
	689.5	27281.9	25416.2	23448.8	21892.9
	827.4	28417.6	26465.5	24402.6	22764.5
	965.3	29598.5	27556.8	25322.8	23613.4
	1103.2	30795.9	28628.6	26275.6	24476.7

Atmospheric-pressure cells

Solution number	Salt	Temperature (°C) 26.61	35.00	45.01	54.83
1.	Me_4NI	3662.96	3467.40	3277.37	3110.71
	Et_4NI	1781.85	1689.49	1601.32	1523.21
	$\underline{n}$-Pr_4NI	1784.31	1691.97	1598.72	1521.48
2.	Me_4NI	3708.70	3512.61	3322.56	3154.61
	Et_4NI	1479.36	1403.79	1327.50	1264.44
	$\underline{n}$-Pr_4NI	2142.33	2030.57	1915.51	1821.18
3.	Me_4NI	3930.56	3727.03	3504.65	3294.46
	Et_4NI	1942.18	1838.94	1728.98	1639.31
	$\underline{n}$-Pr_4NI	1847.48	1746.69	1643.93	1561.50
4.	Me_4NI	5547.02	5253.27	4947.32	4711.08
	Et_4NI	1954.82	1852.99	1757.08	1666.52
	$\underline{n}$-Pr_4NI	3082.98	2914.74	2747.28	2601.84
5.	Me_4NI	6733.67	6342.46	5958.04	5651.29
	Et_4NI	2698.26	2555.07	2413.57	2290.04
	$\underline{n}$-Pr_4NI	3460.28	3270.94	3080.49	2916.60
6.	Me_4NI	6026.34	5696.14	5355.40	5038.30
	Et_4NI	3634.12	3433.67	3207.37	3038.04
	$\underline{n}$-Pr_4NI	3608.82	3407.79	3193.17	3013.80
7.	Me_4NI	8634.16	8142.60	7667.67	7275.85
	Et_4NI	4787.54	4536.90	4258.47	4045.25
	$\underline{n}$-Pr_4NI	9729.69	9185.60	8597.55	8146.76
8.	Me_4NI	13144.1	12395.7	11641.2	11018.9
	Et_4NI	13207.9	12458.8	11687.8	11028.0
	$\underline{n}$-Pr_4NI	18860.2	17824.4	16625.9	15663.3

(b) Concentrations of acetone solutions at atmospheric pressure and 26.61°C

(moles l^{-1})x10^4

High-pressure cell	Salt		
	Me_4NI	Et_4NI	$n\text{-}Pr_4NI$
1	4.4682	9.7287	10.669
2	4.2011	11.250	8.1184
3	3.0912	6.5892	7.6156
4	2.8066	8.7703	5.7834
5	2.1695	5.7462	4.7770
6	1.9456	3.3412	3.6471
7	1.7243	3.2916	1.6966
8	1.0707	1.0684	0.8000

Atmospheric-pressure cells in the order 1,2,3,1,2,3,1, and 2 were filled with the eight solutions listed above starting from the top.

APPENDIX III

1.
Shedlovsky Program

List of Abbreviations

TEMP	temperature (^{o}K)
PRES	pressure (bar)
DIELT	dielectric constant
VISCY	viscosity ($g\ cm^{-1}sec^{-1}$)
TAITB	B constant in the Tait equation (bar)
TAITC	C constant in the Tait equation
AMBDA	equivalent conductivity ($cm^2\Omega^{-1}mole\text{-}1$)
CONC	concentration ($mole\ l^{-1}$)
ONGSL	Onsager slope ($cm^2\Omega^{-1}mole^{-1}x(mole\ l^{-1})^{-\frac{1}{2}}$)
SHEDL	Shedlovsky constant
ZFUOS	Z variable in the Shedlovsky treatment
AMBIN	limiting equivalent conductivity ($cm^2\Omega^{-1}mole^{-1}$)
SAMIN	standard deviation in AMBIN
DICON	dissociation constant ($mole\ l^{-1}$)
SDICO	standard deviation in DICON
HETAM	energy of activation for conductivity at constant pressure ($cal\ mole^{-1}$)
SHEAM	standard deviation in HETAM
VOLAM	volume of activation for conductivity ($ml\ mole^{-1}$)
SVOAM	standard deviation in VOLAM
HEATK	enthalpy of dissociation ($cal\ mole^{-1}$)
SHETK	standard deviation in HEATK
ENTPK	entropy of dissociation ($cal\ deg^{-1}mole^{-1}$)
SENPK	standard deviation in ENTPK
GIBEK	Gibbs free energy of dissociation ($cal\ mole^{-1}$)
SGIEK	standard deviation in GIBEK
VOLMK	volume of dissociation ($ml\ mole^{-1}$)
SVOMK	standard deviation in VOLMK
ACOF2	molar activity coefficient squared
SAMBI	standard deviation in AMBIN
DEG	degree of dissociation

```
.0001            DOUBLE PRECISION TEMP(44),PRES(44),DIELT(44),VISCY(44),TAITB(44),
                1TAITC(44),X(14,7),Y(14,7),AMBDA(14,44),
                2A(16,16),CONC(14,44),ONGSL(7,44),SHEDL(14,7),ZFUOS(14,7),
                3AMBIN(7,44),SAMIN(7,44),DICON(7,44),SDICO(7,44),HEIAM(4,9),
                4SHEAM(4,9),VOLAM(9,4),SVOAM(9,4),HEATK(4,9),SHETK(4,9),ENTPK(4,9),
                5SENPK(4,9),GIBEK(4,9),SGIEK(4,9),VOLMK(9,4),SVOMK(9,4),
                6W(14),ACOF2(14,7),XX(14),YY(14),E(16),SAMBI(7,44),DEG(14,7)
.0002            DIMENSION JJ(44),N(44),KKK(44)
.0003            COMMON A,E
.0004       2000 READ(1,1002)M
.0005       2001 WRITE(3,1002)M
.0006       3000 DO 9900 J=1,M
.0007       4000 READ(1,1004)JJ(J),N(J),TEMP(J),PRES(J),DIELT(J),VISCY(J),TAITB(J),
                1TAITC(J)
.0008       4001 WRITE(3,1004)JJ(J),N(J),TEMP(J),PRES(J),DIELT(J),VISCY(J),
                1TAITB(J),TAITC(J)
.0009       5000 NN=N(J)
.0010       6000 DO 8000 I=1,NN
.0011       7000 READ(1,1007)AMBDA(I,J),CONC(I,J)
.0012       7001 WRITE(3,1007)AMBDA(I,J),CONC(I,J)
.0013       8000 CONTINUE
.0014       9000 CONTINUE
.0015       1100 DO 4600 J=1,M
.0016       1101 WRITE(3,3011)
.0017       1102 NN=N(J)
.0018       1200 DO 1700 L=1,NN
.0019       1201 LAST=1
.0020       1202 NO=N(J)
.0021       1203 WRITE(3,1002)NO
.0022       1900 K=1
.0023       1300 X(L,K)=DSQRT(CONC(L,J))
.0024       1301 WRITE(3,3013)X(L,K)
.0025       1302 XX(L)=X(L,K)
.0026       1400 Y(L,K)=AMBDA(L,J)
.0027       1401 WRITE(3,3013)Y(L,K)
.0028       1402 YY(L)=Y(L,K)
.0029       1500 W(L)=1
.0030       1600 SDCHK=0
.0031       1700 CONTINUE
.0032       1800 CALL DFIT(XX,YY,W,NO,LAST,SDCHK)
.0033       2100 AMBIN(K,J)=A(1,3)
.0034       2201 WRITE(3,3022)AMBIN(K,J)
.0035       2202 WRITE(3,3055)
.0036       2504 WRITE(3,3025)
.0037       2203 WRITE(3,3055)
.0038       2300 DO 4500 K=1,6
.0039       2301 Z1= 0.8204D+06
.0040       2400 ONGSL(K,J)=Z1/((DIELT(J)*TEMP(J))**(1.5))*AMBIN(K,J)+
                182.5/(VISCY(J)*((DIELT(J)*TEMP(J))**(0.5)))
.0041       2502 WRITE(3,3022)ONGSL(K,J)
.0042       2503 WRITE(3,3055)
.0043       2501 NN=N(J)
.0044       2600 DO 3300 I=1,NN
```

```
S.0045      2601 NO=N(J)
S.0046      2700 ZFUOS(I,K)=(ONGSL(K,J)/((AMBIN(K,J))**(1.5)))*DSQRT(CONC(I,J)*
               1AMBDA(I,J))
S.0047      2701 WRITE(3,3013)ZFUOS(I,K)
S.0048      2800 SHEDL(I,K)=(0.5*(ZFUOS(I,K))+((1+((0.5*ZFUOS(I,K))**2))**0.5))**2
S.0049      2801 WRITE(3,3013)SHEDL(I,K)
S.0050      2802 DEG(I,K)=SHEDL(I,K)*AMBDA(I,J)/AMBIN(K,J)
S.0051      2803 WRITE(3,3013)DEG(I,K)
S.0052      2900 ACOF2(I,K)=(DEXP((0.15848D+07*DSQRT(CONC(I,J)*DEG(I,K)))/
               1(DIELT(J)*TEMP(J))**(1.5)))**(-1)
S.0053      2901 WRITE(3,3013)ACOF2(I,K)
S.0054      3100 X(I,K)=((SHEDL(I,K)*AMBDA(I,J))**2)*(ACOF2(I,K)*CONC(I,J))
S.0055      3101 XX(I)=X(I,K)
S.0056      3200 Y(I,K)=(SHEDL(I,K)*AMBDA(I,J))
S.0057      3201 YY(I)=Y(I,K)
S.0058      3202 W(I)=1
S.0059      3300 CONTINUE
S.0060      3301 WRITE(3,3055)
S.0061      3400 NO=N(J)
S.0062      3500 LAST=1
S.0063      3600 SDCHK=0
S.0064      3700 CALL DFIT(XX,YY,W,NO,LAST,SDCHK)
S.0065      3800 AMBIN(K+1,J)=A(1,3)
S.0066      3803 SAMBI(K+1,J)=E(1)
S.0067      3801 WRITE(3,1007)A(1,3),E(1)
S.0068      3802 WRITE(3,1007)A(2,3),E(2)
S.0069      3900 DICON(K+1,J)=-1/(A(1,3)*A(2,3))
S.0070      3901 WRITE(3,4022)DICON(K+1,J)
S.0071      4100 SDICO(K+1,J)=(A(1,3)*E(2)-A(2,3)*E(1))/(A(1,3)*A(2,3))**2
S.0072      4101 WRITE(3,4022)SDICO(K+1,J)
S.0073      4300 IF (AMBIN(K,J)/AMBIN(K+1,J)-0.9995)4500,4400,4400
S.0074      4400 IF (AMBIN(K,J)/AMBIN(K+1,J)-1.0005)4501,4501,4500
S.0075      4500 CONTINUE
S.0076      4501 KKK(J)=K
S.0077      4502 WRITE(3,1002)KKK(J)
S.0078      4600 CONTINUE
S.0079      4800 DO 5600 J=1,M
S.0080      4900 WRITE(3,3055)
S.0081      4901 K=1
S.0082      5400 WRITE(3,3054)
S.0083      5101 WRITE(3,3013)AMBIN(K,J)
S.0084      5201 WRITE(3,3013)ONGSL(K,J)
S.0085      5202 WRITE(3,3055)
S.0086      5203 KK=KKK(J)
S.0087      5204 DO 5500 K=1,KK
S.0088      5301 WRITE(3,3053)AMBIN(K+1,J),SAMBI(K+1,J),DICON(K+1,J),SDICO(K+1,J)
S.0089      5401 WRITE(3,3055)
S.0090      5500 CONTINUE
S.0091      5600 CONTINUE
S.0092      1002 FORMAT(I4)
S.0093      1004 FORMAT(2I4,3D16.8/3D16.8)
S.0094      1007 FORMAT(2D16.8)
S.0095      3011 FORMAT(//2X,'ONSAGER SQRT CONC FIT')
S.0096      3013 FORMAT(D25.16)
S.0097      3025 FORMAT(//2X,'SHEDLOVSKY FITS')
```

```
S.0098      4022 FORMAT(D25.16)
S.0099      3022 FORMAT(D25.16)
S.0100      3053 FORMAT(4D16.8)
S.0101      3054 FORMAT(//2X,' LAMBDA AT INFINITE DILUTION AND DISOCIATION CONSTANT
                1 FOR ONE CONDITION OF TEMP AND PRES')
S.0102      3055 FORMAT(//2X)
S.0103      5700 RETURN
S.0104           END

                    SIZE OF COMMON  002176   PROGRAM  039878

                                END OF COMPILATION  MAIN
```

Least-mean-square subroutines: DFIT

DSOLV

```
S.0001            SUBROUTINE DFIT (X,Y,W,NO,LAST,SDCHK)
                C                    ***SPECIFICATION STATEMENTS***
S.0002            DOUBLE PRECISION X(100),Y(100),W(100),POWX(100),WY(100),DIFF(100),
                 1 YC(100),SUMX(31),SUMY(16),A(16,16),E(16),DET,TEST,SWR2,TEMP,XI,
                 2 RMSD,ORMSD,BIGX,SMLX
S.0003            INTEGER SDCHK
S.0004            COMMON A,E
                C                    ***CHECK MAXIMUM ORDER AND NUMBER OF DATA POINTS***
S.0005          4 IF (LAST + 1 - NO) 2,1,1
S.0006          1 LAST=NO-2
S.0007            IF (LAST) 3,3,2
S.0008          3 WRITE (3,108)
S.0009         12 RETURN
                C                    *** FIND RANGE OF X ***
S.0010          2 BIGX = X(1)
S.0011            SMLX = X(1)
S.0012            DO 40 I=2,NO
S.0013            XI = X(I)
S.0014            IF (BIGX - XI) 41,42,42
S.0015         41 BIGX = XI
S.0016            GO TO 40
S.0017         42 IF (XI - SMLX) 43,40,40
S.0018         43 SMLX = XI
S.0019         40 CONTINUE
S.0020            WRITE (3,102) NO,SMLX,BIGX
                C                    *** INITIALIZE FOR NORMAL EQUATIONS ***
S.0021            SUMX(1) = 0.D0
S.0022            SUMY(1) = 0.D0
S.0023            DO 6 I=1,NO
S.0024            SUMX(1) = SUMX(1) + W(I)
S.0025            WY(I) = W(I) * Y(I)
S.0026            SUMY(1) = SUMY(1) + WY(I)
S.0027          6 POWX(I) = 1.D0
S.0028            NORD = 0
                C                    *** INCREMENT ORDER AND SET UP NORMAL EQUATIONS ***
S.0029         26 NORD = NORD + 1
S.0030            L = NORD + 1
S.0031            J = 2 * NORD
S.0032            JP1 = J+1
S.0033            SUMX(J) = 0.D0
S.0034            SUMX(JP1) = 0.D0
S.0035            SUMY(L) = 0.D0
S.0036            DO 25 I=1,NO
S.0037            TEMP = POWX(I) * X(I)
S.0038            XI = W(I) * TEMP
S.0039            SUMX(J) = SUMX(J) + XI * POWX(I)
S.0040            SUMX(JP1) = SUMX(JP1) + XI * TEMP
S.0041            SUMY(L) = SUMY(L) + WY(I) * TEMP
S.0042         25 POWX(I) = TEMP
S.0043            KK=L+1
S.0044            DO 8 I=1,L
S.0045            DO 7 J=1,L
S.0046            IK=I+J-1
```

```
S.0047          7 A(I,J)=SUMX(IK)
S.0048          8 A(I,KK)=SUMY(I)
                C                       ***CALL MATRIX INVERT ROUTINE***
S.0049            CALL DSOLV (A,L,KK,1.D-25,DET,TEST)
S.0050            IF (TEST) 10,13,10
                C                       ***OUTPUT ERROR MESSAGE-TERMINATE FITTING***
S.0051         10 WRITE (3,101) NORD
S.0052            GO TO 12
                C                       ***CALCULATE RESIDUALS, RMS ERROR***
S.0053         13 SWR2=0.DO
S.0054            DO 16 I=1,NO
S.0055            XI = X(I)
S.0056            TEMP = A(L,KK)
S.0057            LM1 = L-1
S.0058            DO 15 J=1,LM1
S.0059            LMJ = L-J
S.0060         15 TEMP = TEMP * XI + A(LMJ,KK)
S.0061            YC(I) = TEMP
S.0062            DIFF(I) = Y(I) - TEMP
S.0063         16 SWR2=SWR2+W(I)*(DIFF(I)*DIFF(I))
S.0064            RMSD = DSQRT(SWR2 / (NO - L))
                C                       ***CALCULATE ERROR IN COEFFICIENTS***
S.0065            DO 19 I=1,L
S.0066         19 E(I)=RMSD *DSQRT(DABS(A(I,I)))
                C                       ***OUTPUT RESULTS***
S.0067            WRITE (3,103) NORD,RMSD
S.0068            WRITE (3,104)
S.0069            DO 30 I=1,L
S.0070            IM1 = I-1
S.0071         30 WRITE (3,1004) IM1,A(I,KK),E(I)
S.0072            WRITE (3,105)
S.0073            DO 31 I=1,NO
S.0074         31 WRITE (3,1005) W(I),X(I),Y(I),YC(I),DIFF(I)
                C                       ***HAS LAST ORDER BEEN REACHED***
S.0075         18 IF (NORD-LAST) 20,21,21
S.0076         21 WRITE (3,106)
S.0077            GO TO 12
                C                       ***ARE THE ERRORS INCREASING***
S.0078         20 IF (SDCHK) 22,22,27
S.0079         27 IF (NORD-2) 22,23,23
S.0080         23 IF (ORMSD - RMSD) 24,22,22
                C                       ***OUTPUT MESSAGE AND TERMINATE FITTING***
S.0081         24 WRITE (3,107)
S.0082            GO TO 12
                C                       *** SAVE RMSD ***
S.0083         22 ORMSD = RMSD
S.0084            GO TO 26
                C                       ***END OF JOB***
                C                       ***FORMATS***
S.0085        101 FORMAT (// 2X 'MATRIX OF NORMAL EQUATIONS IS SINGULAR FOR DEGREE'
                  1 I3,'. FITTING IS TERMINATED')
S.0086        102 FORMAT (// I5,' OBSERVATIONS WHERE X RANGES FROM' D25.16,' TO'
                  1 D25.16)
S.0087        103 FORMAT (//// 2X 'DEGREE' I3, 5X 'STANDARD DEVIATION' D25.16)
S.0088        104 FORMAT (///2X,'POWER',2X,'COEFFICIENT',14X,'STANDARD ERROR',/)
```

```
S.0089        105 FORMAT (// 2X 'WEIGHT' 4X 'IND. VARIABLE X' 10X 'Y OBSERVED' 15X
     1  'Y COMPUTED' 16X 'RESIDUAL'/)
S.0090       1004 FORMAT (4X,I3,2X,D23.16,2X,D23.16)
S.0091       1005 FORMAT (2X,F14.3,2X,D23.16,2X,D23.16,2X,D23.16,2X,D23.16)
S.0092        106 FORMAT (//2X,'MAXIMUM ORDER HAS BEEN REACHED. FITTING IS TERMINATE
     1D')
S.0093        107 FORMAT (//2X,'STANDARD DEVIATION IS INCREASING. FITTING IS TERMINA
     1TED')
S.0094        108 FORMAT (// 2X 'INSUFFICIENT POINTS. FITTING IS TERMINATED')
S.0095            END
```

```
      C.LPG00090B        DSOLV-SUBROUTINE     66.206     NEW
S.0001      SUBROUTINE DSOLV (X,M,N,PREC,DET,TEST)                        DSOLV082
            C                                                             DSOLV083
S.0002      DIMENSION I1(50),I2(50)                                       DSOLV084
S.0003      DOUBLE PRECISION X(16,16),V,T,DET,BIG,PREC,TEST,FLTM,PIV,TEMP DSOLV085
S.0004      EQUIVALENCE (BIG,TEMP,PIV)                                    DSOLV086
S.0005      DET = 1.D0                                                    DSOLV087
S.0006      TEMP = PREC                                                   DSOLV088
S.0007      IF(TEMP)202,201,202                                           DSOLV089
S.0008  201 TEMP = .5D-14                                                 DSOLV090
S.0009  202 V = 0.D0                                                      DSOLV091
S.0010      DO 1 I = 1,M                                                  DSOLV092
S.0011      I2(I) = 0                                                     DSOLV093
S.0012      DO 1 J = 1,M                                                  DSOLV094
S.0013    1 V = V + X(I,J)*X(I,J)                                         DSOLV095
S.0014      FLTM = M                                                      DSOLV096
S.0015      V = TEMP *DSQRT(V)/FLTM                                       DSOLV097
S.0016      DO 9 K = 1,M                                                  DSOLV098
S.0017      BIG = 0.D0                                                    DSOLV099
S.0018      DO 3 I = 1,M                                                  DSOLV100
S.0019      IF(I2(I))3,103,3                                              DSOLV101
S.0020  103 DO 2 J = 1,M                                                  DSOLV102
S.0021      IF(I2(J))2,102,2                                              DSOLV103
S.0022  102 T =DABS(X(I,J))                                               DSOLV104
S.0023      IF(T - BIG)2,2,1002                                           DSOLV105
S.0024 1002 BIG = T                                                       DSOLV106
S.0025      IROW = I                                                      DSOLV107
S.0026      JCOL = J                                                      DSOLV108
S.0027    2 CONTINUE                                                      DSOLV109
S.0028    3 CONTINUE                                                      DSOLV110
S.0029      IF(BIG - V)104,4,4                                            DSOLV111
S.0030  104 TEST = V                                                      DSOLV112
S.0031      RETURN                                                        DSOLV113
S.0032    4 I1(K) = JCOL                                                  DSOLV114
S.0033      I2(JCOL) = IROW                                               DSOLV115
S.0034      IF(JCOL - IROW)106,6,106                                      DSOLV116
S.0035  106 DO 5 J = 1,N                                                  DSOLV117
S.0036      TEMP = X(IROW,J)                                              DSOLV118
S.0037      X(IROW,J) = X(JCOL,J)                                         DSOLV119
S.0038    5 X(JCOL,J) = TEMP                                              DSOLV120
S.0039      DET = -DET                                                    DSOLV121
S.0040    6 DET = DET * X(JCOL,JCOL)                                      DSOLV122
S.0041      PIV = 1.D0/X(JCOL,JCOL)                                       DSOLV123
S.0042      DO 7 J = 1,N                                                  DSOLV124
S.0043      IF(J - JCOL)107,7,107                                         DSOLV125
S.0044  107 X(JCOL,J) = PIV * X(JCOL,J)                                   DSOLV126
S.0045    7 CONTINUE                                                      DSOLV127
S.0046      X(JCOL,JCOL) = PIV                                            DSOLV128
S.0047      DO 9 I = 1,M                                                  DSOLV129
S.0048      IF(I - JCOL)109,9,109                                         DSOLV130
S.0049  109 PIV = -X(I,JCOL)                                              DSOLV131
S.0050      DO 8 J = 1,N                                                  DSOLV132
S.0051      IF(J - JCOL)108,8,108                                         DSOLV133
```

```
S.0052      108 X(I,J) = X(I,J) + PIV*X(JCOL,J)                                   DSOLV134
S.0053        8 CONTINUE                                                          DSOLV135
S.0054          X(I,JCOL) = PIV * X(JCOL,JCOL)                                    DSOLV136
S.0055        9 CONTINUE                                                          DSOLV137
S.0056          DO 11 K = 1,M                                                     DSOLV138
S.0057          I = M+1 - K                                                       DSOLV139
S.0058          JCOL = I1(I)                                                      DSOLV140
S.0059          IROW = I2(JCOL)                                                   DSOLV141
S.0060          IF(IROW - JCOL)111,11,111                                         DSOLV142
S.0061      111 DO 10 I = 1,M                                                     DSOLV143
S.0062          TEMP = X(I,IROW)                                                  DSOLV144
S.0063          X(I,IROW) = X(I,JCOL)                                             DSOLV145
S.0064       10 X(I,JCOL) = TEMP                                                  DSOLV146
S.0065       11 CONTINUE                                                          DSOLV147
S.0066          TEST = 0.0D0                                                      DSOLV148
S.0067          RETURN                                                            DSOLV149
S.0068          END                                                               DSOLV150
```

2. Program to calculate conductivity and ion-pair dissociation parameters

List of Abbreviations

AMBIO	limiting equivalent conductivity based on the high-pressure cells
SAMIO	standard deviation in AMBIO ($cm^2\Omega^{-1}mole^{-1}$)
SPVOL	specific volume ($ml\ g^{-1}$)
AMBI1	limiting equivalent conductivity based on the atmospheric-pressure cells ($cm^2\Omega^{-1}mole^{-1}$)
SAMI1	standard deviation in AMBI1
DICOO	dissociation constant based on the high-pressure cells ($mole\ l^{-1}$)
SDICO	standard deviation in DICOO
DICO1	dissociation constant based on the atmospheric-pressure cells ($mole\ l^{-1}$)
SDIC1	standard deviation in DICO1
GIBK1	Gibbs free energy of dissociation ($cal\ mole^{-1}$)
SGIK1	standard deviation in GIBK1
HETKO	enthalpy of dissociation based on the high-pressure cells ($cal\ mole^{-1}$)
SHEKO	standard deviation in HETKO
ENTKO	entropy of dissociation based on the high-pressure cells ($cal\ mole^{-1}$)
SENKO	standard deviation in ENTKO
ENTK1	entropy of dissociation based on the atmospheric-pressure cells ($cal\ deg^{-1}mole^{-1}$)
SENK1	standard deviation in ENTK1
MOVOL	molal volume (ml)
AMVLO	logarithm of the limiting equivalent conductivity at constant volume
HETKV	energy of activation for conductivity at constant volume ($cal\ mole^{-1}$)
SHEKV	standard deviation in HETKV
VIAMO	Walden product based on the high-pressure cells
SVIAO	standard deviation in VIAMO
VIAM1	Walden product based on the atmospheric-pressure cells
SVIA1	standard deviation in VIAM1
DICVO	logarithm of the dissociation constant at constant volume
HEDIV	internal energy of dissociation at constant volume ($cal\ mole^{-1}$)
SHEDV	standard deviation in HEDIV

```
S.0001          DOUBLE PRECISION TEMP(36),PRES(36),DIELT(36),
               1VISCY(36),TAITB(36),TAITC(36),AMBIO(36),SAMIO(36),SPVOL(36),
               2AMBI1(12),SAMI1(36),DICOO(36),DICOI(12),SDICO(36),SDIC1(12),X(99),
               3Y(99),W(99),E(16),A(16,16),VOLAM(36),SVOAM(36),HETAM(11),
               4SHEAM(11),GIBEK(36),SGIEK(36),GIBK1(12),SGIK1(12),HETKO(11),
               5SHEKO(11),ENTKO(36),SENKO(36),ENTK1(12),SENK1(12),VOLMK(36),
               6SVOMK(36),MOVOL(36),AMVLO(4,36),HETKV(12),SHEKV(12),VIAMO(36),
               7SVIAO(36),VIAM1(12),SVIA1(12),
               8X1(9),Y1(9),W1(9),X2(4),Y2(4),W2(4),HEDIV(12),SHEDV(12),
               9DICVO(4,36)
S.0002          DIMENSION JJ(36),JJJ(12),N(36)
S.0003          COMMON A,E
S.0004    1000  DO 5000 J=1,36
S.0005    2000  READ(1,1002)JJ(J),N(J),TEMP(J),PRES(J),DIELT(J),VISCY(J),
               1TAITB(J),TAITC(J)
S.0006          WRITE(3,1002)JJ(J),N(J),TEMP(J),PRES(J),DIELT(J),VISCY(J),
               1TAITB(J),TAITC(J)
S.0007    3000  READ(1,1003)AMBIO(J),SAMIO(J),SPVOL(J)
S.0008          WRITE(3,1003)AMBIO(J),SAMIO(J),SPVOL(J)
S.0009    4000  READ(1,1004)DICOO(J),SDICO(J)
S.0010          WRITE(3,1004)DICOO(J),SDICO(J)
S.0011    5000  CONTINUE
S.0012    6000  DO 9000 I=1,12
S.0013    7000  READ(1,1007)AMBI1(I),SAMI1(I),JJJ(I)
S.0014          WRITE(3,1007)AMBI1(I),SAMI1(I),JJJ(I)
S.0015    8000  READ(1,1004)DICOI(I),SDIC1(I)
S.0016          WRITE(3,1004)DICOI(I),SDIC1(I)
S.0017    9000  CONTINUE
S.0018    1100  DO 3200 L=1,4
S.0019    1400  DO 2200 J=1,9
S.0020    1300  J1=J+9*(L-1)
S.0021    1500  LAST=2
S.0022    1600  NO=9
S.0023    1700  SDCHK=0
S.0024    1900  X1(J)=PRES(J1)
S.0025    1800  W1(J)=(AMBIO(J1)/SAMIO(J1))**2
S.0026    2100  Y1(J)=DLOG(AMBIO(J1))
S.0027    2200  CONTINUE
S.0028    2300  CALL DFIT(X1,Y1,W1,NO,LAST,SDCHK)
S.0029    2600  DO 3100 J1=1,9
S.0030    2500  J=J1+9*(L-1)
S.0031    2700  R=0.831460D+02
S.0032    2800  VOLAM(J)=-R*TEMP(J)*((A(2,4)+2*A(3,4)*PRES(J))+((0.6667)*TAITC(J)/
               1(TAITB(J)+PRES(J))))
S.0033    2900  SVOAM(J)=R*TEMP(J)*((E(2)+2*E(3)*PRES(J)+2*A(3,4)*0.7)+((0.6667)*
               1(TAITC(J)*14.8+(TAITB(J)+PRES(J))*0.0011)/(TAITB(J)+PRES(J))**2))
S.0034    3100  CONTINUE
S.0035    3200  CONTINUE
S.0036    3300  DO 4900 L=1,9
S.0037    3600  DO 4400  J3=1,4
S.0038    3601  J1=1+9*(J3-1)
S.0039    3500  J=J1+(L-1)
S.0040    3700  LAST=1
```

```
S.0041      3800 NO=4
S.0042      3900 SDCHK=0
S.0043      4200 X2(J3)=1/TEMP(J)
S.0044      4300 Y2(J3)=DLOG(AMBIO(J))
S.0045      4100 W2(J3)=(AMBIO(J)/SAMIO(J))**2
S.0046      4400 CONTINUE
S.0047      4500 CALL DFIT(X2,Y2,W2,NO,LAST,SDCHK)
S.0048      4600 RCAL=1.9872
S.0049      4700 HETAM(L)=-RCAL*(A(2,3))
S.0050      4800 SHEAM(L)=RCAL*(E(2))
S.0051      4900 CONTINUE
S.0052      5100 DO 6600 L=10,11
S.0053      5101 DO 6300 I3=1,4
S.0054      5104 I1=2+3*(I3-1)
S.0055      5102 IF (L-10)5103,5103,5200
S.0056      5103 I=I1
S.0057      5200 IF (L-10)5400,5400,5300
S.0058      5300 I=I1+1
S.0059      5400 LAST=1
S.0060      5600 NO=4
S.0061      5700 SDCHK=0
S.0062      5800 J=JJJ(I1)
S.0063      5900 W2(I3)=(AMBI1(I)/SAMI1(I))**2
S.0064      6200 Y2(I3)=DLOG(AMBI1(I))
S.0065      6100 X2(I3)=1/TEMP(J)
S.0066      6300 CONTINUE
S.0067      6301 CALL DFIT(X2,Y2,W2,NO,LAST,SDCHK)
S.0068      6400 HETAM(L)=-RCAL*(A(2,3))
S.0069      6500 SHEAM(L)=RCAL*(E(2))
S.0070      6600 CONTINUE
S.0071      6700 DO 7100 J=1,36
S.0072      6800 GIBEK(J)=-RCAL*TEMP(J)*DLOG(DICOO(J))
S.0073      6900 SGIEK(J)=RCAL*TEMP(J)*SDICO(J)/DICOO(J)
S.0074      7100 CONTINUE
S.0075      7200 DO 7500 I=1,12
S.0076      7201 J=JJJ(I)
S.0077      7300 GIBK1(I)=-RCAL*TEMP(J)*DLOG(DICO1(I))
S.0078      7400 SGIK1(I)=RCAL*TEMP(J)*SDIC1(I)/DICO1(I)
S.0079      7500 CONTINUE
S.0080      7600 DO 9200 L=1,9
S.0081      7900 DO 8700 J3=1,4
S.0082      7901 J1=1+9*(J3-1)
S.0083      7800 J=J1+(L-1)
S.0084      8100 LAST=1
S.0085      8200 NO=4
S.0086      8300 SDCHK=0
S.0087      8500 X2(J3)=1/TEMP(J)
S.0088      8600 Y2(J3)=DLOG(DICOO(J))
S.0089      8400 W2(J3)=(DICOO(J)/SDICO(J))**2
S.0090      8700 CONTINUE
S.0091      8600 CALL DFIT(X2,Y2,W2,NO,LAST,SDCHK)
S.0092      8900 HETKO(L)=-RCAL*(A(2,3))
S.0093      9100 SHEKO(L)=RCAL*(E(2))
S.0094      9200 CONTINUE
S.0095      9300 DO 9010 J=10,11
```

```
S.0096      9600 DO 9010 I3=1,4
S.0097      9603 I1=2+3*(I3-1)
S.0098      9601 IF (L-10)9602,9602,9400
S.0099      9602 I=I1
S.0100      9400 IF (L-10)9700,9700,9500
S.0101      9500 I=I1+1
S.0102      9700 LAST=1
S.0103      9800 NO=4
S.0104      9900 SDCHK=0
S.0105      2010 J=JJJ(I1)
S.0106      3010 X2(I3)=1/TEMP(J)
S.0107      1010 W2(I3)=(DICO1(I)/SDIC1(I))**2
S.0108      4010 Y2(I3)=DLOG(DICO1(I))
S.0109      5010 CONTINUE
S.0110      6010 CALL DFIT(X2,Y2,W2,NO,LAST,SDCHK)
S.0111      7010 HETKO(L)=-RCAL*(A(2,3))
S.0112      8010 SHEKO(L)=RCAL*(E(2))
S.0113      9010 CONTINUE
S.0114      1110 DO 2110 M=1,4
S.0115      1610 DO 1811 J=1,9
S.0116      1510 L=J+(M-1)*9
S.0117      1710 ENTKO(L)=(HETKO(J)-GIBEK(L))/TEMP(L)
S.0118      1810 SENKO(L)=(SHEKO(J)+SGIEK(L))/TEMP(L)
S.0119      1811 CONTINUE
S.0120      2110 CONTINUE
S.0121      2210 DO 2610 I=1,10,3
S.0122      2310 J=JJJ(I)
S.0123      2410 ENTK1(I)=(HETKO(1)-GIBK1(I))/TEMP(J)
S.0124      2510 SENK1(I)=(SHEKO(1)+SGIK1(I))/TEMP(J)
S.0125      2610 CONTINUE
S.0126      2710 DO 3210 I=2,11,3
S.0127      2810 J=JJJ(I)
S.0128      2910 ENTK1(I)=(HETKO(10)-GIBK1(I))/TEMP(J)
S.0129      3110 SENK1(I)=(SHEKO(10)+SGIK1(I))/TEMP(J)
S.0130      3210 CONTINUE
S.0131      3310 DO 3710 I=3,12,3
S.0132      3410 J=JJJ(I)
S.0133      3510 ENTK1(I)=(HETKO(11)-GIBK1(I))/TEMP(J)
S.0134      3610 SENK1(I)=(SHEKO(11)+SGIK1(I))/TEMP(J)
S.0135      3710 CONTINUE
S.0136      3810 DO 5412 L=1,4
S.0137      4210 DO 4910 J1=1,9
S.0138      4110 J=J1+9*(L-1)
S.0139      4310 LAST=2
S.0140      4410 NO=9
S.0141      4510 SDCHK=0
S.0142      4610 Y1(J1)=DLOG(DICOO(J))
S.0143      4610 W1(J1)=(DICOO(J)/SDICO(J))**2
S.0144      4710 X1(J1)=PRES(J)
S.0145      4910 CONTINUE
S.0146      5110 CALL DFIT(X1,Y1,W1,NO,LAST,SDCHK)
S.0147      5210 DO 5411 J1=1,9
S.0148      5212 J=J1+9*(L-1)
S.0149      5310 VOLPK(J)=-R*TEMP(J)*((A(2,4)+2*A(3,4)*PRES(J))+((1.0)*TAITC(J)/
                 1(1.0+TAITB(J)*PRES(J)))
```

```
S.0150      5410 SVOMK(J)=R*TEMP(J)*((E(2)+2*E(3)*PRES(J)+2*A(3,4)*0.7)+((1.0)*
                1(TAITC(J)*14.8+(TAITB(J)+PRES(J))*0.011)/(TAITB(J)+PRES(J))**2))
S.0151      5411 CONTINUE
S.0152      5412 CONTINUE
S.0153      5510 DO 7210 L=1,4
S.0154      5810 DO 6610 J1=1,9
S.0155      5710 J=J1+9*(L-1)
S.0156      5910 LAST=3
S.0157      6110 NO=9
S.0158      6210 SDCHK=0
S.0159      6310 W1(J1)=(AMBIO(J)/SAMIO(J))**2
S.0160      6410 X1(J1)=58.081*SPVOL(J)
S.0161      6510 Y1(J1)=DLOG(AMBIO(J))
S.0162      6610 CONTINUE
S.0163      6710 CALL DFIT(X1,Y1,W1,NO,LAST,SDCHK)
S.0164      6810 DO 7110 J=1,36,3
S.0165      6811 MOVOL(J)=58.081*SPVOL(J)
S.0166      6910 AMVLO(L,J)=(A(1,5)+A(2,5)*MOVOL(J)+A(3,5)*MOVOL(J)**2+A(4,5)*
                1MOVOL(J)**3)
S.0167      7110 CONTINUE
S.0168      7210 CONTINUE
S.0169      7310 DO 8610 M=1,12
S.0170      7410 DO 8310 L=1,4
S.0171      7411 MMM=1+3*(M-1)
S.0172      7510 LAST=1
S.0173      7610 NO=4
S.0174      7710 SDCHK=0
S.0175      7910 J=9*L-8
S.0176      8110 X2(L)=1/TEMP(J)
S.0177      7810 W2(L)=1
S.0178      8210 Y2(L)=AMVLO(L,MMM)
S.0179      8310 CONTINUE
S.0180      8311 CALL DFIT(X2,Y2,W2,NO,LAST,SDCHK)
S.0181      8410 HETKV(M)=-RCAL*(A(2,3))
S.0182      8510 SHEKV(M)=RCAL*(E(2))
S.0183      8610 CONTINUE
S.0184      5519 DO 7219 L=1,4
S.0185      5819 DO 6619 J1=1,9
S.0186      5719 J=J1+9*(L-1)
S.0187      5919 LAST=3
S.0188      6119 NO=9
S.0189      6219 SDCHK=0
S.0190      6319 W1(J1)=(DICOO(J)/SDICO(J))**2
S.0191      6419 X1(J1)=58.081*SPVOL(J)
S.0192      6519 Y1(J1)=DLOG(DICOO(J))
S.0193      6619 CONTINUE
S.0194      6719 CALL DFIT(X1,Y1,W1,NO,LAST,SDCHK)
S.0195      6819 DO 7119 J=1,36,3
S.0196      6818 MOVOL(J)=58.081*SPVOL(J)
S.0197      6919 DICVO(L,J)=(A(1,5)+A(2,5)*MOVOL(J)+A(3,5)*MOVOL(J)**2+A(4,5)*
                1MOVOL(J)**3)
S.0198      7119 CONTINUE
S.0199      7219 CONTINUE
S.0200      7319 DO 8619 M=1,12
S.0201      7419 DO 8319 L=1,4
```

```
S.0202      7418 MMM=1+3*(M-1)
S.0203      7519 LAST=1
S.0204      7619 NO=4
S.0205      7719 SDCHK=0
S.0206      7919 J=9*L-8
S.0207      8119 X2(L)=1/TEMP(J)
S.0208      7819 W2(L)=1
S.0209      8219 Y2(L)=DICVO(L,MMM)
S.0210      8319 CONTINUE
S.0211      8318 CALL DEFIT(X2,Y2,W2,NO,LAST,SDCHK)
S.0212      8419 HEDIV(M)=-RCAL*(A(2,3))
S.0213      8519 SHEDV(M)=RCAL*(E(2))
S.0214      8619 CONTINUE
S.0215      8710 DO 9110 J=1,36
S.0216      8810 VIAMO(J)=VISCY(J)*AMBIO(J)
S.0217      8910 SVIAO(J)=VISCY(J)*SAMIO(J)
S.0218      9110 CONTINUE
S.0219      9210 DO 9610 I=1,12
S.0220      9310 J=JJJ(I)
S.0221      9410 VIAM1(I)=VISCY(J)*AMBI1(I)
S.0222      9510 SVIA1(I)=VISCY(J)*SAMI1(I)
S.0223      9610 CONTINUE
S.0224      9710 WRITE(3,1099)
S.0225      9810 WRITE(3,1098)
S.0226      9910 WRITE(3,1091)
S.0227      1020 DO 1220 LN=1,4
S.0228      4020 JI=9*LN-8
S.0229      5020 WRITE(3,1092)TEMP(JI)
S.0230      6020 WRITE(3,1093)
S.0231      8020 DO 1120 J1=1,9
S.0232      3020 J=J1+(LN-1)*9
S.0233      9020 WRITE(3,1094)PRES(J),VOLAM(J),SVOAM(J)
S.0234      1120 CONTINUE
S.0235      1220 CONTINUE
S.0236      1320 WRITE(3,1099)
S.0237      1321 WRITE(3,1095)
S.0238      1420 WRITE(3,1096)
S.0239      1620 DO 2320 L=1,11
S.0240      1720 IF (L-10)1820,1920,1920
S.0241      1820 JL=L
S.0242      1920 IF (L-10)2220,2120,2120
S.0243      2120 JL=1
S.0244      2220 WRITE(3,1094)PRES(JL),HETAM(L),SHEAM(L)
S.0245      2320 CONTINUE
S.0246      2420 WRITE(3,1099)
S.0247      2520 WRITE(3,1097)
S.0248      2620 WRITE(3,1089)
S.0249      2720 DO 3120 M=1,12
S.0250      2820 J=1+3*(M-1)
S.0251      2920 WRITE(3,1094)MOVOL(J),HETKV(M),SHEKV(M)
S.0252      3120 CONTINUE
S.0253      3220 WRITE(3,1099)
S.0254      3320 WRITE(3,1088)
S.0255      3420 WRITE(3,1099)
S.0256      3520 WRITE(3,1087)
```

```
S.0257      3620 DO 4820 M=1,4
S.0258      3720 JI=9*M-8
S.0259      3820 WRITE(3,1092)TEMP(JI)
S.0260      3921 WRITE(3,1096)
S.0261      4120 DO 4320 J1=1,9
S.0262      3920 J=J1+9*(M-1)
S.0263      4220 WRITE(3,1094)PRES(J),GIBEK(J),SGIEK(J)
S.0264      4320 CONTINUE
S.0265      4520 DO 4720 MLL=1,3
S.0266      4420 ML=MLL+3*(M-1)
S.0267      4620 WRITE(3,1094)PRES(1),GIBK1(ML),SGIK1(ML)
S.0268      4720 CONTINUE
S.0269      4820 CONTINUE
S.0270      4920 WRITE(3,1099)
S.0271      5120 WRITE(3,1086)
S.0272      5220 WRITE(3,1085)
S.0273      5320 DO 5920 M=1,11
S.0274      5420 IF (M-10)5620,5520,5520
S.0275      5520 J=1
S.0276      5620 IF (M-10)5720,5820,5820
S.0277      5720 J=M
S.0278      5820 WRITE(3,1094)PRES(J),HETKO(M),SHEKO(M)
S.0279      5920 CONTINUE
S.0280      5921 WRITE(3,1099)
S.0281      5922 WRITE(3,1197)
S.0282      5923 WRITE(3,1089)
S.0283      5924 DO 5927 M=1,12
S.0284      5925 J=1+3*(M-1)
S.0285      5926 WRITE(3,1094)MOVOL(J),HEDIV(M),SHEDV(M)
S.0286      5927 CONTINUE
S.0287      5928 WRITE(3,1099)
S.0288      6120 WRITE(3,1084)
S.0289      6220 DO 7520 M=1,4
S.0290      6320 JI=M*9-8
S.0291      6420 WRITE(3,1092)TEMP(JI)
S.0292      6620 WRITE(3,1083)
S.0293      6720 DO 6920 J1=1,9
S.0294      6520 J=J1+9*(M-1)
S.0295      6820 WRITE(3,1094)PRES(J),ENTKO(J),SENKO(J)
S.0296      6920 CONTINUE
S.0297      7220 DO 7420 MMM=1,3
S.0298      7120 MM=MMM+3*(M-1)
S.0299      7320 WRITE(3,1094)PRES(1),ENTK1(MM),SENK1(MM)
S.0300      7420 CONTINUE
S.0301      7520 CONTINUE
S.0302      7620 WRITE(3,1082)
S.0303      7720 DO 8420 M=1,4
S.0304      7820 JI=M*9-8
S.0305      8120 WRITE(3,1092)TEMP(JI)
S.0306      8121 WRITE(3,1093)
S.0307      7920 DO 8320 J1=1,9
S.0308      7921 J=J1+9*(M-1)
S.0309      8220 WRITE(3,1094)PRES(J),VOLMK(J),SVOMK(J)
S.0310      8320 CONTINUE
S.0311      8420 CONTINUE
```

```
S.0312      8520 WRITE(3,1081)
S.0313      8620 DO 9320 M=1,4
S.0314      8621 JI=1+9*(M-1)
S.0315      8920 WRITE(3,1092)TEMP(JI)
S.0316      8921 WRITE(3,1079)
S.0317      8820 DO 9220 J1=1,9
S.0318      8720 J=J1+9*(M-1)
S.0319      9120 WRITE(3,1094)PRES(J),VIAMO(J),SVIAO(J)
S.0320      9220 CONTINUE
S.0321      9320 CONTINUE
S.0322      9420 WRITE(3,1078)
S.0323      9520 WRITE(3,1077)
S.0324      9620 DO 9920 M=1,12
S.0325      9720 MI=JJJ(M)
S.0326      9820 WRITE(3,1094)TEMP(MI),VIAM1(M),SVIA1(M)
S.0327      9920 CONTINUE
S.0328      1002 FORMAT(2I4,3D16.8/3D16.8)
S.0329      1003 FORMAT(3D16.8)
S.0330      1004 FORMAT(2D16.8)
S.0331      1007 FORMAT(2D16.8,I4)
S.0332      1098 FORMAT(//2X,'CONDUCTIVITY PARAMETERS')
S.0333      1099 FORMAT(//2X)
S.0334      1091 FORMAT(//2X,'VOLUMES OF ACTIVATION')
S.0335      1092 FORMAT(//2X,'TEMPERATURE =',D16.8)
S.0336      1093 FORMAT(/'      PRESSURE              VOLUME              ERROR     ')
S.0337      1094 FORMAT(/3D16.8)
S.0338      1095 FORMAT(//2X,'ENERGY OF ACTIVATION AT CONSTANT PRESSURE')
S.0339      1096 FORMAT(/'      PRESSURE              ENERGY              ERROR     ')
S.0340      1097 FORMAT(//2X,'ENERGY OF ACTIVATION AT CONSTANT VOLUME')
S.0341      1197 FORMAT(//2X,'ENTHALPY OF DISSOCIATION AT CONSTANT VOLUME ')
S.0342      1089 FORMAT(/'      VOLUME              ENERGY              ERROR     ')
S.0343      1088 FORMAT(//2X,'THERMODYNAMIC PARAMETERS OF ION ASSOCIATION')
S.0344      1087 FORMAT(//2X,'GIBBS FREE ENERGY OF DISSOCIATION')
S.0345      1086 FORMAT(//2X,'ENTHALPY OF DISSOCIATION')
S.0346      1085 FORMAT(/'      PRESSURE              HEAT                ERROR     ')
S.0347      1084 FORMAT(//2X,'ENTROPY OF DISSOCIATION')
S.0348      1083 FORMAT(/'      PRESSURE              ENTROPY             ERROR     ')
S.0349      1082 FORMAT(//2X,'VOLUME OF DISSOCIATION')
S.0350      1081 FORMAT(//2X,'WALDEN PRODUCT AS A FUNCTION OF PRESSURE')
S.0351      1079 FORMAT(/'      PRESSURE              PRODUCT             ERROR     ')
S.0352      1078 FORMAT(//2X,'WALDEN PRODUCT AS A FUNCTION OF TEMPERATURE AT ONE
                 1BAR PRESSURE')
S.0353      1077 FORMAT(/'      TEMPERATURE           PRODUCT             ERROR     ')
S.0354      9999 RETURN
S.0355           END
```

3.
Program to calculate ion separations based on the Fuoss equation for the dissociation constant

List of Abbreviations

SEPEX ion separation ($\mathring{A}$)
DICTE dissociation constant (mole l^{-1})
other abbreviations identified above

```
S.CCC1            DIMENSION RR(360),ARGUM(360),SEPEX(360),TEMP(10),DIELT(10),
                 1DICTE(360)
S.CCC2      1000  DO 3000 J=1,10
S.CCC3      2000  READ(1,1001)TEMP(J),DIELT(J)
S.CCC4      3000  CONTINUE
S.CCC5      3601  DO 3603 II=1,10
S.CCC6      3702  DO 3708 I=1,360
S.CCC7      3752  RR(I)=(I-1)*5.0+100.0
S.CCC8      3704  SEPEX(I)=RR(I)*0.10-09
S.CCC9      9151  ARGUM(I)=DEXP((0.167061D-02)/(DIELT(II)*TEMP(II)*SEPEX(I)))
S.CC10      3306  DICTE(I)=3000.0/(0.125664D+02*0.60238D+24*(SEPEX(I)**3)*ARGUM(I))
S.CC11      3707  WRITE(3,1001)SEPEX(I),DICTE(I)
S.CC12      3708  CONTINUE
S.CC13      3709  WRITE(3,1099)
S.CC14      3603  CONTINUE
S.CC15      1099  FORMAT(//2X)
S.CC16      1001  FORMAT(2E16.8)
S.CC17            RETURN
S.CC18            END
```

CLAIMS TO ORIGINAL RESEARCH

1. Measurements of the temperature and pressure coefficients of the conductivity of three tetraalkylammonium iodide compounds in acetone solution have been made.
2. A Shedlovsky procedure has been used to analyse the conductivity results to obtain the limiting equivalent conductivity and the ion-pair dissociation constant as a function of temperature and pressure.
3. The conductivity results have been interpreted in terms of the activated-complex theory and correlations between viscosity, self-diffusion, and conductivity have been made using a hole theory of liquids.
4. Thermodynamic parameters of ion-pair dissociation, including the internal energy at constant volume, have been calculated and the ion pairs formed in acetone shown to be solvent-shared or solvent-separated depending on the conditions of temperature and pressure.

REFERENCES

1. P. C. Blokker. Rec. des Trav. des Pay Bas 54, 975 (1935).

2. Handbook of Chemistry and Physics. The Chemical Rubber Publishing Co., Cleveland. 1961. p. 2339.

3. S. Minc and L. Werblan. Roczniki Chemii Ann. Soc. Chim. Polonorum 40, 1537, 1753, 1989 (1966).

4. S. Glasstone, K. J. Laidler, and H. Eyring. The Theory of Rate Processes. McGraw-Hill, New York. 1941. Ch. 10.

5. G. J. Hills. Chemical Physics of Ionic Solutions, eds. B. E. Conway and R. G. Barradas. John Wiley and Sons, New York. 1966. Ch. 23.

6. H. S. Green. Encyclopedia of Physics, ed. S. Flugge. Springer-Verlag, Berlin. 1960. Volume X, p. 1.

7. C. A. Angell. J. Phys. Chem. 70, 2793 (1966).

8. O. Ya. Samoilov. Structure of Aqueous Electrolyte Solutions and the Hydration of Ions, trans. D. J. G. Ives. Consultants Bureau, New York. 1965.

9. W. Good. Electrochemica Acta 9, 203 (1964).

10. W. Good. Electrochemica Acta 10, 1 (1965).

11. W. Good. Electrochemica Acta 11, 759,767 (1966).

12. R. L. Kay and D. F. Evans. J. Phys. Chem. 70, 2325 (1966).

13. R. A. Horne, R. A. Courant, D. S. Johnson, and F. F. Margosian. J. Phys. Chem. 69, 3988 (1965).

14. R. A. Horne, B. R. Myers, and G. R. Frysinger. J. Chem. Phys. 39, 2666 (1963).

15. R. A. Horne and D. S. Johnson. J. Phys. Chem. 70, 2182 (1966).

16. B. E. Conway. Ann. Rev. Phys. Chem. 17, 481 (1966).

17. M. Falk and T. A. Ford. Can. J. Chem. 44, 1699 (1966).

18. J. Lennard-Jones and J. Pople. Proc. Roy. Soc. London, Ser. A, 202, 166,323 (1950).

19. R. F. Kruh. Chem. Rev. 62, 319 (1962).

20. H. S. Frank and W. Y. Wen. Disc. Faraday Soc. 24, 133 (1957).

21. K. J. Mysels. J. Am. Chem. Soc. 86, 3503 (1964).

22. J. H. Hildebrand. Disc. Faraday Soc. 15, 9 (1953).

23. J. L. Kavanau. Water and Solute-Water Interactions. Holden-Day, San Francisco. 1964.

24. J. H. Hildebrand and R. L. Scott. Regular Solutions. Prentice-Hall, New Jersey. 1962. p. 152.

25. P. W. Allen, H. J. M. Bowen, L. E. Sutton, and O. Bastiansen. Trans. Faraday Soc. 48, 991 (1952).

26. M. D. Zeidler. Ber. Bunsenges. Physik. Chem. 69, 659 (1965).

27. J. N. Wilson. Chem. Rev. 25, 377 (1939).

28. L. Pauling. The Nature of the Chemical Bond. Cornell University Press, Ithaca. 1939. Ch. 10.

29. V. I. Danilov, A. M. Zubko, and A. I. Danilova. Zhur. Eksptl. i Teoret. Fiz. 19, 242 (1949).

30. G. W. Stewart. Chem. Rev. 6, 483 (1929).

31. R. W. Harris and G. T. Clayton. J. Chem. Phys. 45, 2681 (1966).

32. G. G. Harvey. J. Chem. Phys. 7, 878 (1939).

33. G. G. Harvey. J. Chem. Phys. 6, 111 (1938).

34. S. D. Hamann. Physico-Chemical Effects of Pressure. Butterworths Scientific Publications, London. 1957. p. 225.

35. P. W. Bridgman. Proc. Am. Acad. Arts and Sci. 47, 438 (1912).

36. P. W. Bridgman. J. Chem. Phys. 5, 964 (1937).

37. J. O'M. Bockris. Quart. Rev. 3, 173 (1949).

38. E. Glueckauf. Chemical Physics of Ionic Solutions, eds. B. E. Conway and R. G. Barradas. John Wiley and Sons, New York. 1966. p. 102.

39. B. E. Conway, R. E. Verrall, and J. E. Desnoyers. Z. phys. Chem. 230, 157 (1965).

40. R. E. Verrall. Ph.D. Thesis. University of Ottawa. 1966. p. 52.

41. E. R. Nightingale. Chemical Physics of Ionic Solutions, eds. B. E. Conway and R. G. Barradas. John Wiley and Sons, New York. 1966. Ch. 7.

42. O. Ya. Samoilov. Structure of Aqueous Electrolyte Solutions and the Hydration of Ions, trans. D. J. G. Ives. Consultants Bureau, New York. 1965. Ch. 5.

43. H. S. Frank. Chemical Physics of Ionic Solutions, eds. B. E. Conway and R. G. Barradas. John Wiley and Sons, New York. 1966. Ch. 4.

44. M. Born. Z. Physik 1, 45 (1920).

45. K. J. Laidler and C. Pegis. Proc. Roy. Soc. London, Ser. A, 241, 80 (1957).

46. J. E. Desnoyers, R. E. Verrall, and B. E. Conway. J. Chem. Phys. 43, 243 (1965).

47. E. Whalley. J. Chem. Phys. 38, 1400 (1963).

48. J. D. Bernal and R. H. Fowler. J. Chem. Phys. 1, 515 (1933).

49. J. O'M. Bockris and B. E. Conway. Modern Aspects of Electrochemistry. Butterworths, London. 1954. Ch. 2.

50. S. Golden and C. Guttman. J. Chem. Phys. 43, 1894 (1965).

51. E. J. W. Verwey. Rec. Trav. Chim. Phys. Bas 61, 127 (1942).

52. F. Vaslow. J. Phys. Chem. 67, 2777 (1963).

53. J. Miller and A. J. Parker. J. Am. Chem. Soc. 83, 117 (1961).

54. A. J. Parker. Quart. Rev. 16, 163 (1962).

55. S. Winstein, L. G. Savedoff, S. Smith, I. D. R. Stevens, and J. S. Gall. Tetrahedron Letters 9, 24 (1960).

56. K. P. Mishchenko and V. V. Sokolov. Z. Struk. Khim. 4, 184 (1963).

57. H. S. Frank and A. L. Robinson. J. Chem. Phys. 8, 933 (1940).

58. G. N. Lewis and M. Randall. Thermodynamics. McGraw-Hill, New York. 1923. p. 90.

59. W. Kireeff. Acta Phys. Chem. 13, 531 (1940).

60. K. P. Mishchenko and V. V. Sokolov. Z. Struk. Khim. 5, 819 (1964).

61. R. Macy and E. W. Thomas. J. Am. Chem. Soc. 48, 1547 (1926).

62. P. Thirion and E. C. Craven. J. Appl. Chem. 2, 210 (1952).

63. R. L. Meeker, F. E. Critchfield, and E. T. Bishop. Anal. Chem. 34, 1510 (1962).

64. J. F. J. Dippy and S. R. C. Hughes. J. Chem. Soc. 953 (1954).

65. Prof. N. Muller. Purdue University, Indiana. Personal communication.

66. Handbook of Chemistry and Physics. The Chemical Rubber Publishing Co., Cleveland. 1961. p. 451.

67. L. F. Gordon. J. Am. Chem. Soc. 87, 4347 (1965).

68. R. H. Davies and E. G. Taylor. J. Phys. Chem. 68, 3901 (1964).

69. Dictionary of Organic Compounds, 4th Edition. Eyre and Spottiswoode Publishers Ltd., London. 1965. p. 3016.

70. I. M. Kolthoff and E. B. Sandell. Textbook of Quantitative Inorganic Analysis. Macmillan Co., New York. 1952. pp. 455, 545.

71. G. J. Hills. Chemical Physics of Ionic Solutions, eds. B. E. Conway and R. G. Barradas. John Wiley and Sons, New York. 1966. p. 521.

72. P. J. Ovenden. Thesis. Southampton University, England. 1964.

73. T. Shedlovsky. J. Am. Chem. Soc. 52, 1806 (1930).

74. J. E. Prue and P. J. Sherrington. Trans. Faraday Soc. 57, 1795 (1961).

75. G. Jones and D. M. Bollinger. J. Am. Chem. Soc. 57, 280 (1935).

76. G. Jones and S. M. Christian. J. Am. Chem. Soc. 57, 272 (1935).

77. P. Debye and H. Falkenhagen. Z. Physik. 29, 121, 401 (1928).

78. R. A. Robinson and R. H. Stokes. Electrolyte Solutions, revised 2nd Edition. Butterworths, London. 1965. p. 93.

79. J. O'M. Bockris and B. E. Conway. J. Chem. Phys. 28, 707 (1958).

80. T. R. Nanney and W. R. Gilkerson. J. Phys. Chem. 69, 1338 (1965).

81. J. E. Lind Jr., J. J. Zwolenik, and R. M. Fuoss. J. Am. Chem. Soc. 81, 1557 (1959).

82. A. A. Maryott and E. R. Smith. Table of Dielectric Constants of Pure Liquids. National Bureau of Standards Circular 514, 1951. p. 10.

83. F. V. Grimm and W. A. Patrick. J. Am. Chem. Soc. 45, 2794 (1923).

84. S. Kyropoulos. Z. Physik. 40, 507 (1926).

85. B. B. Owen and S. R. Brinkley Jr. Phys. Rev. 64, 32 (1943).

86. H. Hartmann, A. Neumann, and G. Rinck. Z. Phys. Chem. Neue Folge 44, 218 (1965).

87. K. Howard and R. A. McAllister. A. I. Ch. E. J. 4, 362 (1958).

88. P. W. Bridgman. Proc. Am. Acad. Arts and Sci. 61, 57 (1926).

89. E. Kuss. Z. angew. Phys. 8, 372 (1955).

90. H. S. Harned and B. B. Owen. The Physical Chemistry of Electrolyte Solutions. Reinhold Publishing Corp., New York. 1950. p. 154.

91. L. Onsager. Physikal. Z. 28, 277 (1927).

92. S. Arrhenius. Z. physik. Chem. 1, 631 (1887).

93. W. Ostwald. Z. physik. Chem. 2, 36 (1888).

94. H. S. Harned and B. B. Owen. The Physical Chemistry of Electrolyte Solutions. Reinhold Publishing Corp., New York. 1950. p. 206.

95. T. Shedlovsky. J. Franklin Inst. 225, 739 (1938).

96. R. M. Fuoss and T. Shedlovsky. J. Am. Chem. Soc. 71, 1496 (1949).

97. P. G. Sears, E. D. Wilhoit, and L. R. Dawson. J. Phys. Chem. 60, 169 (1956).

98. L. G. Savedoff. J. Am. Chem. Soc. 88, 664 (1966).

99. F. B. Hildebrand. Introduction to Numerical Analysis. McGraw-Hill, New York. 1956. Ch. 7.

100. R. A. Robinson and R. H. Stokes. Electrolyte Solutions, revised 2nd Edition. Butterworths, London. 1965. p. 230.

101. H. S. Harned and B. B. Owen. The Physical Chemistry of Electrolyte Solutions. Reinhold Publishing Corp., New York. 1950. p. 12.

102. S. B. Brummer and G. J. Hills. Trans. Faraday Soc. 57, 1823 (1961).

103. H. D. Young. Statistical Treatment of Experimental Data. McGraw-Hill, New York. 1962. pp. 108,95.

104. P. Walden. Z. physik. Chem. 55, 207, 246 (1906).

105. J. F. Skinner and R. M. Fuoss. J. Phys. Chem. 70, 1426 (1966).

106. R. A. Robinson and R. H. Stokes. Electrolyte Solutions, revised 2nd Edition. Butterworths, London. 1965. p. 125.

107. K. H. Stern and E. S. Amis. Chem. Rev. 59, 1 (1959).

108. M. B. Reynolds and C. A. Kraus. J. Am. Chem. Soc. 70, 1707 (1948).

109. M. J. McDowell and C. A. Kraus. J. Am. Chem. Soc. 73, 3293 (1951).

110. D. F. Evans, C. Zawoyski, and R. L. Kay. J. Phys. Chem. 69, 3878 (1965).

111. P. Walden, H. Ulich, and G. Busch. Z. physik. Chem. 123, 429 (1926).

112. E. R. Nightingale Jr. J. Phys. Chem. 63, 1381 (1959).

113. R. W. Gurney. Ionic Processes in Solution. Dover Publications, New York. 1953. p. 51.

114. R. E. Pennington and K. A. Kobe. J. Am. Chem. Soc. 79, 300 (1957).

115. R. Gopal and S. A. Rizvi. J. Indian Chem. Soc. 43, 104 (1966).

116. R. A. Robinson and R. H. Stokes. Electrolyte Solutions, revised 2nd Edition. Butterworths, London. 1965. p. 44.

117. O. L. Hughes and Hartley. Phil. Mag. 15, 610 (1933).

118. B. S. Gourary and F. J. Adrian. Solid State Phys. 10, 127 (1960).

119. S. B. Brummer. J. Chem. Phys. 42, 1636 (1965).

120. A. E. Stearn and H. Eyring. J. Chem. Phys. 5, 113 (1937).

121. S. Glasstone, K. J. Laidler, and H. Eyring. The Theory of Rate Processes. McGraw-Hill, New York. 1941. pp. 552, 563.

122. J. O'M. Bockris, J. A. Kitchener, S. I. Ignatowicz, and J. W. Tomlinson. Trans. Faraday Soc. 48, 75 (1952).

123. J. O'M. Bockris, E. H. Crook, H. Bloom, and N. E. Richards. Proc. Roy. Soc. London, Ser. A, 255, 588 (1960).

124. S. B. Brummer. Ionic Conductance at Constant Volume. Ph.D. Thesis, University of London. 1960.

125. S. B. Brummer and G. J. Hills. Trans. Faraday Soc. 57, 1816, 1823 (1961).

126. S. Glasstone, K. J. Laidler, and H. Eyring. The Theory of Rate Processes. McGraw-Hill, New York. 1941. Ch. 9.

127. M. G. Evans and M. Polanyi. Trans. Faraday Soc. 31, 875 (1935).

128. A. Jobling and A. S. C. Lawrence. Proc. Roy. Soc. London, Ser. A, 206, 257 (1951).

129. F. C. Collins. J. Chem. Phys. 26, 398 (1957).

130. A. Bondi. J. Chem. Phys. 14, 591 (1946).

131. M. K. Nagarajan and J. O'M. Bockris. J. Phys. Chem. 70, 1854 (1966).

132. C. A. Angell. J. Phys. Chem. 69, 399 (1966).

133. D. M. Newitt and A. Wasserman. J. Chem. Soc. 735 (1940).

134. E. Whalley. Ber. Bunsenges. Physik. Chem. 70, 958 (1966).

135. C. F. Goodeve. Trans. Faraday Soc. 34, 115 (1938).

136. J. H. Hildebrand and R. L. Scott. Regular Solutions. Prentice-Hall, New Jersey. 1962. Ch. 5.

137. J. O'M. Bockris and S. R. Richards. J. Phys. Chem. 69, 671 (1965).

138. R. Fürth. Proc. Cambridge Phil. Soc. 37, 252 (1941).

139. H. Watts, B. J. Alder, and J. H. Hildebrand. J. Chem. Phys. 23, 657 (1955).

140. B. J. Alder and T. E. Wainwright. Molecular Dynamics by Electronic Computers. Transport Properties in Statistical Mechanics. Interscience Publishers, New York. 1958.

141. R. A. Swalin. Acta Met. 7, 736 (1959).

142. C. A. Angell. J. Phys. Chem. 69, 399, 2137 (1965).

143. P. W. Bridgman. The Physics of High Pressure. Bell and Sons, London. 1931. p. 352.

144. D. B. Davies and A. J. Matheson. J. Chem. Phys. 45, 1000 (1966).

145. A. J. Matheson. J. Chem. Phys. 44, 695 (1966).

146. M. H. Cohen and D. Turnbull. J. Chem. Phys. 31, 1164 (1959).

147. R. A. Robinson and R. H. Stokes. Electrolyte Solutions, revised 2nd Edition. Butterworths, London. 1965. Ch. 11.

148. J. Frenkel. Kinetic Theory of Liquids. Dover Publications, New York. 1955. Ch. 1.

149. B. Howard. Ph. D. Thesis. University of London. 1963.

150. D. W. McCall, D. C. Douglas, and E. W. Anderson. J. Chem. Phys. 31, 1555 (1959).

151. J. D. Mackenzie. J. Chem. Phys. 28, 1037 (1958).

152. F. Blankenship and B. Clampitt. Proc. Oklahoma Acad. Sci. 31, 106 (1950).

153. R. A. Horne, R. A. Courant, and D. S. Johnson. Electrochemica Acta 11, 987 (1966).

154. K. Shimizu, H. Takizawa, and J. Osugi. Rev. Phys. Chem. Japan 33, 1 (1963).

155. J. Osugi, K. Shimizu, and H. Takizawa. Rev. Phys. Chem. Japan 36, 1 (1966).

156. F. H. Fisher and D. F. Davis. J. Phys. Chem. 69, 2595 (1965).

157. T. R. Griffiths and M. C. R. Symons. Mol. Phys. 3, 90 (1960).

158. T. R. Griffiths and R. K. Scarrow. International Conference on Non-Aqueous Solvent Chemistry. McMaster University, Canada. June, 1967.

159. T. R. Griffiths and R. H. Wijayanayake. XIII Colloquium Spectroscopicum Internationale, Ottawa, Canada. June, 1967.

160. R. M. Fuoss. J. Am. Chem. Soc. 80, 5059 (1958).

161. S. D. Hamann, P. J. Pearce, and W. Strauss. J. Phys. Chem. 68, 375 (1964).

162. E. H. Amagat. Ann. Chim. et phys. 11, 520 (1877).

163. E. H. Amagat. Ann. Chim. et phys. 29, 68 (1893).

164. P. W. Bridgman. Proc. Am. Acad. Arts and Sci. 49, 1 (1913).

165. D. M. Newitt and K. E. Weale. J. Chem. Soc. 3092 (1951).

166. E. D. Fryer, J. C. Hubbard, and D. H. Andrews. J. Am. Chem. Soc. 51, 759 (1929).

167. L. A. K. Staveley, W. I. Tupman, and K. R. Hart. Trans. Faraday Soc. 51, 323 (1955).

168. L. A. K. Staveley and D. N. Parham. Soc. de Chim. phys. 2^{e} Reunion, 366 (1952).

169. D. I. R. Low and E. A. Moelwyn-Hughes. Proc. Roy. Soc. London, Ser. A, 267, 384 (1962).

170. G. S. Kell and E. Whalley. Phil. Trans. Roy. Soc. London, Ser. A, 258, 565 (1965).

171. R. E. Gibson and O. H. Loeffler. J. Am. Chem. Soc. 63, 898 (1941).

172. R. E. Gibson and O. H. Loeffler. J. Am. Chem. Soc. 61, 2515 (1939).

173. D. Harrison and E. A. Moelwyn-Hughes. Proc. Roy. Soc. London, Ser. A, 239, 230 (1957).

174. Dr. G. S. Kell has informed us that their results (170) indicate that the sign of $(\partial C_V/\partial V)_T$ is positive from 25 to 60°C.

175. R. H. Cole. J. Chem. Phys. 9, 251 (1941).

176. I. S. Jacobs and A. W. Lawson. J. Chem. Phys. 20, 1161 (1952).